

2808970049

REFERENCE ONLY

UNIVERSITY OF LONDON THESIS

Degree PhD Year 2006 Name of Author SMILJANIC
Ela

COPYRIGHT

This is a thesis accepted for a Higher Degree of the University of London. It is an unpublished typescript and the copyright is held by the author. All persons consulting the thesis must read and abide by the Copyright Declaration below.

COPYRIGHT DECLARATION

I recognise that the copyright of the above-described thesis rests with the author and that no quotation from it or information derived from it may be published without the prior written consent of the author.

LOANS

Theses may not be lent to individuals, but the Senate House Library may lend a copy to approved libraries within the United Kingdom, for consultation solely on the premises of those libraries. Application should be made to: Inter-Library Loans, Senate House Library, Senate House, Malet Street, London WC1E 7HU.

REPRODUCTION

University of London theses may not be reproduced without explicit written permission from the Senate House Library. Enquiries should be addressed to the Theses Section of the Library. Regulations concerning reproduction vary according to the date of acceptance of the thesis and are listed below as guidelines.

- A. Before 1962. Permission granted only upon the prior written consent of the author. (The Senate House Library will provide addresses where possible).
- B. 1962 - 1974. In many cases the author has agreed to permit copying upon completion of a Copyright Declaration.
- C. 1975 - 1988. Most theses may be copied upon completion of a Copyright Declaration.
- D. 1989 onwards. Most theses may be copied.

This thesis comes within category D.

☐

This copy has been deposited in the Library of UCC

☐

This copy has been deposited in the Senate House Library, Senate House, Malet Street, London WC1E 7HU.

University College London

Department of Chemistry



Some Studies of Artificial Enzyme Systems

A thesis presented by

Ela Smiljanic

**In Partial Fulfilment of The Requirements For The Award of The
Degree of**

Doctor of Philosophy

of the

University of London

**Sir Christopher Ingold Laboratories
Department of Chemistry
University College London
20 Gordon Street
London
WC1H 0AJ**

UMI Number: U592413

All rights reserved

INFORMATION TO ALL USERS

The quality of this reproduction is dependent upon the quality of the copy submitted.

In the unlikely event that the author did not send a complete manuscript and there are missing pages, these will be noted. Also, if material had to be removed, a note will indicate the deletion.



UMI U592413

Published by ProQuest LLC 2013. Copyright in the Dissertation held by the Author.
Microform Edition © ProQuest LLC.

All rights reserved. This work is protected against
unauthorized copying under Title 17, United States Code.



ProQuest LLC
789 East Eisenhower Parkway
P.O. Box 1346
Ann Arbor, MI 48106-1346

Abstract

This thesis describes a novel approach to the rational design of artificial esterases and aldolases.

The Introduction provides a literature summary of the previous approaches that have been employed towards the design and synthesis of artificial enzyme systems.

Chapter 2 describes the preparation and reactivity of a number of polymer based artificial enzymes, which are capable of catalysing ester hydrolysis. The study has involved the incorporation of a histidine catalytic group together with specifically designed peptide binding groups within a polymeric backbone. The binding groups were specifically selected according to their binding affinity towards an appropriate transition state analogue. The synthesis of peptide binding sites and thus incorporation of these, together with the histidine catalytic group into a polymer backbone, using standard peptide chemistry has been outlined. The results to an investigation of the influence of different pH, solvent and substrate concentration on the activity of artificial esterases are presented.

Chapter 3 describes preliminary work undertaken towards the design and synthesis of artificial aldol catalysts. The aldolases, which feature a proline residue attached to a polymer backbone are shown to selectively catalyse aldol reactions using aromatic aldehydes as electrophilic partner.

Chapter 4 describes the detailed experimental procedures used.

Contents

Abstract	2
Contents	3
Contents of Tables, Figures, Schemes and Equations	7
Abbreviations	17
Acknowledgements	19
Chapter 1 Introduction	22
1.1 Introduction	23
1.2 Principles of Enzyme Catalysis	23
1.2.1 Transition State Theory	24
1.2.2 Contribution of Intermolecular Forces in Transition State Stabilisation	26
1.2.3 Functional Group Cooperativity	30
1.3 Previous Approaches to Artificial Enzymes	33
1.3.1 Cyclodextrins as Enzyme Mimics	34
1.3.2 Cyclophanes as Enzyme Mimics	38
1.3.3 Cyclic Metalloporphyrin Oligomers	42
1.3.4 Catalytic Antibodies	43
1.3.4.1 The 'Bait-and-Switch' Approach	46
1.3.4.2 The Reactive Immunisation Approach	47
1.3.4.3 Cofactor Dependent Antibodies	49
1.3.4.4 Summary	50
1.3.5 Molecularly Imprinted Polymers	51
1.3.6 Synthetic Polymers as Artificial Enzymes	56
1.3.7 Combinatorial Polymers as Enzyme Mimics	61
1.3.8 Directed Evolution of Enzymes	64

1.4 Summary	68
Chapter 2 Results and Discussion	70
Studies related to the development of artificial esterases	
2.1 Introduction	71
2.1.1 The protocol for selection of a binding group (receptor site)	73
2.1.2 Selection of the catalytic functional group	76
2.1.3 Constructing an artificial esterase	77
2.2 Objectives of the current research programme	80
2.3 Development of artificial esterases	81
2.3.1 Preparation of binding groups	82
2.3.2 Synthesis of artificial esterases containing a polyallylamine backbone	85
2.3.3 Characterisation of polymers	88
2.4 Synthesis of initial ester substrates	88
2.4.1 Preparation of cinnamyl ester substrate	89
2.4.2 Synthesis of phenethyl ester substrate	92
2.5 Activity of artificial esterases	92
2.5.1 Hydrolysis of phenethyl ester 127	93
2.5.2 The activity of artificial esterases containing different binding sites	97
2.5.3 Initial velocities of reactions with active polymers	100
2.5.4 Hydrolysis of cinnamyl ester 169	103
2.5.5 The activity of artificial esterases at different pH	107
2.5.6 The activity of artificial esterases at different ester concentrations	111
2.6 Preparation of a histidine catalytic unit with an additional caproic acid spacer	113
2.6.1 The activity of the artificial esterase containing an extended histidine catalytic unit with the caproic acid spacer	119
2.7 Synthesis of artificial esterase containing a tentagel resin backbone	119
2.8 Hydrolysis of other ester substrates	121
2.9 Conclusions from the esterase studies	122
2.10 Future Outlook	123

Chapter 3 Results and Discussion	125
Artificial Aldol Catalysts	
3.1 Introduction	126
3.2 Preliminary studies with artificial aldolases	127
3.3 Organocatalysts in aldol reactions	131
3.4 Synthesis of aldol catalysts containing proline	135
3.4.1 Tentagel based aldol catalyst	135
3.4.2 Polyallylamine based aldol catalyst	138
3.4.3 Aldol reaction using proline and its derivatives as catalysts	140
3.4.3.1 Aldol reactions using proline derivative 242	141
3.4.3.2 Testing the dipeptide 242 as a catalyst in aldol reaction	143
3.4.4 Re-investigation of catalytic activity of tentagel catalyst 238	144
3.4.4.1 Optimising reaction conditions for an aldol reaction	144
3.4.4.2 Aldol substrate specificity studies (part 1)	145
3.4.4.3 Enantioselectivity of aldol reaction	149
3.4.4.4 Aldol substrate specificity studies (part 2)	151
3.4.5 Development of alternative tentagel based catalysts	152
3.4.6 Re-investigation of catalytic activity of polyallylamine catalyst 240	155
3.4.7 Development of a Merrifield resin based aldol catalyst	156
3.4.8 Designing an aldol catalyst with improved selectivity	162
3.4.8.1 Development of transition state analogues	163
3.4.8.2 Synthesis of sulfoxide transition state analogues	164
3.4.8.3 Selecting a binding group for the transition state analogues	165
3.4.8.4 Synthesis of aldol catalyst containing a serine binding group	167
3.4.8.5 Activity of aldol catalyst 326 containing serine binding group	168
3.5 Exploring artificial aldolases through supramolecular assembly	171
3.5.1 Introduction	171
3.5.2 Synthesis of monomer units	173
3.6 Conclusions and Perspectives from the aldolase studies	177
3.7 Final Remarks	179

Chapter 4 Experimental	180
4.1 General Experimental	181
4.2 Artificial Esterases	184
4.2.1 Synthesis of Ester Substrates	184
4.2.2 Synthesis of Binding Units	196
4.2.3 Synthesis of Artificial Esterases	222
4.2.4 Synthesis of Acid Product For Use as a Standard in HPLC	243
4.2.5 Calibration of HPLC by the External Standard Method	244
4.2.6 General Procedures for Ester Hydrolysis with Polymers	248
4.3 Artificial Aldolases	249
4.3.1 Synthesis of Artificial Aldolases With Incorporated Lysine	249
4.3.2 Synthesis of Catalytic Units Containing Proline for Artificial Aldolase Catalysts	252
4.3.3 Synthesis of Artificial Aldolases With Incorporated Proline	264
4.3.4 Synthesis of Racemic Aldol Products	283
4.3.5 General Procedures for Aldol Reactions	290
4.3.6 Synthesis of Sulfoxide Transition State Analogues	297
4.3.7 NMR Binding Studies	302
4.3.8 Supramolecular Chemistry	303
References	308
 Appendix	 319

Contents of Tables, Figures, Schemes and Equations

Table 1.3.1	Comparison of catalytic efficiencies of imidazole, α -chymotrypsin and polyethyleneimine.	58
Table 2.1.1	NMR binding studies of potential dipeptide binding sites.	76
Table 2.4.1	Different conditions attempted for trifluoroacetamide deprotection of 173 .	90
Table 2.5.1	Effect of aqueous wash on polymer (132) activity.	94
Table 2.5.2	The influence of changing the binding group on polymer activity.	97
Table 2.5.3	Initial velocities of reactions with active polymers.	102
Table 2.5.4	Hydrolysis of cinnamyl ester 169 .	104
Table 2.5.5	Initial velocities of reactions with polymer 132 , at pH 6, pH 7 and pH 8.	108
Table 2.5.6	Initial velocities of reactions with polymer 168 , at pH 6, pH 7 and pH 8.	110
Table 2.5.7	Initial velocities of reactions with polymer 132 , at different ester concentrations.	111
Table 2.6.1	Attempted reaction conditions for the synthesis of dipeptide 189 .	115
Table 3.2.1	Aldol reaction (Scheme 3.2.2) monitored by UV and NMR.	128
Table 3.2.2	Aldol reaction (Scheme 3.2.4) monitored by UV and NMR.	130
Table 3.2.3	Aldol reaction (Scheme 3.2.6) monitored by UV and NMR.	131
Table 3.4.1	Aldol reaction (Scheme 3.4.4) monitored by UV and NMR.	138
Table 3.4.2	Aldol reaction (Scheme 3.4.6) monitored by UV and NMR.	139
Table 3.4.3	Optimising reaction conditions for aldol reaction in Scheme 3.4.13 .	145

Table 3.4.4	Activity of aldol catalyst 238 with varying aldehyde substrates.	148
Table 3.4.5	Selectivity of aldol catalyst 238 .	150
Table 3.4.6	Reaction of 4-nitrobenzaldehyde with different ketones.	152
Table 3.4.7	Reaction conditions attempted for the aldol reaction catalysed by polymer 240 .	156
Table 3.4.8	Results of NMR binding studies between Boc protected amino acids and sulfoxide TSAs 316 and 317 .	166
Table 3.4.9	Selectivity of the aldol catalyst 238 , 325 and 326 .	170
Table 4.2.1		244
Table 4.2.2		245
Table 4.2.3		246
Table 4.2.4		247
Figure 1.2.1	Energy level diagram of enzyme-substrate pathway following transition state theory.	25
Figure 1.2.2	Representation of electrostatic interactions occurring between cytochrome c and cytochrome oxidase.	27
Figure 1.2.3	HIV-2 protease inhibitors.	28
Figure 1.2.4	a) Initial step of amide bond cleavage by serine protease. b) Representation of dynamic binding.	30
Figure 1.2.5	Representation of the active site of chymotrypsin-like enzymes.	32
Figure 1.3.1	α -cyclodextrin 6 which can be represented in a more simplified manner as 7 or 8 .	34
Figure 1.3.2	AB, AC and AD isomers of cyclodextrin bis-imidazoles.	35
Figure 1.3.3	Cyclodextrin dimer and its cyclopropene substrate.	37
Figure 1.3.4	Cyclodextrin dimer with an incorporated copper (II) and its benzyl ester substrate.	37
Figure 1.3.5	Thymine diphosphate and flavin adenine dinucleotide.	38
Figure 1.3.6	Pyruvate oxidase mimic.	39
Figure 1.3.7	Steroid 33 and cyclophane cytochrome P-450 mimic 34 .	40
Figure 1.3.8	Cyclodextrin cytochrome P-450 mimic.	41
Figure 1.3.9	Metalloporphyrin oligomers.	42

Figure 1.3.10	Phosphonate transition state analogue for ester hydrolysis.	44
Figure 1.3.11	Transition state analogue for oxy-Cope rearrangement.	45
Figure 1.3.12	Transition state analogue for phosphodiester hydrolysis.	47
Figure 1.3.13	Molecule 70 containing the succinic anhydride moiety, which is coordinated to CuCl ₂ prior to forming a complex with antibody 38C2.	50
Figure 1.3.14	The general molecular imprinting process.	52
Figure 1.3.15	Triamine 79 , phosphonate transition state analogue 80 and diphenylcarbonate 81 .	54
Figure 1.3.16	Poly(4-vinylpyridine) (82), poly(<i>N</i> -vinylimidazole) (83) and nitrophenyl ester (84).	56
Figure 1.3.17	Polyethyleneimine.	57
Figure 1.3.18	Trinuclear macrocyclic complex 92 , multinuclear metalloprotease 93 and amide substrates.	59
Figure 1.3.19	Hydrolysis of amides by metalloprotease 93 .	60
Figure 1.3.20	Co(III)Cyc complex 99 and proposed mechanism of DNA hydrolysis.	60
Figure 1.3.21	PCD derivative incorporating Co(III)Cyc complex.	61
Figure 1.3.22	General representation of directed evolution process.	65
Figure 2.1.1	A diagrammatic representation of an artificial “millipede” enzyme.	72
Figure 2.1.2	Ester substrate used for hydrolysis studies.	73
Figure 2.1.3	Representation of the interaction between a guanidine and a carboxylic acid.	76
Figure 2.1.4	Polyallylamine	77
Figure 2.1.5	The tripeptide 131 binding group.	78
Figure 2.1.6	a) Graphical representation of artificial esterase. b) Chemical representation of artificial esterase.	79
Figure 2.1.7	Examples of further artificial esterases prepared.	79
Figure 2.3.1	Initial artificial esterases targeted.	82

Figure 2.3.2	Fulvene-piperidine adduct.	83
Figure 2.3.3	Additional tripeptide binding groups prepared.	85
Figure 2.4.1	Initial ester substrates targeted.	89
Figure 2.4.2	By-product 175 detected during sodium borohydride deprotection of 173 .	90
Figure 2.5.1	Scanning electron micrograph showing a) Polymer 132 before aqueous wash, b) The same polymer 132 after aqueous wash.	94
Figure 2.5.2	A plot of ester concentration against time for polymer 132 over the first 225 min of the reaction.	95
Figure 2.5.3	A plot of acid concentration against time for polymer 132 over the first 225 min of the reaction.	96
Figure 2.5.4	A plot of acid concentration against time for polymers 132 , 136 and 168 over the first 400 min of the reaction.	98
Figure 2.5.5	The graph in Figure 2.5.4 , expanded to show the first 60 min of the reaction for clarity.	99
Figure 2.5.6	A plot of ester concentration against time for polymers 132 and 136 – 139 over the first 300 min of the reaction.	100
Figure 2.5.7	Representation of product formation for a typical enzyme catalysed reaction.	101
Figure 2.5.8	A plot of ester concentration against time for polymers 132 and 168 over the first 300 min of the reaction.	105
Figure 2.5.9	A plot of alcohol concentration against time for polymers 132 and 168 over the first 300 min of the reaction.	106
Figure 2.5.10	The effect of pH on the velocity of a typical enzymatic reaction.	107
Figure 2.5.11	A plot of acid concentration against time for polymer 132 , at pH 6, pH 7 and pH 8 over the first 180 min of the reaction.	108
Figure 2.5.12	A plot of acid concentration against time for polymer 168 , at pH 6, pH 7 and pH 8 over the first 180 min of the reaction.	109
Figure 2.5.13	A plot of acid concentration against time for polymer 132 , at different concentrations of phenethyl ester 127 , over 180 min of the reaction.	111

Figure 2.6.1	a) Artificial esterase containing a spacer between both the binding group and histidine catalytic unit. b) An example of a potential dipeptide to be synthesised with the appropriate protecting groups before incorporation into polyallylamine.	112
Figure 2.6.2	Artificial esterase 181 .	118
Figure 2.8.1	Ethyl phenylacetate.	120
Figure 3.1.1	Representation of artificial aldolase catalyst.	126
Figure 3.1.2	Enamine attack on aldehyde during an aldol reaction.	126
Figure 3.4.1	Aldol catalysts 242 and 294 , used by Li and co-workers in their studies.	157
Figure 3.4.2	Representation of aldol catalyst with incorporated chiral binding group.	162
Figure 3.4.3	β -diketo-sulfone TSA.	163
Figure 3.4.4	Sulfoxide TSAs (316 and 317) and representation of the aldol transition state.	164
Figure 3.4.5	Target sulfoxide transition state analogues.	164
Figure 3.5.1	Representation of hydrogen bonded monomer units.	172
Figure 3.5.2	Hydrogen bonded dimers.	172
Figure 3.5.3	Target dimer unit.	173
Figure 3.5.4	Target dimer unit consisting of proline catalytic group and carboxylic acid proton donor.	173
Figure 3.5.5	Example of a possible hydrogen bonded complex between 335 and 341 .	176
Scheme 1.2.1	Functional group cooperativity in chymotrypsin.	31
Scheme 1.3.1	Hydrolysis of aryl acetate by cyclodextrin.	34

Scheme 1.3.2	Mechanism of hydrolysis of cyclic phosphodiester by cyclodextrin bis imidazole.	36
Scheme 1.3.3	The reaction cascade from pyruvate to acetyl phosphate, catalysed by pyruvate oxidase	38
Scheme 1.3.4	The transformation of naphthalene-2-carbaldehyde to methyl naphthalene-2-carboxylate catalysed by pyruvate oxidase mimic.	39
Scheme 1.3.5	Regiospecific Diels-Alder reaction between 4-pyridyl butadiene and 3-nitroso pyridine.	42
Scheme 1.3.6	Hydrolysis of ester by catalytic antibody.	44
Scheme 1.3.7	Oxy-Cope rearrangement catalysed by antibody AZ-28.	45
Scheme 1.3.8	Phosphodiester hydrolysis catalysed by antibody MATT.F-1.	46
Scheme 1.3.9	Mechanism of aldol reaction within active site of natural aldolases.	48
Scheme 1.3.10	Transformation of a 1, 3-diketone to a vinylogous amide.	48
Scheme 1.3.11	Examples of aldol reactions catalysed by antibody 33F12.	49
Scheme 1.3.12	Ester hydrolysis catalysed by 38C2-70-CuCl ₂ complex.	50
Scheme 1.3.13	Imprinting a polymer with sterol acrylate and ketone reduction with polymer catalyst 76 .	53
Scheme 1.3.14	Schematic representation of a) the molecular imprinting with TSA 80 and monomer 79 in the presence of Zn ²⁺ ; b) removal of the template; c) and d) catalysis step.	55
Scheme 1.3.15	Ester hydrolysis by polyethyleneimine.	57
Scheme 1.3.16	Hydrolysis of albumin by catalyst 89 .	58
Scheme 1.3.17	Synthesis of a polymer library consisting of polyallylamine and carboxylic acids.	62
Scheme 1.3.18	Reduction of benzoylformic acid using combinatorial polymers.	63
Scheme 1.3.19	Combinatorial polymer 115 and dehydration of β -	63

	hydroxyketone catalysed by 115.	
Scheme 1.3.20	Hydrolytic kinetic resolution of ester 118 catalysed by <i>Pseudomonas Aeruginosa</i> lipase.	66
Scheme 1.3.21	Baeyer-Villiger reaction catalysed by CHMO enzyme.	67
Scheme 1.3.22	Baeyer-Villiger reaction catalysed by CHMO enzyme.	68
Scheme 2.1.1	General ester hydrolysis.	74
Scheme 2.1.2	Hydrolysis of ester 127 <i>via</i> a tetrahedral intermediate, which is mimicked by transition state analogue 128.	75
Scheme 2.1.3	General acid/base catalysis in ribonucleases.	77
Scheme 2.3.1	Synthesis of Fmoc 6-aminocaproic acid 142.	83
Scheme 2.3.2	Solid phase synthesis of tripeptide binding group 131.	84
Scheme 2.3.3	Synthesis of artificial esterases 132 and 136 – 139.	86
Scheme 2.3.4	Synthesis of artificial esterase 168 (no lys).	87
Scheme 2.4.1	Attempted route to cinnamyl ester 169.	89
Scheme 2.4.2	Synthesis of cinnamyl ester substrate 169.	91
Scheme 2.4.3	Synthesis of phenethyl ester substrate 127.	92
Scheme 2.5.1	Hydrolysis of phenethyl ester 127.	93
Scheme 2.5.2	Hydrolysis of cinnamyl ester 169.	103
Scheme 2.6.1	Attempted synthesis of histidine ester 183.	113
Scheme 2.6.2	Attempted synthesis of dipeptide 184.	114
Scheme 2.6.3	Synthesis of benzyl protected 6-aminocaproic acid 186.	114
Scheme 2.6.4	Synthesis of Boc protected histidine 188.	115
Scheme 2.6.5	Synthesis of dipeptide 189.	115
Scheme 2.6.6	Synthesis of dipeptide 190.	116
Scheme 2.6.7	Synthesis of artificial esterase 181.	117
Scheme 2.7.1	Synthesis of artificial esterase 196, containing a tentagel resin backbone.	119
Scheme 2.8.1	Synthesis of ester 199.	120
Scheme 2.8.2	Synthesis of ester 200.	121
Scheme 2.8.3	Synthesis of ester 202.	121
Scheme 3.2.1	Synthesis of aldolase catalyst 207.	127
Scheme 3.2.2	Attempted aldol reaction between acetophenone and	128

	benzaldehyde, using polymer catalyst 207 .	
Scheme 3.2.3	Synthesis of aldol catalyst 211 .	129
Scheme 3.2.4	Attempted aldol reaction between benzophenone and benzaldehyde, using polymer 211 as a catalyst.	129
Scheme 3.2.5	Synthesis of aldol catalyst 212 .	130
Scheme 3.2.6	Attempted aldol reaction between benzophenone and <i>p</i> -tolualdehyde, using polymer 212 as a catalyst.	131
Scheme 3.3.1	Proline catalysed intramolecular aldol reaction.	132
Scheme 3.3.2	Proline catalysed intermolecular aldol reaction.	132
Scheme 3.3.3	Proposed mechanism of the proline catalysed aldol reaction.	133
Scheme 3.3.4	Proline catalysed aldol reaction.	133
Scheme 3.3.5	Aldol reactions catalysed by proline derivatives.	134
Scheme 3.3.6	Proline derivative catalysed nitro-Michael addition.	134
Scheme 3.3.7	Proline catalysed Mannich reaction.	135
Scheme 3.4.1	Synthesis of Boc proline 230 .	135
Scheme 3.4.2	Synthesis of tentagel based aldol catalyst 233 .	136
Scheme 3.4.3	An improved synthesis of tentagel based aldol catalyst 238 .	137
Scheme 3.4.4	Attempted aldol reaction between acetophenone and <i>p</i> -tolualdehyde, using polymer catalyst 238 .	137
Scheme 3.4.5	Synthesis of polyallylamine based aldolase catalyst 240 .	138
Scheme 3.4.6	Attempted aldol reaction between acetophenone and <i>p</i> -tolualdehyde, using polymer catalyst 240 .	139
Scheme 3.4.7	Attempted aldol reaction, using L-proline as a catalyst.	140
Scheme 3.4.8	Attempted aldol reactions, using L-proline as a catalyst.	140
Scheme 3.4.9	Aldol reaction performed by Li <i>et al.</i> , using dipeptide 242 as a catalyst.	141
Scheme 3.4.10	Attempted synthesis of dipeptide 242 .	142
Scheme 3.4.11	Synthesis of dipeptide 242 .	143
Scheme 3.4.12	Aldol reaction catalysed by polymer 238 .	144
Scheme 3.4.13	Aldol reaction catalysed by polymer 238 .	144

Scheme 3.4.14		146
Scheme 3.4.15	Synthesis of racemic aldol product.	151
Scheme 3.4.16	Reaction of 4-nitrobenzaldehyde with different ketones.	151
Scheme 3.4.17	Synthesis of aldol catalyst 286 .	153
Scheme 3.4.18	Aldol reaction catalysed by polymer 286	153
Scheme 3.4.19	Synthesis of polymer 287 .	153
Scheme 3.4.20	Synthesis of 290 .	154
Scheme 3.4.21	Synthesis of aldol catalyst 293 with incorporated internal base.	154
Scheme 3.4.22	Aldol reaction catalysed by polymer 293 .	155
Scheme 3.4.23	Aldol reaction catalysed by polyallylamine based polymer 240 .	156
Scheme 3.4.24	Synthesis of Boc protected hydroxy proline 296 .	157
Scheme 3.4.25	Synthesis of protected hydroxyproline 300 .	158
Scheme 3.4.26	Synthesis of protected phenylalanine ester 303 .	159
Scheme 3.4.27	Synthesis of protected phenylalanine ester 303 .	159
Scheme 3.4.28	Attempted synthesis of phenylalanine ester 306 .	160
Scheme 3.4.29	Attempted synthesis of phenylalanine ester 306 .	160
Scheme 3.4.30	Attempted synthesis of protected phenylalanine ester 310 .	161
Scheme 3.4.31	Attempted synthesis of polymer catalyst 312 .	162
Scheme 3.4.32	Synthesis of sulfoxide TSAs 316 and 317 .	165
Scheme 3.4.33	Synthesis of serine derivative 323 .	167
Scheme 3.4.34	Synthesis of aldolase catalyst 326 with incorporated serine binding group.	168
Scheme 3.4.35	Attempted aldol reaction using aldol catalyst 326 .	171
Scheme 3.5.1	Synthesis of diaminopyridine derivative 333 .	174
Scheme 3.5.2	Attempted synthesis of uracil derivative 334 .	174
Scheme 3.5.3	Synthesis of uracil derivative 339 .	175
Scheme 3.5.4	Aldol reaction using diaminopyridine derivative 333 as a catalyst.	175
Scheme 3.5.5	Towards the synthesis of diaminopyridine derivative 342 .	176

Scheme 3.5.6	Towards the synthesis of orotic acid derivative 346.	177
Equation 1.2.1	Representation of enzymic reaction pathway.	24
Equation 2.3.1		83
Equation 2.5.1		101
Equation 2.5.2		102
Equation 4.2.1		244
Equation 4.2.2		245
Equation 4.2.3		246
Equation 4.2.4		247

Abbreviations

Ab	Antibody
AMP	Adenosine monophosphate
Arg	Arginine
ATP	Adenosine triphosphate
Boc	<i>Tert</i> -butoxycarbonyl
BPP-LED	Bipolar Pulse Pair Longitudinal Encode-Decode
br	Broad
CA	6-aminocaproic acid
CHMO	Cyclohexanone monooxygenase
d	Doublet
DCC	<i>N, N'</i> -dicyclohexylcarbodiimide
DCM	Dichloromethane
DCU	Dicyclohexylurea
DIC	Diisopropylcarbodiimide
DIPEA	Diisopropylethylamine
DMAP	Dimethylaminopyridine
DMF	<i>N, N'</i> -Dimethylformamide
DMSO	Dimethylsulfoxide
DNA	Deoxyribonucleic acid
E	Enzyme
EDCI	1-[3-(dimethylamino)propyl]-3-ethylcarbodiimide hydrochloride
<i>ee</i>	Enantiomeric excess
EP	Enzyme-product complex
ES	Enzyme-substrate complex
FAB	Fast atom bombardment
FAD	Flavin adenine dinucleotide
Fmoc	9-fluorenylmethoxycarbonyl
Glu	Glutamic acid
Gly	Glycine
HATU	O-(7-azabenzotriazol-1-yl)- <i>N, N, N', N'</i> -tetramethyluronium hexafluorophosphate
His	Histidine
HIV	Human immunodeficiency virus
HOBt	1-hydroxybenzotriazole
HPLC	High Performance Liquid Chromatography
HRMS	High Resolution Mass Spectrometry
Im	Imidazole
IR	Infra Red
<i>J</i>	Coupling constant
k_{cat}	First order rate constant
Lys	Lysine
m	Multiplet
MIP	Molecularly Imprinted Polymer

MS	Mass spectrometry
NAD	Nicotineamide adenine dinucleotide
NHS	<i>N</i> -Hydroxysuccinimide
NMR	Nuclear Magnetic Resonance
P	Product
Pbf	2,2,4,6,7-pentamethyldihydrobenzofuran-5-sulfonyl
PCD	Poly(chloromethylstyrene- <i>co</i> -divinylbenzene)
PEI	Polyethyleneimine
PFG	Pused Field Gradient
ppm	Parts per million
PyBOP	(1H-benzotriazol-1-yloxy)tripyrrolidinophosphonium hexafluorophosphate
q	quartet
r.t.	Room temperature
RNA	Ribonucleic acid
S	Substrate
s	singlet
SEM	Scanning Electron Microscopy
t	triplet
t.l.c.	Thin layer chromatography
TBDMS	Tertbutyldimethylsilane
TFA	Trifluoroacetic acid
TFAA	Trifluoroacetic anhydride
ThDP	Thymine diphosphate
Trt	Trityl
TSA	Transition state analogue
UV	Ultraviolet
<i>v/v</i>	Volume for volume
w	Weak

Acknowledgements

I would like to thank my supervisor, Prof. Willie Motherwell, for his continuous support, help, encouragement and belief in me over the past years. The experience I gained from working in his group and on this project has been invaluable. I would also like to thank my industrial supervisors from GSK, Stephanie Wong and Prof. Brian Warrington for sharing their expertise with me.

There have been a large number of people that helped me during the course of my PhD, especially with the more technical side of things. I would like to thank Dr. Abil Aliev, for all his help with NMR and for taking time to train me to manually run NMRs, especially the binding studies. My thanks also goes to David Butler, who spent a lot of time running the solid state NMR of my polymer samples. In addition, I am very grateful to the following people for their help and support: John Hill for mass spectrometry; Kevin Reeves (UCL Institute of Archaeology) for training me on scanning electron microscope; Dr. Dave Selwood and his group (especially Cristina Visintin) for allowing me to use solid state IR; Dr. Chris Hoyle from GSK for all his advice on enzyme kinetics; Dr. Peter Grice (Cambridge University) for running the NMRs on tentagel resin.

In the lab, special thanks goes to Steve, for always being there for me and for being the best bench mate and a wonderful friend. All his help, incredible patience and support are much appreciated. I would also like to thank Tom, for always being available for advice and all the assistance he has given me with my research. Thanks to Gui Gui for all the 'entertainment' he has provided both in the lab and on nights out. Thanks also to Rob, Phil, Bert, Alex, Lorna, Joelle and outside WBM lab, Chris White. My appreciation goes to Dr. Robyn Motherwell, for providing me with all the advice and support on both personal and professional level; without her, the lab would fall to pieces!

Finally, I am eternally grateful to Chris Hurley, for all his infinite love, kindness, support and patience and for being fun and making me laugh so much – I couldn't have

done this without him! I would like to express my deepest gratitude to my family for their endless love and support.

To Chris, Mum, Dad and Ana

CHAPTER 1

INTRODUCTION

1.1 Introduction

Enzymes are highly evolved catalysts that have been developed by nature over billions of years.¹ The capability of enzymes to catalyse reactions with remarkable regio- and chemo stereoselectivity has inspired chemists to investigate synthetic equivalents. An understanding of the underlying principles behind enzyme catalysis would enable us to develop ‘artificial enzymes’, which would rival natural enzymes in terms of rate accelerations, turnover and specificity. Furthermore, research into artificial enzymes provides us with a unique opportunity to design a catalyst for reactions for which there is no natural enzyme equivalent.

Since the present thesis is concerned with the synthesis of artificial enzymes, it is appropriate to place the present study into context, by providing a discussion of the main principles behind enzyme catalysis and an overview of the previous approaches to artificial enzymes.

1.2 Principles of Enzyme Catalysis

Nature has developed enzymes into sophisticated three-dimensional structures, which differ from synthetic chemical catalysts in several ways. Firstly, enzymatically catalysed reactions occur at reaction rates typically in the range of 10^6 to 10^{12} greater than those of corresponding chemically catalysed reactions.¹ Secondly, enzymes function under very mild reaction conditions – lower temperatures, atmospheric pressure and usually neutral pH. Thirdly, many of them have a great degree of specificity for their substrate, producing a product with a high degree of regio- and stereoselectivity and directing reactive intermediates towards only one of several potential products.

The manner by which an enzyme performs the above functions will be discussed in more detail in the following section.

1.2.1 Transition State Theory

Illustrated below is a simplistic representation of the reaction pathway that occurs between an enzyme (E) and a substrate (S) (**Equation 1.2.1**).² The substrate binds to the enzyme to form an enzyme-substrate complex in the first step. The substrate molecule then passes through a series of intermediate forms of altered geometry and electronic distribution before it converts to the final product (P) of the reaction.



Equation 1.2.1 Representation of enzymic reaction pathway.

The free energies of these intermediates forms, especially of those in the most unstable transition states are the major determinants of the reaction rate. Hence, in order for catalysis to occur, the enzyme must be able to recognise and stabilise the transition state of the reaction.³ This theory was originally proposed by Pauling in 1948 and is still the most widely accepted view of enzyme catalysis.³ This is illustrated below (**Figure 1.2.1**).

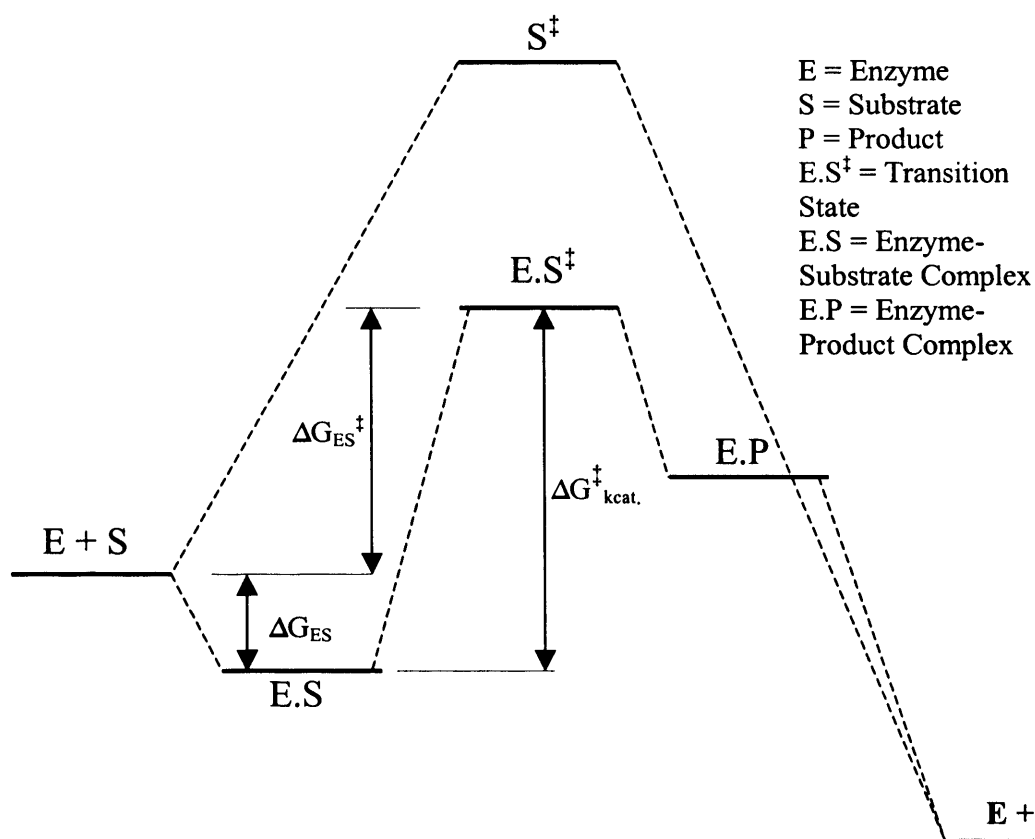


Figure 1.2.1 Energy level diagram of enzyme-substrate pathway following transition state theory, under k_{cat} conditions.²

The overall activation energy ($\Delta G_{\text{ES}}^{\ddagger}$) of the system is composed of ΔG_{ES} and $\Delta G_{\text{kcat}}^{\ddagger}$. ΔG_{ES} represents the net energy gain that results from the formation of the enzyme-substrate complex, while $\Delta G_{\text{kcat}}^{\ddagger}$ is the amount of energy that must be expended to reach the transition state of the reaction. In the absence of the enzyme, the reaction has to overcome a large energy barrier in order to reach the transition state S^{\ddagger} . In the presence of the enzyme, the reaction first proceeds through the E.S complex, an intermediate that is not available during the uncatalysed reaction. The energy gained from the formation of this complex can in part be used to form the transition state of the reaction E.S^{\ddagger} . During the formation of E.S^{\ddagger} , the molecular forces between the enzyme and the substrate (discussed in the next section), have the effect of destabilizing the ground state configuration of the bound substrate molecule and energetically favouring the transition state complex E.S^{\ddagger} which therefore occurs at a lower energy level than S^{\ddagger} . The reaction

then goes through the formation of the E.P complex before final release of the product. It can be seen from the diagram that although the initial and final states for catalysed and uncatalysed reactions are energetically the same, the overall activation energy barrier has been reduced for the enzyme catalysed reaction.^{2;3} In addition to this, in order for true catalysis to occur, the system must also exhibit a turnover. The turnover number of an enzyme is the number of reaction processes that each active site catalyses per unit time.¹ The enzyme-substrate binding must be stronger than enzyme-product binding, *i.e.* E.S must be lower in energy than E.P; if the opposite of this is true, then product inhibition would be observed. The important conclusion to make from this picture of enzyme action, is that when designing an enzyme mimic, we must consider both transition state stabilisation and thermodynamically favourable release of the product. In more complex cases of enzyme catalysis (e.g. bimolecular processes and reactions involving covalent enzyme-bound intermediates), the above model of transition state stabilisation is evidently much less straightforward.

1.2.2 Contribution of Intermolecular Forces in Transition State Stabilisation

From previous studies, it is clear that there are many weak intermolecular forces involved during the binding of a substrate to the enzyme. In general, the overall binding is due to hydrogen bonding⁴, electrostatic forces⁵, hydrophobic interactions⁴, Van der Waals forces⁵ and π -stacking.⁶

Hydrogen bonding contributes significantly to the total energy of the enzyme – substrate complex. However, since enzymes operate in water, these effects are generally disrupted by solvation.⁷ Fersht and co-workers have quantified the contribution of hydrogen bonding from investigation of the coupling of tyrosine to adenosine triphosphate (ATP) to yield tyrosyl-adenosine monophosphate (AMP).⁸ The reaction is catalysed by tyrosyl ³H RNA synthase. Because the crystal structure of the complex was known, a series of point mutations were conducted. This determined which specific hydrogen bonds were important for binding. It was found that a neutral – neutral hydrogen bond contributes only 0.5 - 1.5 kcal mol⁻¹ (2.1 – 6.3 kJ mol⁻¹), which is approximately a 15-fold increase in binding.^{8;9} However, the contribution of a charged

hydrogen bond was found to be more significant, approximately $4.7 \text{ kcal mol}^{-1}$ (19.7 kJ mol^{-1}), which is about a 3000-fold increase in binding.

Electrostatic interactions usually occur between a charged amino acid side chain and a charged group on a ligand. An example that demonstrates the importance of electrostatic interactions comes from mitochondrial electron transfer cascade.² During this process, the electrons that are transferred from the protein cytochrome c to the enzyme cytochrome oxidase are used to reduce oxygen to water during cellular respiration. For the electrons to jump from one protein to another, the two must form a tight complex. The crystal structure of cytochrome c showed that the molecule contained an unusually high number of positively charged lysine residues. The corresponding binding site for cytochrome c on the cytochrome oxidase consists of a high density of aspartic and glutamic acid residues. Consequently, it is believed that the formation of the tight complex between the two proteins is assisted by a large number of electrostatic interactions formed between the charged amino acid residues (**Figure 1.2.2**).

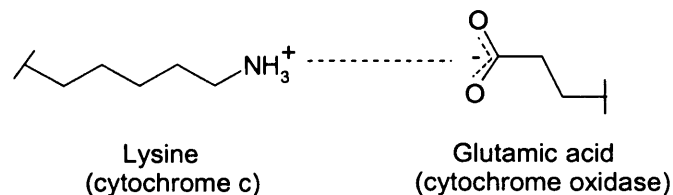


Figure 1.2.2 Representation of electrostatic interactions occurring between cytochrome c and cytochrome oxidase.

The work of Cudd and Fridovich also highlighted the importance of lysine residues within the active site of superoxide dismutase.¹⁰ The enzyme catalyses dismutation of superoxide $\text{O}_2^{\cdot -}$ to O_2 and H_2O_2 . It is evident that there is an interaction between $\text{O}_2^{\cdot -}$ and positively charged lysine residues within the enzyme active site. Following removal of the positive charge of the active site lysines by acetylation, a decrease in enzyme activity was observed indicating the significance of electrostatic interactions for catalytic activity.

Hydrophobic interactions are another major source of binding in enzyme-substrate interactions. When non-polar groups are present in an aqueous environment, the

surrounding water molecules are believed to possess an ordered structure.⁷ When these non-polar structures come together *via* formation of a hydrophobic interaction, the cage like water structures are broken down, resulting in a net gain of freedom and movement. This results in increased entropy and favourable enthalpy changes.⁷ Removal of the hydrophobic surface area from water, by binding into a hydrophobic region within a receptor is worth approximately $0.68 \text{ kcal mol}^{-1}$ (2.85 kJ mol^{-1}) per methyl group.⁴ Although the contribution of hydrophobic effects to substrate binding is considered to be important, it is generally believed that it is a non-specific interaction and that it may not contribute to the specificity of enzyme-substrate binding compared to hydrogen bonding. However, hydrophobic interactions can significantly stabilise substrate binding. For example **Figure 1.2.3** shows two HIV-2 protease inhibitors, both of which have similar affinities for the enzyme, despite the fact that the quinoline amide in **1** has been replaced by the lipophilic dimethylphenoxy substituent in **2**.¹¹ X-ray analysis of **1** revealed hydrogen bonds between the quinoline amide and Asp29' and Gly48'. However, the complex of **2** with the enzyme shows an induced fit to the dimethylphenoxy group through a shift of 1 \AA for Asp29' and 4 \AA for the side chain of Asp30'. The similar activities of **1** and **2** demonstrate that affinity can be maintained through hydrophobic interactions, even at the cost of losing significant hydrogen bonds. This example also illustrates the very important point that enzymes can undergo conformational changes to accommodate substrates ('induced fit') in order to optimise the favourable binding interactions.

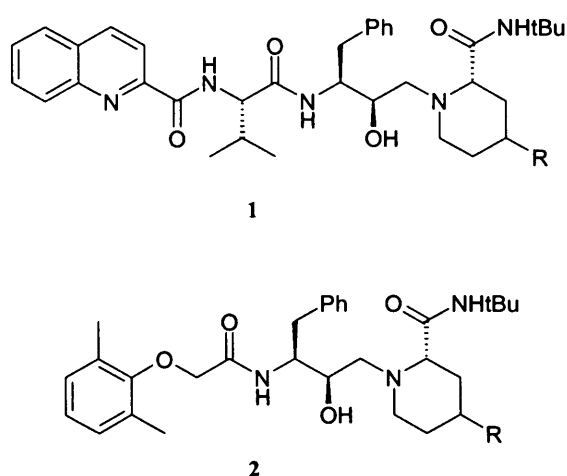


Figure 1.2.3 HIV-2 protease inhibitors.

Van der Waals forces are typically worth about 1 kcal mol⁻¹ in binding stabilisation.² Although this is a very small contribution, when conditions permit a large number of Van der Waals forces to form, they can collectively provide a significant contribution to the stabilising energy to the enzyme-substrate complex.² However, they are often neglected when analysing their contribution to binding equilibria because the Van der Waals interactions between the elements of the first and second row of periodic table are insensitive to the nature of atoms involved. This means that the forces do not change significantly on replacing solvent-substrate contacts with solvent-solvent or enzyme-substrate contacts.⁵

π – Stacking interactions have also been explored as one of the driving forces in molecular recognition. The cation – π interactions formed between the side chains of phenylalanine, tyrosine or tryptophan and the side chains of lysine or arginine have received particular attention, because of their important role in the functioning of potassium channels.¹⁰ Many models have been proposed for potassium channels, and suggest that there are numerous aromatic residues found within the channel pore which seem to be involved in cation – π interactions.^{6;12} As a result of this, it has been proposed that it is the cation – π interactions which are responsible for ion selectivity in potassium channels.⁶

All of the above intermolecular interactions involve binding between a discrete ligand and a binding site. However, the changes in active site interactions on going from ground state to transition state are much more difficult to assess. This is mainly because these bonding interactions are dynamic in nature, as a result of changing charge distribution due to bond formation or cleavage. This binding phenomenon is called ‘dynamic binding’ and it allows us to distinguish between ground state and transition state recognition.¹³ For example, Kirby has illustrated this process in serine proteases, where the initial step of amide cleavage involves an intermediate such as **4** (**Figure 1.2.4**).¹³

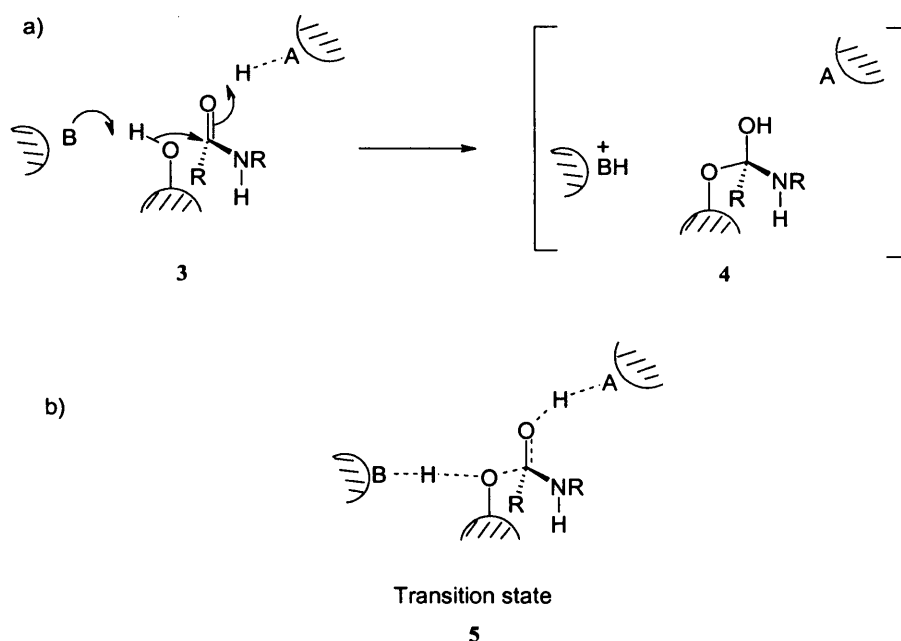


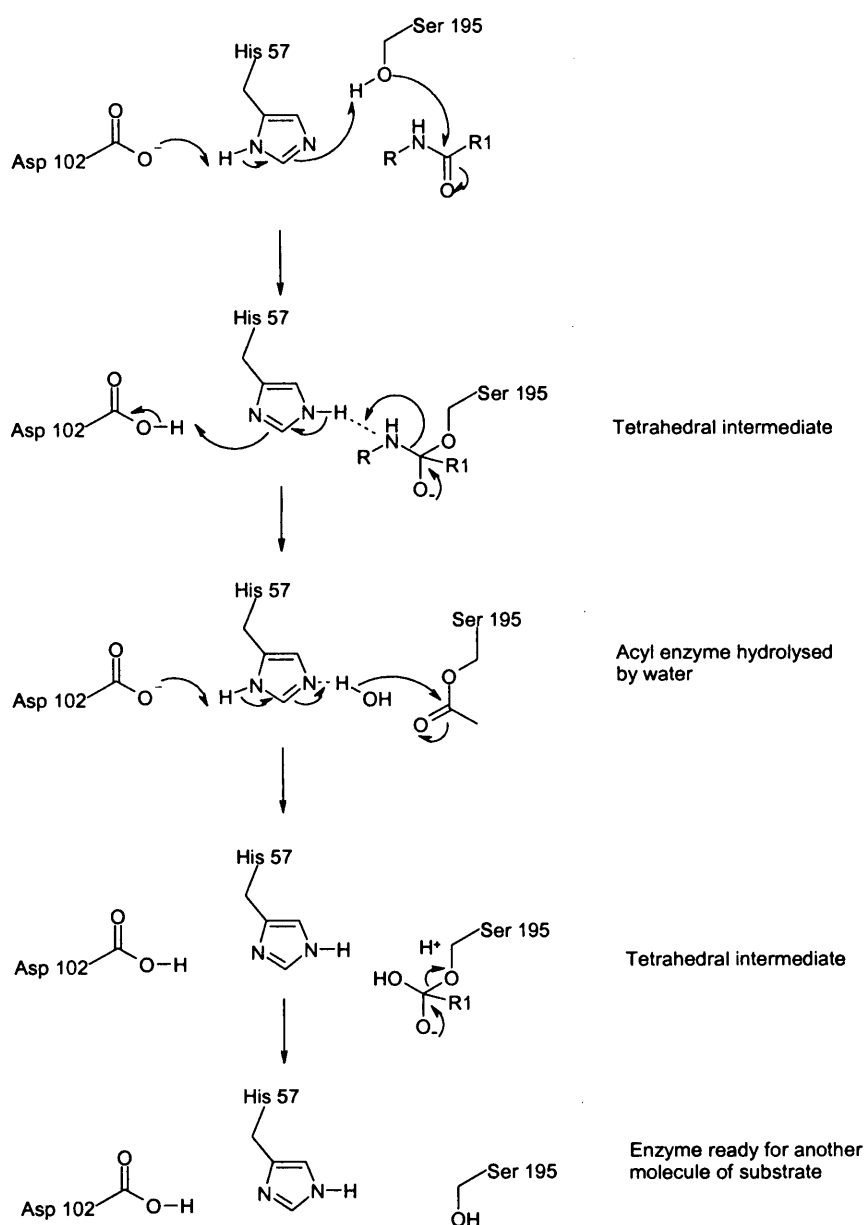
Figure 1.2.4 a) Initial step of amide bond cleavage by serine protease. b) Representation of dynamic binding.

The transition state (5) for this reaction involves at least six bonds being broken or formed. The partially formed covalent bonds at the reaction centre represent ‘dynamic binding’ interactions, which have no corresponding ground state counterpart. Hence, this partial covalent bonding can distinguish between ground state and transition state recognition and makes an important contribution to binding and stabilisation of the transition state in enzyme reactions.

1.2.3 Functional Group Cooperativity

Naturally occurring biomolecules use the cooperativity concept to carry out catalysis or substrate binding and recognition. By way of example, amide bond hydrolysis, catalysed by chymotrypsin, illustrates this concept.¹⁴ The enzyme is involved in the cleavage of amides through a mechanism which involves a catalytic triad of serine, histidine and aspartic acid (**Scheme 1.2.1**).¹⁴ The hydrolysis sequence is initiated by the aspartate-102 side chain polarising the imidazole of histidine-57. This leads to the hydroxyl proton of serine-195 being transferred to histidine, which results in the formation of an alkoxide. Serine-195 then attacks the amide, forming a tetrahedral intermediate with an oxyanionic centre on the carbonyl carbon. This transition state is stabilised by specific hydrogen-bonding interactions between amino acids in the active

site and the oxyanion centre of the substrate. It is believed that the hydrogen bonds are provided by the backbone nitrogens of the nucleophilic serine and a glycine residue found within the active site.² The reaction proceeds with a histidine residue donating a proton to the amino leaving group, which leads to dissociation of the tetrahedral intermediate and formation of the covalent acyl-enzyme intermediate. Subsequent nucleophilic attack by water allows the formation of another tetrahedral transition state, followed by the release of hydrolysed product.



Scheme 1.2.1 Functional group cooperativity in chymotrypsin.

The stereochemical relationship between the groups on the substrate and the binding groups in the enzyme active site is also important for determining the substrate specificity of the enzyme. In chymotrypsin, the substrate binding affinity is partially determined by the hydrogen bonding that forms between β -sheet structures of the residues in the enzyme active site and residues of the substrate. However, in order to actually distinguish one peptide from another, chymotrypsin-like enzymes contain a deep cleft into which part of the substrate must fit (**Figure 1.2.5**).^{2;15} It is the specific amino acid residues within this cleft which influence the nature of the substrate which would be able to bind to the active site. For example, enzymes within the trypsin-like subclass have an aspartate residue within this cleft, which perhaps explains their selectivity for substrates with arginine or lysine residues.¹⁵

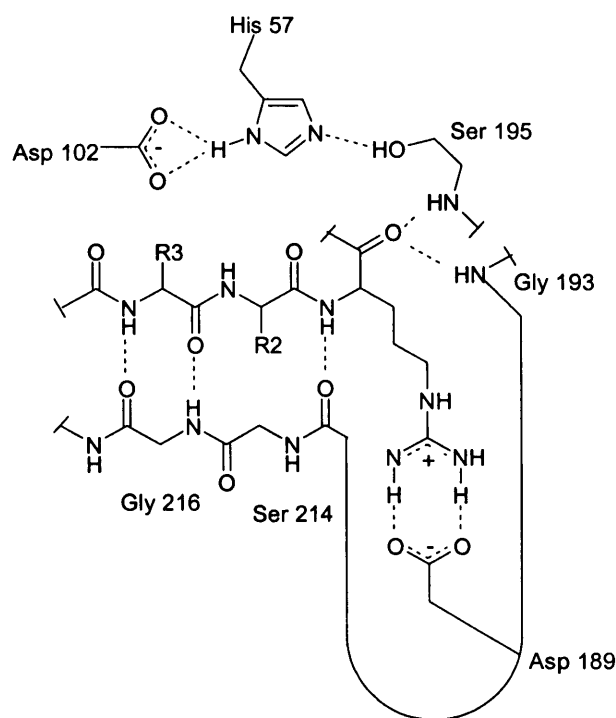


Figure 1.2.5 Representation of the active site of chymotrypsin-like enzymes.

Considering the short overview of chymotrypsin given above and the binding interactions discussed previously, the active site of an enzyme needs to bind the substrate in an appropriate orientation for catalysis, stabilise the transition state of the reaction, and also be able to differentiate between potential substrates. While the

molecular details differ from one enzyme to another, the general interactions illustrated above can broadly be applied to most naturally occurring enzymes.

1.3 Previous Approaches to Artificial Enzymes

The most traditional approach to enzyme mimics has involved rational design, which entails synthesising a macromolecule with appropriately attached functional groups.¹⁶ The functional groups are chosen on the basis of amino acid residues that are found in the natural enzyme active site and are known to participate in the catalysis of a particular reaction. Although the use of this idea has been exemplified in catalytic cyclodextrins^{16;17} and cyclophanes^{18;19} with some impressive results, it can be very time consuming, and in a number of cases, an idea that may give promising results in theory is not always successful in practice because of a tiny design error. As a result, research has moved away from this approach to the selection strategy. The selection strategy involves simultaneous screening of a wide range of possible catalysts for enzyme-like activity, thereby reducing the time required for the identification of potentially useful catalysts.⁷ Furthermore, the introduction of combinatorial chemistry and improved screening techniques has made this approach very attractive.^{20;21} The earliest examples of this approach, use the idea of a transition state analogue (TSA).²² A TSA is a stable molecule that is able to mimic the geometry and charge distribution of the transition state of a reaction. A library of molecules is generated and the best molecule selected solely on the fact that it has the best binding towards the TSA. Such an approach forms the essence of generating catalytic antibodies.^{23;24} The logic behind this is that any macromolecule that is able to bind the TSA, should also be able to bind and stabilise the transition state of that particular reaction. More recently, it was recognised that selection based upon the binding of the TSA alone is not enough to produce enzyme mimics which rival the catalytic efficiency of natural enzymes. Hence, using a combination of different approaches as for example by incorporating a catalytic group into a macromolecule, together with the TSA host selection, has led to some impressive advances in this field.²⁵ Specific examples are discussed in more detail below.

1.3.1 Cyclodextrins as Enzyme Mimics

Cyclodextrins are stable, water-soluble cyclic oligomers of α -D-glucose (**Figure 1.3.1**). The two main features of cyclodextrins are: (i) they consist of a central cavity capable of binding hydrophobic molecules in water; (ii) they allow the possibility of the hydroxyl groups being functionalised around the rim of cyclodextrin. Both of these characteristics have made cyclodextrins very attractive as potential artificial enzymes.¹⁶

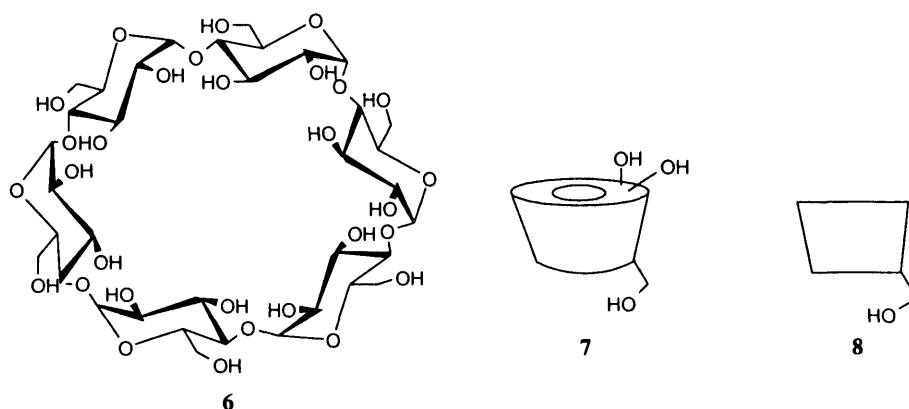
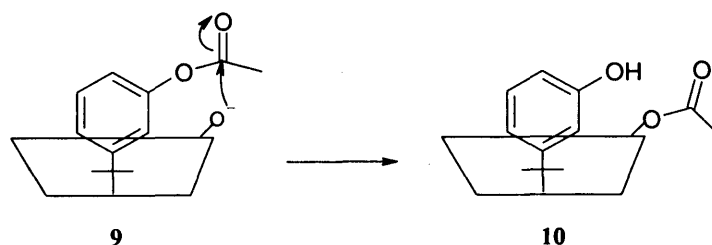


Figure 1.3.1 α -Cyclodextrin **6** which can be represented in a more simplified manner as **7** or **8**.¹⁶

A simple example that demonstrates the catalytic activity of a cyclodextrin is the hydrolysis of esters, such as aryl acetates (**Scheme 1.3.1**).¹⁶ Initially, the substrate binds within the cyclodextrin cavity, *via* a favourable hydrophobic interaction. Hydrolysis can then proceed *via* nucleophilic attack on the carbonyl of the acetate group by a hydroxyl functionality on the cyclodextrin, resulting in the formation of alcohol and acylated cyclodextrin (**10**).¹⁶



Scheme 1.3.1 Hydrolysis of aryl acetate by cyclodextrin.¹⁶

Although significant rate enhancements, up to about 2150-fold were observed with the system described above, several problems were revealed. Firstly, the hydrophobic phenol product was usually bound so tightly within the cavity, that product inhibition was often observed. Secondly, the nucleophilic mechanism proceeded *via* an acylated cyclodextrin intermediate, where the rate determining step of the reaction was the hydrolysis of this resultant cyclodextrin intermediate. In many cases, this intermediate was therefore found to be less reactive towards hydrolysis than the original substrate.

To increase the reactivity of cyclodextrins, functionalisation of cyclodextrin rings with groups which are more reactive at pH 7 than a hydroxyl has been undertaken.¹⁷ Breslow and co-workers were inspired by ribonuclease A, to synthesise three different isomers of cyclodextrin bis-imidazoles as shown in **Figure 1.3.2**.¹⁷ Ribonuclease A is an enzyme which cleaves ribonucleic acid (RNA) using two histidine residues found within its active site, following a general acid-base catalysis mechanism.

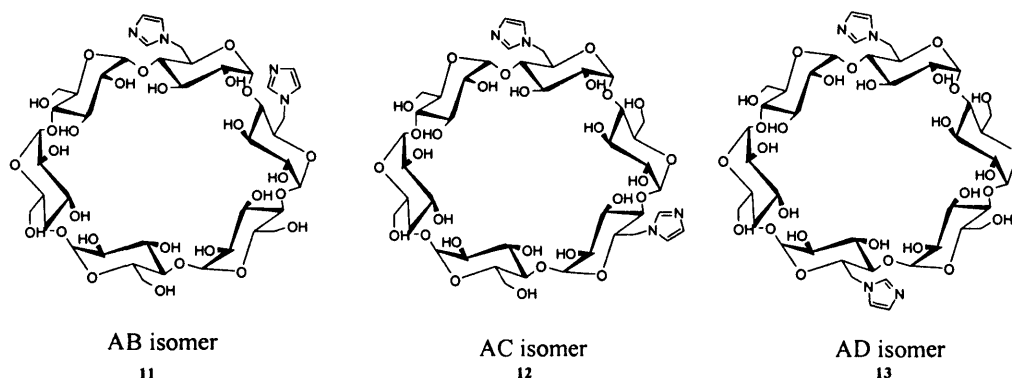
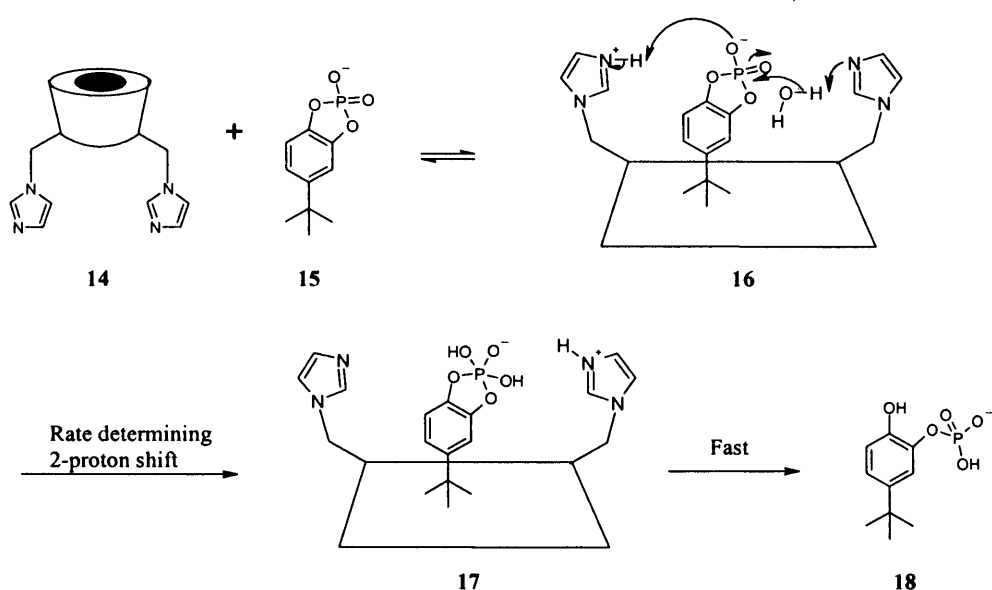


Figure 1.3.2 AB, AC and AD isomers of cyclodextrin bis-imidazoles.

The mechanism of the hydrolysis of a cyclic phosphodiester is shown in **Scheme 1.3.2**.²⁶ The proposed mechanism suggests that both imidazoles are involved in hydrolysis. This has been confirmed from a pH rate profile of this reaction.²⁶ Additionally, it was discovered that the AB isomer was the most efficient cyclodextrin at carrying out the hydrolysis and further investigations into the mechanism reveal an explanation for this. By using proton inventory (a technique that determines whether acid and base groups act simultaneously), it was discovered that the transition state involves two protons.²⁶ The mechanism proceeds by stabilisation of phosphate oxyanion *via* a hydrogen bond to ImH⁺ of 14. Water, hydrogen bonded to the remaining Im, then

attacks the phosphorus atom. As the O-P bond forms, the ImH⁺ proton transfers along with the water proton to produce a phosphorane monoanion. This then proceeds to give the product of the reaction. Hence, the AB isomer (**11**) must have the two imidazoles placed in a more favourable position for more efficient hydrolysis to occur. This example highlights the importance of the geometric and electronic preferences of functional groups in the artificial enzyme. Additionally, the functional groups have displayed cooperativity which is a property observed in many enzyme active sites.



Scheme 1.3.2 Mechanism of hydrolysis of cyclic phosphodiester by cyclodextrin bis imidazole.²⁶

In order to create artificial enzymes that could bind substrates in aqueous solution, with defined geometry, cyclodextrin dimers have been investigated.²⁷ Most cyclodextrins that bind substrates in water have a binding constant of *ca.* 10^4 M^{-1} .²⁷ Breslow,^{27,28} and Tabushi,²⁹ conjugated two cyclodextrin rings using a variety of linkers. These dimers demonstrated improved binding. For example, dimer **19** (**Figure 1.3.3**), was found to bind its cyclopropene substrate **20**, with a binding constant of 10^8 M^{-1} .²⁷

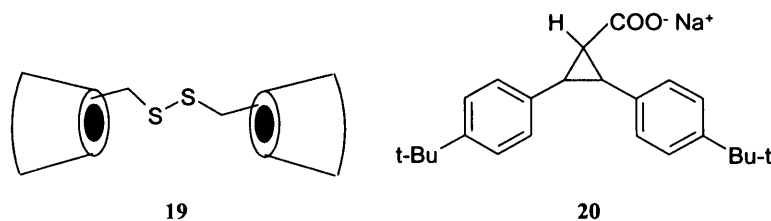


Figure 1.3.3 Cyclodextrin dimer and its cyclopropene substrate.²⁷

The group used these findings and incorporated a catalytic group within the linker of the system. The resulting dimer **21** consisted of a copper (II) complex, which was used to investigate the hydrolysis of the unactivated benzyl ester **22** (**Figure 1.3.4**).³⁰ The reaction mechanism was reported to proceed with the ester **22** binding both of its ends into the cyclodextrin rings of **21**. This is followed by the metal ion delivering a water molecule as a bound hydroxide species, attacking the ester group. This behaviour is similar to that exhibited by many metalloenzymes.³⁰

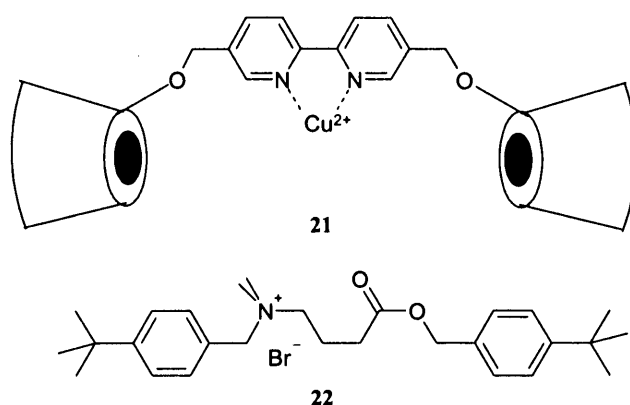


Figure 1.3.4 Cyclodextrin dimer with an incorporated copper (II) and its benzyl ester substrate.³⁰

The field of cyclodextrins has also been extended to incorporate trimers and tetramers of cyclodextrins, with different transition metals. A famous example is the cytochrome P450 mimic which is illustrated in Section 1.3.2.³¹

1.3.2 Cyclophanes as Enzyme Mimics

Pyruvate oxidase is a flavin adenine dinucleotide (FAD) and thiamine diphosphate (ThDP) **23** dependent enzyme found in lactobacteria (**Figure 1.3.5**).^{32;33} The enzyme catalyses the reaction cascade from pyruvate **26** to acetyl phosphate **29** (**Scheme 1.3.3**, pathway I). The thiazolium group of ThDP forms an activated enol (**27**) which is oxidised by the flavin co-factor (**24**) to give an electrophilic intermediate **28**. This is then attacked by the inorganic phosphate nucleophile to give the product **29** and regenerate the thiazolium ylide (**25**). In a similar way, aldehydes are oxidised by either water or alcohols to carboxylic acids or esters respectively by thiazolium ions in the presence of flavin (**Scheme 1.3.3**, pathway II).

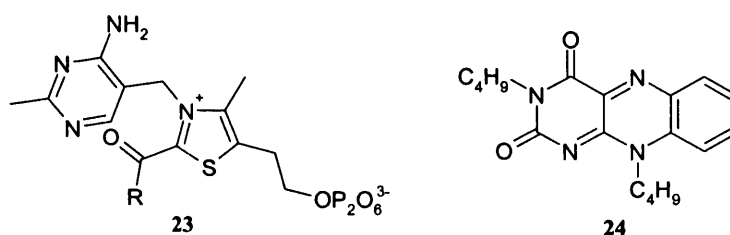
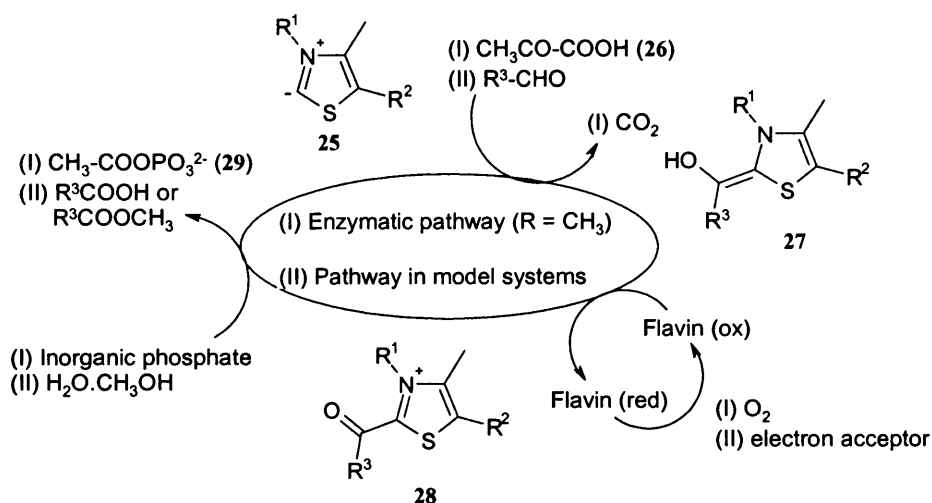


Figure 1.3.5 Thiamine diphosphate **23** and flavin **24**.



Scheme 1.3.3 The reaction cascade from pyruvate to acetyl phosphate, catalysed by pyruvate oxidase. (I) Enzymatic pathway. (II) Pathway in model systems.

Pyruvate oxidase mimics have been synthesised by Diederich, who reported the catalytic use of cyclophane **30** (Figure 1.3.6).^{18;19} This model of pyruvate oxidase is advantageous because it combines a binding site for aromatic substrates together with both the flavin and thiazolium prosthetic groups covalently bound. The substrate was expected to be bound within the cavity, hence the close proximity of the flavin and thiazolium moieties to the binding site was expected to lead to an improvement in catalysis. The enzyme mimic **30** was found to catalyse the oxidation of 2-naphthaldehyde **31** in the presence of triethylamine, with a k_{cat} of 0.22 s^{-1} (Scheme 1.3.4). In order for the system to exhibit true catalysis, the flavin was reoxidised *in situ* by regeneration at a working electrode potential of -0.3 V vs Ag/AgCl. Under these conditions, the cyclophane had a catalytic turnover of up to 100 cycles.

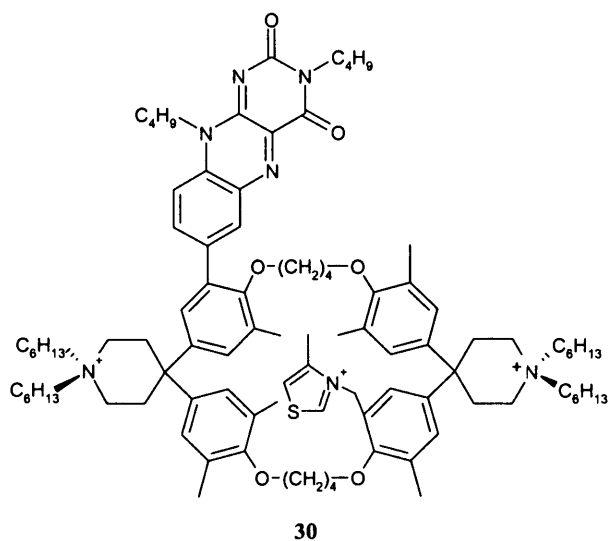
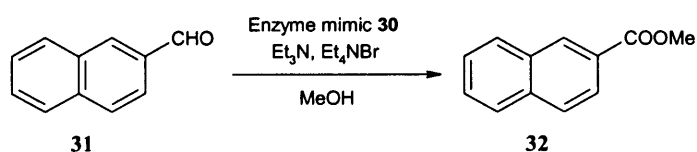


Figure 1.3.6 Pyruvate oxidase mimic.



Scheme 1.3.4 The transformation of naphthalene-2-carbaldehyde to methyl naphthalene-2-carboxylate catalysed by pyruvate oxidase mimic.

Cyclophanes have also been used in other enzyme mimics. For example, Breslow and co-workers described the construction of a cytochrome P-450 mimic **34**, in which a manganese-porphyrin unit is linked to 4 hydrophobic cyclophane binding groups (**Figure 1.3.7**).³⁴ Catalyst **34** was utilised to catalyse the hydroxylation of steroid **33**, with approximately 70 turnovers. It was observed that 60% of the hydroxylation occurs at C-9, while 40% occurs at various other positions.

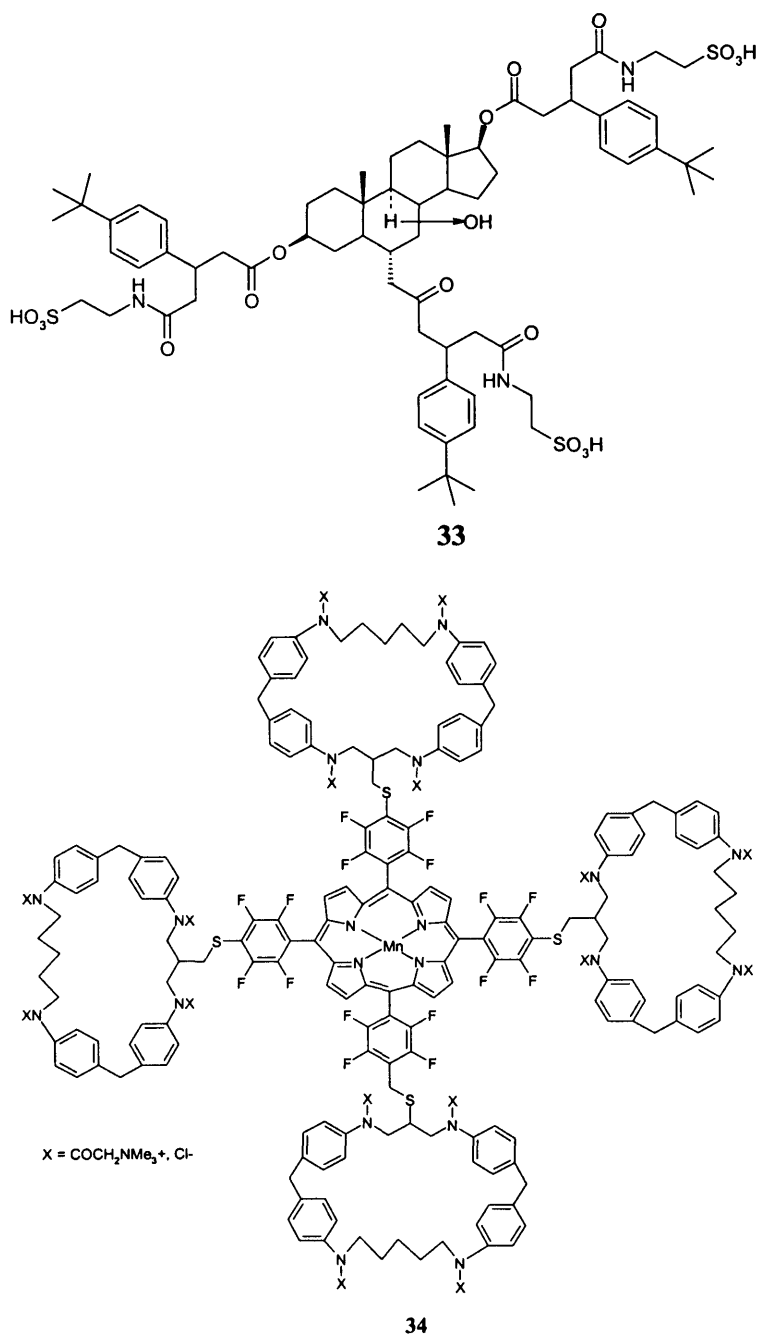


Figure 1.3.7 Steroid **33** and cyclophane cytochrome P-450 mimic **34**.

As a comparison, **35** a catalyst similar to **34** (**Figure 1.3.8**), using cyclodextrins instead of cyclophanes as binding groups was also prepared for the same steroid substrate in **Figure 1.3.8**.³⁴ This catalyst displayed selective hydroxylation at C-9, with 70 turnovers.³⁴ The poorer selectivity of the cyclophane based catalyst does not necessarily make it less useful, but it does provide important information about the behaviour of these types of catalysts and their substrates. The geometry established by substrate **33** when bound to the cyclophane catalyst **34** is thought to be too flexible. This allows the oxidising Mn=O moiety to reach more than one site within the substrate where oxidation is possible. This highlights that simple binding of the substrate to the catalyst itself is insufficient to achieve regiospecific hydroxylation and just as with natural enzymes, a unique geometry is required.

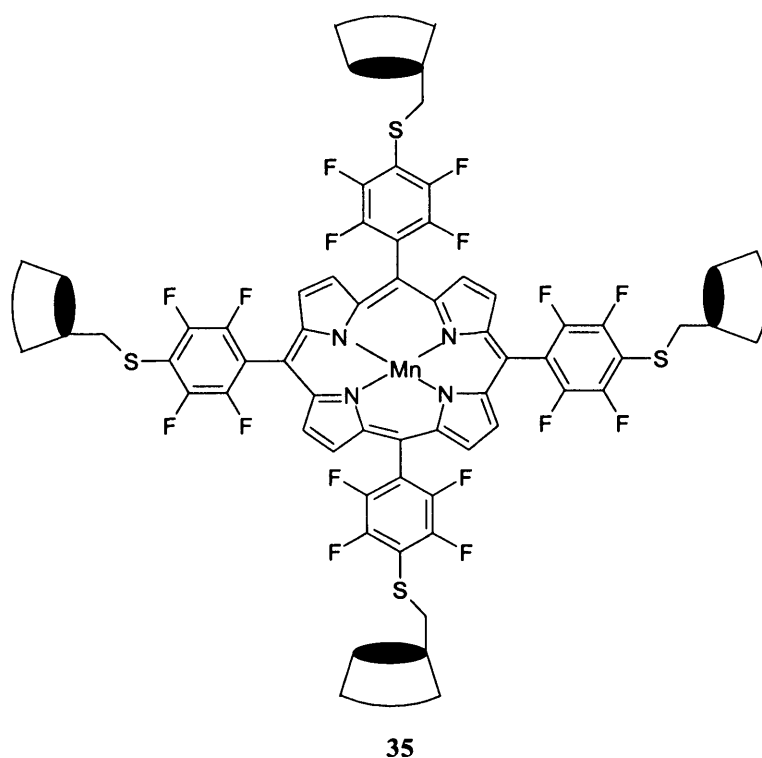
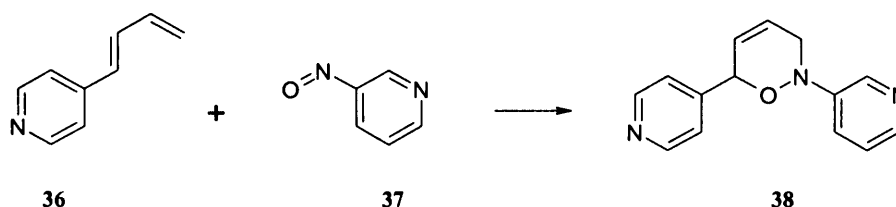


Figure 1.3.8 Cyclodextrin cytochrome P-450 mimic.

1.3.3 Cyclic Metalloporphyrin Oligomers

Whilst a lot of studies have looked at cyclodextrins as a backbone for artificial enzymes, other types of macromolecules have also been explored. One of the problems faced with cyclodextrins is that the hydrophobic cavity always remains a fixed dimension and hence it can only accommodate substrates of a certain size. Sanders' group have extensively investigated cyclic metalloporphyrins which possess hydrophobic cavities that have flexibility (**Figure 1.3.9**).³⁵⁻³⁸ The research has focused on the design of metalloporphyrin catalysts for a regiospecific Diels-Alder reaction between 4-pyridyl butadiene (**36**) and 3-nitroso pyridine (**37**) to give the oxazine **38** (**Scheme 1.3.5**).^{37;38}



Scheme 1.3.5 Regiospecific Diels-Alder reaction between 4-pyridyl butadiene and 3-nitroso pyridine.

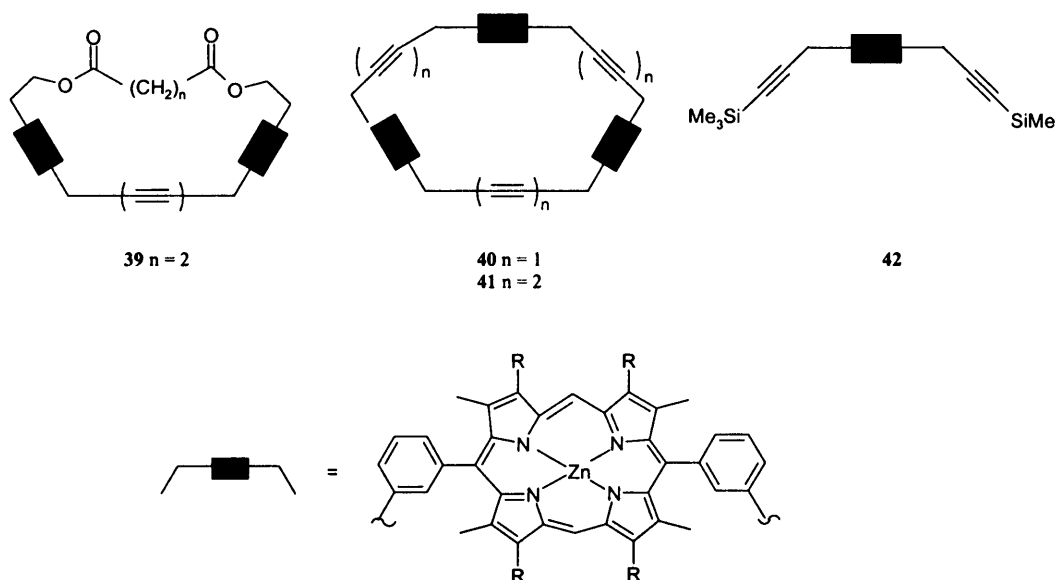


Figure 1.3.9 Metalloporphyrin oligomers.³⁸

Initially, catalyst **39** was tested, and found to accelerate the reaction 65-fold (**Figure 1.3.9**).³⁸ The x-ray structure of the host-product complex **39.38** revealed that when the

product was bound within the cavity, it induced structural changes in **39**. The two porphyrin units were pushed apart, increasing the Zn-Zn distance across the acetylene linkage from 10.6 Å (**39** alone) to 13.5 Å (once the **39.38** complex has formed). The estimated distance of the transition state complex was ~13.5 Å, which meant that catalyst **39** was able to distort enough to accommodate the complex. Much better rate acceleration was exhibited by **40** (approximately 1030-fold) where the Zn-Zn distance was measured to be 14 Å of the catalyst alone. Further studies with catalyst **41**, which has a Zn-Zn distance of 16 Å (much longer than that expected in the transition state complex), established that it was less effective than catalyst **40** at accelerating the Diels-Alder reaction (only ~250-fold). This is perhaps not surprising since the substrates are not spending enough time in productive orientations, making cycloaddition unfavourable. Additionally, when the reaction was attempted with catalyst **42**, a minimal 2-fold rate acceleration was observed, suggesting that only the cyclic catalysts which can hold the reactants at close proximity within the cavity can increase the rate of reaction. This example illustrates the importance of flexibility of the enzyme mimic, as this allows it to respond to changing geometrical demands of the reactants and transition state, which is a key factor in controlling the reaction rate and regioselectivity.

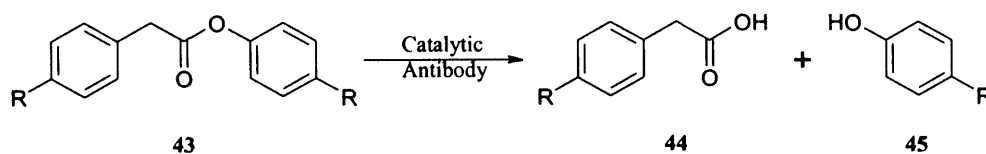
1.3.4 Catalytic Antibodies

Antibodies are proteins belonging to the immunoglobulin family, that are generated by the immune system as a response to foreign species (antigens) that have entered the bloodstream.¹ The first examples of truly catalytic antibodies have been simultaneously identified by Lerner²³ and Schultz²⁴ in the mid 1980s.

Early work on catalytic antibodies focused on the TSA approach. The idea, originally described by Jencks proposed that if a molecule carrying chemical information about a reaction mechanism (TSA) was used to induce an immune response, this would then increase the probability of identifying antibodies with catalytic properties for that particular reaction.²² Antibodies that evolve to bind such a compound tightly, should also be able to stabilise the transition state of that reaction and hence speed up the conversion to the product. This methodology, has now been well established and involves attachment of a TSA to a carrier protein (this complex is then termed a hapten),

which is then introduced into the bloodstream of a mouse. Once the immune response has occurred, the desired monoclonal antibody can then be selected from the isolated polyclonal population on the basis of its binding activity towards the TSA.²³

An example of this approach was demonstrated by Lerner through his early work on the hydrolysis of ester **43** (**Scheme 1.3.6**).²³ Ester hydrolysis proceeds through a tetrahedral intermediate, which was mimicked by a phosphonate TSA **46** (**Figure 1.3.10**). The monoclonal antibody that was isolated in the presence of TSA **46** was tested in the hydrolysis reaction. The catalyst showed approximately 960-fold acceleration in the rate of hydrolysis.



Scheme 1.3.6 Hydrolysis of ester by catalytic antibody.

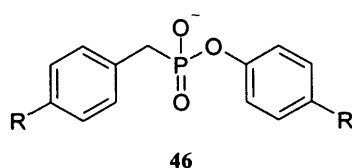
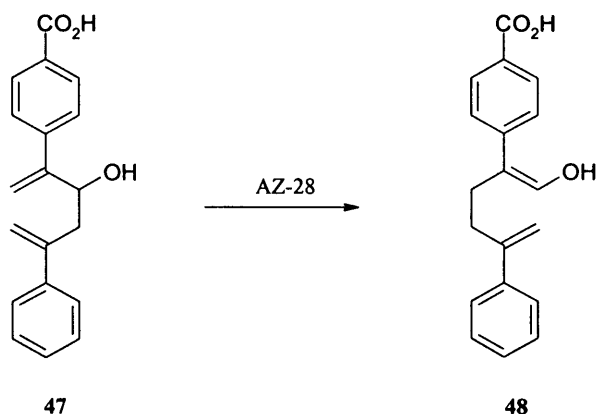


Figure 1.3.10 Phosphonate transition state analogue for ester hydrolysis.

Catalytic antibodies have also been utilised in the oxy-Cope rearrangement (**Scheme 1.3.7**).³⁹ The [3, 3] sigmatropic shift occurs *via* a chair-like transition state,³⁹ hence TSA **49** was designed to mimic the transition state (**Figure 1.3.11**).⁴⁰ Antibody AZ-28 was raised against TSA **49** and was found to catalyse the oxy-Cope rearrangement of **47** to **48**.⁴⁰



Scheme 1.3.7 Oxy-Cope rearrangement catalysed by antibody AZ-28.

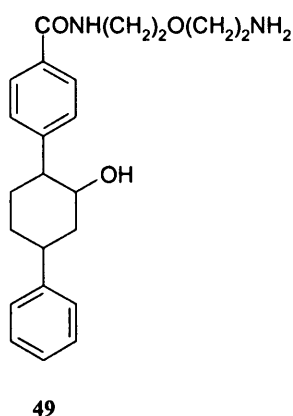


Figure 1.3.11 Transition state analogue for oxy-Cope rearrangement.

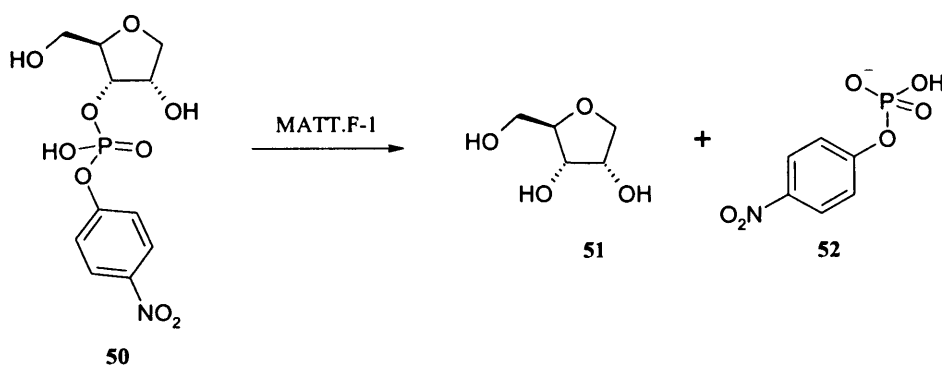
Using the TSA approach, a large number of other reactions have been catalysed including Diels-Alder reactions,⁴¹ cyclopropanations,⁴² elimination reactions,^{43;44} and cationic cyclisations.⁴⁴

Although this approach has yielded promising results, with rate enhancements in most cases, there are a few problems associated with it. During the immune response, it is the affinity of the antibody towards the TSA rather than catalytic activity that drives the maturation of the immune response. Therefore although the antibody may be good at binding the TSA, it may not possess useful catalytic activity. The second major drawback is the inaccurate design of the TSA itself. The transition state of a particular reaction can share recognition elements with ground state molecules, hence it is very difficult to design an accurate TSA with the precise geometry and charge distribution of

a transition state. This problem is illustrated by the fact that the transition state of a reaction is not a discrete entity and in many cases, there are multiple transition states to consider.

1.3.4.1 The 'Bait-and-Switch' Approach

As a result of the above problems, chemists have explored other strategies to design catalytic antibodies. The 'bait-and-switch' approach involves designing a TSA with a point charge, which mimics a chemical functional group that is expected to transform a corresponding substrate.⁴⁵ The charge on the hapten is expected to induce a complementary charge at the active site of the antibody. The resulting charged amino acid residues that are recruited usually tend to catalyse the reaction *via* a general acid/base or nucleophilic mechanism. An example of this approach can be seen in the phosphodiester hydrolysis reaction (**Scheme 1.3.8**).⁴⁵ The TSA **53** (**Figure 1.3.12**) was designed in the hope that during an immune response, a general base will be incorporated within the antibody active site. The base should be in proximity to the 2' hydroxyl group of substrate **50** and should therefore facilitate nucleophilic attack of this hydroxyl on the adjacent phosphorus centre. Antibody MATT.F-1 was found to catalyse the phosphodiester hydrolysis with a proficiency three orders of magnitude lower than that of the naturally occurring enzyme RNase A for the same substrate.⁴⁵



Scheme 1.3.8 Phosphodiester hydrolysis catalysed by antibody MATT.F-1.

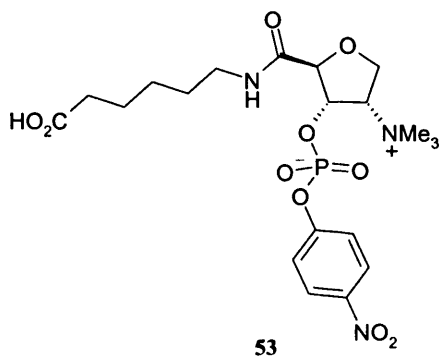
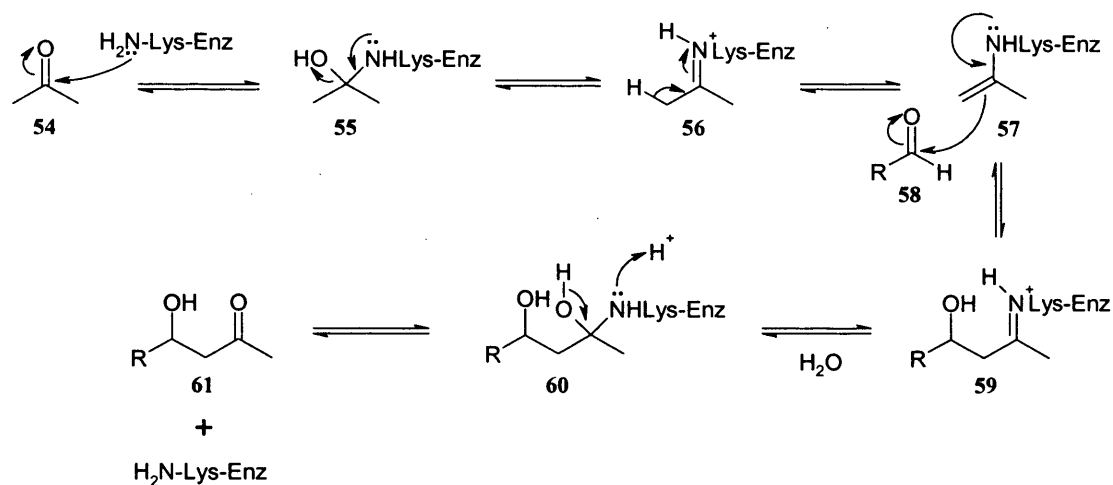


Figure 1.3.12 Transition state analogue for phosphodiester hydrolysis.

1.3.4.2 The Reactive Immunisation Approach

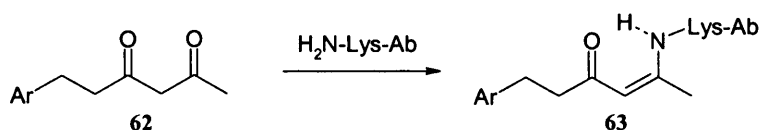
Both the TSA and the bait-and-switch approaches rely on chemically inert antigens. Reactive immunisation is a different approach, pioneered by Lerner and co-workers in 1995, which relies upon a highly reactive antigen to react covalently with a specific functionality within the antibody binding site during immunisation.⁴⁶ This allows direct selection of active antibodies from a large pool of inactive ones. The success of this strategy has been exemplified by a number of versatile aldolase catalysts that have been created.

The mechanism of natural aldolases is shown in **Scheme 1.3.9**. A lysine residue in the enzyme active site forms a covalently bound intermediate with the substrate, which proceeds to form an imine, which then tautomerises to give an enamine **57**. The enamine **57** can then react with another equivalent of the carbonyl substrate to give Schiff base **59**. After hydrolysis with water the aldol product **61** is generated.²⁵



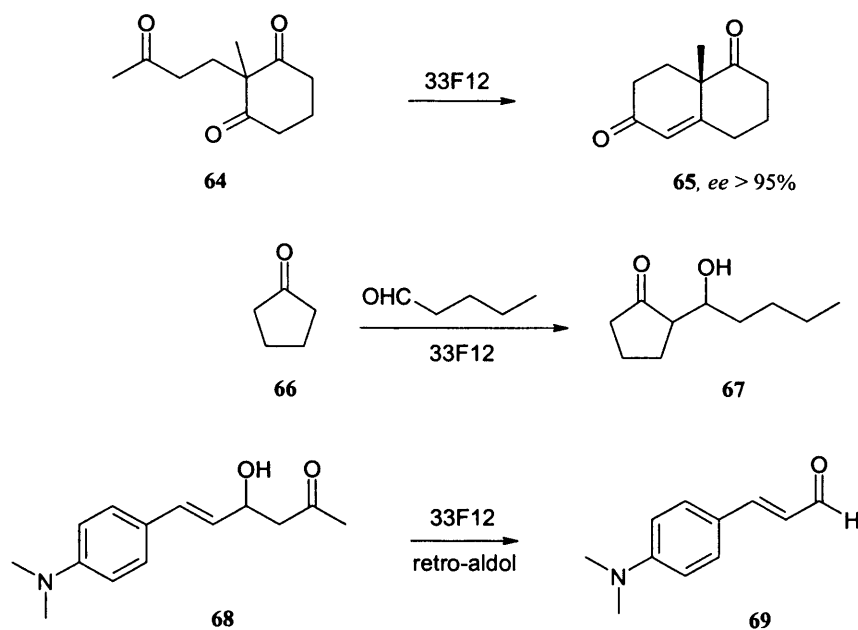
Scheme 1.3.9 Mechanism of aldol reaction within active site of natural aldolases.

By creating an immunogenic 1, 3-diketone **62**, Lerner reasoned that this should be able to trap reactive lysines within the antibody's active site, *via* Schiff base formation and subsequent rearrangement to a more stable vinylogous amide **63** (**Scheme 1.3.10**).²⁵ The resulting vinylogous amide **63** has a strong ultraviolet (UV) absorption at 316 nm, which is outside the range of the protein. Hence, once the library of antibodies raised against the diketone has been generated, the most successful candidates can be simply identified on the basis of their ability to absorb in that UV region.



Scheme 1.3.10 Transformation of a 1, 3-diketone to a vinylogous amide.

Antibody 33F12 was isolated and shown to have the ability to catalyse over 100 aldehyde-aldehyde, aldehyde-ketone and ketone-ketone reactions, with very high selectivity.^{25;47} A few of these examples are shown in **Scheme 1.3.11**.



Scheme 1.3.11 Examples of aldol reactions catalysed by antibody 33F12.

When compared to their natural enzyme counterparts, these antibodies accept a wider range of substrates, with a catalytic turnover approximately within 10 times that of the natural aldolase.²⁵ The mechanism of action was shown to be the same as for the natural aldolase. X-ray crystal structure of the antibody 33F12 revealed that the nucleophilic lysine residue, which should usually be protonated at physiological pH, is contained within a hydrophobic pocket, which disfavours protonation.²⁵ This suggests that the pKa of the ϵ -amino group of lysine is lowered, which may explain its enhanced nucleophilicity.²⁵

Although reactive immunisation does not appear to have solved the problem of creating an active site with multiple catalytic residues, it has the advantage of selecting antibodies on the basis of their ability to initiate a chemical reaction as opposed to binding to a TSA.

1.3.4.3 Cofactor Dependent Antibodies

Metal coordinated enzymes are very common in nature, and the metallic species within the active site plays an important role in the reaction pathway by enhancing substrate selectivity and accelerating reaction rates. Nicholas *et al.* have modified the antibody

38C2 by incorporating a copper bis-imidazole cofactor within its active site.⁴⁸ In the absence of the co-factor, antibody 38C2 catalyses an aldol reaction, but after addition of the copper complex, the properties of this antibody are altered, resulting in the antibody now being able to catalyse ester hydrolysis.⁴⁸ During the immune response, it was found that the lysine residue within the 38C2 active site undergoes covalent bond formation with the succinic anhydride moiety of **70** (**Figure 1.3.13**) (which was previously pre-coordinated with CuCl_2), forming a 38C2-**70**- CuCl_2 complex. This metalloantibody was then used to catalyse the hydrolysis of ester **71** (**Scheme 1.3.12**). The study demonstrated how the introduction of a metal-coordinated ligand can completely alter the nature and the catalytic activity of the parent antibody.

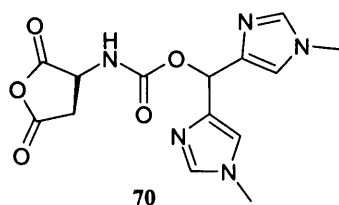
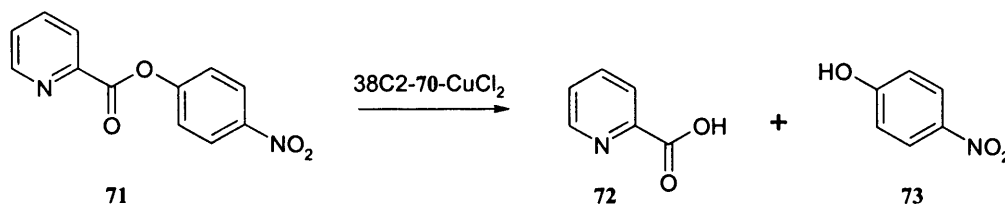


Figure 1.3.13 Molecule **70** containing the succinic anhydride moiety, which is coordinated to CuCl_2 prior to forming a complex with antibody 38C2.



Scheme 1.3.12 Ester hydrolysis catalysed by 38C2-**70**- CuCl_2 complex.

1.3.4.4 Summary

As the foregoing discussion has hopefully indicated, catalytic antibody technology can be a very powerful approach for creating new catalysts and some impressive advances have been made in this field. It has been demonstrated that it is possible to carry out transformations with good catalytic rates and turnover numbers, producing products with high yields with good selectivity. Reactions that were difficult to carry out with

previous methodologies have been successfully performed with catalytic antibodies. Despite these advances, there are still many problems remaining with this technology and the production of truly efficient enzyme mimics has proven to be very difficult. The requirement for the use of mice to generate catalytic antibodies is undesirable and new methods such as phage display⁴⁹ and ribosome display⁵⁰ that are able to create protein libraries, may provide an alternative to the immunisation techniques used thus far. The isolation of monoclonal antibodies and screening for the best catalyst can be a very time consuming process, although the advances in technology have made the screening protocol slightly easier.^{20;21;51} Finally, improvements in the design of transition state analogues may allow the isolation of antibodies whose properties rival those of natural enzymes.

1.3.5 Molecularly Imprinted Polymers

Molecular imprinting is a technique which involves a cross-linked polymer being assembled around a template. If the template is a TSA, then the resulting polymer should behave as an artificial enzyme for the chosen reaction.⁵² The general molecular imprinting process is outlined in **Figure 1.3.14**. Firstly, the template is mixed with monomers that contain functional groups which can interact with it, to form the template-monomer complex. The template-monomer complex can be formed by covalent or non-covalent associations. A mixture of standard monomer and cross-linker is then co-polymerised around the template monomer complex forming a macroporous polymer. This contains sites on which the template molecule is bound. Finally, the template molecule is removed to leave the imprinted polymer with well defined, shape specific cavities, which are complementary in shape to the template.⁵²

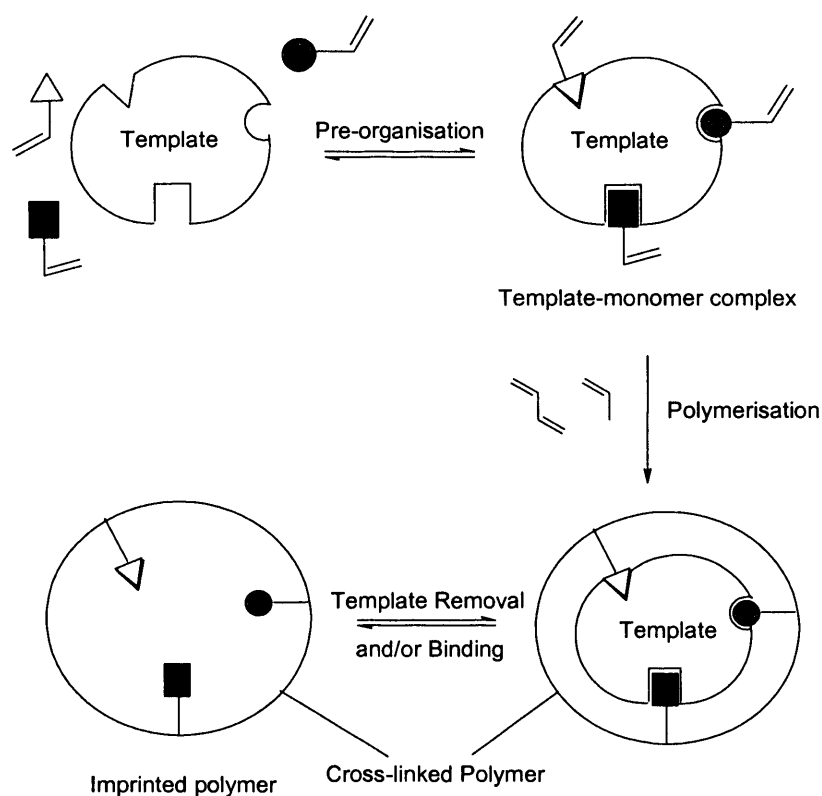
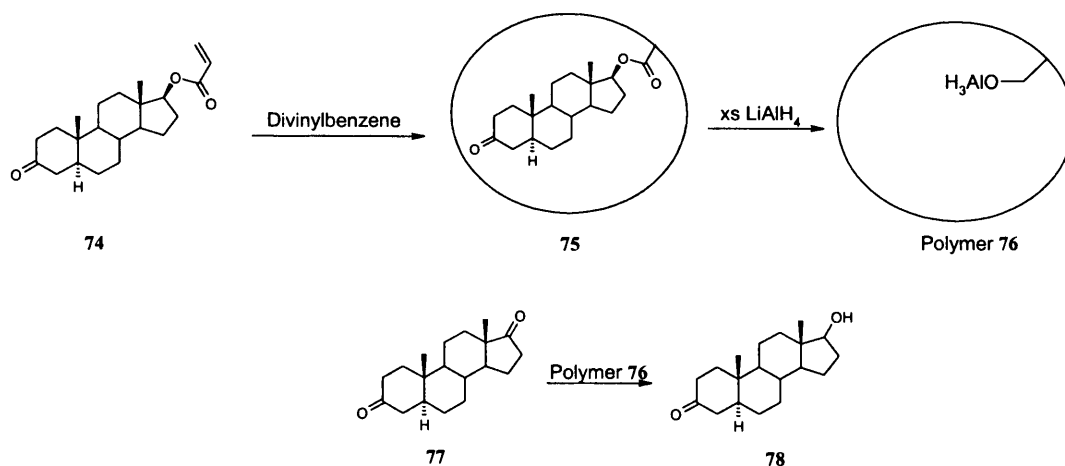


Figure 1.3.14 The general molecular imprinting process.⁵²

A good example of the use of imprinted polymer sites was demonstrated by Bystrom and co-workers.⁵³ Polymer beads were imprinted with a sterol acrylate ester **74** template (**Scheme 1.3.13**). The template was then removed by the reduction of the ester linkage, followed by reaction of the hydroxyl group in the vacant sites with excess lithium aluminium hydride. The hydride functionality was thus positioned at a specific position within the cavity. Polymer **76**, containing reducing agents, was then used to selectively reduce the ketone of androstan-3, 17-dione **77** at position C-17 only.⁵³



Scheme 1.3.13 Imprinting a polymer with sterol acrylate and ketone reduction with polymer catalyst **76**.

Under conventional conditions, in the absence of the polymer, there was a complete regiochemical preference for reduction at the less hindered C-3 carbonyl group, whereas in the geometrically defined environment of the polymer **76**, only the C-17 ketone is allowed access to the reducing agent. Furthermore, some stereochemical control was also observed with the final product containing a mixture of $17\alpha\text{-OH}$ and $17\beta\text{-OH}$ (30:70).

Another elegant use of molecularly imprinted polymers (MIPs) originates from Wulff and co-workers, who mimicked the activity of carboxypeptidase A.⁵⁴ The active site of carboxypeptidase A consists of two guanidinium groups of arginine and a Zn^{2+} ion bound to His 69, Glu 72 and His 196. During the reaction, the oxyanion generated in the rate limiting step involving the breakdown of the tetrahedral transition state is stabilised by Arg 127, which is followed by zinc, which undertakes the catalytic role in the hydrolysis step.⁵⁵ Substrate specificity is increased through the presence of a hydrophobic pocket in the active site and binding of the substrate to another guanidinium of Arg 145. The system Wulff designed contained an amidinium group, in addition to the triamine **79** (**Figure 1.3.15**) would act as co-ordination site for the Zn^{2+} ion (**Scheme 1.3.14**).⁵⁴ The rationale was that the amidinium group should stabilise the transition state of the reaction as well as polarise the carbonyl moiety of the substrate, making it more susceptible to nucleophiles. The TSA **80** (**Figure 1.3.15**) was used as a tetrahedral transition state mimic of carbonate hydrolysis, capable of being stabilised by

both guanidinium and zinc moieties. Using **80** as an imprint molecule, the activity of the resulting MIP was then investigated in the hydrolysis of diphenylcarbonate (**81**). The catalyst displayed a 3200-fold rate acceleration and it also exhibited typical Michaelis-Menten kinetics.⁵⁴ The ratio $k_{\text{cat}}/k_{\text{uncat}}$ is used to express the catalytic activity of enzymes and antibodies. By using k_{soln} as k_{uncat} for the MIP, it was calculated that the ratio $k_{\text{cat}}/k_{\text{soln}}$ had the value of 6900.⁵⁴ This value is remarkably higher than the one which has been reported for carbonate hydrolysis by catalytic antibodies ($k_{\text{cat}}/k_{\text{uncat}} = 810$).⁵⁶

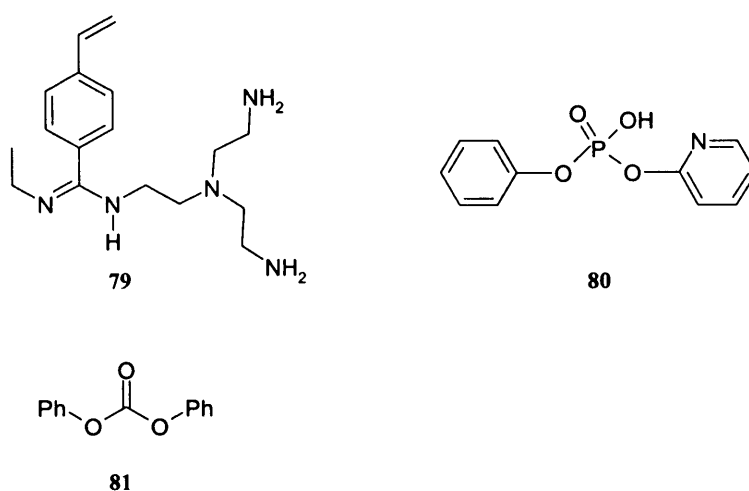
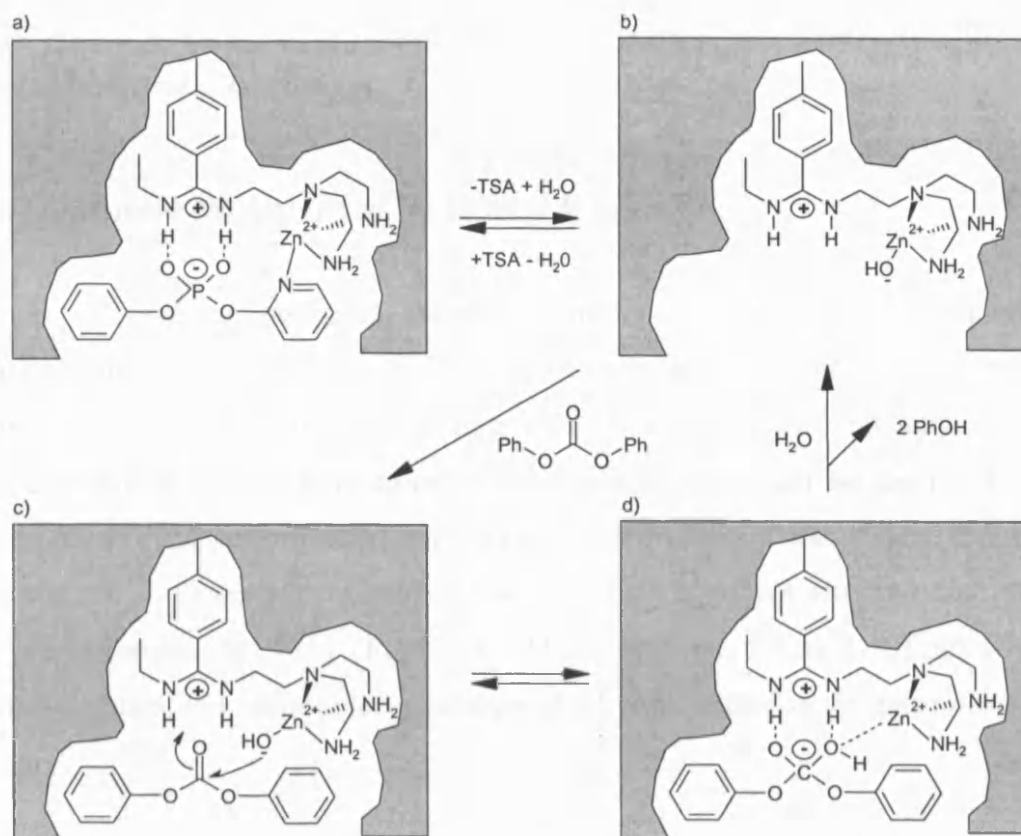


Figure 1.3.15 Triamine **79**, phosphonate transition state analogue **80** and diphenylcarbonate **81**.



Scheme 1.3.14 Schematic representation of a) the molecular imprinting with TSA **80** and monomer **79** in the presence of Zn^{2+} ; b) removal of the template; c) and d) catalysis step.⁵⁴

The utilisation of molecular imprinting has also been reported for Diels-Alder reactions,⁵⁷ ester hydrolysis^{58;59} and isomerisation reactions⁶⁰ as well as in protecting group strategies.⁶¹ MIPs are generally stable to harsh conditions such as extreme pH and temperature and although these characteristics can be used to advantage, their scope remains limited. This may partially be due to the problems associated with the formation of the template-monomer complex. As previously mentioned, covalent and non-covalent interactions are involved in the formation of the template-monomer complex. In the non-covalent case, the combination of weak intermolecular forces leads to the pre-organisation step being a dynamic equilibrium, with the free and complex forms in a constant exchange. As a result, the molecular recognition sites formed within the polymer become heterogeneous, which can lead to problems in the catalytic applications of these polymers. One of the most important factors in enzyme catalysis is that an enzyme can change its conformation in order to accommodate the substrate into

its active site. MIPs often have very rigid structures, which means that they cannot undergo conformational changes.

1.3.6 Synthetic Polymers as Artificial Enzymes

The use of synthetic polymers as enzyme mimics has always been an attractive approach, due to their compatibility with organic solvents and stability to higher temperatures. Synthetic polymers can form a backbone to the artificial enzyme allowing the attachment of various binding or catalytic groups which can aid the recognition of substrates and even perform catalysis. As early as the 1960s, it was noticed that flexible, water soluble polymers with suitable side chains, such as poly(4-vinylpyridine) (**82**) and poly(*N*-vinylimidazole) (**83**) (**Figure 1.3.16**), displayed different affinities towards small molecules and were able to catalyse the hydrolysis of *ortho* nitrophenyl esters **84**.⁶²

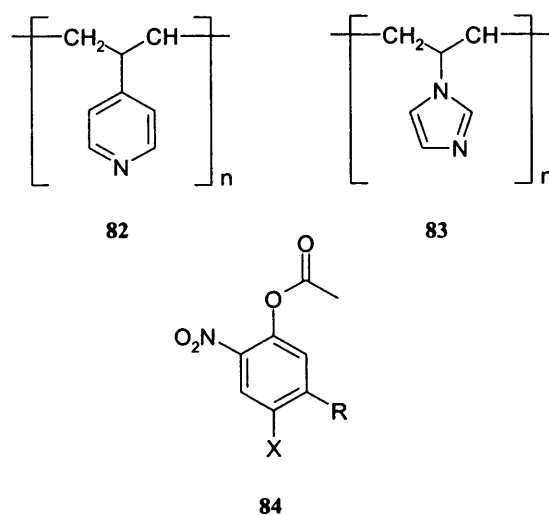


Figure 1.3.16 Poly(4-vinylpyridine) (**82**), poly(*N*-vinylimidazole) (**83**) and nitrophenyl ester (**84**).

The behaviour of these polymers had intrigued Klotz and co-workers and since then, the group have conducted a number of detailed studies using water soluble polymers such as polyethyleneimine (PEI) (**Figure 1.3.17**).⁶³ PEI is usually prepared as a highly branched macromolecule, with a very compact, locally concentrated conformation.⁶³

This is believed to help with its increased binding ability towards small molecules, compared with the much more extended and open conformation of linear polymers. The compact conformation of PEI has been compared to that of serum albumin, which has an incredibly strong affinity for small molecules of widely different structures.⁶³

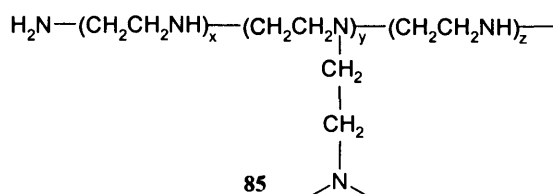
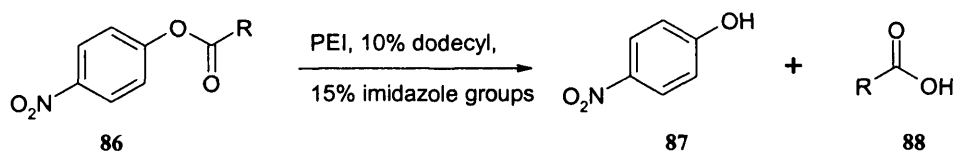


Figure 1.3.17 Polyethyleneimine.

The fact that such a polymer with strong ligand binding was so readily available led Klotz to graft functional groups onto the polymer matrix. A notable discovery was that alkylation of PEI with 10% dodecyl groups and 15% with imidazole gave a polymer which was able to hydrolyse *para* nitrophenyl esters **86** (Scheme 1.3.15) in a truly catalytic manner.⁶⁴



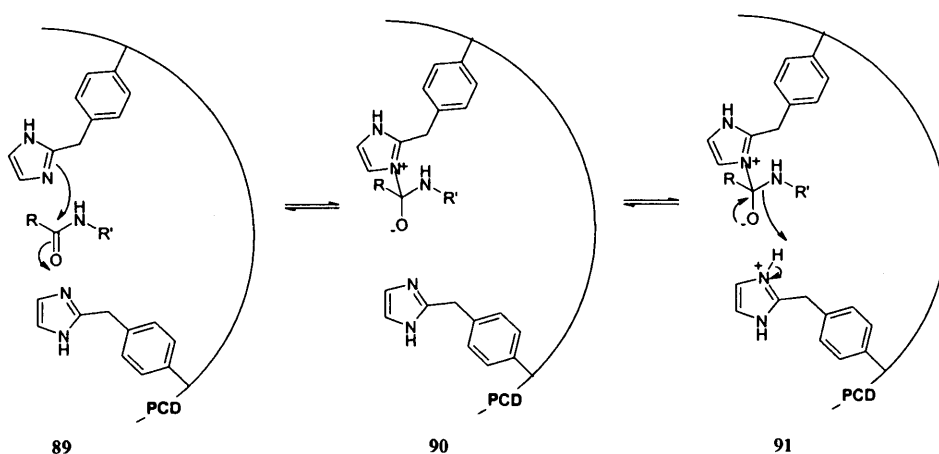
Scheme 1.3.15 Ester hydrolysis by polyethyleneimine.

Table 1.3.1, shows a comparison between the effectiveness of different catalysts towards the hydrolysis of a nitrophenyl ester **86**. PEI derivative is 270 times more effective than free imidazole, however it does not match the activity of α -chymotrypsin, even with activated unnatural ester substrates.^{64;65}

Catalyst	Catalytic Constant k ($\text{m}^{-1} \text{min}^{-1}$)
Imidazole	10
α -Chymotrypsin	10000
PEI, 10% dodecyl gp, 15% imidazole	2700

Table 1.3.1 Comparison of catalytic efficiencies of imidazole, α -chymotrypsin and polyethyleneimine.

Branched insoluble polymers have more rigid backbones and more hydrophobic pockets than branched soluble polymers such as PEI, which may be more advantageous in some catalysts. This encouraged Suh to synthesise an effective polymer catalyst with protease activity.⁶⁶ Imidazoles were randomly attached to poly(chloromethylstyrene-*co*-divinylbenzene) (PCD), to give catalyst **89** (Scheme 1.3.16), which was able to hydrolyse albumin, with the optimum activity between pH 7 – 9. Catalyst **89** contained 22 mol% of imidazoles and when this is lowered to 5 mol%, a marked reduction in proteolytic activity was observed (k_o decreased from $3.13 \times 10^{-2} \text{ m}^{-1}$ to $0.13 \times 10^{-3} \text{ m}^{-1}$). It is believed that the mechanism of action involves two imidazoles as depicted in Scheme 1.3.16.⁶⁶



Scheme 1.3.16 Hydrolysis of albumin by catalyst **89**.

Many enzymes contain two or more metal ions within their active site and examples of these include methionine aminopeptidases,⁶⁷ metallo- β -lactamases,⁶⁸ and proline dipeptidases.⁶⁹ Suh constructed an artificial multinuclear metalloprotease **93** through transfer of three moieties of tris(2-aminoethyl)amine (tren) from the trinuclear macrocyclic complex **92** to PCD (**Figure 1.3.18**).^{70;71}

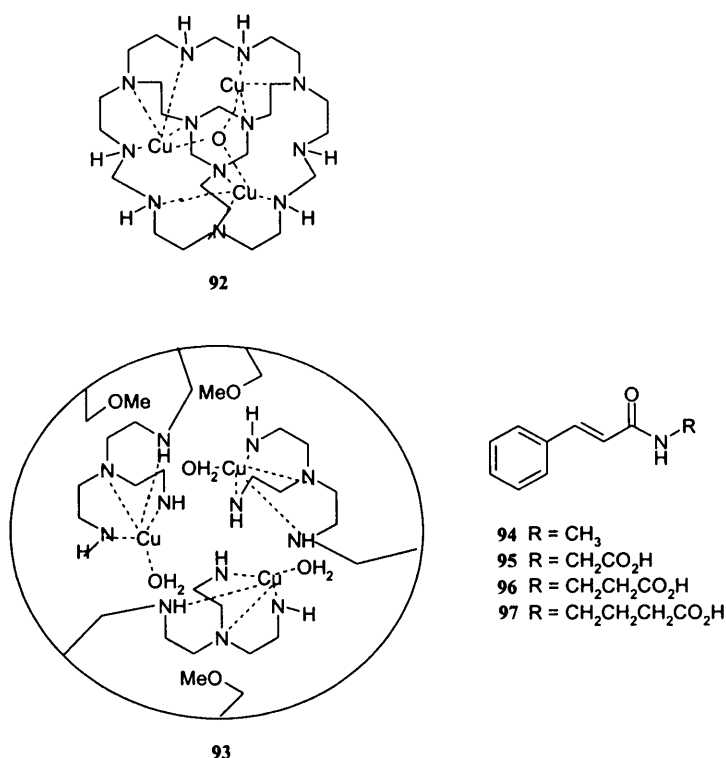


Figure 1.3.18 Trinuclear macrocyclic complex **92**, multinuclear metalloprotease **93** and amide substrates.

The catalytic activity of **93** was investigated using amides **94** – **97**. It was found that the catalyst only hydrolysed amides **95** - **97** which contained carboxyl groups. To account for this selectivity, the mechanism in **Figure 1.3.19** was proposed. The first copper (II) ion complexes to the carboxyl group and the second copper (II) coordinates to the oxygen of the amide. This leaves the third copper (II) with the attached hydroxyl group to position itself in the correct geometry for nucleophilic attack. The estimated k_{cat} for the amide hydrolysis was 0.1 h^{-1} at pH 8.5 and 50°C .⁷⁰ This is compatible with a k_{cat} of 0.18 h^{-1} for hydrolysis of an amide substrate at pH 9 and 25°C observed with a catalytic antibody.⁷¹

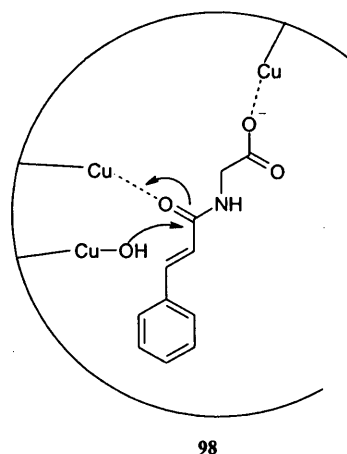


Figure 1.3.19 Hydrolysis of amides by metalloprotease 93.

Another PCD based artificial metalloenzyme has been used in phosphodiester hydrolysis. Deoxyribonucleic acid (DNA) is very stable to hydrolysis, the half-life for spontaneous hydrolysis is estimated at about 10^{11} years at pH 7 and 25 °C.⁷² However, DNA can be hydrolysed using a Co(III) complex of cyclen and Co(III)Cyc **99**, is one of the most effective catalysts for the hydrolysis of DNA.⁷³ The mechanism illustrated in **Figure 1.3.20** has been proposed for the catalytic action of Co(III)Cyc.

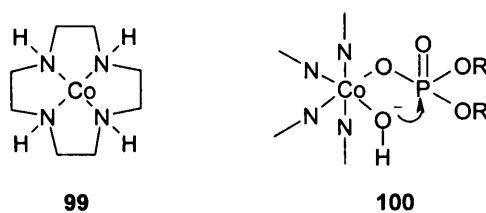


Figure 1.3.20 Co(III)Cyc complex **99** and proposed mechanism of DNA hydrolysis.

A PCD derivative incorporating Co(III)Cyc was prepared (**101**, **Figure 1.3.21**) and assessed for hydrolytic activity.⁷⁴ **101** was shown to be a very efficient catalyst, with the DNA hydrolysis half life measured to be 30 min at 25 °C. A comparison of the rate constants for Co(III)Cyc alone and PCD-based Co(III)Cyc complex showed that attachment to PCD increased the activity of the catalyst by 200 times.⁷⁴ It has been

estimated that only a small number of Co(III)Cyc moieties are exposed to the resin surface and hence only a small fraction of these would function as the catalytic groups. Consequently, the co-operation between two or more metal centres is unlikely and instead, it has been proposed that the increased activity of the PCD – based catalyst may possibly be due to the gel-like microenvironment of PCD exerting favourable effects on the reactivity of Co(III)Cyc complex.⁷⁴

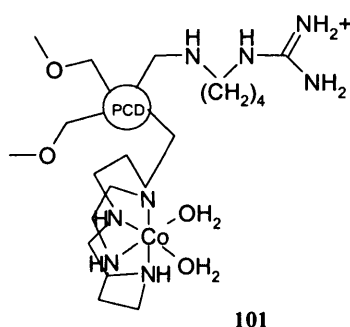
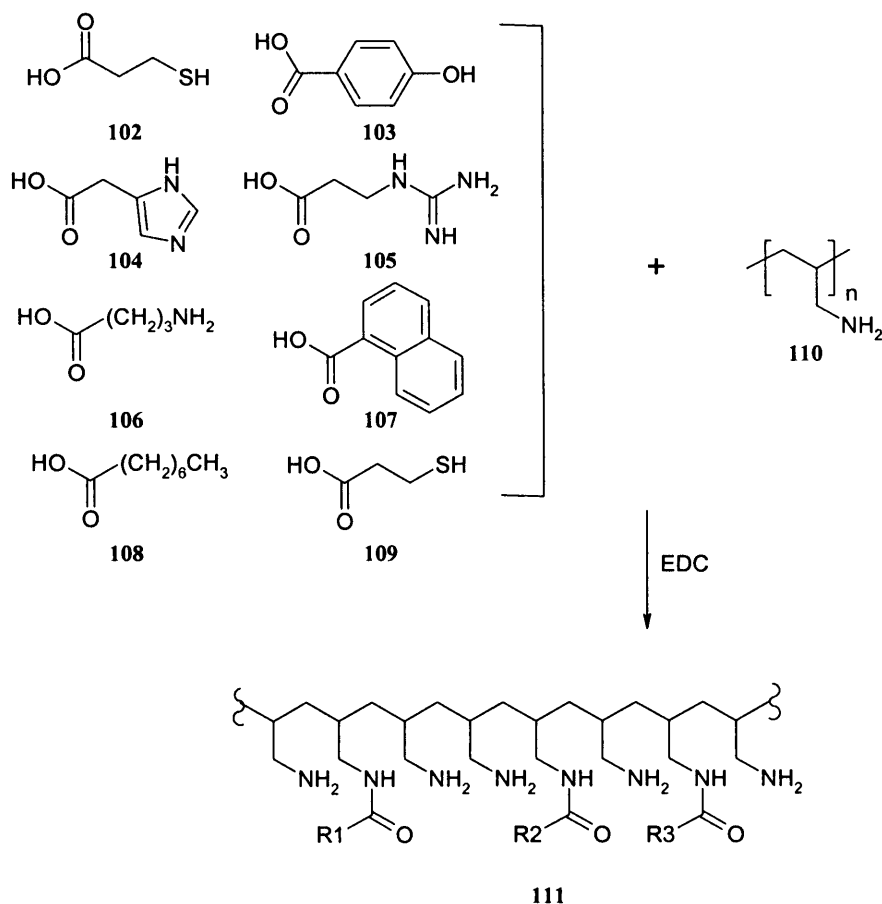


Figure 1.3.21 PCD derivative incorporating Co(III)Cyc complex.

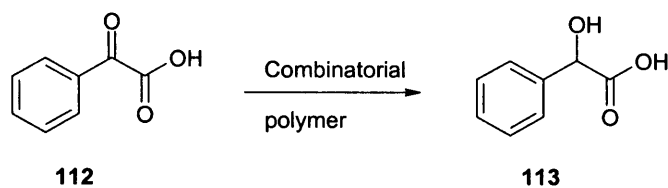
1.3.7 Combinatorial Polymers as Enzyme Mimics

During the mid nineties, Menger and co-workers introduced a highly creative approach towards artificial enzymes by generating a large library of randomly functionalised polymers.⁷⁵⁻⁷⁷ In an attempt to create a reducing agent, mixtures of three or four carboxylic acids (102 – 109), selected from **Scheme 1.3.17**, were randomly attached to polyallylamine 110. This allowed the group to create a large and diverse polymer library.⁷⁷ Furthermore, each polymer contained 5 – 10% of dihydropyridine in addition to metals such as zinc (II), magnesium (II) and iron (II). Dihydropyridines are known to convert ketones to alcohols in nicotinamide adenine dinucleotide (NADH) models.⁷⁸



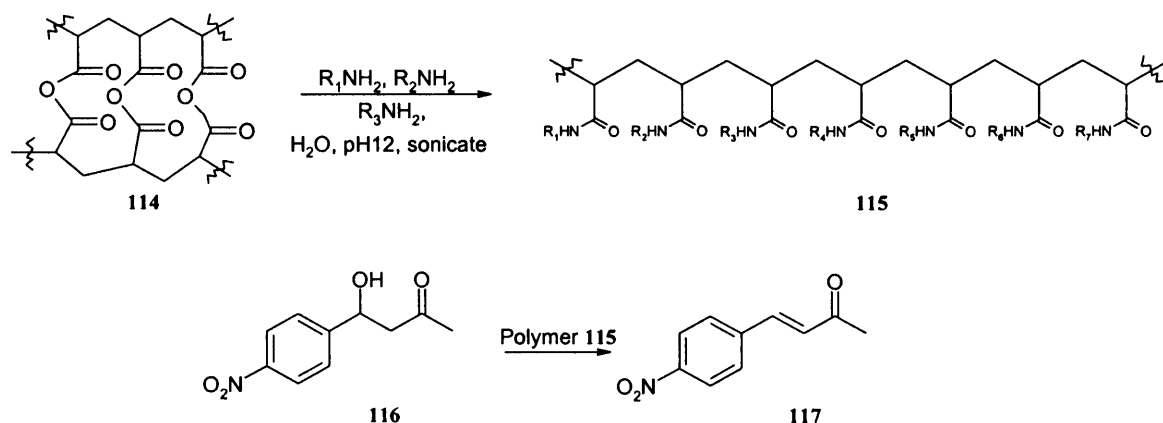
Scheme 1.3.17 Synthesis of a polymer library consisting of polyallylamine and carboxylic acids.

Each of 8198 combinatorially generated polymers with and without the presence of a metal ion were then screened for catalytic activity towards benzoylformic acid (**Scheme 1.3.18**). 92% of these yielded less than 10% of product and were hence considered inactive. The polymers that were found to be most active had a number of things in common which are believed to have contributed to catalysis: a metal ion, a hydrophobic chain and the presence of an imidazole or guanidine moiety.⁷⁷ The half-life of one of the better reductions was 2 hours, which was faster relative to many other NADH models.⁷⁸



Scheme 1.3.18 Reduction of benzoylformic acid using combinatorial polymers.

Combinatorial polymers have also been used to catalyse the dehydration of β -hydroxyketone **116** (Scheme 1.3.19).⁷⁶ The general design of these polymers was essentially the same as described above, however in this instance, poly(acrylic anhydride) **114** was used, and amines were attached to the polymer instead of carboxylic acids. The best polymer screened displayed rate acceleration of 920 times above the background reaction.



Scheme 1.3.19 Combinatorial polymer **115** and dehydration of β -hydroxyketone catalysed by **115**.

Although this combinatorial approach has generated some promising results, the polymeric mixtures generated are complex systems, which are impossible to separate, thus making it difficult to determine their structure, and perhaps even more frustratingly, making meaningful mechanistic conclusions all but impossible.

1.3.8 Directed Evolution of Enzymes

Many enzymes are commercially available today and work well in catalysing enantioselective transformations of a number of unnatural compounds. However, their great degree of specificity means that they cannot be used on a wider range of substrates. In an attempt to deal with such problems, directed evolution strategies have been employed (**Figure 1.3.22**).⁷⁹ The starting point of this technique involves obtaining a wild-type enzyme which catalyses a particular reaction of interest, but not with an acceptable level of enantioselectivity. The gene that encodes the wild-type enzyme is then subjected to random mutagenesis methods, such as the error-prone polymerase chain reaction⁸⁰ or DNA shuffling.⁸¹ The library of mutant genes is then inserted into a microorganism and mutant enzymes are expressed. The enzymes are then screened for catalytic activity (using techniques such as infrared thermography⁸²) and enantioselectivity in the reaction of interest. The mutant gene of the optimal enzyme variant is then subjected once more through the whole process of mutagenesis, expression and screening. This process can be repeated as many times as required and it creates a type of 'Darwinistic evolution', leading to the formation of a superior enzyme, every time it is performed.

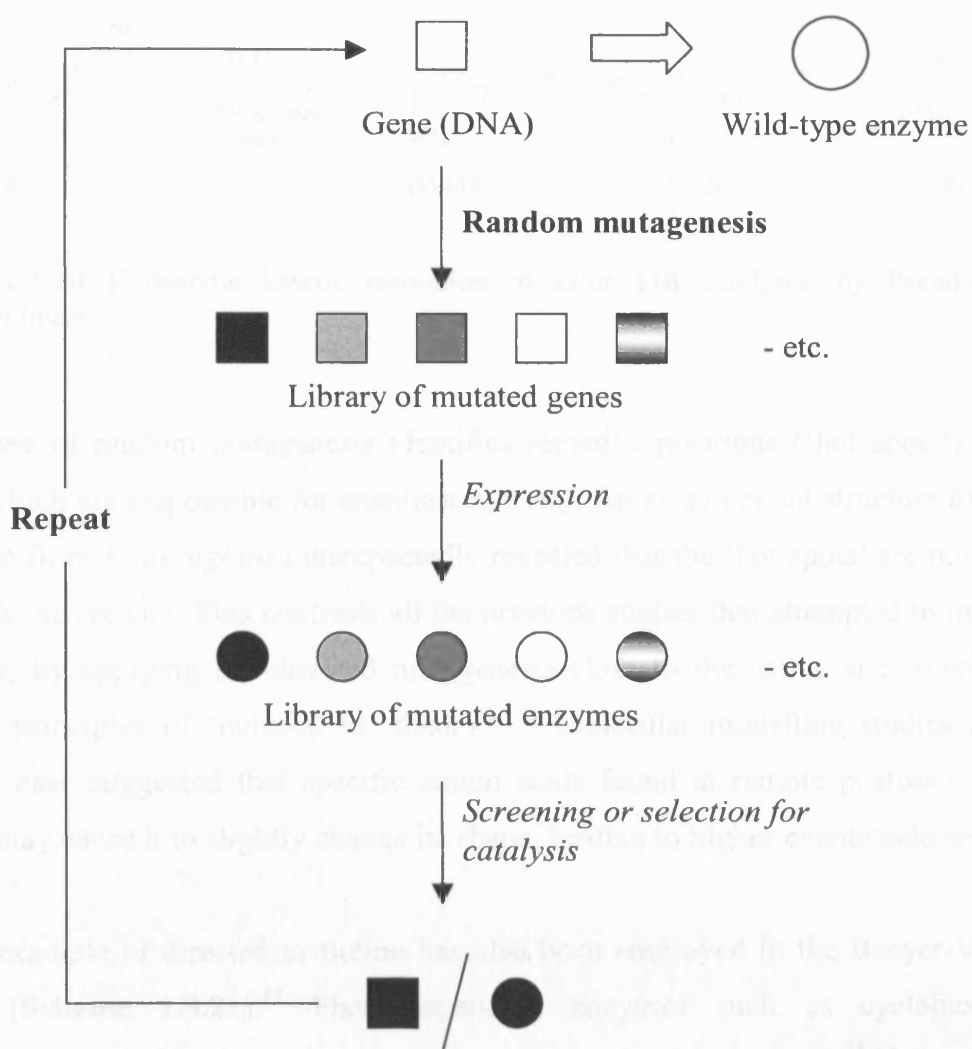
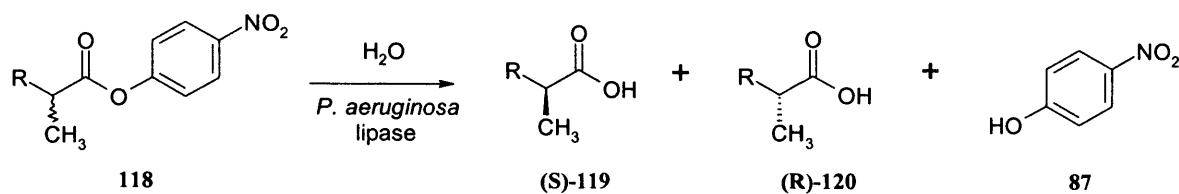


Figure 1.3.22 General representation of directed evolution process.

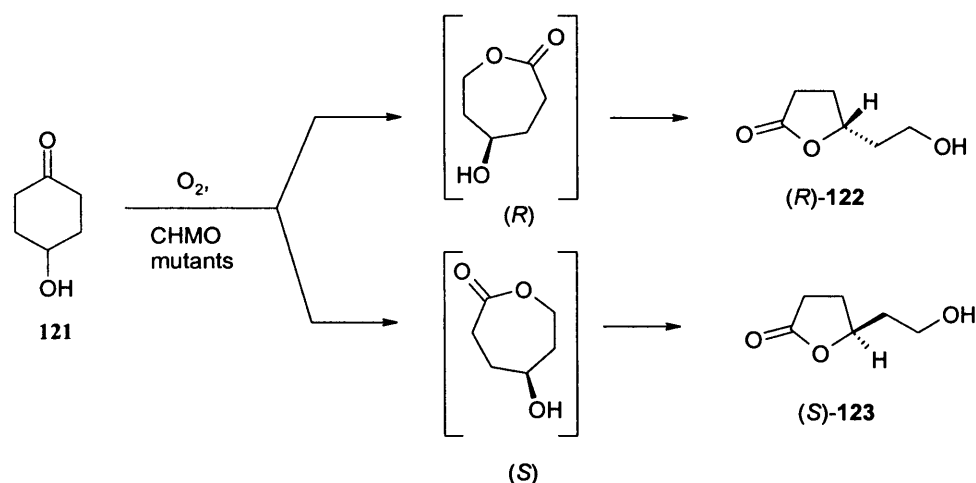
To demonstrate this approach, Reetz *et al* selected a hydrolytic kinetic resolution of ester **118**, catalysed by a bacterial lipase from *Pseudomonas aeruginosa* (**Scheme 1.3.20**).⁸³ The wild-type lipase showed an *ee* of only 2% for the (*S*)-acid **119**. The first round of mutagenesis, expressed about 1000 lipase mutants, which were isolated and screened on the basis of released *p*-nitrophenol product, which has an absorption at 410 nm. The candidates which favoured the hydrolysis of the (*S*) enantiomer of ester **118** were then isolated and exposed to further mutagenesis. After four generations, the group obtained an artificial enzyme which catalysed the hydrolysis reaction with an *ee* of 81% for (*S*)-acid **119**.⁸³



Scheme 1.3.20 Hydrolytic kinetic resolution of ester **118** catalysed by *Pseudomonas Aeruginosa* lipase.

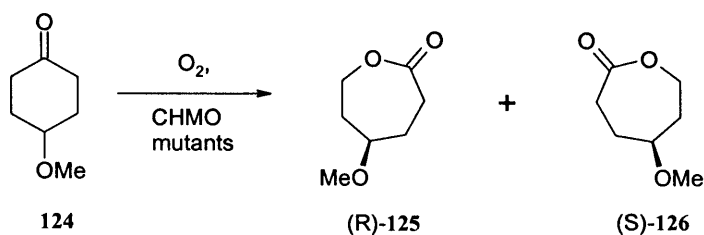
The process of random mutagenesis identifies sensitive positions ('hot spots') in the enzyme which are responsible for enantioselectivity. An x-ray crystal structure of wild-type lipase from *P. aeruginosa* unexpectedly revealed that the 'hot spots' are not really close to the active site. This contrasts all the previous studies that attempted to improve selectivity, by applying site-directed mutagenesis close to the active site, keeping in mind the principles of 'induced fit' theory.⁸⁴⁻⁸⁶ Molecular modelling studies in this particular case suggested that specific amino acids found at remote positions of the enzyme, may cause it to slightly change its shape, leading to higher enantioselectivity.⁸³

Another example of directed evolution has also been employed in the Baeyer-Villiger reaction (**Scheme 1.3.21**).⁸⁷ Flavin-dependent enzymes such as cyclohexanone monooxygenase (CHMO) can be used as a catalyst for this reaction.^{88,89} During the enzymatic process, dioxygen reacts with the enzyme-bound flavin adenine dinucleotide (FAD) to form an intermediate hydroperoxide, which initiates the Baeyer-Villiger reaction by transferring one oxygen atom from O_2 to the substrate (ketone). As a model reaction, the rearrangement of 4-hydroxycyclohexanone **121** was chosen, using CHMO from *Acinetobacter* sp. NCIMB 9871. The Baeyer-Villiger reaction of ketone **121** leads to lactone ((*R*) or (*S*)), which can then rearrange to **122** or **123**, with retention of stereochemistry (**Scheme 1.3.21**).⁸⁷ Using the wild-type enzyme, the reaction pathway favours (*R*)-**122** with an *ee* of 9%. After performing mutagenesis, the best selected enzyme, 2-D19-E6, was shown to catalyse the reaction with an *ee* of 90% in favour of (*R*)-**122**.



Scheme 1.3.21 Baeyer-Villiger reaction catalysed by CHMO enzyme.

It is believed that one factor influencing the enantioselectivity during the rearrangement is that the hydroxy group of the substrate is acting as a potential hydrogen donor, placing the substrate in two different protein environments, depending on whether the favoured product is (*R*) or (*S*). This hypothesis led the group to use 4-methoxycyclohexanone as a substrate to provide them with further information. The enzyme 2-D19-E6, shown to have high selectivity in the reaction of hydroxy ketone **121** for (*R*)-**122** (90 % *ee*), only showed 25% *ee* in favour of (*R*)-**125** in the reaction of methoxy ketone **124** (**Scheme 1.3.22**).⁸⁷ However, the enzyme 1-K2-F5 that showed the most *S*-enantiomer selectivity in reaction of **121**, showed nearly complete enantioselectivity (98.6% *ee* in favour of (*S*)-**126**) when catalysing the reaction of methoxy ketone **124**. Since the methoxy functionality is a hydrogen acceptor, this suggests that enzyme 1-K2-F5 had undergone an amino acid substitution in order to be able to form an additional hydrogen bond to the methoxy group during the transition state of the reaction. Characterisation of 1-K2-F5 confirmed that this was the case, with serine replacing phenylalanine at position 432.⁸⁷



Scheme 1.3.22 Baeyer-Villiger reaction catalysed by CHMO enzyme.

The group also demonstrated that enzymes generated by direct evolution can be used on a wider range of substrates.⁸⁷ Reactions of other 4-substituted cyclohexanone derivatives such as methyl, ethyl, chloro, bromo and iodo were also catalysed with selectivities of 95 – 99% *ee*.

1.4 Summary

As illustrated from the above discussion, there have been many approaches taken towards developing artificial enzymes. We have seen the use of more traditional, rational design approach, where a molecule is designed by incorporating a group that is known to be catalytic within the active site of a natural enzyme. Although much information has been learned about different aspects of enzyme catalysis and functional group cooperativity, this approach can be very time consuming and even the most careful planning of the design can lead to unproductive results. More successful outcomes have been seen with approaches which have employed a selection event, allowing one to choose the most efficient catalyst from a large library of molecules. The catalyst can be selected on the basis of its binding towards an appropriate TSA and this approach has been successful in several cases as illustrated by catalytic antibodies. However, problems associated with designing a TSA which has the electronic and geometric features that closely resemble the transition state of the reaction has prevented this approach from generating catalytic molecules that rival enzymes. Alternatively, incorporating a catalytically active group within the active site in combination with TSA binding as exemplified by reactive immunisation in catalytic antibodies has led to more significant results. In general, the problems associated with all selection events are the large number of possible combinations generated and the

necessity for screening techniques in order to detect catalytic activity. The development of new technology, such as UV/Vis spectroscopy, IR thermography⁸² and automated mass spectrometry has allowed for the use of improved and new screening methods.^{20;21;51} However, despite this, screening techniques remain a crucial area that needs developing in order for greater success to be achieved. Developments in combinatorial chemistry have also facilitated progress in this area, however difficulties in isolating and characterising the selected host have been identified. Finally, advances in molecular biology techniques have allowed for the development of more efficient artificial enzyme systems. However, these artificial enzymes, together with catalytic antibodies still share the same undesirable properties as natural enzymes, such as lack of thermal stability and pH sensitivity.

Despite the fact that there have been a number of impressive advances in this field, the development of an artificial enzyme, which has the efficiency, stereoselectivity and turnover of a natural enzyme still remains to be seen. Clearly, there are many factors involved in enzyme catalysis, and for us, the one thing that remains is to continue to learn from Nature's principles. Combining this knowledge, together with technological advances, will hopefully allow us to eventually create more efficient and sophisticated artificial enzymes.

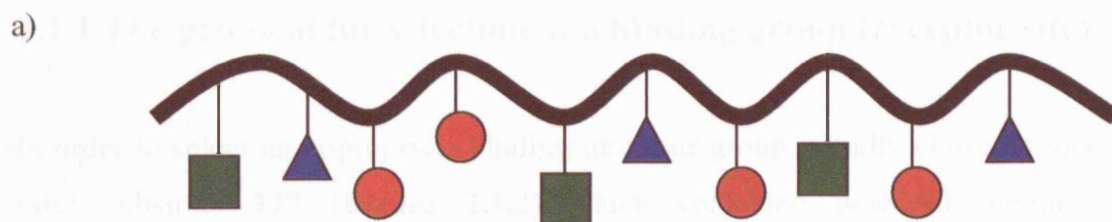
CHAPTER 2

RESULTS AND DISCUSSION

STUDIES RELATED TO THE DEVELOPMENT OF ARTIFICIAL ESTERASES

2.1 Introduction

A novel approach towards the construction of an artificial esterase was taken by our own research group and first described in 2001.^{90;91} Thus a protocol was developed for the modular assembly of artificial enzymes, which combined the positive elements of both the design and selection approaches. The basic principle was to consider an enzyme at its most simplistic level – as a molecule that can both “hold” and “bite”, and also possess the flexibility to achieve the operation of bringing the “hands” (recognition and substrate binding) to the mouth (catalytically active group). The resultant artificial enzyme (**Figure 2.1.1**) therefore consisted of a flexible polymer backbone, inspired by the work of Menger^{76;77} and Klotz,⁶⁴ with two differing threads attached to it, one whose function was to facilitate the reaction through substrate recognition and transition state binding, whilst the second was to contain a necessary functional group for catalysis. The binding group was a specifically designed and selected unit, which could act, to stabilise the transition state of the reaction. This binding group would also hopefully hold the ester substrate in the correct orientation for effective hydrolysis by the catalytic group, thus resulting in an increase in the catalytic activity of the polymer. Although the exact tertiary structure of the polymer was unknown, it was thought that the random attachment of such groups and the overall flexibility of the system would increase the possibility of the “esterase” developing effective regions for catalysis to occur. The modular assembly of an artificial esterase in this way was also envisaged to permit rapid variation of both the binding site and/or the catalytically active group, and this would allow the assessment of a range of factors which are essential for enzyme catalysis.



● = Binding group ▲ = Catalytic Group
■ = Hydrophilic/hydrophobic group | = Spacer

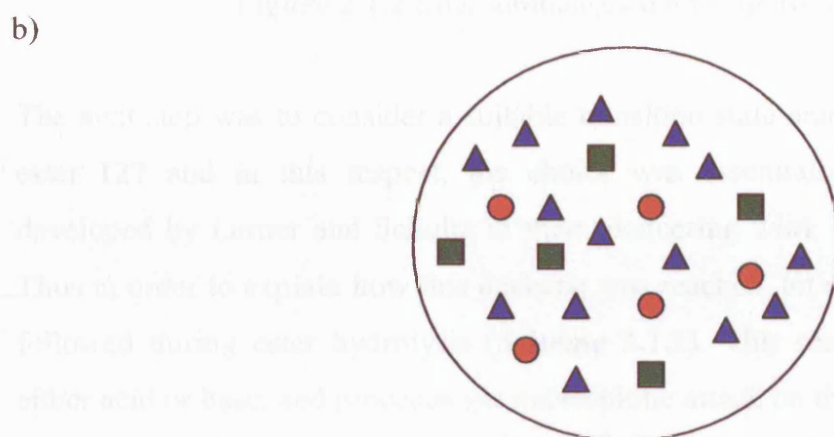


Figure 2.1.1 A diagrammatic representation of an artificial “millipede” enzyme. a) Binding, catalytic and hydrophilic/hydrophobic groups are randomly grafted onto a polymeric backbone. b) Aerial view – each receptor site is surrounded by a number of catalytic groups, and once a substrate is bound, any one of these may be in correct position to attack the substrate and act as catalyst.⁹¹

2.1.1 The protocol for selection of a binding group (receptor site)

In order to select an appropriate binding unit, our group initially chose an unactivated ester substrate **127** (Figure 2.1.2) which contained potential binding groups (highlighted in red) and was also UV active thus allowing the hydrolysis reaction to be monitored.

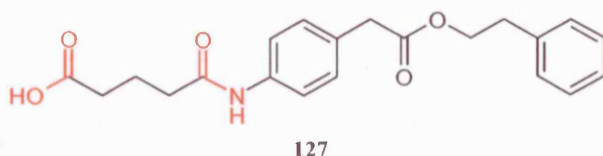
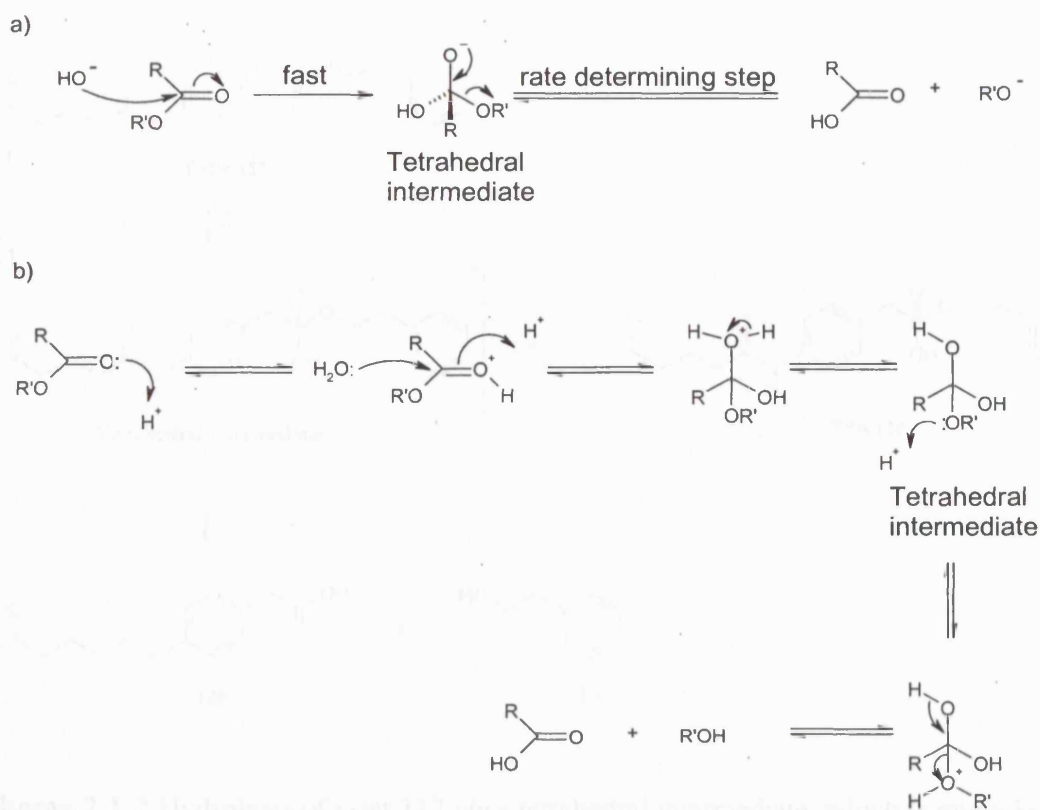


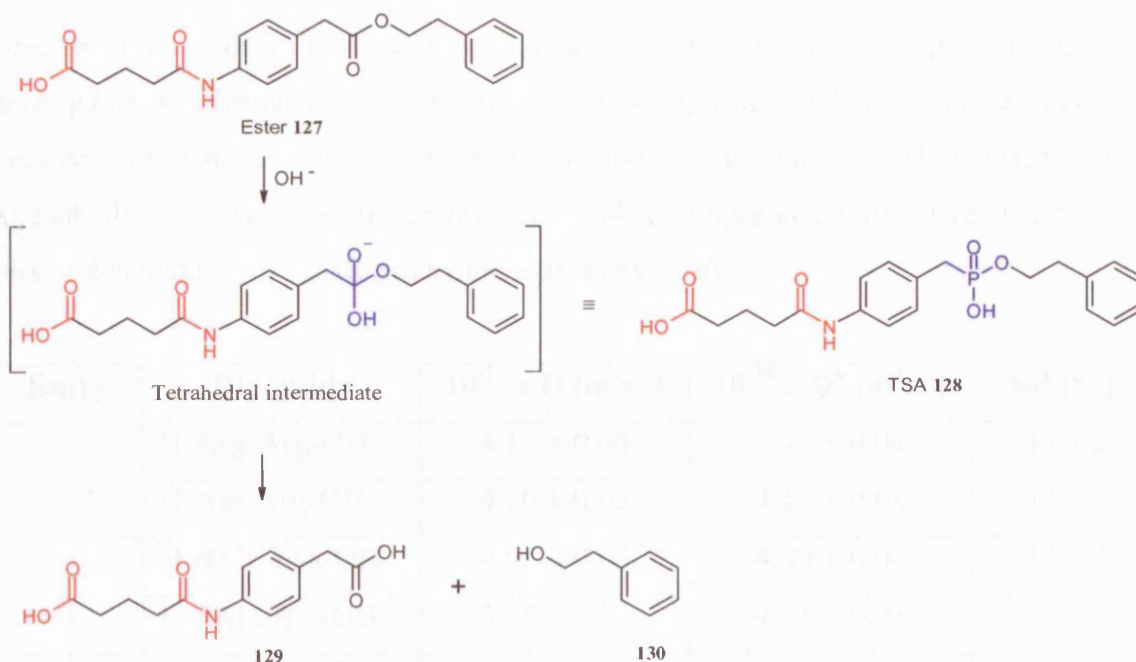
Figure 2.1.2 Ester substrate used for hydrolysis studies.^{90;91}

The next step was to consider a suitable transition state analogue for the hydrolysis of ester **127** and in this respect, the choice was essentially based on the principles developed by Lerner and Schultz in their pioneering work on catalytic antibodies.^{23;24} Thus in order to explain how this decision was reached, let us first analyse the pathway followed during ester hydrolysis (Scheme 2.1.1). This reaction can be catalysed by either acid or base, and proceeds *via* nucleophilic attack on the carbonyl group, resulting in a change of hybridisation from sp^2 to sp^3 when the tetrahedral intermediate is formed. This then breaks down in the rate determining step to liberate the acid and the alcohol.⁹²



Scheme 2.1.1 General ester hydrolysis. a) Base catalysed hydrolysis, b) Acid catalysed hydrolysis.

Since the transition state of the reaction involves a tetrahedral intermediate, any stable analogue which mimics the geometry and charge distribution of this tetrahedral intermediate should, in theory, function as a good TSA. Phosphonates have often been used as inhibitors of natural esterases because of their tetrahedral geometry around the phosphorus centre. Hence, they were considered to be good mimics of the ester hydrolysis transition state.⁹³ Phosphonate **128** was therefore synthesised as a TSA for the hydrolysis reaction of ester **127** (**Scheme 2.1.2**). Thus the requisite phosphonate contained both a carboxylic acid and a phosphonate moiety which can form salts with basic groups and amide linkages which can form hydrogen bonds with other polar groups.⁹¹



Scheme 2.1.2 Hydrolysis of ester **127** via a tetrahedral intermediate, which is mimicked by transition state analogue **128**.

Dipeptides were chosen as potentially suitable binding units because they are rich in acidic, basic and hydrogen bond donor/acceptor functionalities. Nine commercially available dipeptides were selected (**Table 2.1.1**) and analysed for their binding affinity towards the TSA **128** using Pulsed Field Gradient (PFG) NMR techniques.⁹⁴⁻⁹⁶ This technique employs the use of the translational diffusion coefficient (D), which is molecular mass dependent: small molecules diffuse faster than larger molecules in solution. When two molecules form a complex in solution, the overall molecular mass changes and this can be observed as a slowing or decrease in the translational diffusion coefficient. Although this technique is normally employed to study the binding of a small molecule with a high molecular weight receptor, our own group were able to detect binding of the dipeptide to the TSA in an aqueous environment through the simple expedient of using Le Chatelier's principle. The translational diffusion coefficients of the dipeptides were measured in D_2O at pD 7 and the results obtained are shown in **Table 2.1.1**.^{91;96} From these studies, it was found that the dipeptide H-Arg-Arg-OH and TSA complex displayed the greatest change in the diffusion coefficient, *i.e.* this dipeptide displayed the best binding potential towards the TSA. This is perhaps not surprising, since the interaction between the guanidine of arginine and the

carboxylic acid of the TSA **128** is well documented (**Figure 2.1.3**), and was also confirmed by molecular modelling studies.⁹⁰ Although the Arg-Arg dipeptide was selected as the strongest binder for incorporation into the artificial esterase, it does not necessarily mean that it will be the most effective unit for catalysis. However, the ability to rank the binding affinities of the TSA with a simple selection of readily available dipeptides makes this NMR procedure extremely useful.

Entry	Dipeptide	$10^{-10} \times D \text{ [m}^2\text{s}^{-1}\text{]}$	$10^{-10} \times D' \text{ [m}^2\text{s}^{-1}\text{]}$	Rd [%] ^a
1	H-Arg-Arg-OH	4.10 ± 0.04	3.40 ± 0.04	17 ± 2
2	H-Ala-Arg-OH	4.76 ± 0.05	4.18 ± 0.08	12 ± 2
3	H- β Ala-Lys-OH	4.91 ± 0.03	4.39 ± 0.04	11 ± 1
4	H- β Ala-His-OH	5.18 ± 0.03	4.71 ± 0.05	9 ± 1
5	H-Ser-His-OH	4.89 ± 0.03	4.46 ± 0.05	9 ± 1
6	H-Gly-Tyr-OH	4.97 ± 0.04	4.64 ± 0.07	7 ± 1
7	H- β Ala-Leu-OH	4.97 ± 0.04	4.62 ± 0.09	7 ± 1
8	H-Gly-Thr-OH	5.54 ± 0.04	5.19 ± 0.04	6 ± 1
9	H-Ala-Gly-OH	6.08 ± 0.05	5.72 ± 0.08	6 ± 1

Table 2.1.1 NMR binding studies of potential dipeptide binding sites. D is the observed diffusion coefficient for 3 mM solution of dipeptide in D₂O at 298 K. D' is the observed diffusion coefficient for mixtures containing dipeptide (3 mM) and TSA **128** (30 mM) in D₂O at 298 K. ^aR_d is the relative change in diffusion coefficient ($100(D-D')/D$).⁹⁶

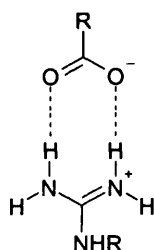
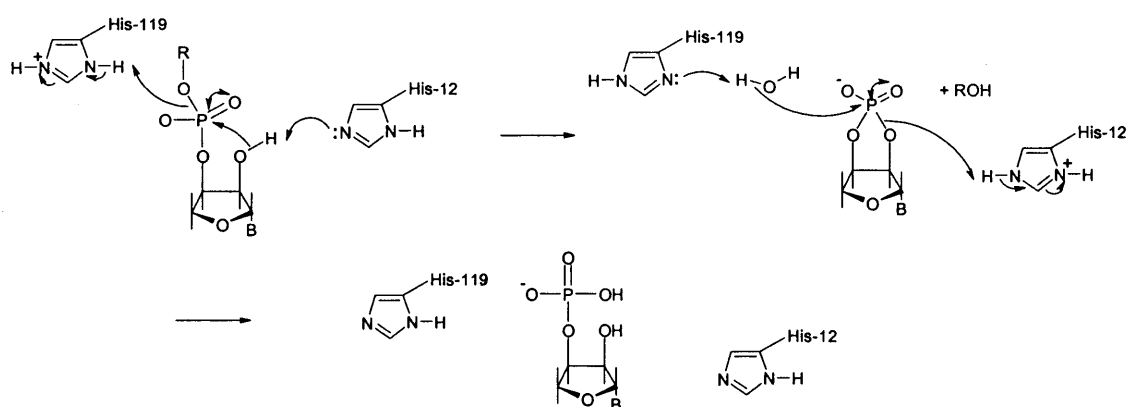


Figure 2.1.3 Representation of the interaction between a guanidine and a carboxylic acid.

2.1.2 Selection of the catalytic functional group

With a suitable binding unit in hand, the next stage was to choose an effective catalytic group. The catalytic group was selected on the basis of amino acids functionalities

which were well known to participate in catalysis during ester hydrolysis within natural enzymes. Therefore cysteine, histidine and serine were all considered.⁹⁷ However, histidine was chosen, because it can function as a general acid/base pair as observed in ribonucleases (**Scheme 2.1.3**).⁹⁷ It was anticipated that it might perform a similar function within this system.



Scheme 2.1.3 General acid/base catalysis in ribonucleases.⁹⁷

2.1.3 Constructing an artificial esterase

Polyallylamine **110** (**Figure 2.1.4**) was chosen as a polymer support, since it is a flexible polymer and also possesses free amino groups thereby providing an easy method for the attachment of the binding and catalytic units using standard peptide coupling techniques.

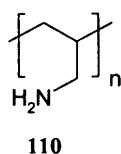


Figure 2.1.4 Polyallylamine

In addition, since it was considered to be essential for the Arg-Arg binding group to be conformationally mobile when attached to the polymer, a spacer unit (6-aminocaproic acid) was attached to the binding unit. The resulting binding unit, which consisted of the protected tripeptide 6-(Fmoc-Arg(Pbf)-Arg(Pbf)-)amido caproic acid **131** (**Figure 2.1.5**) was prepared by solid phase synthesis.⁹¹

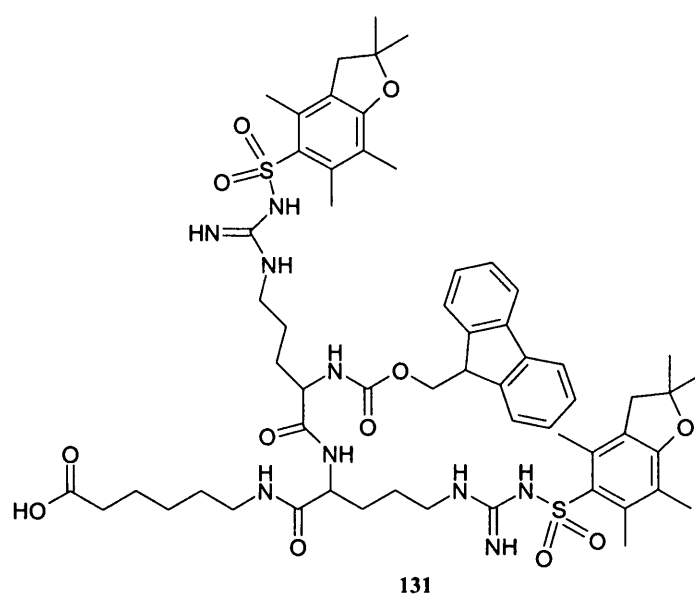
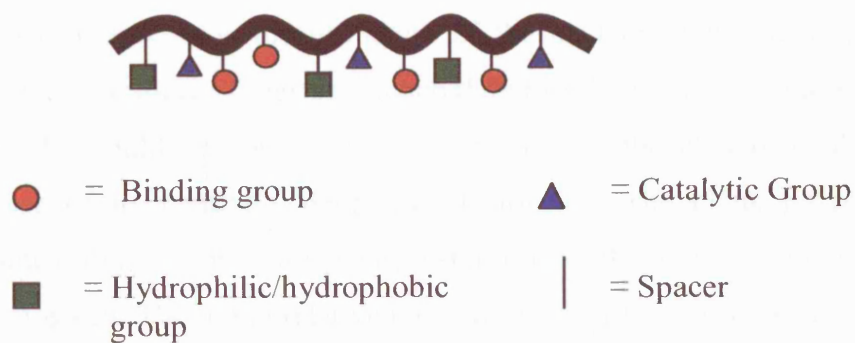


Figure 2.1.5 The tripeptide **131** binding group.

The artificial esterase **132** (**Figure 2.1.6**) was then assembled by simultaneous attachment of the binding unit **131** and the histidine catalytic group, and this process was then followed by the attachment of a lysine residue which could be considered to act as a hydrophilic group. It was envisaged that, by introducing the binding and catalytic groups at the same time, they would influence the positioning of each other on the polymer backbone. Removal of the protecting groups, then gave the desired polymer **132** (**Figure 2.1.6**). Other polymers were also prepared, one containing only lysine and the binding unit **134** (2:1 ratio), another with lysine and the catalytic group **133** (2:1 ratio) and finally a “blank” polymer **135**, containing lysine residues only (**Figure 2.1.7**). In this way, it was possible to explore the relative importance of the units and the possible synergistic effects which contributed to those polymers possessing the best catalytic activities.

a)



b)

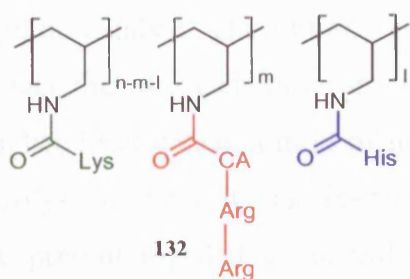


Figure 2.1.6 a) Graphical representation of artificial esterase. b) Chemical representation of artificial esterase.

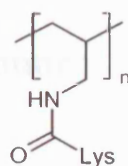
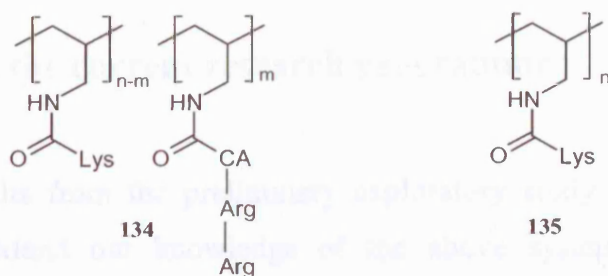
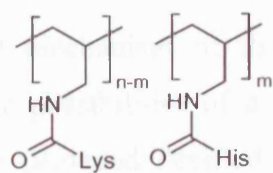


Figure 2.1.7 Examples of further artificial esterases prepared.

The fully deprotected polymers **132 - 135** were then investigated to determine whether they catalysed hydrolysis of ester **127**. The hydrolysis reaction in aqueous phosphate buffer at pH 7 was followed by the formation of the acid product and the resultant decrease in the concentration of starting material both of which were monitored by analytical HPLC. It should be noted that the formation of the alcohol could not be monitored because of its relatively poor UV absorbance. The blank polymer **135**, consisting of lysine only, did not hydrolyse the ester. For all the other polymers **132-134** hydrolysis was observed. The initial relative rates for product formation were calculated to be 890:90:1 for polymers **132:134:133** respectively.⁹¹ The hydrolysis observed for polymer **133** was considered to be due to the presence of the imidazole group which could function as a nucleophilic catalyst. The initially surprising activity of polymer **134**, was attributed to the fact that the guanidine groups of arginine residues were protonated, thus giving a higher local concentration of hydroxide ions in the vicinity, which were then able to hydrolyse the ester. It was clear however, that when the binding and catalytic residues were present together as in polymer **132**, the most efficient catalyst was produced.⁹¹ Within this approach, it was also possible to demonstrate the enzymic phenomenon of competitive inhibition. Thus, exposure of an equimolar mixture of the phosphate TSA and the ester substrate led to a drastic decrease in the rate of ester hydrolysis.

Despite the fact that the detailed mechanism of the catalysis was unknown, this preliminary study demonstrated the possibilities of a valuable new approach for the creation of artificial enzymes and provided detailed information about the relative importance and cooperativity of the groups within the active site.

2.2 Objectives of the current research programme

In light of the results from the preliminary exploratory study discussed above, our intention was to extend our knowledge of the above system, and by using the information acquired, to further explore these types of polymer systems. Consequently, the main objectives of the present study, using the same design concept were:

- a) To further investigate the activity of artificial esterases by modifying the binding groups within the polymer.

- b) To analyse the effect of changing pH, solvent and substrate concentration on artificial esterase activity.
- c) To evaluate ester substrate specificity.
- d) To extend this design concept to the synthesis of other classes of artificial enzymes.

2.3 Development of artificial esterases

Since it was our intention to synthesise several different analogues of artificial esterases, containing different binding sites, the first step was to synthesise the protected peptides. Using the previously conducted NMR binding studies as a guide⁹⁶ (**Table 2.1.1**), we wished to incorporate the moderate binding H-Ala-Arg-OH motif and the poor binding H-Ala-Gly-OH dipeptide within our enzyme mimic. It was our desire to correlate the NMR binding strength to the effectiveness of artificial esterase. Since the dipeptides H-Ala-Arg-OH and H-Ala-Gly-OH are comprised of two different amino acid residues, these motifs also allow us to vary the relative positions of the two amino acids with respect to the polymer backbone. Hence, the protected forms of both H-Ala-Arg-OH and the reverse, H-Arg-Ala-OH would have to be synthesised. The fact that the amino acids are placed in different positions in relation to the polymer backbone, may affect the behaviour of the polymer during ester hydrolysis. The same argument applies to H-Ala-Gly-OH, hence H-Gly-Ala-OH was also selected for incorporation. Additionally, it was reasoned that the synthesis of the polymer containing the previously used H-Arg-Arg-OH binding unit should be repeated for comparison purposes and this would hopefully give us a more complete picture of the behaviour of these types of polymer systems. Hence, in summary, the initial aim was to synthesise the five artificial esterases illustrated in **Figure 2.3.1**.

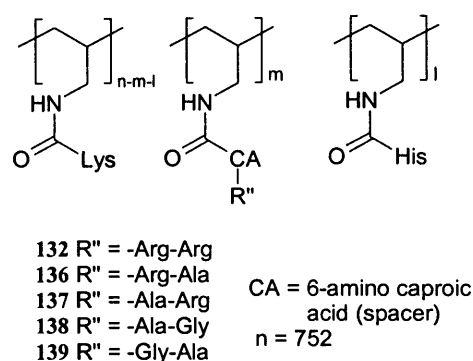
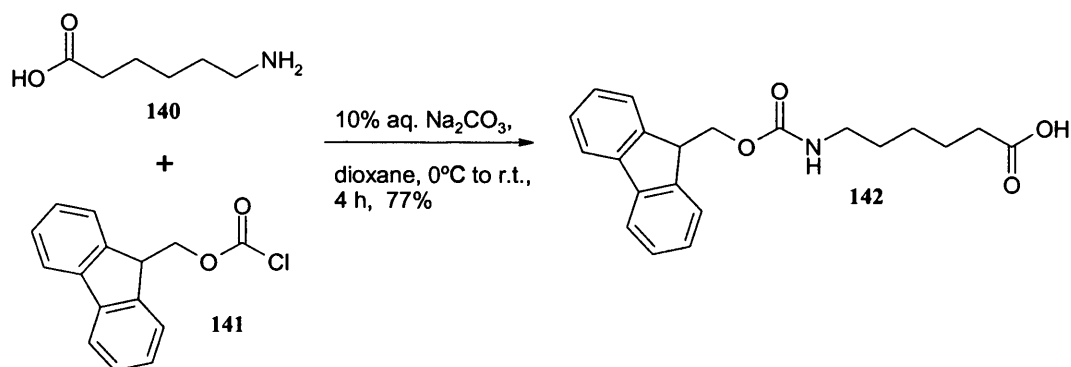


Figure 2.3.1 Initial artificial esterases targeted.

2.3.1 Preparation of binding groups

The binding motifs (Arg-Arg, Arg-Ala, Ala-Arg, Gly-Ala and Ala-Gly) were selected on the basis of binding the TSA as assessed by NMR spectroscopy (**Table 2.1.1**, Section 2.1.1).⁹⁶ The binding units were prepared manually on solid phase, utilizing 2-chlorotrityl resin **144** (**Scheme 2.3.2**), following the procedure described previously.⁹¹ Initially, the binding unit **131** consisting of a 6-aminocaproic acid linker and the arginine dipeptide which was protected with 9-fluorenylmethoxycarbonyl (Fmoc) and 2,2,4,6,7-pentamethyldihydrobenzofuran-5-sulfonyl (Pbf) groups was synthesised (**Scheme 2.3.2**). The route commenced with the Fmoc protection of 6-aminocaproic acid **140** using 9-fluorenylmethyl chloroformate (Fmoc-Cl) **141** and 10% aqueous sodium carbonate in dioxane to afford Fmoc protected 6-amino caproic acid **142** (**Scheme 2.3.1**).



Scheme 2.3.1 Synthesis of Fmoc 6-aminocaproic acid **142**.

The acid **142** was then coupled to 2-chlorotrityl resin **144** using diisopropylethylamine (DIPEA) (**Scheme 2.3.2**). At this point and for all the further coupling steps, a test for the level of Fmoc substitution was performed, in order to give an indication of the efficiency of reaction. The substitution was measured by treating a known quantity of resin with piperidine/DMF (2:8) solution in a silica UV cell. Piperidine cleaves the Fmoc protecting group to form dibenzofulvene, which reacts with piperidine to form the fulvene-piperidine by-product **143** (**Figure 2.3.2**). The by-product **143** has a strong UV absorption at 290 nm.⁹⁸

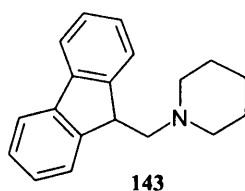


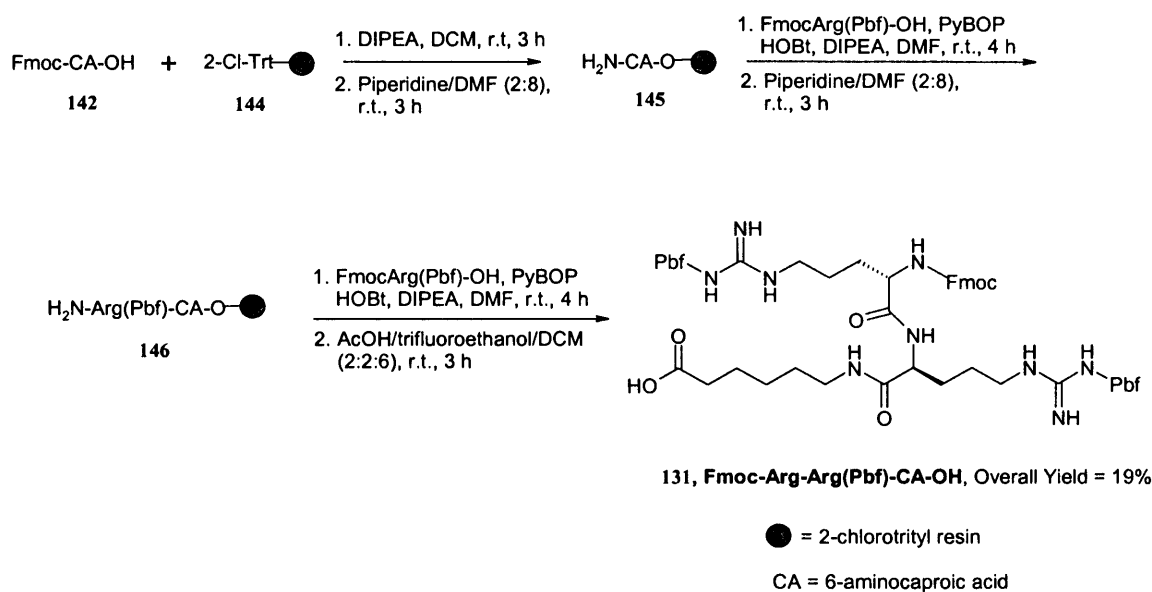
Figure 2.3.2 Fulvene-piperidine adduct.

The level of Fmoc substitution can then be determined in mmol/g from **Equation 2.3.1**.⁹⁸

$$\text{Substitution} = (\text{Absorbance} / \text{mg of sample} \times 1.75)$$

Equation 2.3.1

Fmoc protected caproic acid in piperidine/DMF (2:8) solution afforded resin **145** (**Scheme 2.3.2**). Attachment of the first Pbf protected arginine residue to **145**, was achieved using DIPEA, (1H-benzotriazol-1-yloxy)tripyrrolidinophosphonium hexafluorophosphate (PyBOP) and 1-hydroxybenzotriazole (HOBt) in DMF. This was followed by Fmoc deprotection and coupling of the second arginine unit.



Scheme 2.3.2 Solid phase synthesis of tripeptide binding group **131**.

Cleavage of the tripeptide from the resin, using a mixture of acetic acid/trifluoroethanol/DCM gave the desired binding group **131** in 19% overall yield. The same synthetic sequence shown in **Scheme 2.3.2**, was repeated in an analogous manner for the generation of the further peptides shown in **Figure 2.3.3**.

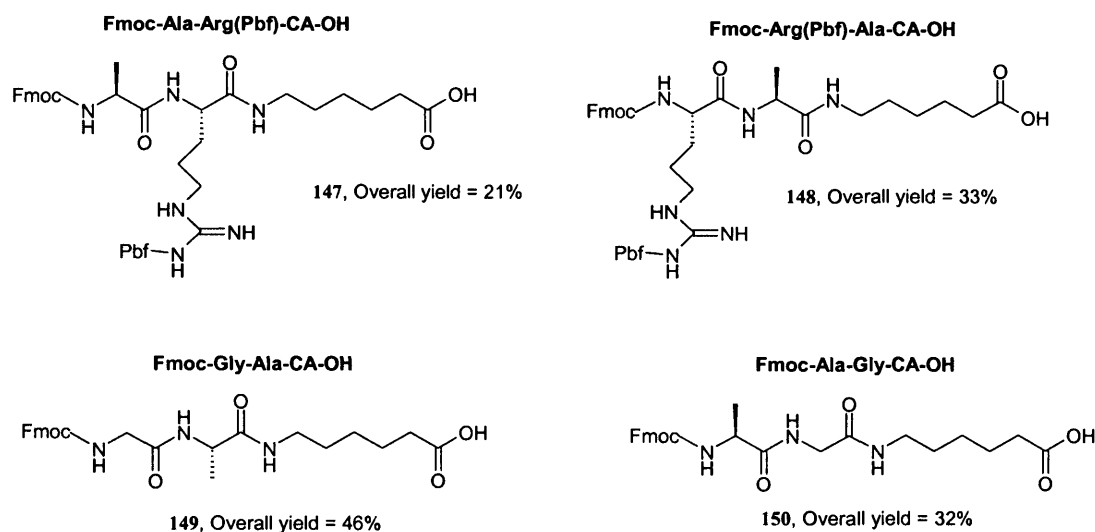
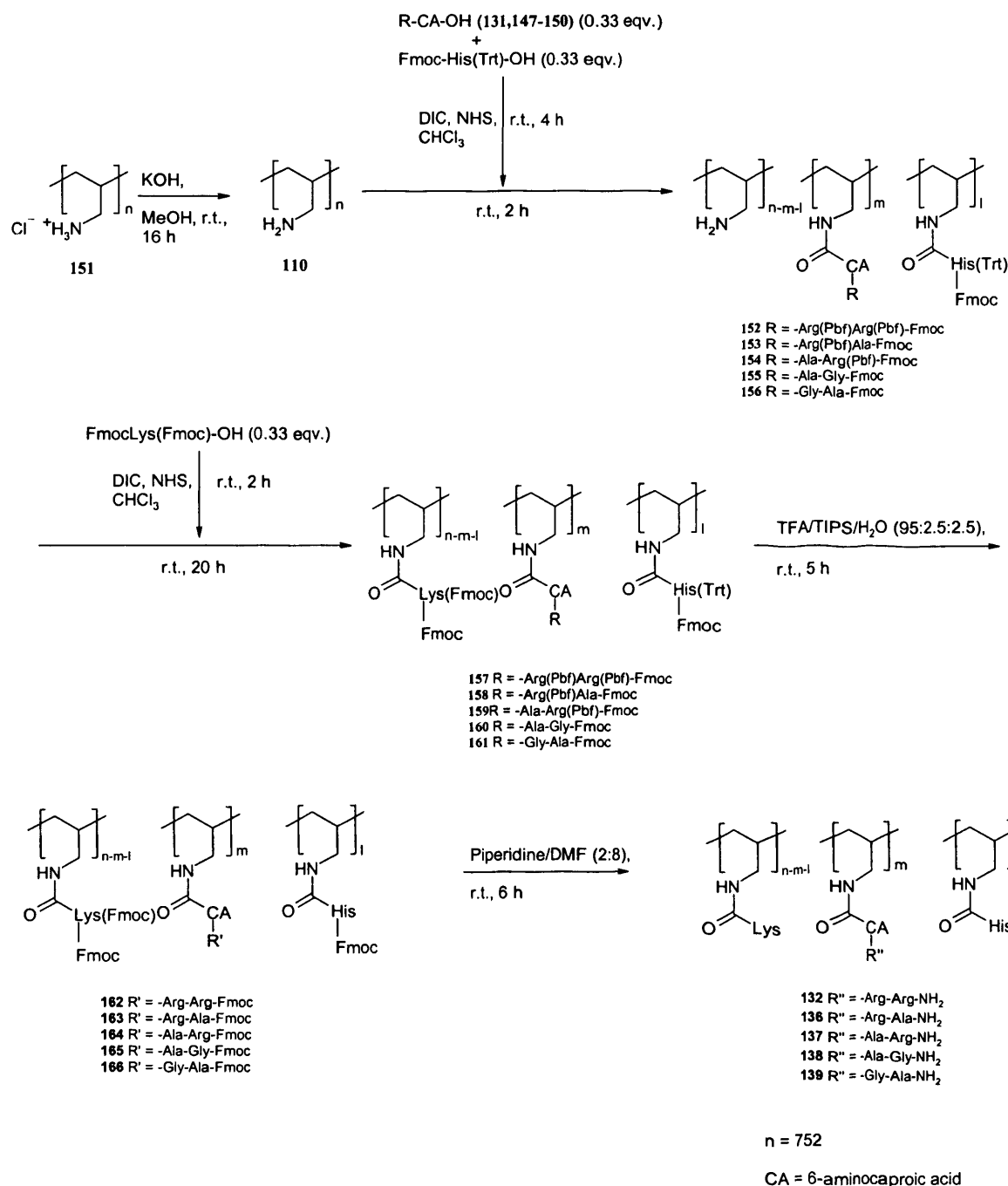


Figure 2.3.3 Additional tripeptide binding groups prepared.

2.3.2 Synthesis of artificial esterases containing a polyallylamine backbone

All of the polymers were synthesised using the same procedure as shown in **Scheme 2.3.3**. Polyallylamine hydrochloride **151** ($n = 752$), was converted to its free base using potassium hydroxide in methanol.⁹⁹ It was important that both the peptide binding sites and histidine catalytic unit were incorporated into the polymer at the same time, as it was hoped that this would allow them to influence the positioning of each other on the polymer backbone. Hence, the peptide binding groups (**131**, **147-150**) and the histidine catalytic residue were coupled to the polymer, simultaneously, using *N*-hydroxysuccinimide and DIC to give **152 – 156** (**Scheme 2.3.3**).

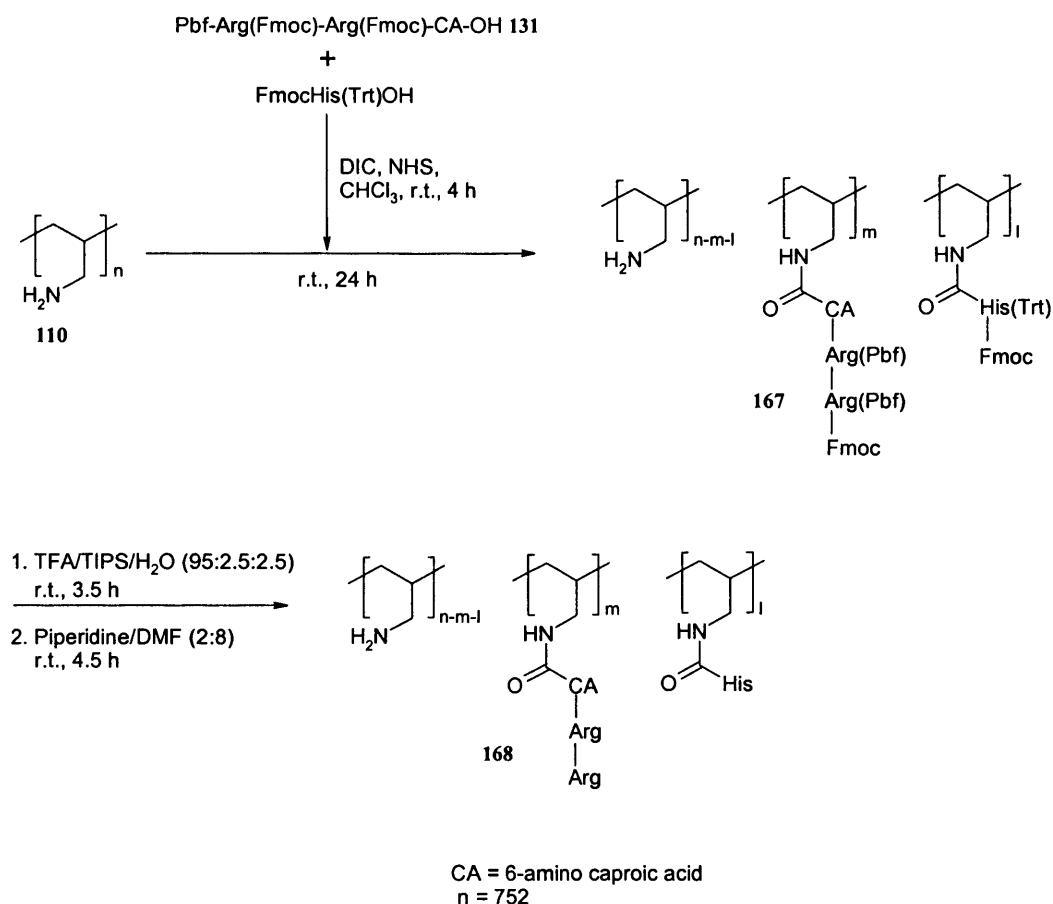


Scheme 2.3.3 Synthesis of artificial esterases **132** and **136 – 139**.

The next step was to couple the lysine residue and this was achieved by attaching Fmoc protected lysine to form polymers **157 – 161**. The resulting polymers (**157 – 161**) consisted of the peptide binding group, a histidine catalytic unit and a hydrophilic lysine group in approximately 1:1:1 ratio (based upon equivalents of amino acids used). The deprotection of the acid labile protecting groups (Pbf and Trt) was achieved by sonication of the polymers in a mixture of TFA/triisopropylsilane(TIPS)/water. Some

problems were encountered during the purification of polymers **162** – **166**. Purification by washing the polymer with TFA and water at the end of the reaction, as previously reported, was only suitable for polymers **162** and **164**.⁹⁰ For all of the other polymers, (**163**, **165** and **166**), purification could not be conducted due to their solubility in TFA. Instead, these polymers were precipitated by addition of water, followed by washing with a suitable organic solvent such as methanol or DCM. The concluding step involved the cleavage of the base labile Fmoc protecting groups using a mixture of piperidine/DMF to give the initial set of artificial esterases (**132**, **136** – **139**) (**Scheme 2.3.3**).

The final artificial esterase (**168**) to be synthesised consisted of the Arg-Arg binding unit and the histidine catalytic residue as before. However, we decided to exclude the lysine moiety leaving a third of the amine sites on the polymer unoccupied. The rationale in this instance was to make the polymer more soluble in an aqueous environment. The synthesis was carried out in an analogous manner to that previously described (**Scheme 2.3.4**).



Scheme 2.3.4 Synthesis of artificial esterase **168** (no lys).

2.3.3 Characterisation of polymers

Several problems were encountered when characterising the polymers due to their solubility in organic/aqueous solvents and the limited range of analytical techniques that could be utilized. For the polymers that were partially soluble in organic solvents, solution phase NMR spectroscopy was used. However, several polymers had solubility problems in organic solvents, especially after the protecting groups were cleaved. For these polymers, solution NMR was not possible and characterisation was attempted using solid state carbon NMR. For cases where no proton or carbon NMR spectra could be obtained, structure assignment was made only on the basis of infra-red (IR) data. For polymer **137**, no NMR characterisation was possible due to formation of an insoluble gum. The gum could not be packed appropriately into the NMR rotor, and hence an acceptable solid state carbon NMR could not be obtained. Hence, the proposed structural assignment was based on the previous compound (**164**) in that synthetic sequence (**Scheme 2.3.3**). See Appendix for selected examples of NMR spectra.

2.4 Synthesis of initial ester substrates

At the outset, we were interested in making two differing ester substrates for studies of hydrolysis reactions including the phenethyl ester **127**, (**Figure 2.4.1**) which was the original ester tested previously,⁹¹ and secondly the cinnamyl ester **169** (**Figure 2.4.1**). As mentioned earlier, during the hydrolysis of **127**, the formation of alcohol could not be monitored due to its poor UV absorbance.⁹⁰ It was hoped that the ester **169** would circumvent this problem, with the cinnamyl alcohol having a much better UV absorbance. It was also desirable to monitor the alcohol formation as well as acid formation after hydrolysis because the acid product is structurally very similar to the ester and hence could stay bound to the artificial esterase, after the hydrolysis reaction has occurred, thus giving an inaccurate indication of the quantity of product that is truly being formed.

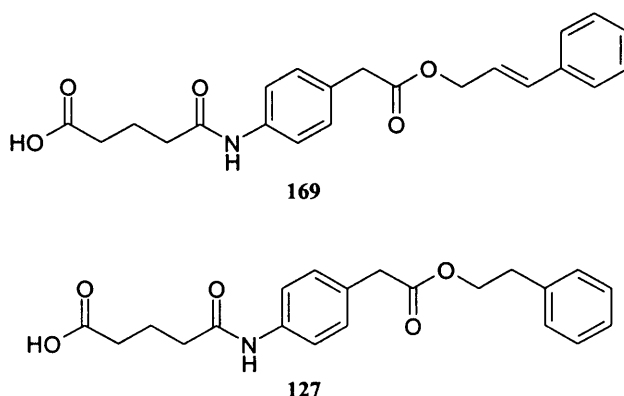
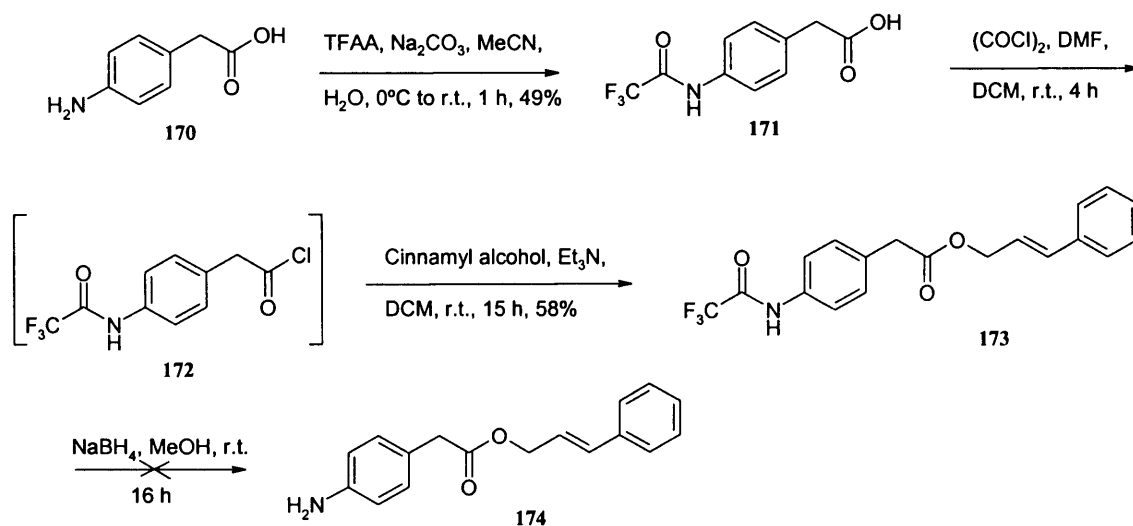


Figure 2.4.1 Initial ester substrates targeted.

2.4.1 Preparation of cinnamyl ester substrate

The synthesis of cinnamyl ester **169** was initially attempted, following the methodology previously used to generate the phenethyl ester **127** (Scheme 2.4.1).^{90,91}



Scheme 2.4.1 Attempted route to cinnamyl ester **169**.

Commercially available *p*-aminophenylacetic acid **170** was protected using trifluoroacetic anhydride to afford carboxylic acid **171**. Acid **171** was then converted to the acid chloride using oxalyl chloride to give **172**. Attempts to isolate **172** were unsuccessful due to degradation of the product. Therefore, the synthesis of ester **173** was attempted by generating the acid chloride *in situ* and then trapping it with cinnamyl

alcohol. This successfully provided ester **173** in 58% yield. Deprotection of the trifluoroacetamide moiety proved problematic. Sodium borohydride in methanol was initially attempted, however only the hydrolysed product **175** (**Figure 2.4.2**) was detected suggesting that either the conditions were too basic or the ester was highly labile.

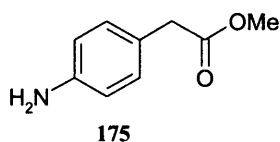


Figure 2.4.2 By-product **175** detected during sodium borohydride deprotection of **173**.

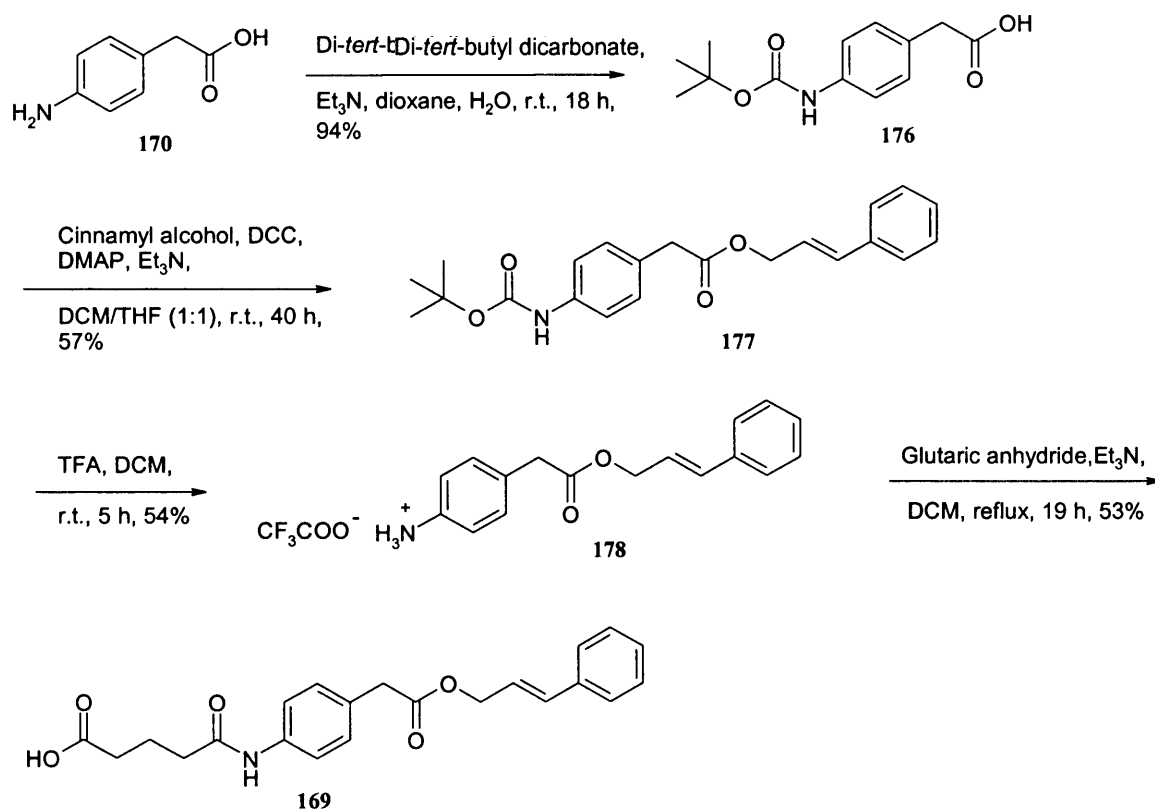
Subsequently, a number of different reaction conditions were investigated to isolate the deprotected amine **174** (**Table 2.4.1**). Initially a shorter reaction time was attempted (entry 1). However, t.l.c. and NMR spectra analysis indicated that the hydrolysis of the ester **173** commences upon addition of NaBH₄. The addition of NaBH₄ in methanol at 0 °C was also attempted (entry 2), because it was thought that NaBH₄ was too reactive at room temperature. However this too resulted in ester hydrolysis. The use of potassium carbonate in water and methanol is another common method of removing the trifluoroacetamide group (entry 3),¹⁰⁰ however hydrolysis of the ester was also observed.

Entry	Reagent Used	Solvent	Temperature (°C)	Reaction Time (hours)
1	NaBH ₄	MeOH	20	2
2	NaBH ₄	MeOH	0, then 20	6
3	K ₂ CO ₃	MeOH, H ₂ O	20	2

Table 2.4.1 Different conditions attempted for trifluoroacetamide deprotection of **173**.

Due to difficulties encountered with the trifluoroacetamide group, it was decided that a different protecting group should be utilized. The Boc group was used as an alternative

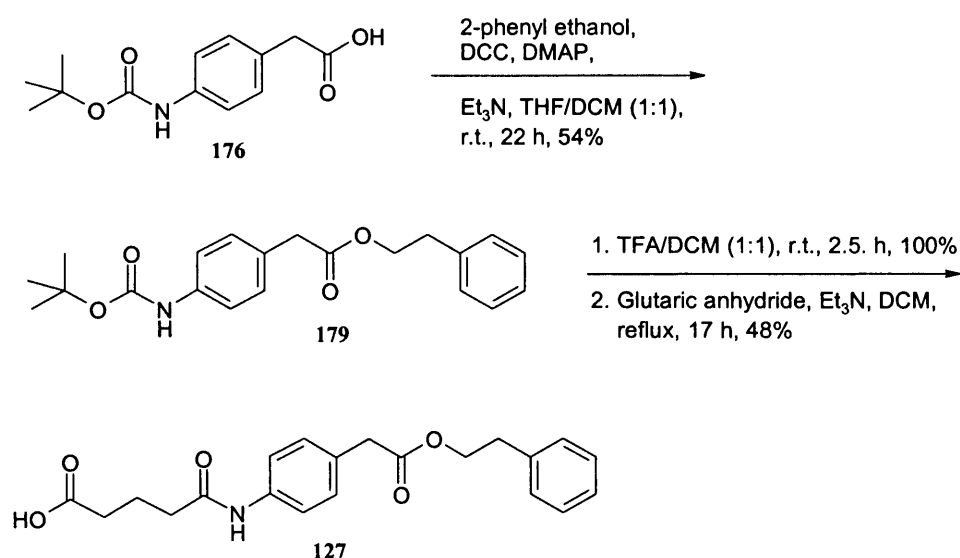
and the synthesis of a Boc protected cinnamyl ester derivative **177** was attempted (**Scheme 2.4.2**). Boc protected amine **176** was prepared using di-*tert*-butyl dicarbonate and triethylamine to give the acid **176** in 94% yield. The carboxylic acid **176** was subsequently converted to the ester **177** using dicyclohexylcarbodiimide (DCC). Initially an attempt to deprotect the amine **177** using a mixture of TFA/DCM (1:1) was unsuccessful, due to hydrolysis of the ester moiety. Several different ratios were investigated for deprotection, and the optimal conditions used a 4% v/v solution of TFA in DCM. This generated the free amine in an acceptable yield of 54%. Subsequent coupling of amine **178** with glutaric anhydride then afforded the desired cinnamyl ester **169**.



Scheme 2.4.2 Synthesis of cinnamyl ester substrate **169**.

2.4.2 Synthesis of phenethyl ester substrate

Due to the problems associated with the trifluoroacetamido protecting group during the synthesis of cinnamyl ester **169**, we decided not to follow this route. Instead, we elected to synthesise phenethyl ester **127** following the route already established for the cinnamyl ester **169** (Scheme 2.4.2). Thus, the acid **176** was coupled to phenethyl alcohol using DCC, giving ester **179** in 54% yield (Scheme 2.4.3). Deprotection of the Boc group using TFA/DCM, and subsequent reaction with glutaric anhydride furnished the desired phenethyl ester substrate **127**.



Scheme 2.4.3 Synthesis of phenethyl ester substrate **127**.

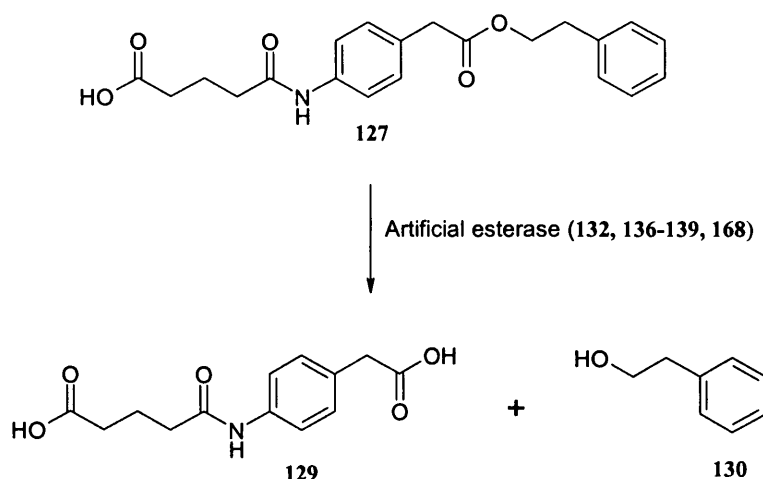
2.5 Activity of artificial esterases

With the polymer catalysts and substrate esters now in hand, we turned our attention towards an investigation of the potential activity of artificial esterases. Before testing the polymers as catalysts for the hydrolysis of ester substrates, a control reaction was carried out in order to assess hydrolysis in the absence of the polymers. A solution of each of the esters **127** and **169** was prepared in phosphate buffer at pH 7 and stirred for

24 hours. The reactions were monitored by HPLC and this confirmed that no hydrolysis had occurred.

2.5.1 Hydrolysis of phenethyl ester **127**

The polymers were first of all tested for their ability to hydrolyse ester **127** (**Scheme 2.5.1**). Although it is difficult to quantify the number of binding sites and catalytic groups within our esterase polymers, we estimated that the amount of polymer used in all of all these reactions was approximately 5 mol % at a 0.5 mM ester concentration. The reactions were initially monitored by observing a decrease in ester concentration and/or an increase in acid production.



Scheme 2.5.1 Hydrolysis of phenethyl ester **127**.

The first polymer to be tested was **132** and contained the Arg-Arg motif which on the basis of binding to the phosphonate transition state analogue, was expected to display good activity. The first observation made was that the isolation technique used for the polymer had an effect on its activity. More specifically, in the final step of the synthesis of **132**, which involved washing the polymer with water, however, it was observed that the polymer changed from a white solid to a gum. This polymer batch (**132**) (**Table 2.5.1**, entry 1) had no hydrolytic activity, whereas another batch of polymer **132**, which had no aqueous wash, was active (**Table 2.5.1**, entry 2). In order to investigate this

further, the two batches of polymer **132** were examined using scanning electron microscopy (SEM) (**Figure 2.5.1**).

Entry	Polymer containing binding site R	Solvent	Hydrolysis observed?	Conversion to product (%) ^a
1.	132 , R = Arg-Arg (aqueous wash)	Phosphate buffer pH 7	No	-
2.	132 , R = Arg-Arg (no aqueous wash)	Phosphate buffer pH 7	Yes	20

Table 2.5.1 Effect of aqueous wash on polymer (**132**) activity. In a typical experiment, the polymer (10 mg) was added to a stirred solution of ester in aqueous buffer (0.5 mM, 1 ml) at room temperature. The reaction was monitored by HPLC. ^a The % conversions shown are the best results obtained after testing several different batches of the same polymer after 24 h.

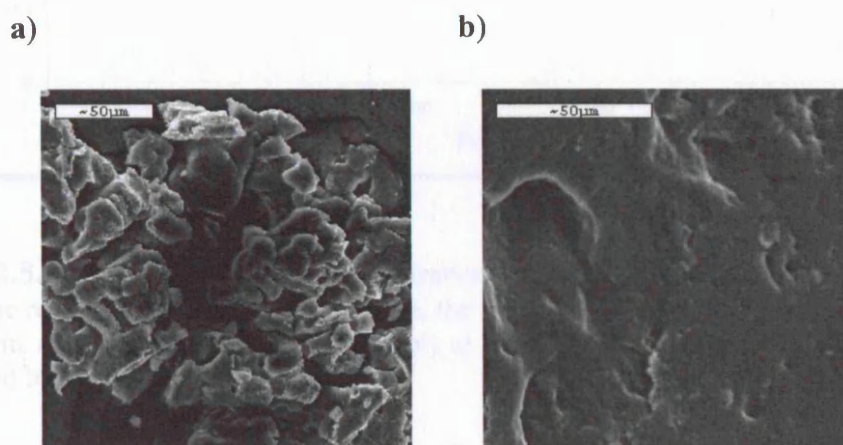


Figure 2.5.1 Scanning electron micrograph showing a) Polymer **132** before aqueous wash and b) Polymer **132** after aqueous wash.

The scanning electron micrograph (a) (**Figure 2.5.1**) indicates that before the aqueous wash, the polymer has an obvious tertiary structure. Conversely the same polymer is shown in picture (b) (**Figure 2.5.1**) after an aqueous wash, indicating that the tertiary structure is completely destroyed and hence a loss of activity is observed.

After establishing, as expected, that polymer **132** could hydrolyse ester **127**, our next goal was to follow the consumption of ester **127** and formation of acid **129** over unit time (**Figure 2.5.2** and **2.5.3**).

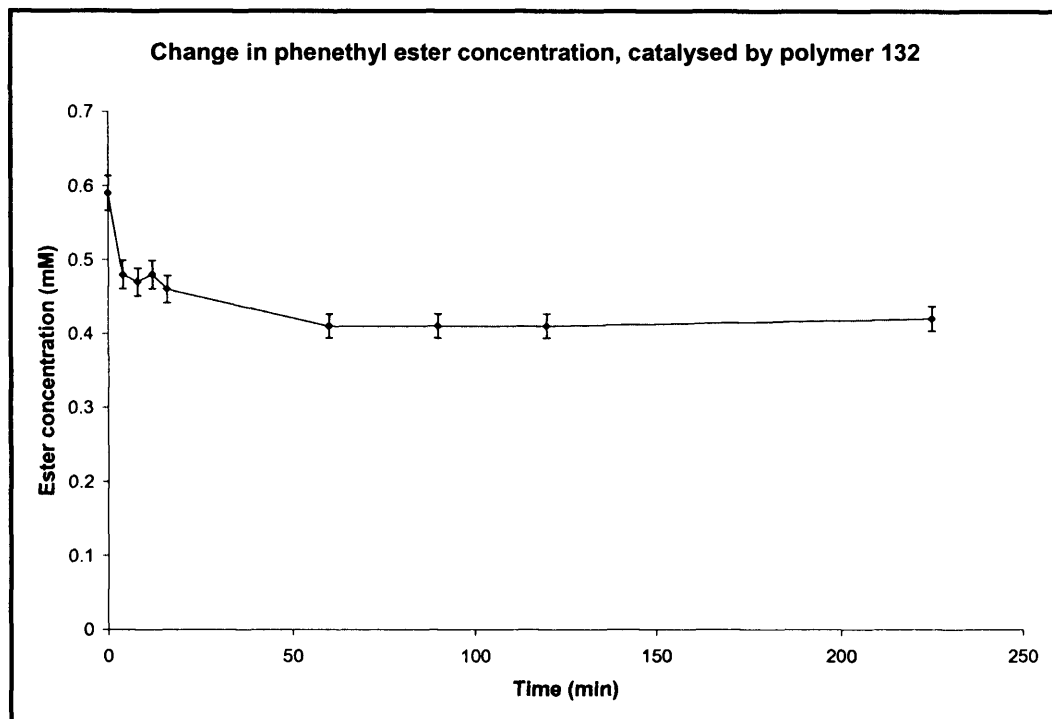


Figure 2.5.2 A plot of ester (**127**) concentration against time for polymer **132** over the first 225 min of the reaction. In a typical experiment, the polymer (10 mg) was added to a stirred solution of ester in aqueous buffer (0.5 mM, 1 ml) at room temperature for 24 h. The reaction was monitored by HPLC.

The hydrolysis reaction was monitored closely over 225 minutes and an additional measurement was recorded at 24 hours. The single measurement taken after 24 hours (not shown in **Figure 2.5.3**) had indicated that there was some further increase in acid concentration overnight. This indicates that it is possible that the acid formation was monitored at the wrong time frame and that perhaps, the ‘real’ catalysis may be occurring after a period of 225 minutes rather than at the beginning of the reaction as initially anticipated. It should be noted that when several different batches of polymer **132** were prepared and tested, they all exhibited some hydrolysis, however not with the same efficiency. Hence, the different batches all give different amounts of acid product, with the best polymer showing 20% conversion to the product, after 24 hours. This is comparable with the results obtained previously with this same polymer, under the same

conditions.⁹¹ It should be highlighted however, that performing the hydrolysis reactions with the *same* batch of polymer, similar results were obtained. Clearly, polymers of this type, as implied by the scanning electron micrograph study, are extremely sensitive to the exact nature of the surrounding environment and may undergo drastic changes in tertiary structure.

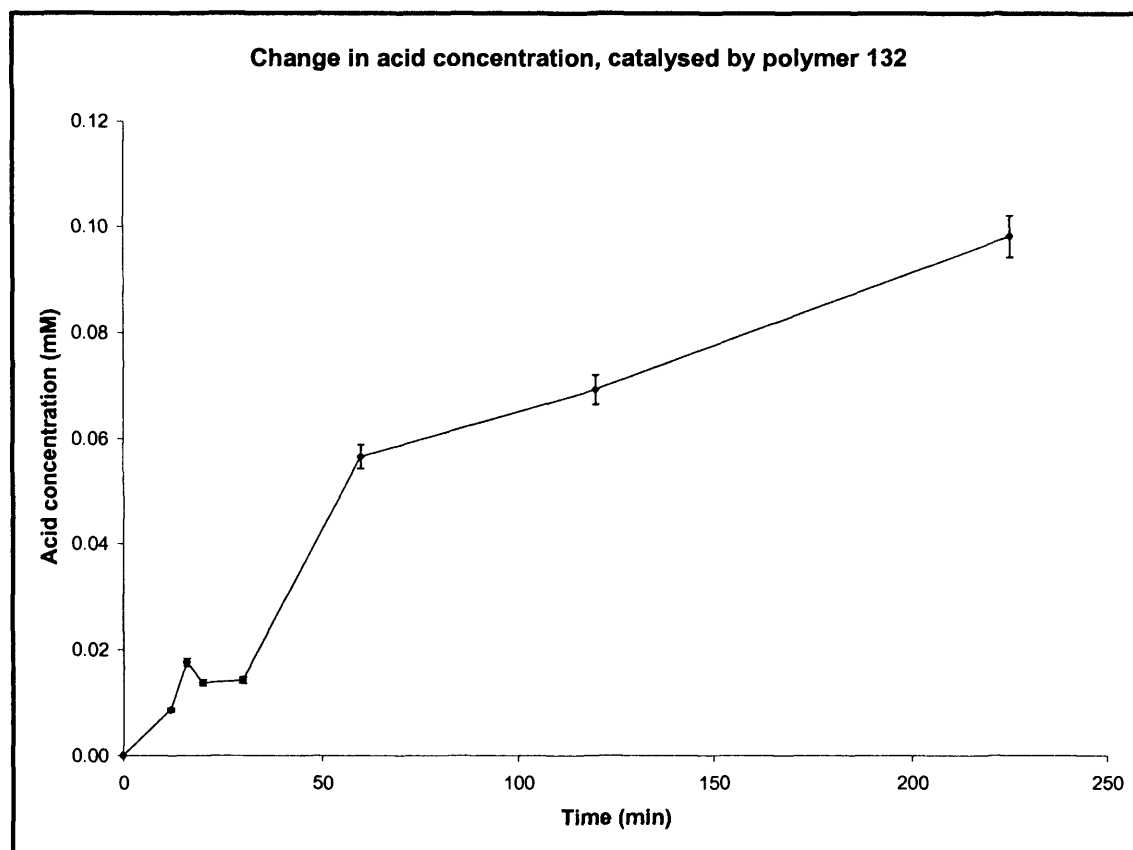


Figure 2.5.3 A plot of acid (**129**) concentration against time for polymer **132** over the first 225 min of the reaction. In a typical experiment, the polymer (10 mg) was added to a stirred solution of ester (**127**) in aqueous buffer (0.5 mM, 1 ml) at room temperature for 24 h. The reaction was monitored by HPLC.

2.5.2 The activity of artificial esterases containing different binding sites

The next stage of our investigation was to determine how changes in the peptide binding site within the polymer would influence activity. The results of the five different polymers in the hydrolysis of ester **127** (Scheme 2.5.1) are presented in Table 2.5.2.

Entry	Polymer containing binding group R	Solvent	Hydrolysis observed?	Conversion to product (%) ^a	NMR binding studies, Rd (%) ⁹¹
1	132 , R = CA-Arg-Arg	Phosphate buffer pH 7	Yes	20	17 ± 2
2	136 , R = CA-Arg-Ala	Phosphate buffer pH 7	No	0	Not determined
3	137 , R = CA-Ala-Arg	Phosphate buffer pH7	Yes	15	12 ± 2
4	138 , R = CA-Ala-Gly	Phosphate buffer pH7	No	0	6 ± 1
5	139 , R = CA-Gly-Ala	Phosphate buffer pH7	No	0	6 ± 1
6	168 , R = CA-Arg-Arg (no lys)	Phosphate buffer pH7	Yes	10	17 ± 2

Table 2.5.2 The influence of changing the binding group on polymer activity. In a typical experiment, the polymer (10 mg) was added to a stirred solution of ester **127** in aqueous buffer (0.5 mM, 1 ml) at room temperature. The reaction was monitored by HPLC. ^a The % conversions shown are the best results obtained after testing several different batches of the same polymer after 24 h.

If we compare how the activity of the polymers correlates with the ranking obtained for the binding groups using NMR binding studies, we see only three of the polymers displayed hydrolytic activity (Table 2.5.2, entries 1, 3 and 6 respectively and see also Figure 2.5.4). Polymer **132** (entry 1), containing the CA-Arg-Arg binding site, exhibited the highest activity, with a 20% conversion to the product. Polymer **137** (entry 3), still showed some activity, but possessing weaker binding ability, it displayed 15% conversion to the product. The polymer **136** (entry 2), containing the CA-Arg-Ala dipeptide gave none of the desired hydrolysis products when tested. These results imply

that the majority of the binding to the transition state is performed by the arginine residue which is furthest away from the polymer backbone. The inactivity of polymer **136** could be explained by the fact that the arginine residue is more hindered and hence is unable to participate in effective binding of the transition state for the reaction.

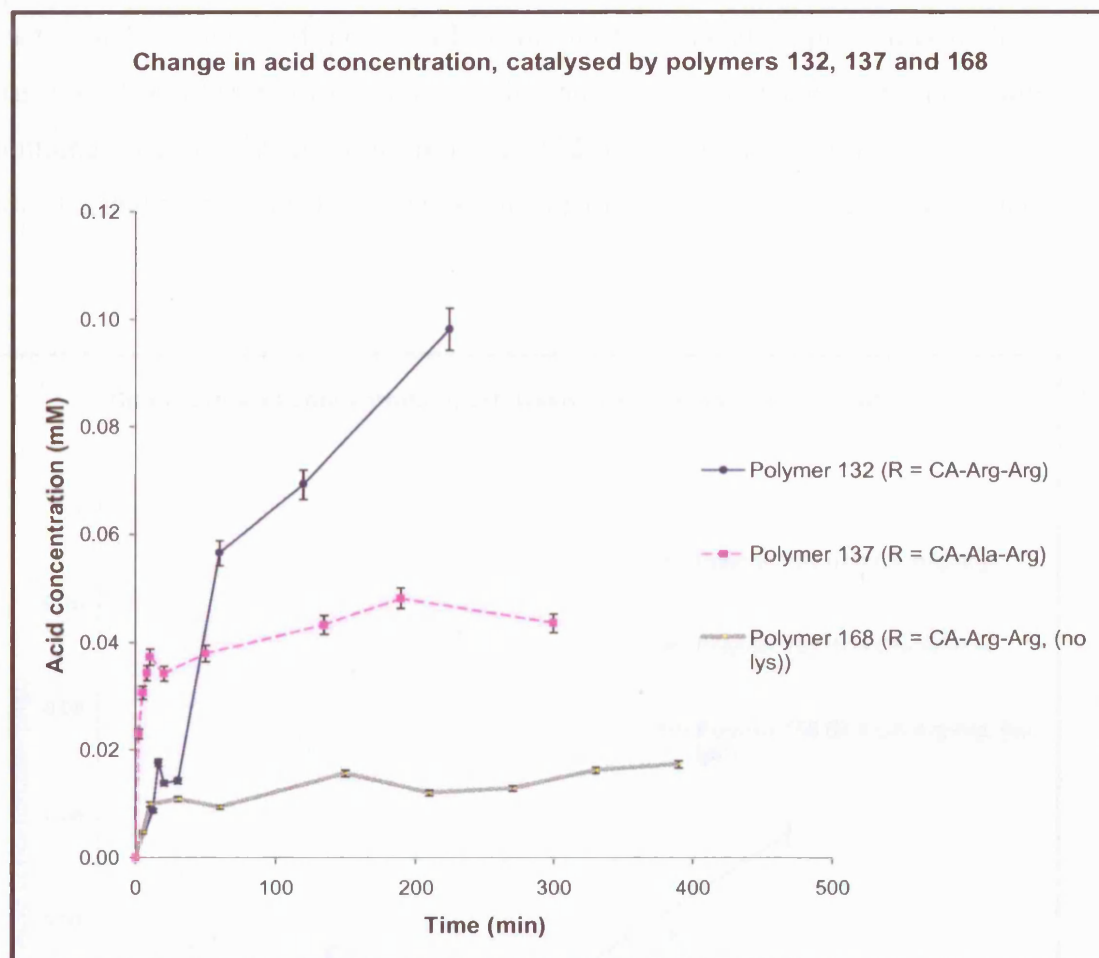


Figure 2.5.4 A plot of acid (**129**) concentration against time for polymers **132**, **137** and **168** over the first 400 min of the reaction. In a typical experiment, the polymer (10 mg) was added to a stirred solution of ester (**127**) in aqueous buffer (0.5 mM, 1 ml) at room temperature for 24 h. The reaction was monitored by HPLC.

The other polymers, containing the weakest binding group, Ala-Gly (Table 2.5.2, entries 4 and 5) demonstrated no activity at all. Finally, polymer **168** (entry 6) which contained no lysine residues also exhibited some hydrolysis (10% product formation, Table 2.5.2). However, unlike all of the other polymers, this polymer was completely soluble in phosphate buffer. We questioned whether the solubility of the polymer might aid catalysis, but this does not seem to be the case, when compared to its analogue,

polymer **132**. One characteristic which all three polymers in **Figure 2.5.4** have in common is the fact that they seem to have the ability to catalyse ester hydrolysis at a very fast initial rate at the beginning of the reaction (within the first 60 min, see **Figure 2.5.5**) and these rates then slow down as illustrated by the curves displaying a type of saturation kinetics. This indicates that product inhibition may be occurring, which is to be expected as the diacid product **129** is produced in the close proximity to the bidentate Arg-Arg. It should be noted again that the same observations apply to these polymers as mentioned previously regarding polymer **132**, the single measurement taken after 24 h, indicates that more hydrolysis was occurring after the period of saturation kinetics.

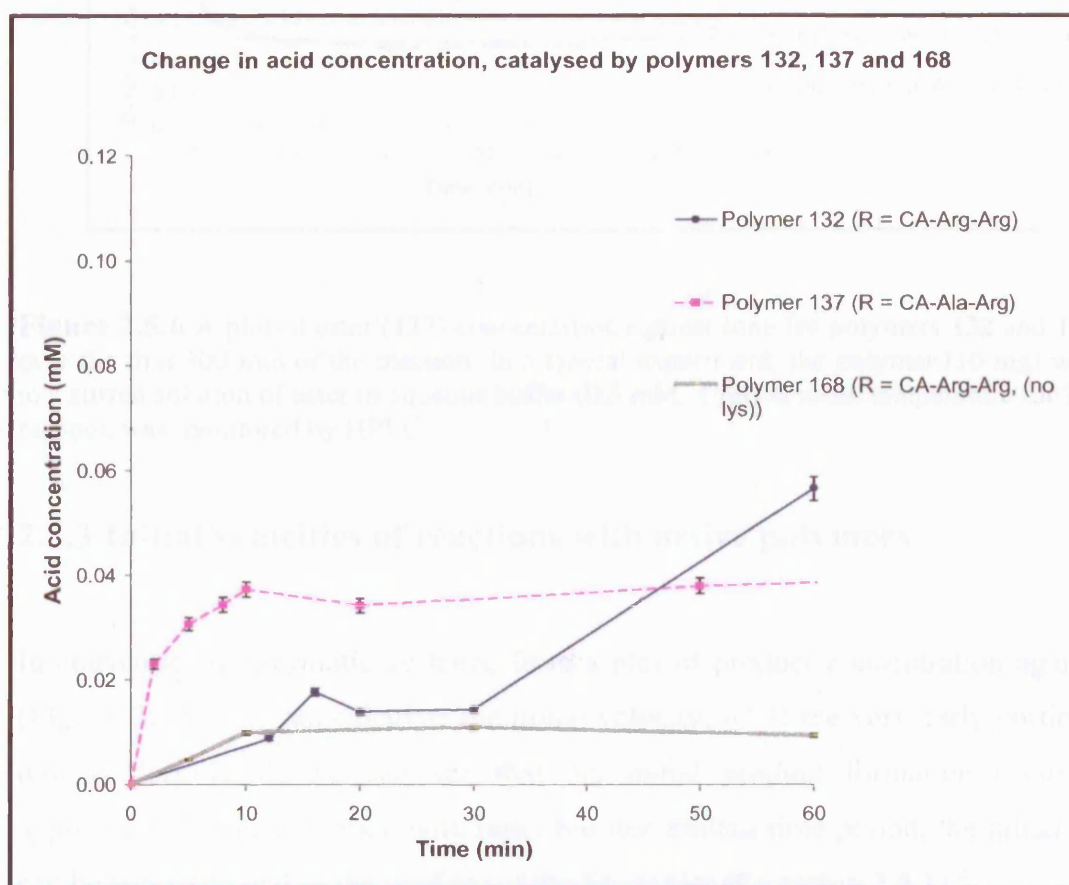


Figure 2.5.5 The graph in **Figure 2.5.4**, expanded to show the first 60 min of the reaction for clarity. In a typical experiment, the polymer (10 mg) was added to a stirred solution of ester **127** in aqueous buffer (0.5 mM, 1 ml) at room temperature for 24 h. The reaction was monitored by HPLC.

One thing that is clear, is that all the polymers are showing a decrease in ester concentration regardless of whether they have the ability to hydrolyse the ester (**Figure**

2.5.6). This is perhaps not surprising, since all the polymers contain a binding group, which should be able to bind the ester substrate to some extent.

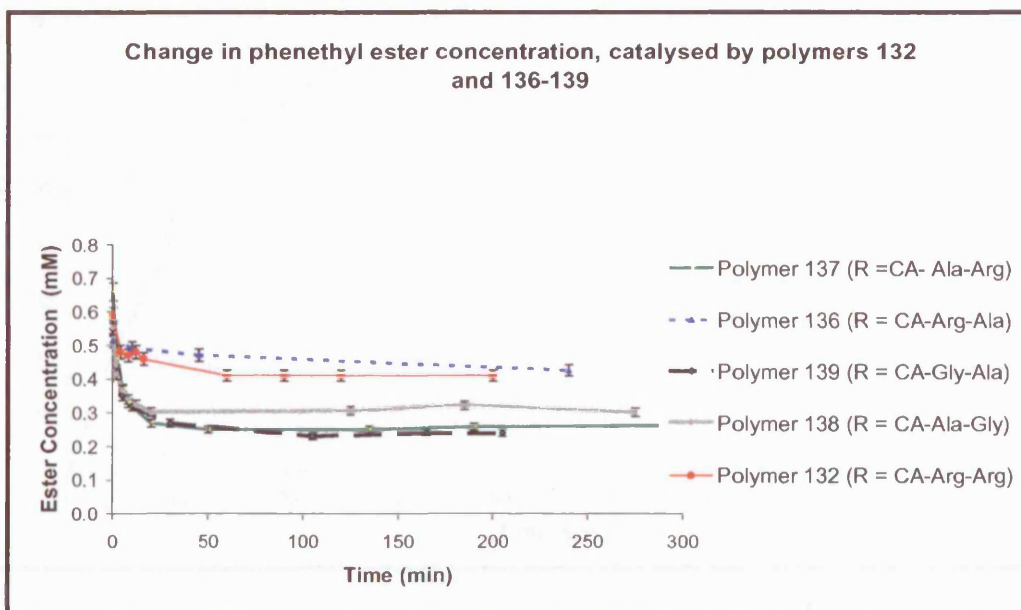


Figure 2.5.6 A plot of ester (**127**) concentration against time for polymers **132** and **136 – 139** over the first 300 min of the reaction. In a typical experiment, the polymer (10 mg) was added to a stirred solution of ester in aqueous buffer (0.5 mM, 1 ml) at room temperature for 24 h. The reaction was monitored by HPLC.

2.5.3 Initial velocities of reactions with active polymers

In conventional enzymatic systems, from a plot of product concentration against time (**Figure 2.5.7**) one can calculate the initial velocity, v .² If the very early portion of the plot is considered, we can see that the initial product formation occurs in an approximately linear fashion with time. For this limited time period, the initial velocity can be approximated as the gradient of the linear plot (**Equation 2.5.1**).²

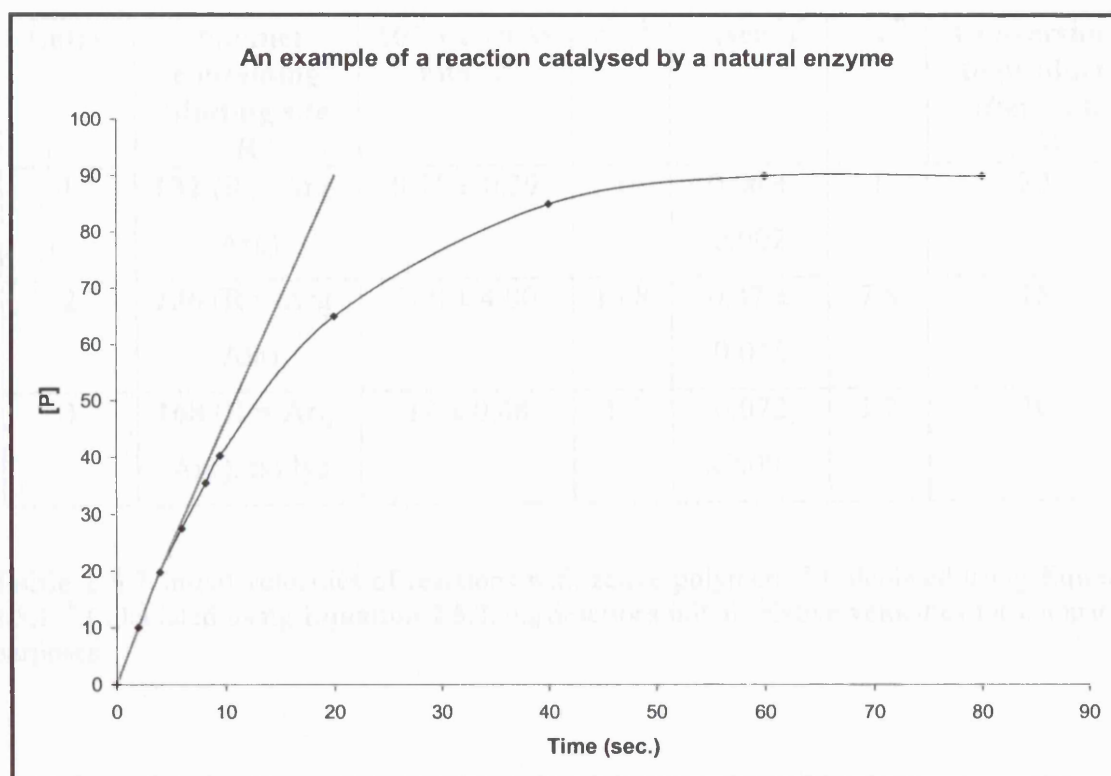


Figure 2.5.7 Representation of product formation for a typical enzyme catalysed reaction.²

$$v = \Delta[P]/\Delta t$$

Equation 2.5.1

Using this technique, we attempted to calculate the initial velocities from the plots shown in **Figure 2.5.4**. This was problematic in the instance of polymer **132**, since the points are very scattered. Hence the initial velocity was calculated on the basis of a best fit line, between the first few points of the graph. For the other two polymers, the method described above was used and the results are presented in **Table 2.5.3**.

Entry	Polymer containing binding site R	$10^{-4} \times v$ (mM min ⁻¹) ^a	v_{rel} ^a	v (sec ⁻¹) ^b	v_{rel} ^b	Conversion to product after 24 h (%)
1	132 (R = Arg-Arg)	9.71 ± 0.39	1	0.06 ± 0.002	1	20
2	136 (R = Arg-Ala)	100 ± 4.00	13.8	0.47 ± 0.018	7.8	15
3	168 (R = Arg-Arg), no lys	12 ± 0.48	1.7	0.072 ± 0.003	1.2	10

Table 2.5.3 Initial velocities of reactions with active polymers. ^a Calculated using **Equation 2.5.1**. ^b Calculated using **Equation 2.5.2**. v_{rel} describes initial relative velocities for comparison purposes.

The calculated initial rates should be interpreted with caution as they are approximated. For example polymer **132** (**Table 2.5.3**, entry 1), which displayed the best binding ability towards the transition state has a very slow initial velocity. However this same polymer (**132**) gave the highest conversion to hydrolysis products after 24 h. It is difficult to conclude what is happening within the micromolecular environment of the polymer from these results. Nevertheless, it is tempting to speculate that the Arg-Arg binding unit in polymer **132** is, in effect, too efficient at both substrate and product binding whereas the Arg-Ala unit (polymer **136**) can release the product more easily hence contribute to enhanced turnover.

There is another way of calculating initial velocities and this is from using the UV absorptions monitored during our reaction. Having established a single specific time point within the linear time period, the initial velocity is determined from the difference in UV absorbance at that time point and at the initiation of the reaction divided by the time (**Equation 2.5.2**):²

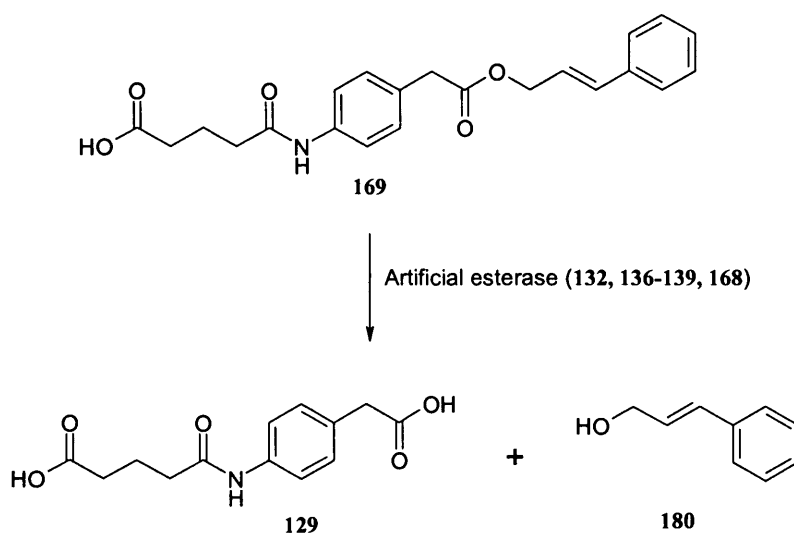
$$v = \Delta I / \Delta t = I_t - I_0 / t_{\text{reading}}$$

Equation 2.5.2

The intensity of the signal being measured at time t and time zero is given by I_t and I_0 , respectively and t_{reading} is the time interval between initiation of the reaction and measurement of the UV response. Using this method, essentially gives similar relative initial velocities compared to the first method.

2.5.4 Hydrolysis of cinnamyl ester 169

The next stage was to test the ability of the polymers to hydrolyse the cinnamyl ester substrate **169** (Scheme 2.5.2). As previously mentioned, we believed that the acid product remained bound to the polymer after hydrolysis (as demonstrated by saturation curves shown in Figure 2.5.4). This meant that the concentration of acid product **129** produced was potentially inaccurately monitored. Hence, monitoring the release of alcohol would be more suitable, as it cannot form ionic salts. Since efforts to monitor the release of the alcohol during the hydrolysis of the phenethyl ester **127** were unsuccessful because of its poor UV absorbance, we felt that the introduction of a more UV active alcohol would help solve this problem.



Scheme 2.5.2 Hydrolysis of cinnamyl ester **169**.

In the event, to our dismay, it was observed that the cinnamyl ester **169**, was completely insoluble in phosphate buffer at pH 7. However, since the ester was soluble in acetonitrile, the hydrolysis reaction was first attempted in a mixture of phosphate

buffer/acetonitrile (1:1) (entry 1, **Table 2.5.4**). At this stage, no reduction in ester or any formation of the products (acid **129** or alcohol **180**) was observed. Fortunately, however, a combination of buffer/acetonitrile in a 99:1 ratio has been employed in comparable artificial systems¹⁰¹ and by using this solvent combination, polymer **132** exhibited catalysis (entry 2, **Table 2.5.4** and **Figures 2.5.8, 2.5.9**). The more soluble analogue, polymer **168** also demonstrated hydrolysis of the ester **169** (entry 3, **Table 2.5.4** and **Figures 2.5.8, 2.5.9**), but gave a smaller conversion to product when compared to **132**. Due to the ester being very labile (as we experienced during the TFA deprotection, see Section 2.4.1), we tested whether the ester would spontaneously hydrolyse, in the absence of polymer, however this was not the case (entry 4, **Table 2.5.4**).

Entry	Polymer	Solvent	Hydrolysis observed?	$10^{-4} \times v$ (mM min ⁻¹) ^a	v_{rel}	Conversion to product after 24 h (%) ^b
1.	132 , R = CA-Arg-Arg	Buffer/ MeCN (1:1)	No	-	-	0
2.	132 , R = CA-Arg-Arg	Buffer/ MeCN (99:1)	Yes	15 ± 0.60	1.8	86
3.	168 , R = CA-Arg-Arg, no lys	Buffer/ MeCN (99:1)	Yes	8.5 ± 0.34	1	49
4.	No polymer	Buffer/ MeCN (99:1)	No	-	-	0

Table 2.5.4 Hydrolysis of cinnamyl ester **169**. In a typical experiment, the polymer (10 mg) was added to a stirred solution of ester in aqueous buffer/acetonitrile (99:1) (0.5 mM, 1 ml) at room temperature. The reaction was monitored by HPLC. ^a Calculated using **Equation 2.5.1**. ^b The % conversions shown are the best results obtained after testing several different batches of the same polymer after 24 h, as monitored by HPLC. v_{rel} describes initial relative velocities for comparison purposes.

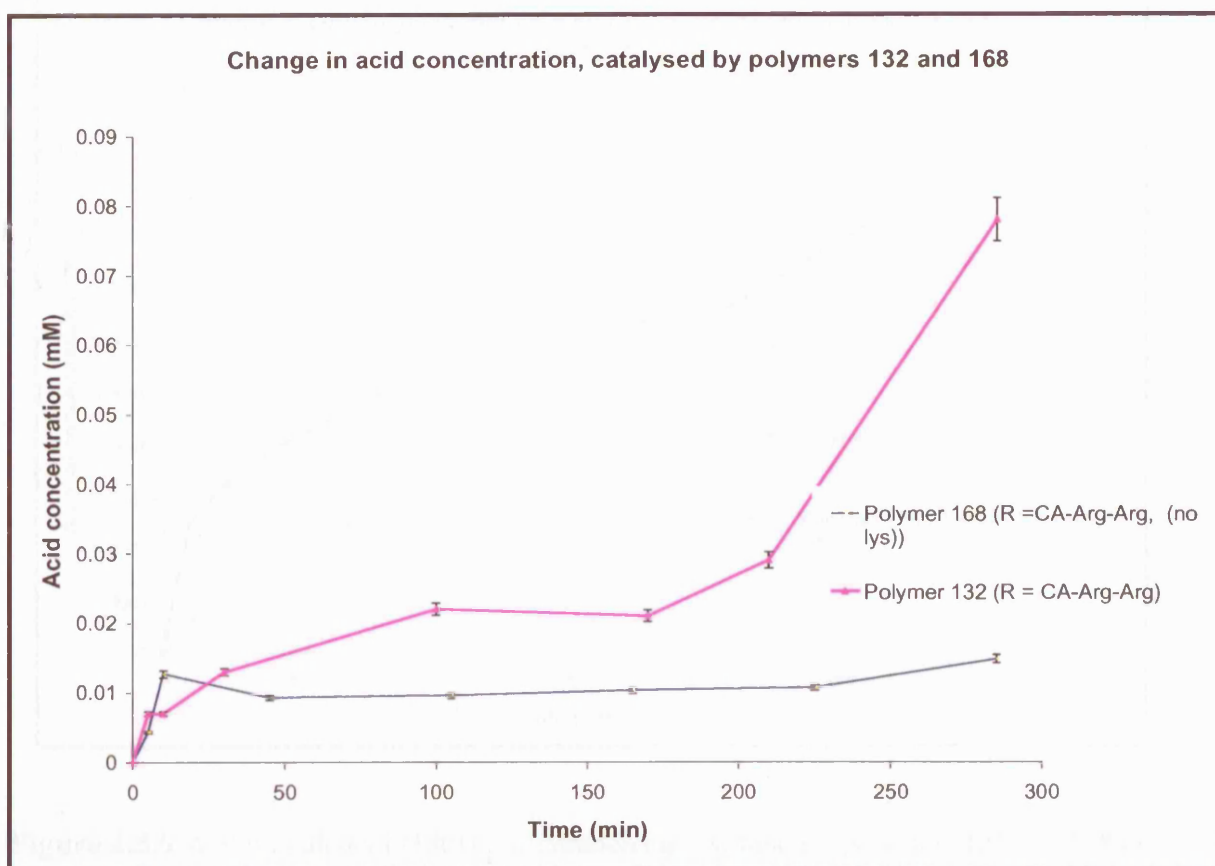


Figure 2.5.8 A plot of acid (**129**) concentration against time for polymers **132** and **168** over the first 300 min of the reaction. In a typical experiment, the polymer (10 mg) was added to a stirred solution of ester (**169**) in aqueous buffer/acetonitrile (99:1) (0.5 mM, 1 ml) at room temperature for 24 h. The reaction was monitored by HPLC.

As predicted, the formation of both acid **129** (**Figure 2.5.8**) and cinnamyl alcohol **180** (**Figure 2.5.9**) was observed. However, a further problem was encountered here. The acid and the alcohol should be formed in equimolar amounts (assuming that neither one is binding to the polymer), but this did not seem to be the case. According to the results, the acid was forming in a much larger quantity when compared with the alcohol. In the event, we discovered that the reason for this behaviour was that the alcohol is insoluble in the buffer/acetonitrile (99:1) mixture. It is therefore very likely that it was precipitating out during the hydrolysis reaction and hence giving unreliable readings. It is nevertheless encouraging that alcohol formation can be followed by UV detection.

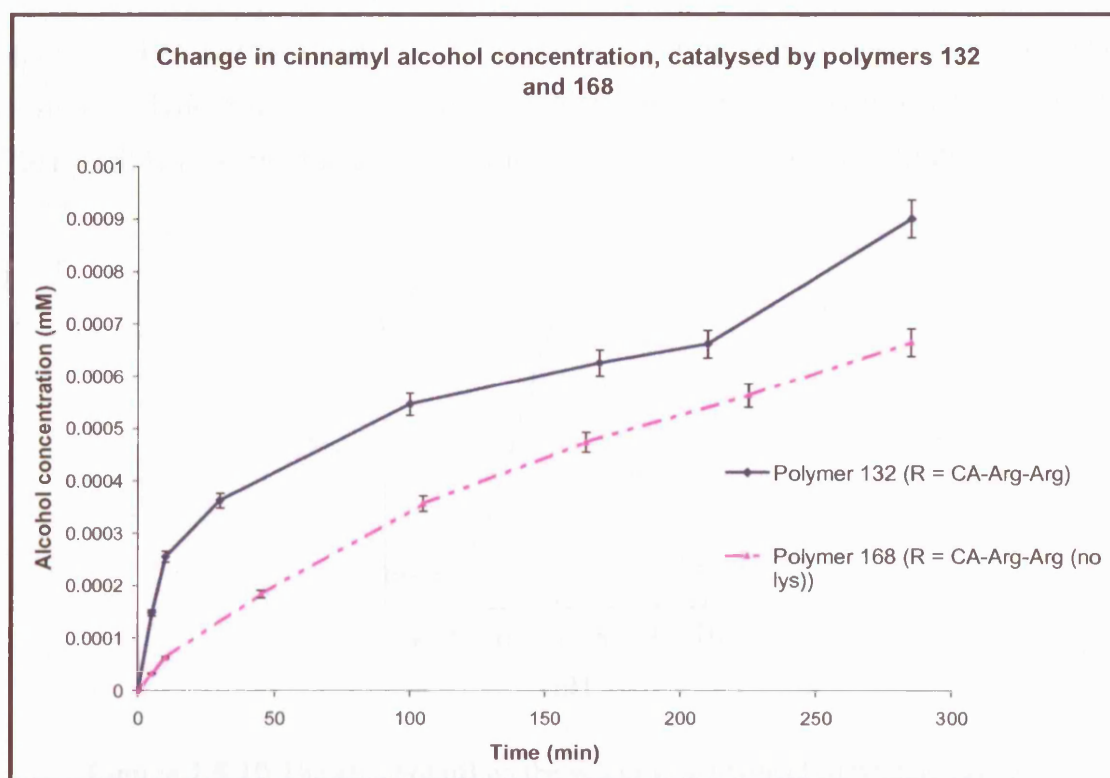


Figure 2.5.9 A plot of alcohol (**180**) concentration against time for polymers **132** and **168** over the first 300 min of the reaction. In a typical experiment, the polymer (10 mg) was added to a stirred solution of ester (**169**) in aqueous buffer/acetonitrile (99:1) (0.5 mM, 1 ml) at room temperature for 24 h. The reaction was monitored by HPLC.

2.5.5 The activity of artificial esterases at different pH

Natural enzymes are very sensitive to the pH of their environment. The pH can affect the binding of substrate, catalytic activity and the tertiary structure of the enzyme.¹ The pH rate profile for a natural esterase enzyme such as chymotrypsin is shown in **Figure 2.5.10** and exhibits a classic bell shaped curve.² The traditional explanation for this behaviour is that the centre (optimum pH) and breadth of the curve depend upon the acid dissociation constant of the relevant amino acid residues within the enzyme. As previously mentioned in the Introduction (Section 1.2.3), chymotrypsin consists of a catalytic triad composed of Asp 102, His 57 and Ser 195. The ability of chymotrypsin to hydrolyse its peptidic substrate depends on hydrogen bonding and proton transfer among the residues of the catalytic triad, which will certainly be affected by the different degrees of ionisation of these residues as the pH is varied. As the diagram in

Figure 2.5.10 illustrates that there is typically a narrow range of pH values over which enzyme catalytic efficiency is maximised. Very extreme pH environments, usually lead to irreversible denaturation of the enzyme, which results in loss of activity.¹

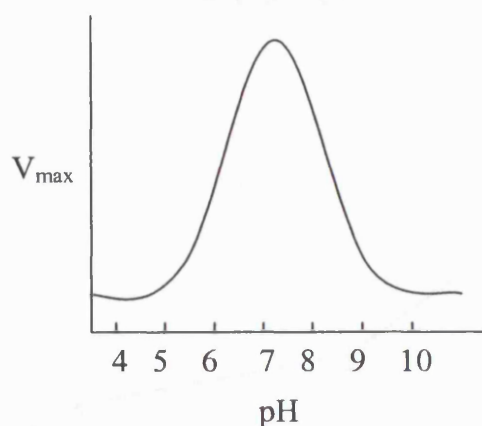


Figure 2.5.10 The effect of pH on the velocity of a typical enzymatic reaction.²

Accordingly, it was of considerable interest to explore the behaviour of our artificial esterase at different pH. For these experiments, it was decided to use the polymer that displayed the most encouraging results, **132** ($R = \text{CA-Arg-Arg}$). The polymer was accordingly stirred in a solution of citrate buffer at pH 6 and borate buffer at pH 8 together with phenethyl ester **127**, under the same conditions as previously employed. The results are shown in **Figure 2.5.11** and **Table 2.5.5**, together with the results at pH 7 for comparison purposes. When comparing the relative initial velocities to the hydrolysis at pH 6, higher initial velocities are observed for reactions at pH 7 (entry 2) and pH 8 (entry 3). The corresponding percentage conversions to the product also show the same trend, with the highest conversion being at pH 8. This indicates that polymer **132**, is more efficient at the beginning of the reaction at pH 7 and pH 8, possibly due to subtle conformational changes within the polymer, which may allow more access to the catalytic residues. The low levels of hydrolysis detected at pH 6 (entry 1), are probably due to most of the free amine sites on the polymer being protonated. As discussed previously, the protonated polymer will be less able to participate in binding both the substrate and the transition state for the reaction. However, in borate buffer at pH 8, when there should be no protonated amines on the residues or backbone, polymer **132** demonstrated significantly higher conversion (entry 3). At pH 8, the acid product **129**

can probably be liberated more easily as its salt, thus freeing the binding site for further reaction.

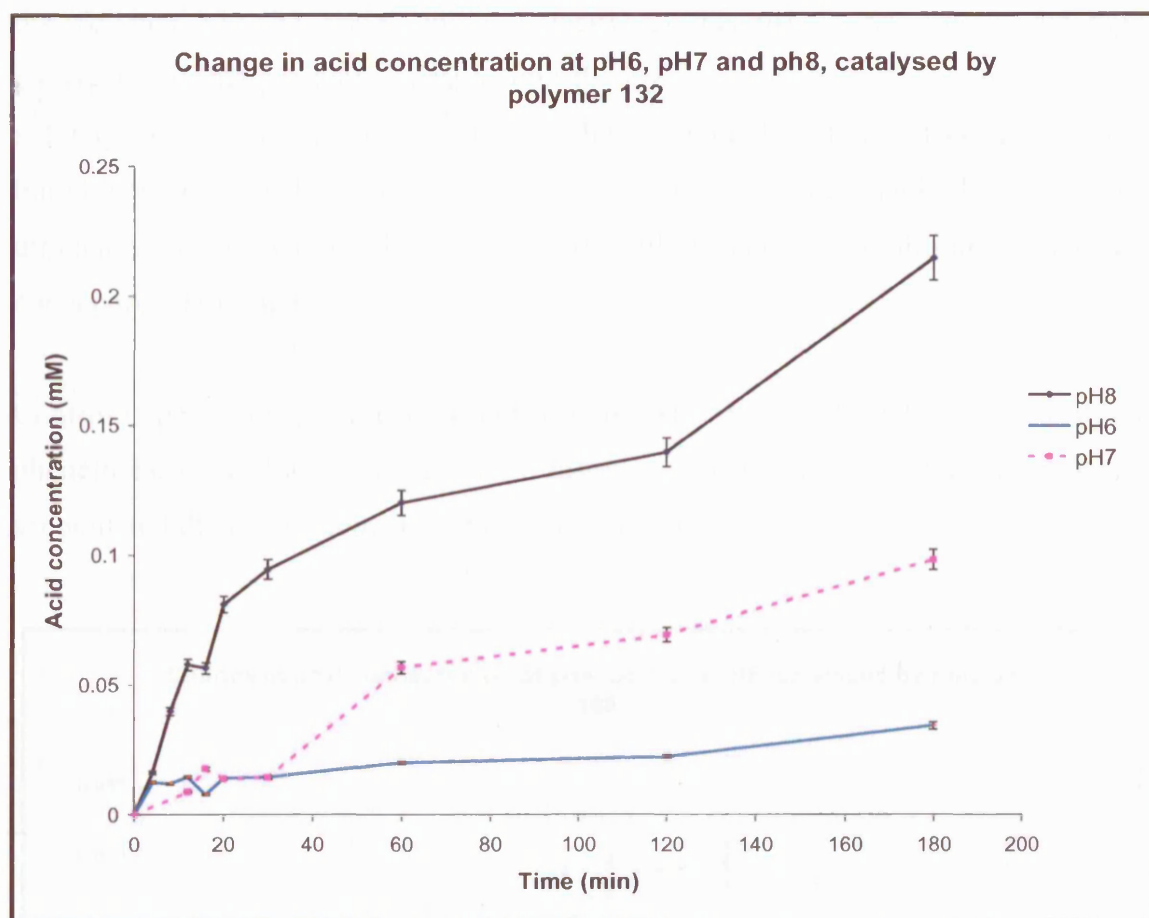


Figure 2.5.11 A plot of acid (**129**) concentration against time for polymer **132**, at pH 6, pH 7 and pH 8 over the first 180 min of the reaction. In a typical experiment, the polymer (10 mg) was added to a stirred solution of ester (**127**) in aqueous buffer (0.5 mM, 1 ml) at room temperature for 180 min. The reaction was monitored by HPLC.

Entry	pH	$10^{-4} \times v$ (mM min ⁻¹) ^a	v_{rel}	Conversion to product after 180 min (%)
1	6	6.87 ± 0.27	1	6
2	7	9.71 ± 0.39	1.4	20
3	8	48.0 ± 1.9	6.9	42

Table 2.5.5 Initial velocities of reactions with polymer **132**, at pH 6, pH 7 and pH 8. ^a Calculated using **Equation 2.5.1**. v_{rel} describes initial relative velocities for comparison purposes.

A similar type of behaviour was also observed with the more soluble polymer **168** (Figure 2.5.12 and Table 2.5.6). However, the percentage conversions to the product do not follow the same pattern as the initial velocities. For example, although at pH 8 the polymer has the lowest initial velocity, at this pH, it also shows the highest conversion to the product. Extrapolating the efficiency of the esterase from the initial velocity alone is risky, as demonstrated here, although polymer **168** has the lowest initial velocity at pH 8, the conversion to product is ultimately higher. Polymer efficiency should therefore be seen as an overall evaluation of both initial velocity and conversion to product.

Control experiments were carried out at both pH 6 and pH 8 and some hydrolysis of phenethyl ester **127** was detected in the absence of the polymer. We have taken this into account and the results shown are the corrected values.

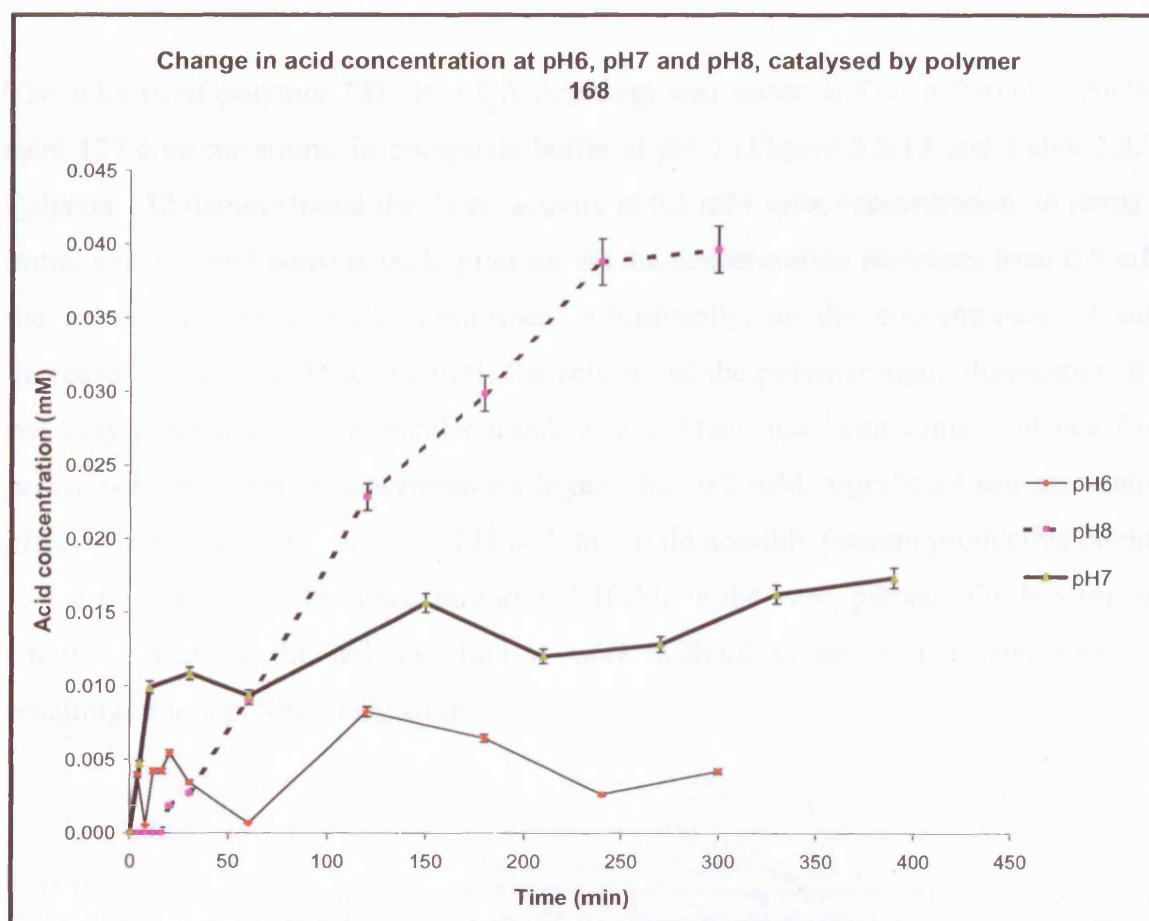


Figure 2.5.12 A plot of acid (**129**) concentration against time for polymer **168**, at pH 6, pH 7 and pH 8 over the first 180 min of the reaction. In a typical experiment, the polymer (10 mg) was added to a stirred solution of ester (**127**) in aqueous buffer (0.5 mM, 1 ml) at room temperature for 24 h. The reaction was monitored by HPLC.

Entry	pH	$10^{-4} \times v$ (mM min ⁻¹) ^a	v_{rel}	Conversion to product after 300 min (%)
1	6	7.11 ± 0.28	4.9	0.8
2	7	9.78 ± 0.39	6.7	2.6
3	8	1.45 ± 0.05	1	7.8

Table 2.5.6 Initial velocities of reactions with polymer **168**, at pH 6, pH 7 and pH 8. ^a Calculated using **Equation 2.5.1**. v_{rel} describes initial relative velocities for comparison purposes.

2.5.6 The activity of artificial esterases at different ester concentrations

The activity of polymer **132** (R = CA-Arg-Arg) was tested at four different phenethyl ester **127** concentrations, in phosphate buffer at pH 7 (**Figure 2.5.13** and **Table 2.5.7**). Polymer **132** demonstrated the ‘best’ activity at 0.5 mM ester concentration, in terms of initial velocity and conversion to product. As the concentration increases from 0.5 mM, the activity of the esterase diminishes. Additionally, as the concentration of ester decreases from 0.5 mM to 0.2 mM, the activity of the polymer again diminishes. It is not very clear why this particular trend occurs. There has been some evidence from previous studies that at concentrations higher than 0.5 mM, significant self-association effects are observed for the ester **127** and this could possibly prevent productive binding to the polymer at higher concentrations.⁹¹ If this is the case, perhaps the binding and catalytic units on the polymer find it more difficult to access the ester substrate, resulting in less product formation.

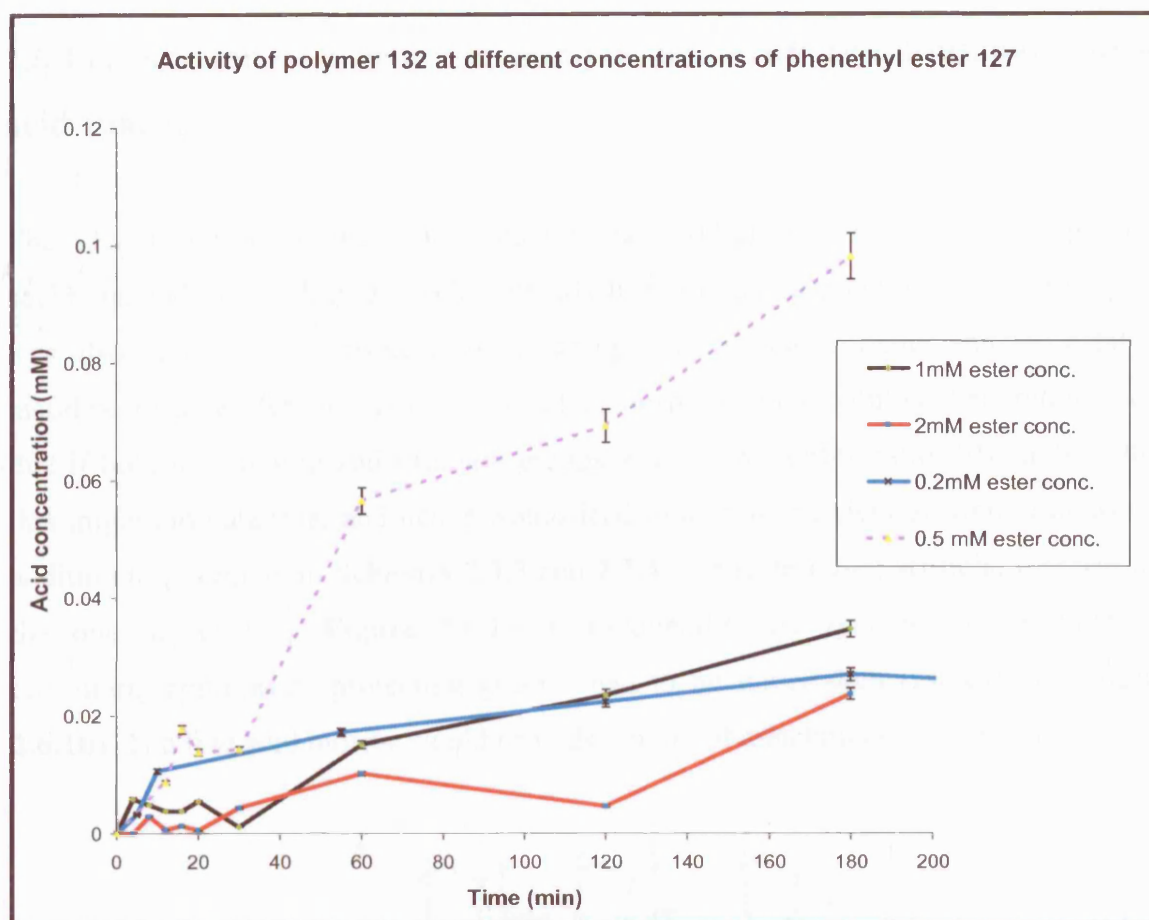


Figure 2.5.13 A plot of acid (**129**) concentration against time for polymer **132**, at different concentrations of phenethyl ester **127**, over 180 min of the reaction. In a typical experiment, the polymer (10 mg) was added to a stirred solution of ester (**127**) in aqueous buffer (0.2 mM, 0.5 mM, 1 mM or 2 mM, 1 ml) at room temperature for 180 min. The reaction was monitored by HPLC.

Entry	Ester conc. (mM)	$10^{-4} \times v$ (mM min ⁻¹) ^a	v_{rel}	Conversion to product after 180 min (%)
1	0.2	4.72 ± 0.19	2	5
2	0.5	9.71 ± 0.39	4.2	20
3	1	12.0 ± 0.48	5	7
4	2	2.33 ± 0.09	1	5

Table 2.5.7 Initial velocities of reactions with polymer **132**, at different ester concentrations.
^aCalculated using **Equation 2.5.1**. v_{rel} describes initial relative velocities for comparison purposes.

2.6 Preparation of a histidine catalytic unit with an additional caproic acid spacer

The idea of inserting the 6-aminocaproic acid (CA) spacer between the polymer backbone and the binding group has already been discussed previously. Accordingly, it was also of interest to insert a spacer group between the polymer and the catalytic histidine residues for the same reason of conformational flexibility. Our rationale was that if both the binding and catalytic groups were more conformationally mobile, then this might aid catalysis, and hence would lead to a more efficient artificial esterase. In addition to polymers in **Schemes 2.3.3** and **2.3.4**, our sixth target artificial esterase was the one depicted in **Figure 2.6.1a**. Consequently, the synthesis of a dipeptide, containing appropriate protecting groups, had to be undertaken (for example **Figure 2.6.1b**). The free acid moiety would provide a point of attachment to the resin.

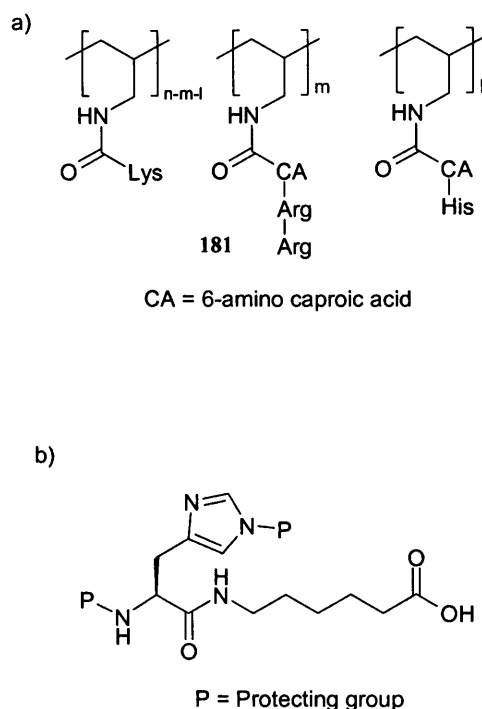
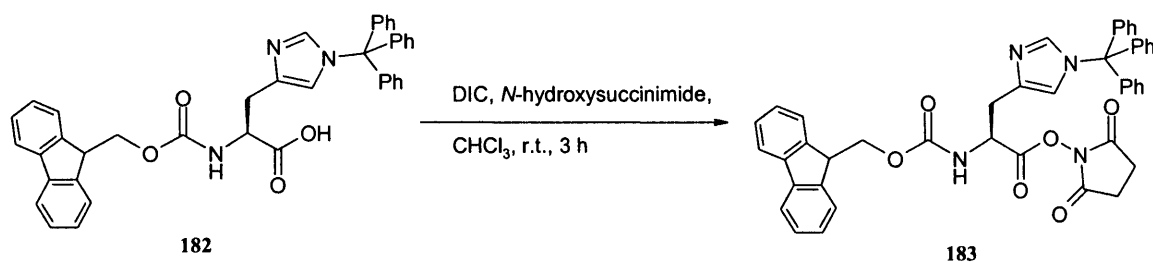


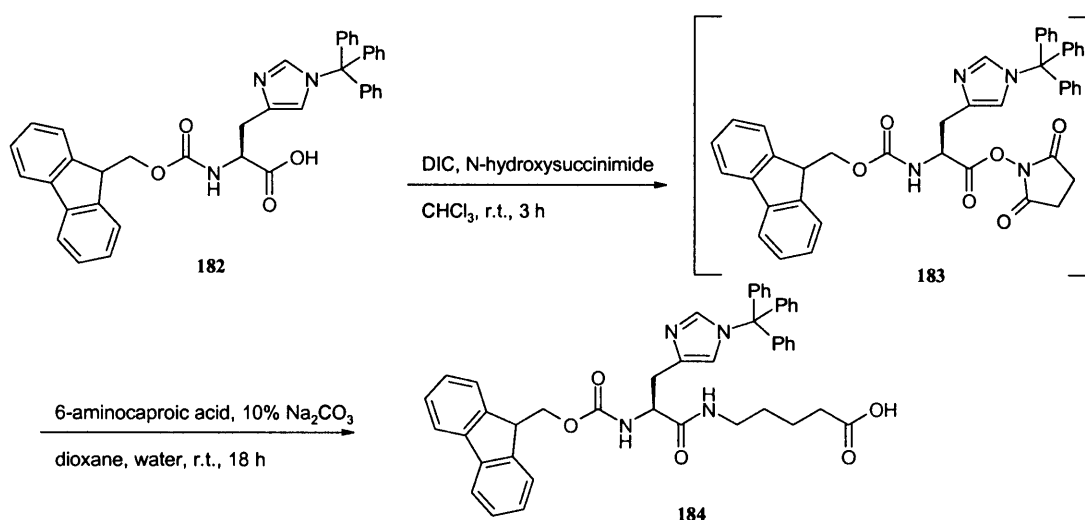
Figure 2.6.1 a) Artificial esterase containing a spacer between both the binding group and histidine catalytic unit. b) An example of a potential dipeptide to be synthesised with the appropriate protecting groups before incorporation into polyallylamine.

Initially, the route commenced with the use of the commercially available protected histidine derivative **182**. This was converted to the corresponding activated ester, using *N*-hydroxysuccinimide and *N,N'*-diisopropylcarbodiimide (DIC), to yield **183** (**Scheme 2.6.1**). Although the ester **183** was obtained successfully, NMR analysis confirmed that there was excess of DIC and its corresponding urea by-product present. Attempts to purify ester **183** by either recrystallisation (ethyl acetate/petroleum spirit) or by flash chromatography did not meet with success. Since DIC forms a urea by-product that is soluble in most organic solvents, it was thought that it would be preferable to use *N,N'*-dicyclohexylcarbodiimide (DCC) instead, since its urea is much less soluble.¹⁰² The reaction was repeated using DCC instead and the resulting *N,N'*-dicyclohexylurea (DCU), which appeared as a white precipitate, was filtered off. However, traces of DCU remained after purification.



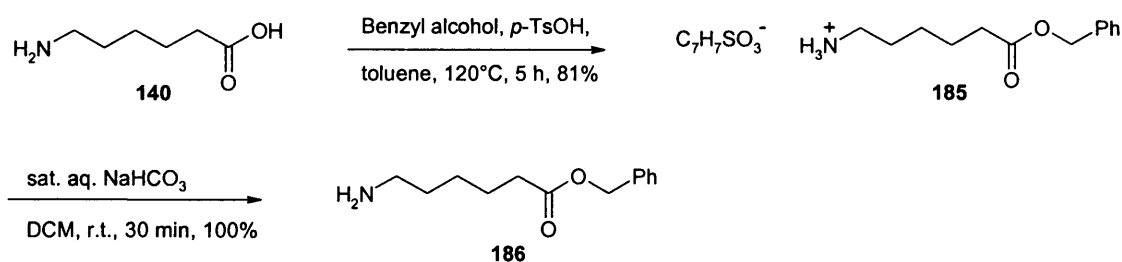
Scheme 2.6.1 Attempted synthesis of histidine ester **183**.

Consequently, the use of DIC was reconsidered due to the more efficient generation of the activated ester. However, the isolation of ester was not attempted and instead, *in situ* conversion to the desired amide was undertaken (**Scheme 2.6.2**). Although the formation of the desired product **184** was confirmed by NMR analysis, a complex mixture of impurities was also present. Furthermore, attempts to purify the dipeptide **184** were unsuccessful, and hence this approach was abandoned.



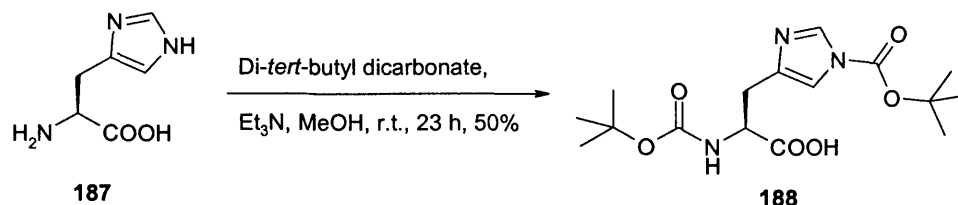
Scheme 2.6.2 Attempted synthesis of dipeptide **184**.

The next strategy attempted was to protect the free carboxylic acid of caproic acid, hopefully preventing the formation of any undesired products. The benzyl protecting group was selected, since it can be deprotected under mild hydrogenation conditions.¹⁰³ However there was reported evidence that the trityl group may be labile under these conditions.¹⁰⁴ Therefore another suitably protected histidine derivative would have to be selected to be compatible with the linker. In view of the fact that the de-benzylation step would involve hydrogenation, Boc protected histidine seemed a good choice since its removal is completely orthogonal with respect to the benzyl group. 6-Aminocaproic acid **140** was protected using benzyl alcohol in the presence of *p*-toluene sulfonic acid to give the benzyl protected caproic acid salt **185** (**Scheme 2.6.3**). Quantitative conversion to the free base (**186**) was achieved using dichloromethane and saturated sodium carbonate.¹⁰⁵



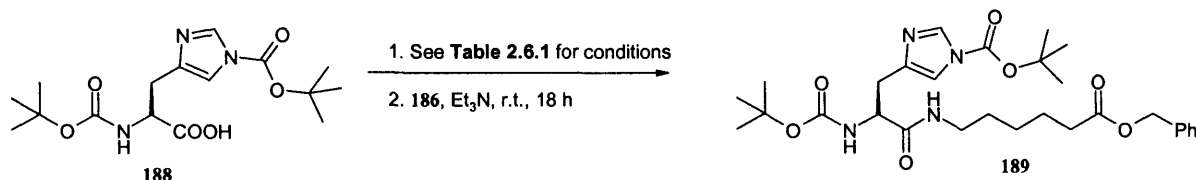
Scheme 2.6.3 Synthesis of benzyl protected 6-aminocaproic acid **186**.

Boc protected histidine **188** (**Scheme 2.6.4**) was then formed in 50% yield, using di-*tert*-butyl dicarbonate and triethylamine.



Scheme 2.6.4 Synthesis of Boc protected histidine **188**.

The peptide coupling with benzyl protected caproic acid **186** was then attempted *via* the formation of the activated *N*-hydroxysuccinimide ester, (**Scheme 2.6.5**, **Table 2.6.1**, entry 1). The best conditions involved the use of DCC as a coupling reagent and compound **189** was isolated in 33% yield. However, NMR analysis indicated that the product once again contained the urea by-product and attempts to purify by flash chromatography and recrystallisation were similarly unsuccessful in this case.

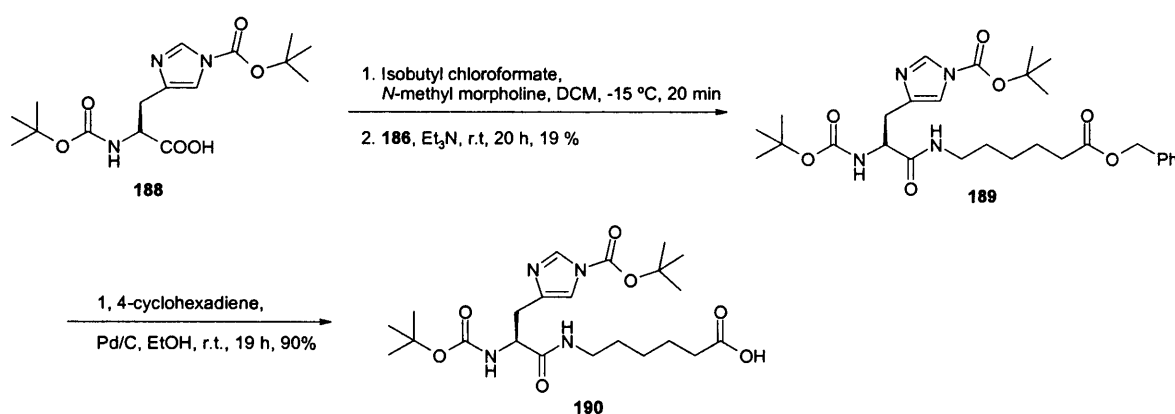


Scheme 2.6.5 Synthesis of dipeptide **189**.

Entry	Reaction Conditions	Yield of 189
1.	DCC, <i>N</i> -hydroxysuccinimide, CHCl ₃ , r.t., 5 h	33% together with DCU
2.	DIC, <i>N</i> -hydroxysuccinimide, CHCl ₃ , r.t., 6 h	10%
3.	EDCI.HCl, <i>N</i> -hydroxysuccinimide, Et ₃ N, CHCl ₃ , r.t., 5 h	0%
4.	PyBOP, Et ₃ N, MeCN, r.t., 5 h	0%
5.	Ethyl chloroformate, Et ₃ N, DCM, r.t., 5 h	0%
6.	HATU, Et ₂ NCH(CH ₃) ₂ , DMF, r.t., 5 h	7%
7.	Isobutyl chloroformate, <i>N</i> -methylmorpholine, DCM, -15°C, 20 min	19%

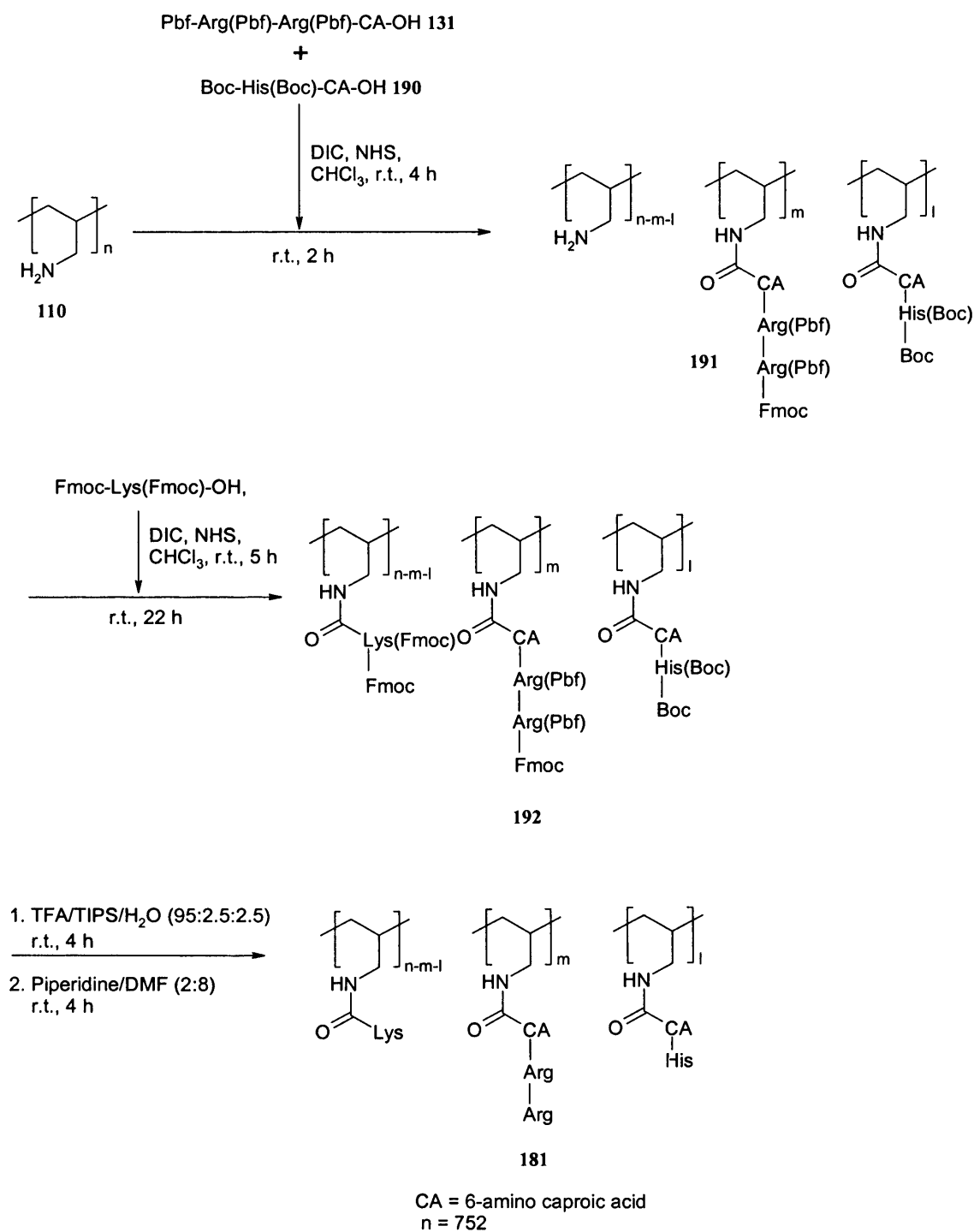
Table 2.6.1 Attempted reaction conditions for the synthesis of dipeptide **189**.

DIC was next attempted (**Table 2.6.1**, entry 2), because as mentioned previously, its urea by-product is soluble in organic solvents, and it was reasoned that this could aid its removal by recrystallisation. Unfortunately **189** was obtained in low yield (*ca.*10%). Due to the problems encountered with the carbodiimides mentioned above, it was decided that the use of 1-[3-(dimethylamino)propyl]-3-ethylcarbodiimide hydrochloride (EDCI) (**Table 2.6.1**, entry 3), which forms a water soluble urea, which can be easily removed in work-up might be more suitable.¹⁰⁶ However, the desired product was not isolated and the NMR analysis confirmed that the peptide coupling had not occurred. Although PyBOP has often been used for sluggish peptide coupling reactions¹⁰⁷ (**Table 2.6.1**, entry 4), in this case, no product was detected. The use of ethyl chloroformate to form a mixed anhydride was also unsuccessful (**Table 2.6.1**, entry 5). The final coupling reagent considered was O-(7-azabenzotriazol-1-yl)-*N,N,N',N'*-tetramethyluronium hexafluorophosphate (HATU) (**Table 2.6.1**, entry 6). The reaction gave a complex mixture of products, with **189** being isolated in only 7% yield.¹⁰⁸ A slight improvement in yield of the reaction was found when it was performed with isobutyl chloroformate in the presence of *N*-methyl morpholine, giving **189** in 19% yield (**Scheme 2.6.6**).¹⁰⁹ Although the yield was modest, the purity of the desired amide was excellent and hence, we proceeded to the next step. Deprotection of the benzyl group was achieved by catalytic transfer hydrogenation, using 1,4-cyclohexadiene in the presence of palladium on carbon and the desired acid **190** was isolated in an excellent 90% yield (**Scheme 2.6.6**).¹¹⁰



Scheme 2.6.6 Synthesis of dipeptide **190**.

The synthesis of polymer **181**, containing a histidine unit attached to the caproic acid spacer is shown in (Scheme 2.6.7) and was carried out in a manner analogous to previous polymers.



Scheme 2.6.7 Synthesis of artificial esterase **181**.

2.6.1 The activity of the artificial esterase containing an extended histidine catalytic unit with the caproic acid spacer

To our enormous surprise, when activity of polymer **181** (**Figure 2.6.2**) was tested in phosphate buffer at pH 7, HPLC analysis confirmed that the esterase was completely inactive. Possible explanations for the lack of activity could be the lack of solubility of the polymer in buffer, the formal increase in the distance between the histidine residue and the binding group or the fact that too many lipophilic methylene units are now concentrated in the “active site” region. This example nevertheless demonstrates that relatively minor alterations can drastically affect the polymer’s ability to hydrolyse the ester.

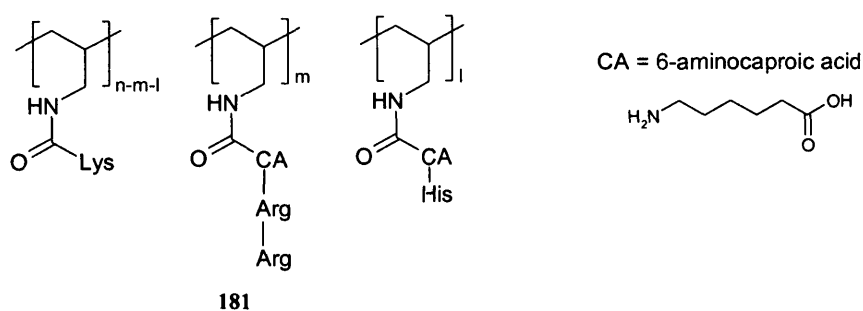
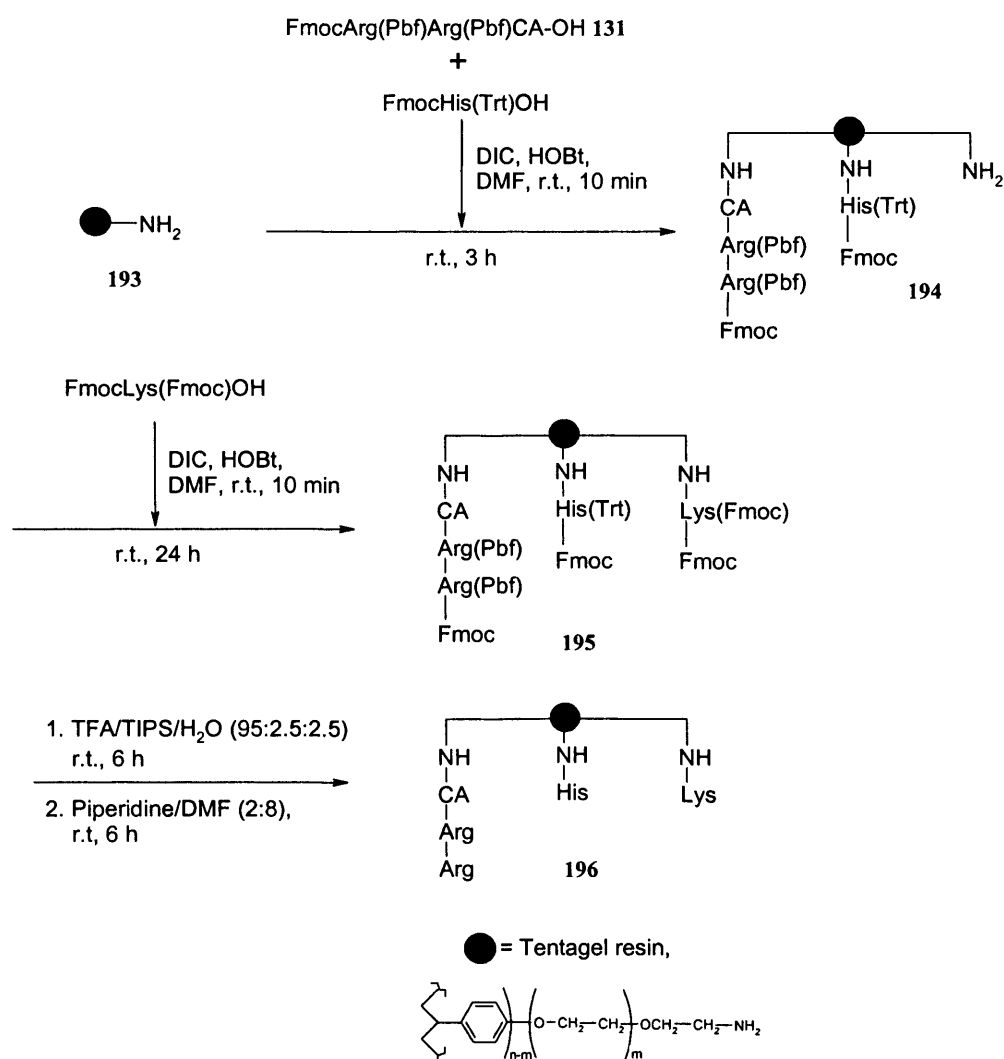


Figure 2.6.2 Artificial esterase **181**.

2.7 Synthesis of artificial esterase containing a tentagel resin backbone

Since all artificial esterases examined thus far were based on a polyallylamine backbone, it was of interest to ascertain how the activity of the artificial esterase would be influenced by using a different polymeric support for the threads. Tentagel resin, for example, unlike polyallylamine, is much more compatible with organic solvents and has very good swelling properties, especially in DCM.^{111;112} We therefore decided to incorporate a tentagel based resin within our system, and to retain the same binding unit Arg-Arg, histidine nucleophile, and lysine spacer which had shown superior activity in our earlier studies. The synthesis was carried out using a similar method to that previously described in Section 2.3.2, and using the Arg-Arg binding unit, histidine and lysine in an approximate 1:1:1 ratio (**Scheme 2.7.1**).



Scheme 2.7.1 Synthesis of artificial esterase **196**, containing a tentagel resin backbone.

The esterase **196** was tested in phosphate buffer pH 7, but no hydrolysis was observed. Since the resin has better swelling properties in organic solvents, the hydrolysis reactions were also attempted in a mixture of THF/phosphate buffer (1:1) and acetonitrile/phosphate buffer (1:1). However, in all of these cases, disappointingly, no hydrolysis was observed.

2.8 Hydrolysis of other ester substrates

At this stage, we also wished to investigate the substrate specificity of our artificial esterases. The hydrolysis of commercially available ethyl phenylacetate **197** (**Figure 2.8.1**) was selected for study because in contrast compared to esters **127** and **169**, it does not contain the additional amide and acid binding groups for recognition. Polymers **132** and **137**, for which ester hydrolysis had previously been observed, did not show any product formation with ethyl phenylacetate **197**. In both cases, however, a reduction in ester concentration was observed.

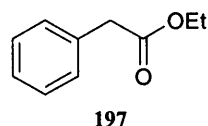
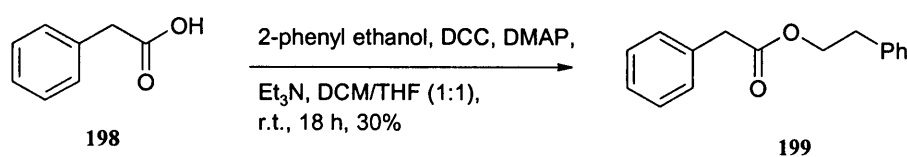
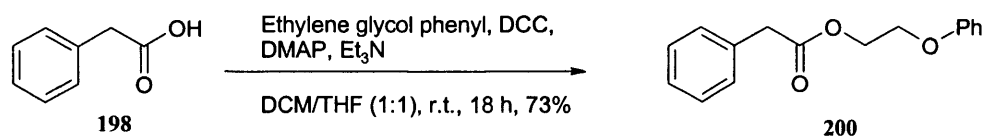


Figure 2.8.1 Ethyl phenylacetate

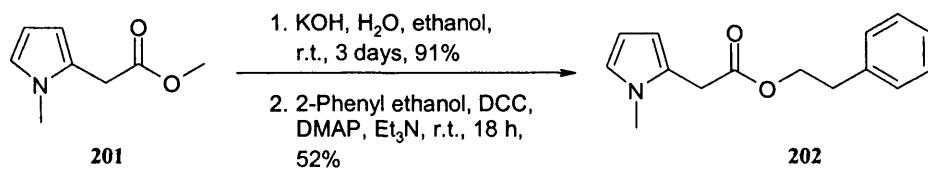
Frustratingly, an additional series of esters **199** (**Scheme 2.8.1**), **200** (**Scheme 2.8.2**) and **202** (**Scheme 2.8.3**) which were also prepared in order to assess substrate behaviour, proved to have problems of solvent incompatibility and hence could not be studied. Nevertheless, in a more encouraging vein, the fact that the esterases **132**, **137** and **168** hydrolysed their designed substrate and did not hydrolyse ethyl phenylacetate demonstrated that our artificial enzymes could indeed, as with many naturally occurring enzymes, be considered as substrate specific.



Scheme 2.8.1 Synthesis of ester **199**.



Scheme 2.8.2 Synthesis of ester **200**.



Scheme 2.8.3 Synthesis of ester **202**.

2.9 Conclusions from the esterase studies

This section has described further developments in our novel strategy for the preparation of artificial enzymes. Our objective was to use this approach to further investigate some different factors which are responsible for catalysis and hence to subsequently find the most efficient artificial esterase.

The dipeptides which displayed quantifiable binding affinity towards the phosphonate transition state analogue **128** as established by the previous NMR studies⁹⁶ were accordingly incorporated into a polymer backbone, together with a histidine catalytic group. As a result, a number of different variants of artificial esterases were prepared. We found that only three of the esterases showed activity, polyallylamine containing Arg-Arg and Ala-Arg binding groups and the soluble polymer with a missing lysine residue. Out of these three, it was found that the esterase **132** containing the peptide which showed the best binding towards the transition state analogue, Arg-Arg, was the most efficient in terms of overall conversion. We have verified the importance of the amino acid sequence within the binding group in relation to the polymer backbone. This was illustrated by the example of the unreactive polymer **136** containing Arg-Ala binding group, with the arginine directly attached to the backbone. Furthermore, we established that the most efficient hydrolysis occurs at pH 8 with the designed substrate. We have also demonstrated that changing the polymer backbone, gives the catalyst completely different properties and although we had the same groups attached to tentagel, the polymer was still inactive.

We have exploited the most significant advantage of this approach, by demonstrating that through simple variation of the groups attached to the polymer backbone, a systematic exploration of catalyst activity could be achieved. This information can now be used in principle to generate new catalysts with even better efficiency. Nevertheless, despite the fact that we have managed to gather a lot of information on cooperativity between binding and catalytic groups, as well as the activity of these polymers under different conditions and their substrate specificity, the methodology of effectively random coupling of the two functional units to a polymer backbone needs some re-thinking. As we observed, by synthesising several different batches of the same

polymer, they have a tendency to exhibit different efficiencies. Although in all cases ester hydrolysis was observed, they performed to different extents, leading us to believe that each polymeric thread that is produced by random attachment of functional groups, forms a distinct molecular entity and ultimately this is undesirable. The sensitivity of the tertiary structure to minor work up modifications is also of some concern.

The method by which the formation of the acid product was monitored needs further improvements and hence the measurements presented in this chapter should only be considered as preliminary. It is possible that the acid formation was monitored at the wrong time frame and that perhaps, the 'real' catalysis may be occurring after a period of 300 minutes rather than at the beginning of the reaction as initially anticipated. The fact that substantially more product formation was observed after a period of 24 hours also indicates that this may be the case. Therefore the polymers could be undergoing an initial period of 'recognition' of the substrate, before catalysing the reaction. In this case, a continuous assay should be designed in order to monitor product formation, which could be more useful in determining the time period when the polymers are at their most active state.

2.10 Future Outlook

In overall terms, we were nevertheless satisfied with the additional results achieved for these artificial esterases especially in an aqueous buffered medium. However, there is still plenty of scope for further studies in the area of artificial esterases.

Investigations into different types of catalytic groups, such as serine or cysteine, which are also found within natural enzymes could certainly be carried out. Although our studies were limited to the small number of binding groups identified by the NMR technique, clearly, these may not be optimal. Finding a more efficient binding group would require research into new binding assays and exploitation of other techniques such as UV or fluorescence in combination with NMR binding studies. Most certainly, this would also involve investigations into more accurate design and understanding of transition state analogues.

Further studies on different polymer backbones, ranging from more or less soluble polymers as desired could also be done to see how the microenvironment of the polymer affects catalysis.

It would also be of interest to complete the competition studies that were initiated, providing that a suitable ester substrate which is soluble in phosphate buffer can be found.

Finally, this approach could be extended to involve kinetic resolution of ester substrates since binding groups on the polymeric backbone could be selected for a single enantiomer.

CHAPTER 3

RESULTS AND DISCUSSION

ARTIFICIAL ALDOL CATALYSTS

3.1 Introduction

Using the design concept previously developed for artificial esterases, it was of interest to explore this approach in terms of an artificial aldolases. As discussed previously (Section 1.3.4.2, **Scheme 1.3.9**), in natural aldolases, a lysine residue performs the key catalytic step, forming a reactive imine/ enamine intermediate for the aldol reaction to proceed.²⁵

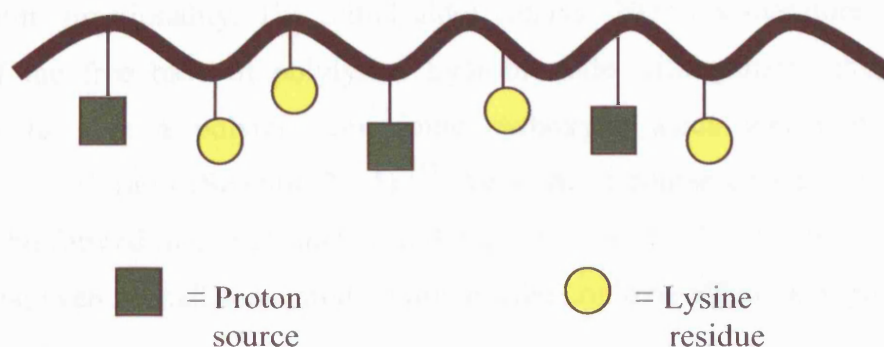


Figure 3.1.1 Representation of artificial aldolase catalyst.

Accordingly, we envisaged that an artificial aldolase would consist of a polymer backbone with two different functional groups attached to it (**Figure 3.1.1**). In the first instance, as a gross simplification of the design we had for esterases, it was decided to select lysine as the first group and a carboxylic acid as the second group. Our hope that this system would have some characteristics of the natural enzyme is expressed in **Figure 3.1.2**, wherein a nucleophilic enamine is formed using the lysine residue and the carboxylic acid functions as a proton source to enhance the electrophilicity of the aldehydic carbonyl group.

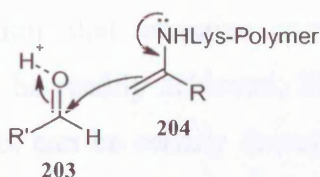
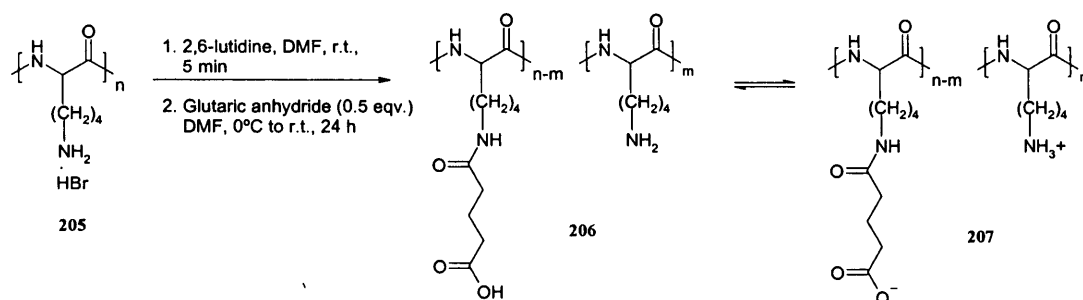


Figure 3.1.2 Enamine attack on aldehyde during an aldol reaction.

3.2 Preliminary studies with artificial aldolases

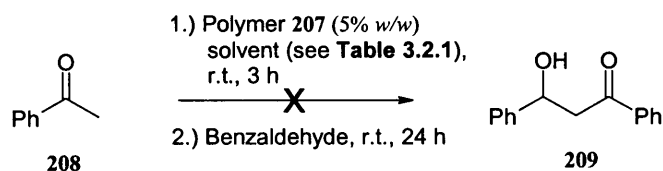
When selecting the polymer backbone for our initial investigations into artificial aldolases, the obvious choice was to utilise polylysine since the lysine residues are already present and hence only the carboxylic acid units would need to be incorporated. As a carboxylic acid source, we elected to use 1,5-pentadioic acid, which after incorporation onto the polylysine backbone should confer conformational mobility on this important functionality. The initial aldol catalyst **207** was therefore formed *via* reaction of the free base of polylysine hydrobromide with glutaric anhydride (0.5 equivalent) to give a polymer containing carboxylic acids and free amines in approximately 1:1 ratio (**Scheme 3.2.1**).¹¹³ We were of course aware that ammonium salts could be formed in equilibrium with the free form of the “amino acid” shown, but reasoned that even a small concentration of the latter could be effective in promoting the desired reaction.



Scheme 3.2.1 Synthesis of aldolase catalyst **207**.

For our preliminary aldol reactions, we decided to study the reaction between acetophenone and benzaldehyde (**Scheme 3.2.2**). There were several reasons for this choice including the expectation that enamine regiospecific formation between acetophenone and lysine should be readily achieved; the fact that both of the starting materials and the known product can be readily detected by UV, hence allowing the reaction to be easily followed. In the event however, our initial attempts to perform an aldol reaction between acetophenone and benzaldehyde, catalysed by polymer **207**, were uniformly unsuccessful. The polymer **207** was tested in a number of solvents as

shown in **Scheme 3.2.2** and **Table 3.2.1**. After 24 hours no aldol product **209** was detected under any of the conditions specified in **Table 3.2.1**.

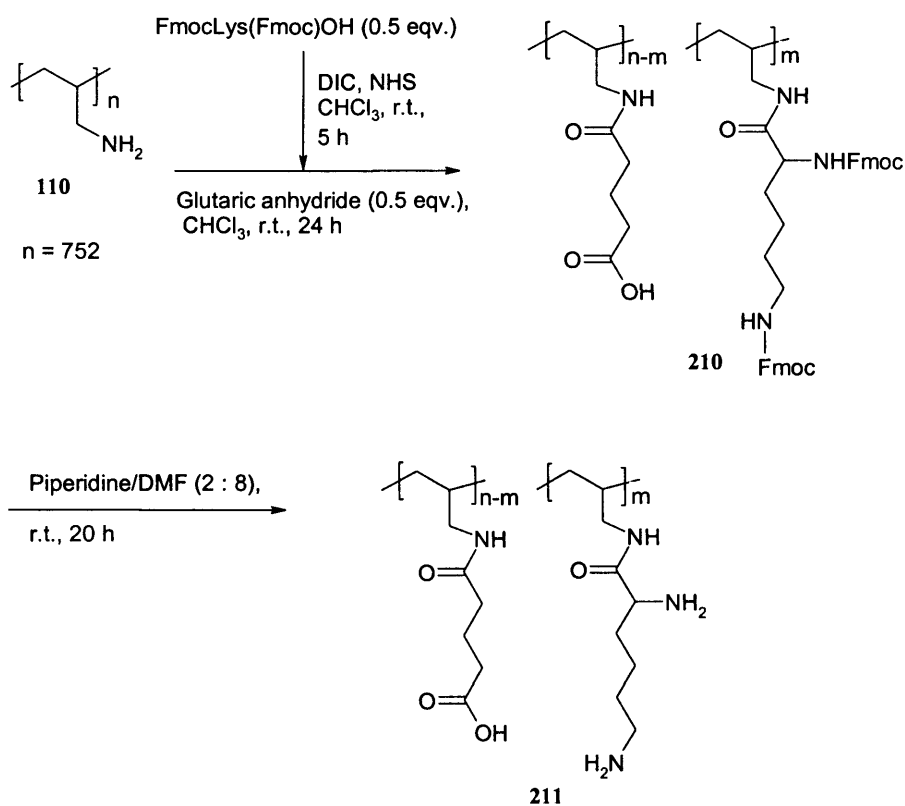


Scheme 3.2.2 Attempted aldol reaction between acetophenone and benzaldehyde, using polymer catalyst **207**.

Entry	Solvent	Product detected?
1.	Ethanol	No
2.	THF	No
3.	DCM	No
4.	Acetonitrile	No
5.	DMF	No

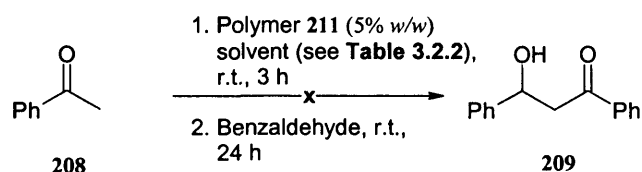
Table 3.2.1 Aldol reaction (**Scheme 3.2.2**) monitored by UV and NMR.

As a result of the failure of our catalyst to generate any product, we questioned whether the lysine residues in polymer **207** were hindered by the morphology of the polymer, which therefore may have inhibited enamine formation in the reaction. Hence, we decided to synthesise an alternative catalyst based on a polyallylamine backbone, onto which we incorporated glutaric anhydride (0.5 equivalent) and Fmoc protected lysine (0.5 equivalent). Again, we envisaged that the lysine and pentadioic acid would be incorporated in 1:1 ratio. The synthesis of this polymeric catalyst **211** is outlined below (**Scheme 3.2.3**).



Scheme 3.2.3 Synthesis of aldol catalyst **211**.

The resulting polymer **211** was tested under the same reaction conditions previously attempted with the polylysine derived polymer (**Scheme 3.2.4** and **Table 3.2.2**).



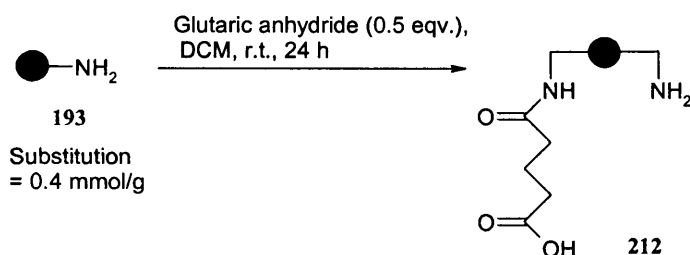
Scheme 3.2.4 Attempted aldol reaction between benzophenone and benzaldehyde, using polymer **211** as a catalyst.

Entry	Solvent and conditions	Products detected?
1.	Ethanol, r.t.	No
2.	THF, r.t.	No
3.	DCM, r.t.	No
4.	MeCN, r.t.	No
5.	DMF, r.t.	No
6.	Ethanol, 60 °C	No
7.	THF, 60 °C	No

Table 3.2.2 Aldol reaction (**Scheme 3.2.4**) monitored by UV and NMR.

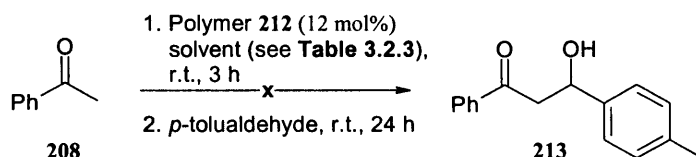
However, under the conditions stated in entries 1 – 7 (**Table 3.2.2**), no aldol adducts were observed in any of the different solvents that were investigated.

Since neither polymer **207** or polymer **211** were able to catalyse the aldol reaction outlined in **Scheme 3.2.4**, we considered whether an alternative polymer backbone might be desirable. Since both polylysine and polyallylamine are more compatible with aqueous media,^{90;113} and due to the fact that we were attempting the aldol reaction in organic solvents, a polymer support more compatible with organic solvents would potentially be of more use. Tentagel resin has been reported to possess good swelling properties in organic medium¹¹¹ and we therefore decided to incorporate this within our system. Tentagel resin was reacted with glutaric anhydride (0.5 equivalents) (**Scheme 212**), resulting in polymer **212** consisting of a free amine and a carboxylic acid in an approximately 1:1 ratio. In the first instance, we decided not to attach lysine to tentagel resin, as we felt that the free primary amino group of tentagel resin should be sufficient to perform the enamine formation.



Scheme 3.2.5 Synthesis of aldol catalyst **212**.

This time, we decided to use tolualdehyde as a substrate, instead of benzaldehyde, since we thought the formation of the aldol product would be monitored more easily by the chemical shift of the methyl group by ^1H NMR spectroscopy. However, under the conditions tested, the desired aldol adduct (**213**) was not detected (**Scheme 3.2.6** and **Table 3.2.3**).



Scheme 3.2.6 Attempted aldol reaction between benzophenone and *p*-tolualdehyde, using polymer **212** as a catalyst.

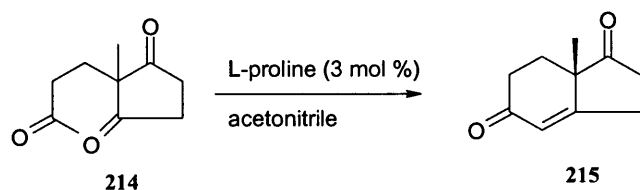
Entry	Solvent and conditions	Products detected?
1.	Ethanol, r.t.	No
2.	THF, r.t.	No
3.	DCM, r.t.	No
4.	MeCN, r.t.	No

Table 3.2.3 Aldol reaction (**Scheme 3.2.6**) monitored by UV and NMR.

As a result of the fact that none of the aldol catalysts (**207**, **211** and **212**) containing a primary amino group had proved successful, we questioned whether the primary amine had the ability to evolve from the derived imine to an enamino species, under the reaction conditions investigated. Secondary amines can of course allow easier enamine formation, and we therefore reasoned that incorporation of proline (a secondary amine) into our polymer system might be more suitable. Before discussing this aspect further, it is appropriate to provide a short overview of the recent literature, on organic catalysts where proline derivatives have been widely used as catalysts in aldol reactions.

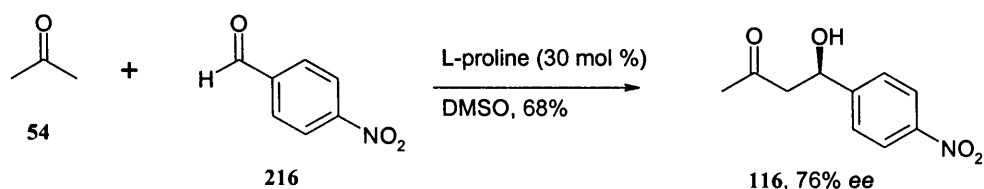
3.3 Organocatalysts in aldol reactions

In 1974, Hajos and Parrish reported the use of L-proline as a catalyst in the asymmetric intramolecular aldol cyclization of the triketone **214** (**Scheme 3.3.1**).¹¹⁴



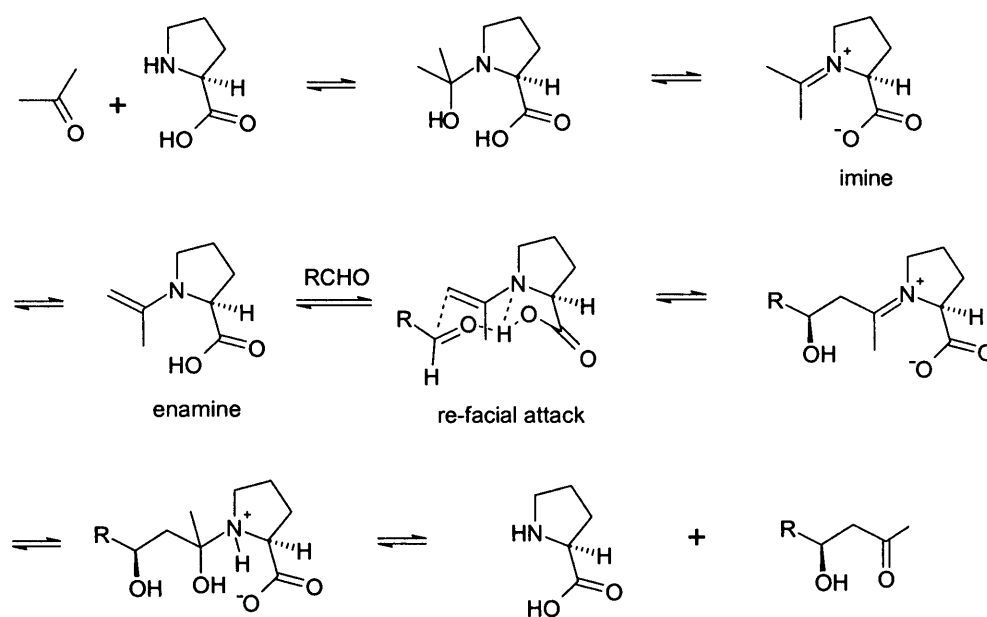
Scheme 3.3.1 Proline catalysed intramolecular aldol reaction.

Subsequently, List and co-workers described the first proline-catalysed intermolecular asymmetric aldol reaction (**Scheme 3.3.2**).¹¹⁵ These proline catalysed reactions had several key advantages: (1) proline was inexpensive, non-toxic and readily available in both enantiomeric forms; (2) The reaction did not require inert conditions and could be run at room temperature; (3) The reaction did not require the pre-generation of enolate equivalents or the presence of a metallic species; (4) The catalyst was water soluble and could be removed in an aqueous work-up.



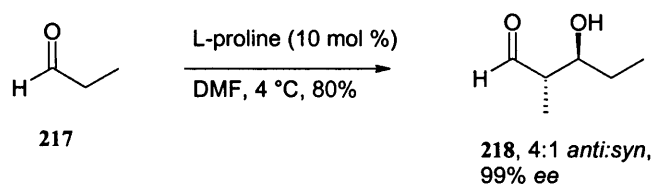
Scheme 3.3.2 Proline catalysed intermolecular aldol reaction.

The proline catalysed reaction has been proposed to proceed through an enamine mechanism, analogous to natural aldolases (**Scheme 3.3.3**).²⁵ The proline functions as a nucleophile and an acid/base co-catalyst in the form of the carboxylate.¹¹⁵ The enantioselectivity can be explained with a metal free version of the Zimmerman-Traxler type transition state,¹¹⁶ where the tricyclic hydrogen bonded network favours the *re*-facial attack.



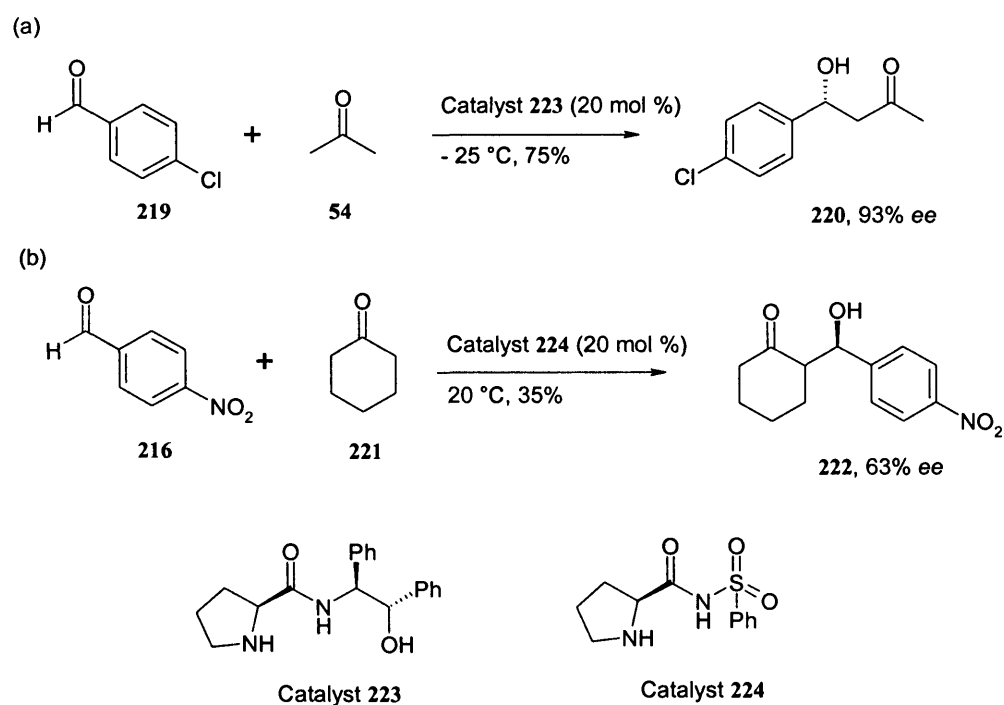
Scheme 3.3.3 Proposed mechanism of the proline catalysed aldol reaction.

As a result of finding such an efficient catalyst, there have been some remarkable advances made in this field. Thus, proline has been used in aldehyde-aldehyde reactions as illustrated by MacMillan and coworkers (**Scheme 3.3.4**).¹¹⁷



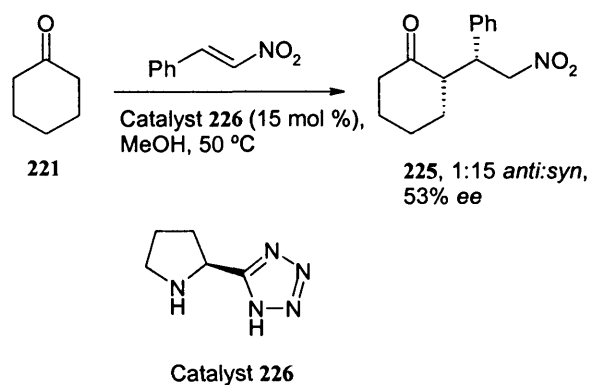
Scheme 3.3.4 Proline catalysed aldol reaction.

Many derivatives of proline have also been synthesised in the attempt to improve selectivity of the reactions. For example, the proline based dipeptide **223** developed by Wu *et al.*¹¹⁸ demonstrated better selectivity over proline (**Scheme 3.3.5, (a)**), whereas a sulfonamide derivative **224** generated by the Ley group¹¹⁹ offered improved solubility in organic solvents (**Scheme 3.3.5, (b)**).

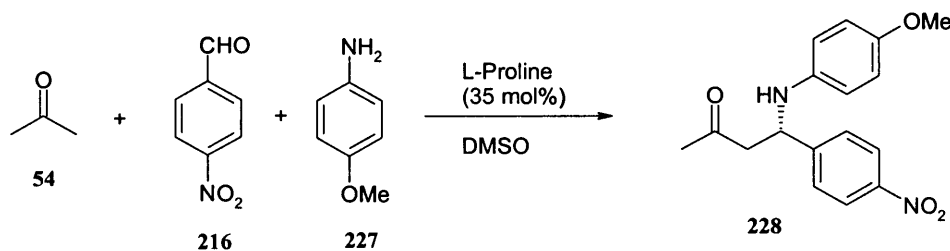


Scheme 3.3.5 Aldol reactions catalysed by proline derivatives.

Proline and its derivatives have also been used as catalysts in nitro-Michael additions (**Scheme 3.3.6**)¹¹⁹ and asymmetric Mannich-type reactions (**Scheme 3.3.7**).^{119;120}



Scheme 3.3.6 Proline derivative catalysed nitro-Michael addition.

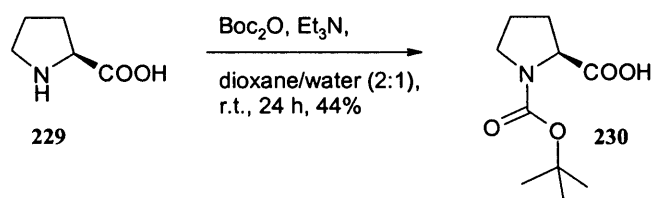


Scheme 3.3.7 Proline catalysed Mannich reaction.

3.4 Synthesis of aldol catalysts containing proline

3.4.1 Tentagel based aldol catalyst

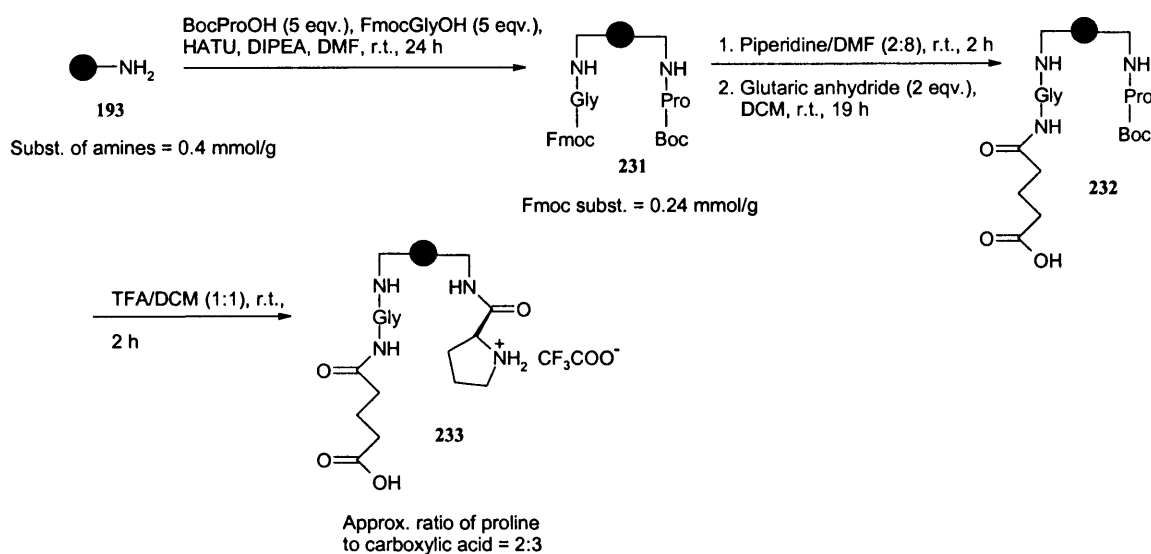
In the light of the foregoing discussion, we felt that it may be more appropriate to replace our lysine catalytic residue with proline. Before incorporating it into the polymer, proline was first protected with a Boc group to give Boc proline **230** (**Scheme 3.4.1**).



Scheme 3.4.1 Synthesis of Boc proline **230**.

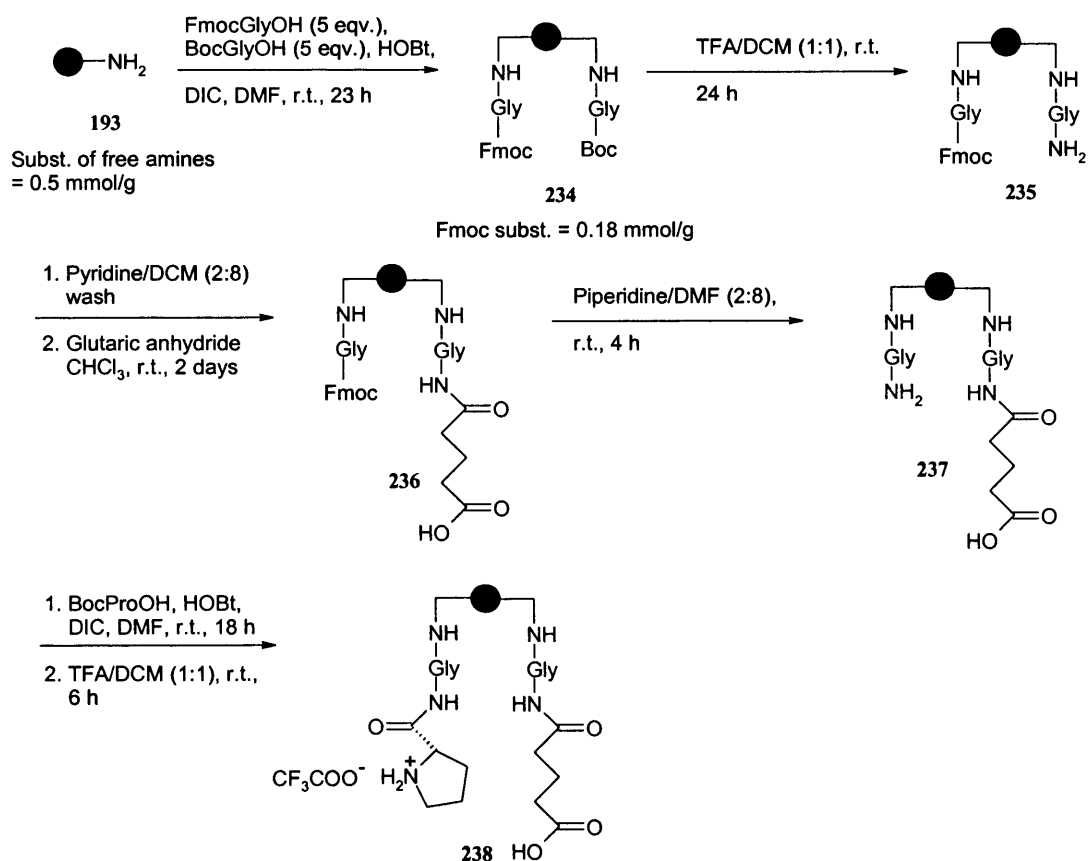
The next step was to synthesise our aldol catalyst, using tentagel resin as the polymeric backbone due to its compatibility with organic solvents. Our intention was to incorporate the proline and pentadioic acid moieties in an approximately 1:1 ratio onto the polymer. Initially, a synthetic route was undertaken whereby Boc protected proline and Fmoc glycine were attached to tentagel resin (**Scheme 3.4.2**). The function of the Fmoc protected glycine spacer was to allow us to monitor the substitution of the glycine residue on the resin, using the Fmoc substitution test outlined in Section 2.3.1. Use of this methodology permits us to approximate the number of proline catalytic groups

attached to the resin. This should in turn allow us to estimate the percentage of the catalyst used in our aldol reactions. Polymer **231** was then deprotected (piperidine/DMF) and treated with glutaric anhydride. Boc deprotection gave our desired catalyst as a trifluoroacetate salt (**233**). However, using this synthetic sequence, Fmoc substitution measurements revealed that the acid and catalytic proline were not attached in a 1:1 ratio.



Scheme 3.4.2 Synthesis of tentagel based aldol catalyst **233**.

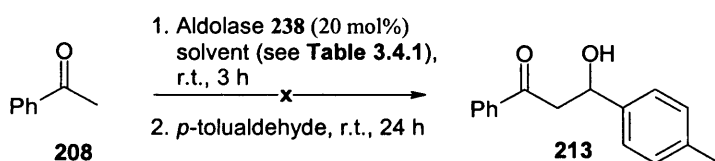
A more controlled synthesis was hence carried out, following the procedure of Ladlow and coworkers,¹²¹ where FmocGlyOH and BocGlyOH were initially attached to the resin in excess (**Scheme 3.4.3**). It was reported that both glycine derivatives should attach to the resin in approximately 1:1 ratio.¹²¹ However, Fmoc substitution analysis revealed that the two glycine residues were attached in approximately 2:3 ratio in compound **234**. The rest of the synthesis was completed using standard procedures to obtain the final aldol catalyst **238**. Although the incorporation was not achieved in the desired 1:1 ratio, this procedure was more reproducible (giving constant Fmoc substitution values) than the previous synthetic route outlined above (**Scheme 3.4.2**).



Ratio of proline to carboxylic acid = 2:3

Scheme 3.4.3 An improved synthesis of tentagel based aldol catalyst **238**.

Initial testing of polymer **238** was carried out using acetophenone and *p*-tolualdehyde and the polymer was assessed for its activity in organic solvents (**Table 3.4.1**). However, no product was again detected under these conditions (**Table 3.4.1**, entries 1-3). It was therefore subsequently tested in a monophasic aqueous system of acetonitrile and buffer at different pH values (**Table 3.4.1**, entries 4 –6). Unfortunately, however, under either acidic (entry 4) or basic conditions (entry 6) no aldol adducts was formed.



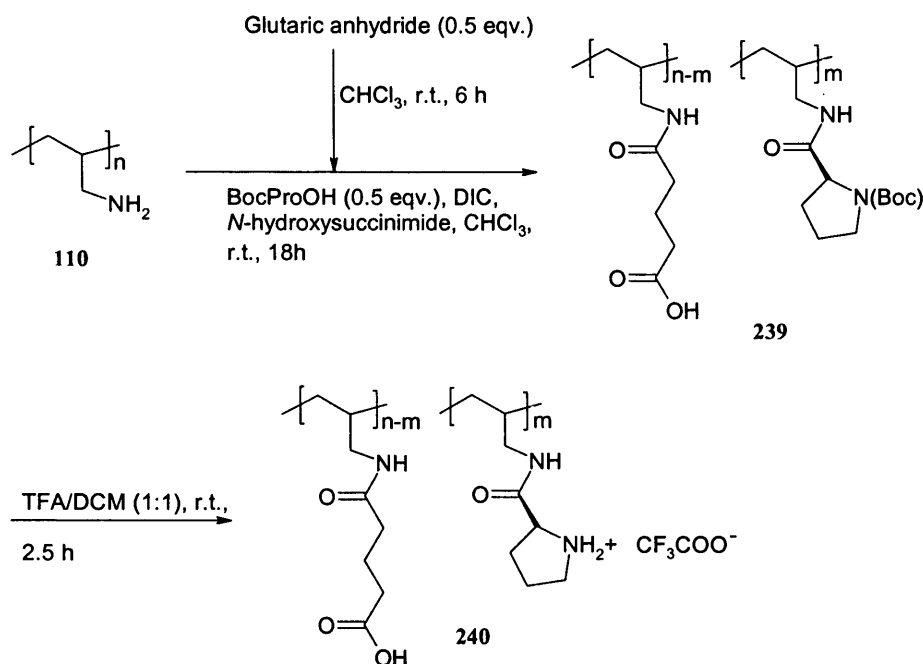
Scheme 3.4.4 Attempted aldol reaction between acetophenone and *p*-tolualdehyde, using polymer catalyst **238**.

Entry	Solvent and conditions	Product detected?
1.	DCM	No
2.	THF	No
3.	MeCN	No
4.	MeCN/Citrate buffer pH6 (1:1)	No
5.	MeCN/Phosphate buffer pH7 (1:1)	No
6.	MeCN/Borate buffer pH8 (1:1)	No

Table 3.4.1 Aldol reaction (**Scheme 3.4.4**) monitored by UV and NMR.

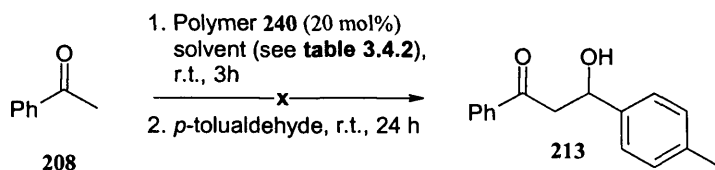
3.4.2 Polyallylamine based aldol catalyst

As a result of the failure of the tentagel based catalyst, our next step was to conjugate the proline and pentadioic acid moieties to a polyallylamine backbone. Polyallylamine based resins are more compatible with aqueous systems and it was anticipated that this could be exploited within our system. The synthesis of the required catalyst **240** is outlined below in **Scheme 3.4.5**.



Scheme 3.4.5 Synthesis of polyallylamine based aldolase catalyst **240**.

The catalytic properties of polymer **240** were then assessed for the reaction in **Scheme 3.4.6**, under the conditions outlined in **Table 3.4.2**. However, under aqueous conditions (entries 2-4) no reaction was detected. This was somewhat disappointing as it had been hoped that the favourable swelling properties of polyallylamine would make the catalytic proline residues more accessible to the ketone.



Scheme 3.4.6 Attempted aldol reaction between acetophenone and *p*-tolualdehyde, using polymer catalyst **240**.

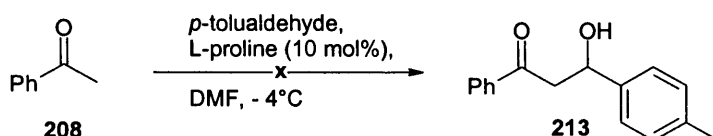
Entry	Solvent and conditions	Product detected?
1.	MeCN, r.t.	No
2.	MeCN/Citrate buffer pH6 (1:1), r.t.	No
3.	MeCN/Phosphate buffer pH7 (1:1), r.t.	No
4.	MeCN/Borate buffer pH8 (1:1), r.t.	No
5.	DMF, r.t.	No
6.	DCM, r.t.	No
7.	THF, r.t.	No
8.	Diethyl Ether, r.t.	No
9.	Ethanol, 75 °C	No

Table 3.4.2 Aldol reaction (**Scheme 3.4.6**) monitored by UV and NMR.

For completeness, a range of organic solvents was also examined (**Table 3.4.2**, entries 5–9), but as before, no reaction was observed.

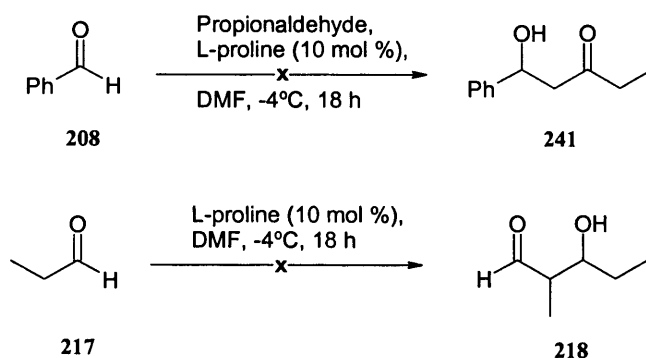
3.4.3 Aldol reaction using proline and its derivatives as catalysts

Following the problems encountered with our catalysts, we decided to establish appropriate reaction conditions with proline on its own, with the aid of information already available in the literature. Once this had been determined, we then planned to use our catalyst under the corresponding conditions. Following the procedure of MacMillan,¹¹⁷ who had carried out aldol reactions between two aldehydes, we attempted to use the same reaction conditions on our substrates, with proline as a catalyst (**Scheme 3.4.7**).



Scheme 3.4.7 Attempted aldol reaction, using L-proline as a catalyst.

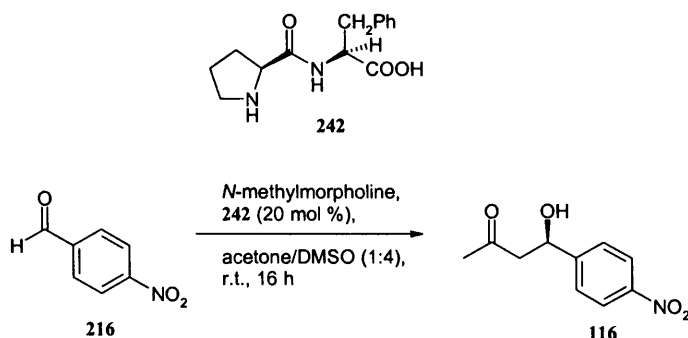
However, these conditions were unsuccessful for our substrates. Therefore, we attempted to reproduce exactly the same results stated in the paper (**Scheme 3.4.8**).¹¹⁷ However, in our hands, we were unable to repeat the reaction between benzaldehyde and propionaldehyde and the self coupling of propionaldehyde. In both cases, we isolated a complex mixture of materials, with no evidence of the desired aldol products **241** and **218** by NMR spectroscopy.



Scheme 3.4.8 Attempted aldol reactions, using L-proline as a catalyst.

3.4.3.1 Aldol reactions using proline derivative **242**

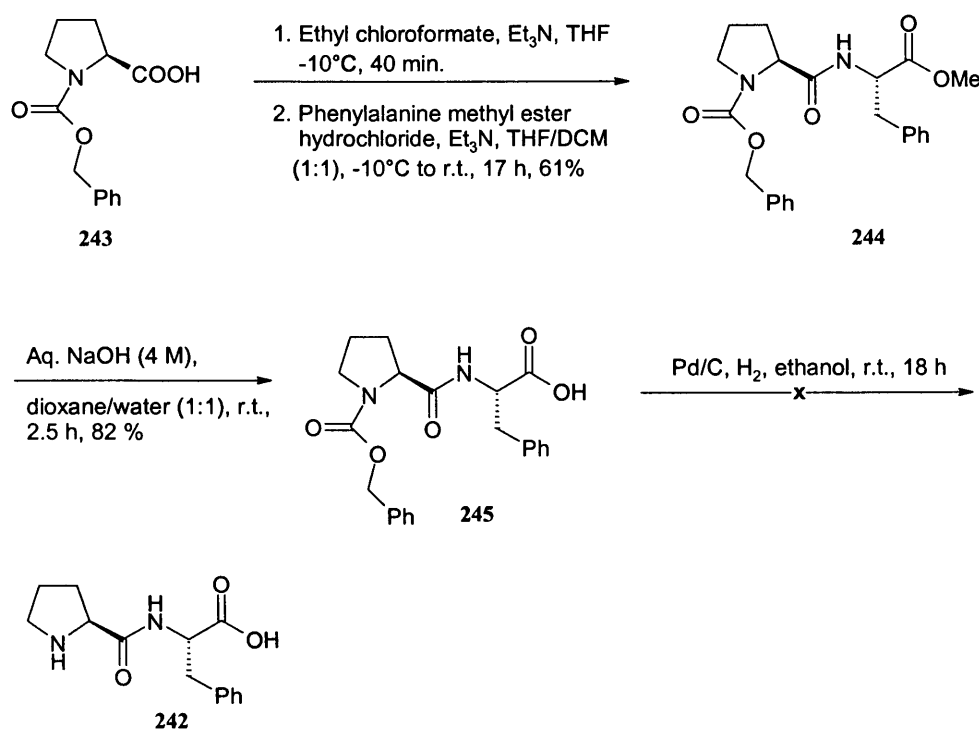
Our next strategy was to investigate the catalytic dipeptide **242** used by Li and co-workers in the aldol reaction between nitrobenzaldehyde and acetone (where acetone was used as a solvent) (Scheme 3.4.9).¹²²



Scheme 3.4.9 Aldol reaction performed by Li *et al.*¹²², using dipeptide **242** as a catalyst.

The first step was to synthesise the dipeptide catalyst **242**, used in their studies, which is described below.

Our initial route to dipeptide **242** involved coupling CBz protected proline to phenylalanine methyl ester (Scheme 3.4.10). The peptide coupling was first attempted *via* activated succinimide ester formation using EDCI and *N*-hydroxysuccinimide. However, low yields of dipeptide **244** were isolated. The coupling was more successfully achieved by formation of the mixed anhydride using ethyl chloroformate and *in situ* reaction with protected phenylalanine (Scheme 3.4.10).¹²³

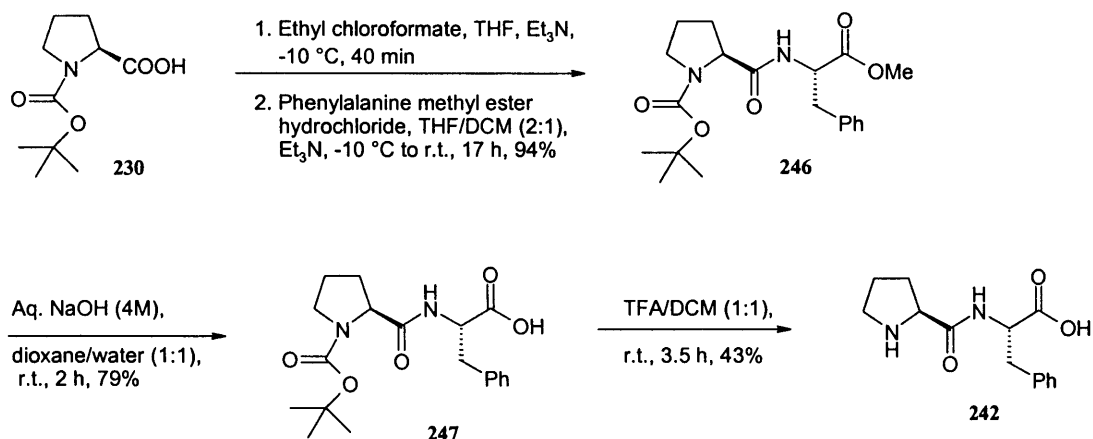


Scheme 3.4.10 Attempted synthesis of dipeptide **242**.

The subsequent step involved cleavage of the methyl ester **244**. This was first carried out using aqueous sodium hydroxide in methanol, however, in this case, starting material was also recovered.¹²⁴ Hydrolysis was then attempted using sodium hydroxide in dioxane, which cleanly gave the desired acid **245** in 82% yield (**Scheme 3.4.10**).¹²⁵ The last step involved deprotection of the Cbz group by hydrogenation. Initially, transfer hydrogenation conditions using palladium on carbon in the presence of 1,4-cyclohexadiene resulted in recovery of starting material and a complex mixture of unknown by-products.¹¹⁰ Heating the reaction to 50 °C did not facilitate deprotection, and once again, the NMR spectra revealed a mixture of products. The final attempt was to use hydrogen gas instead of 1,4-cyclohexadiene, and although the NMR spectra showed a small amount of desired product **242**, our efforts to purify the compound were unsuccessful (**Scheme 3.4.10**).

We therefore turned our attention to the use of an alternative protecting group on the proline residue. Boc protected proline was coupled to phenylalanine methyl ester using the mixed anhydride method to yield **246** (**Scheme 3.4.11**). Hydrolysis of the methyl

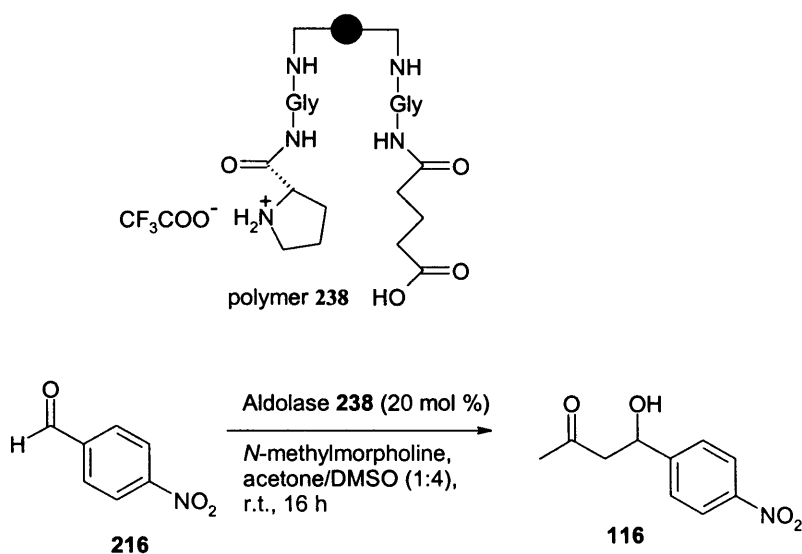
ester and deprotection of the Boc group proceeded smoothly, leading to the desired catalytic dipeptide **242** being isolated in 43% yield.



Scheme 3.4.11 Synthesis of dipeptide **242**.

3.4.3.2 Testing the dipeptide **242** as a catalyst in aldol reaction

The dipeptide **242** was then investigated in the aldol reaction between 4-nitrobenzaldehyde and acetone, in the presence of *N*-methylmorpholine as outlined in **Scheme 3.4.9**, under the same conditions described by Li.¹²² The aldol adduct was successfully obtained in 87% yield. With the successful aldol conditions in hand, we next applied this to the same aldol reaction using our polymer catalyst **238** (**Scheme 3.4.12**). This resulted in a product conversion of 72% by NMR spectroscopy, which was very encouraging. The precise role of *N*-methylmorpholine in this reaction was not obvious. However, Li *et al.* used it to adjust their reaction mixture to pH 8.¹²² As a result, they observed the reaction time was shortened from 192 to 96 hours. In our case, when the reaction was performed in the absence of *N*-methylmorpholine (**Scheme 3.4.12**), no product was detected. In this instance, in addition to adjusting the pH, its role could be the desalting of the TFA salt of the proline on resin **238**. The presence of the TFA salt would most likely prevent the enamine formation between proline and benzaldehyde. Additionally, it should also be noted that when the reaction was performed with *N*-methylmorpholine in the absence of polymer catalyst **238**, no product formation was detected.

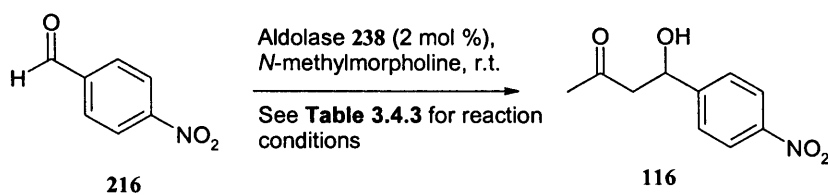


Scheme 3.4.12 Aldol reaction catalysed by polymer **238**.

3.4.4 Re-investigation of catalytic activity of tentagel catalyst **238**

3.4.4.1 Optimising reaction conditions for an aldol reaction

Encouraged by the fact that polymer **238** exhibited some activity, we selected the reaction between 4-nitrobenzaldehyde with acetone as a model, in order to optimise the reaction conditions (**Scheme 3.4.13** and **Table 3.4.3**).



Scheme 3.4.13 Aldol reaction catalysed by polymer **238**.

Using 2 mol % of our tentagel catalyst **238**, the aldol reaction was tested in a variety of organic solvents, which all gave similar NMR conversion yields (entries 2 – 6), albeit over longer reaction times. Addition of water to the reaction enhances the percentage conversion to aldol product (entry 7). As highlighted by Houk, the most energetically

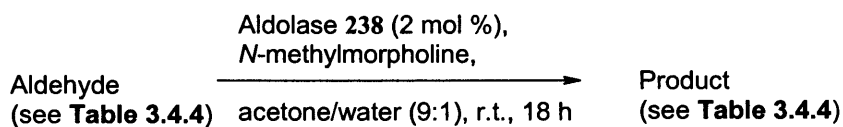
demanding step in the aldol reaction sequence is the breakdown of the carbinolamine which is formed on hydrolysis of the iminium cation, and as suggested by these theoretical studies, an increased concentration of water in the reaction could shift the equilibrium towards the product.¹²⁶ Increasing the reaction duration, gave an impressive 80% conversion to the product (entry 8). Interestingly, doubling the water content of the reaction gave only a trace of product presumably due to premature hydrolysis of the enamine intermediate (entry 9). This may also be partially due to the fact that the resin does not have very good swelling properties in water¹¹¹ and hence ‘shrinks’, making the catalytic site less accessible to the substrate. The solvent system that gave the best results was a mixture of acetone/water (entry 11), which resulted in a quantitative conversion by NMR analysis.

Entry	Solvent	Reaction time (h)	Ratio of aldehyde to product ^a
1.	Acetone/DMSO (1:4)	16	3.5:1
2.	Acetone	40	5:1
3.	Acetone/Acetonitrile (1:4)	40	10:1
4.	Acetone/DCM (1:4)	40	5:1
5.	Acetone/Dioxane (1:4)	40	4:1
6.	Acetone/DMF (1:4)	40	8:1
7.	Acetone/DMSO/Water (1:3.5:0.5)	18	1.6:1
8.	Acetone/DMSO/Water (1:3.5:0.5)	40	1:4
9.	Acetone/DMSO/Water (1:3.5:1)	18	32:1
10.	Acetone/DMSO/Water (1:3.5:0.25)	40	5:1
11.	Acetone/Water (4.5:0.5)	40	0:1

Table 3.4.3 Optimising reaction conditions for aldol reaction in **Scheme 3.4.13**. ^a Molar ratio determined by NMR analysis of crude isolated material.

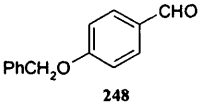
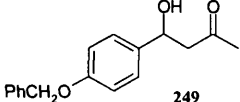
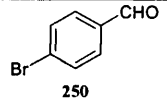
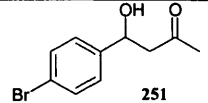
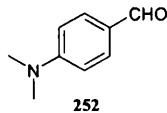
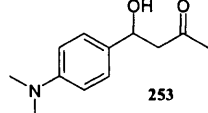
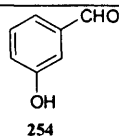
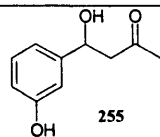
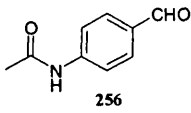
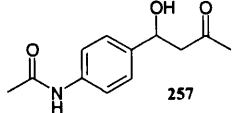
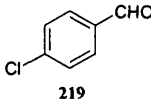
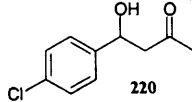
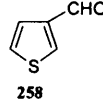
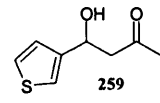
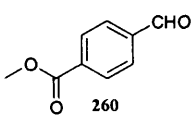
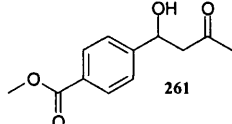
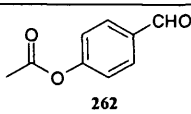
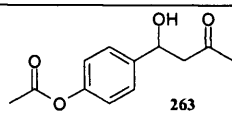
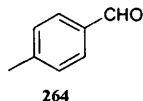
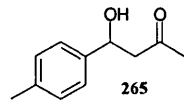
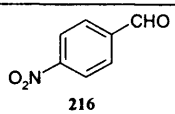
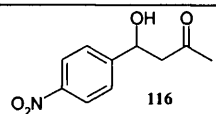
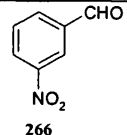
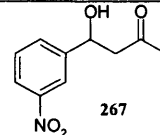
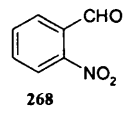
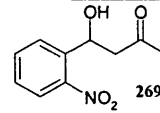
3.4.4.2 Aldol substrate specificity studies (Part 1)

Following the optimisation of the aldol reaction using polymer **238**, the most favourable solvent conditions employing acetone/water (9:1) (**Table 3.4.3**) were applied in aldol reactions, where the aldehyde substrate was varied (**Scheme 3.4.14**). The reaction was stopped after a period of 18 hours.



Scheme 3.4.14

From examination of the results in **Table 3.4.4** it can be concluded that only those aldehydes which contain electron withdrawing groups attached to the benzene ring can undergo an aldol reaction (entries 2,6,8, 11-15) under our conditions. This is perhaps not surprising, since the electron withdrawing groups make the carbon atom of the aldehyde more electron deficient and thus more susceptible to nucleophilic attack by the enamine. Although the NMR analysis of the crude mixtures for some reactions indicated no remaining aldehyde was present, the corresponding isolated yields were much lower than expected (entries 6, 8, 11 and 12). This probably arises due to some of the product remaining trapped on the resin, even though the resin was thoroughly washed after the reaction. The aldol reaction was also attempted with recovered catalyst, and although the catalyst can be re-used, the products were obtained in lower yields. Thus for example, for the aldol reaction shown in entry 11, the product was isolated in 30% yield, however when the same reaction was attempted with the recovered catalyst, the product was isolated in only 17% yield.

Entry	Aldehyde	Expected product	Ratio of aldehyde to product ^a	Isolated yield (%) ^b
1.	 248	 249	1:0	-
2.	 250	 251	1:1	19
3.	 252	 253	1:0	-
4.	 254	 255	1:0	-
5.	 256	 257	1:0	-
6.	 219	 220	0:1	18
7.	 258	 259	3:1	7
8.	 260	 261	0:1	30
9.	 262	 263	1:0	-
10.	 264	 265	1:1	21
11.	 216	 116	0:1	30
12.	 266	 267	0:1	43
13.	 268	 269	1:4	25

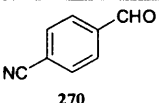
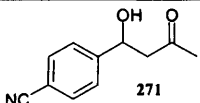
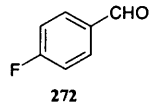
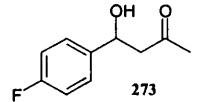
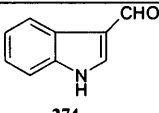
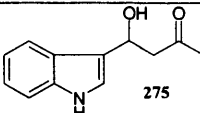
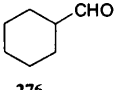
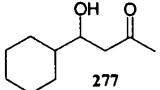
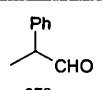
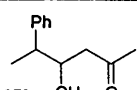
14	 270	 271	1:2.6	32
15.	 272	 273	0:1	-
16.	 274	 275	1:0	-
17.	 276	 277	1:0	-
18.	 278	 279	1:0	-

Table 3.4.4 Activity of aldol catalyst **238** with varying aldehyde substrates. ^a Molar ratio determined by NMR analysis of crude isolated material after 18 h. ^b Isolated yield of product after column chromatography.

When the polymers were tested on hetero-aromatic systems, the reaction of thiophene-3-carboxaldehyde (entry 7) proceeded in modest yield, but, as expected, the more electron rich indole congener (entry 16) proved unsuccessful. Attempted cross aldol reactions with either an alicyclic (entry 17) or acyclic (entry 18) aldehyde did not furnish any detectable product.

3.4.4.3 Enantioselectivity of aldol reaction

Our next goal was to ascertain whether the aldolase **238** exhibited any degree of enantioselectivity for the successful aldol reactions. When analysing the aldol adducts of eight reactions (**Table 3.4.5**), chiral induction was observed for five of the substrates. The R product was favoured for entries 2, 7, and 8. Curiously, whilst the use of 4-bromobenzaldehyde gave no enantiomeric excess (entry 1), the adduct from the 4-chloro derivative was formed with 19% *ee*. The *para* nitro and cyano analogues (entries 7 and 8) displayed moderate chiral enrichment (both 48%), however, the methyl ester derivative was generated as a racemate (entry 4). Interestingly, a substantial difference was observed amongst the *ortho*, *meta* and *para* nitro benzaldehyde derivatives (entries 5 –7). Thus, the *meta* analogue indicated no enantiomeric enhancement, whilst, the *ortho* derivative (entry 6) exhibited some selectivity. However, since the latter is not a literature compound and the enantiomers could not be separated on a chiral HPLC column, the favoured enantiomer could not be determined. It should be noted that when the aldol reactions were attempted with L-proline on its own, under the same conditions stated in **Scheme 3.4.14**, no selectivity was observed. This could be due to the fact that *N*-methylmorpholine can deprotonate the carboxylic acid and the resultant proline salt cannot adopt the Zimmerman-Traxler type transition state¹¹⁶ with the ketone as illustrated in **Scheme 3.3.3**.

As mentioned previously, the low isolated yields of the aldol products imply that some of the products may be trapped on the polymer. This has raised some concern regarding the observed *ee* values in **Table 3.4.5**. If some of the product remains on the polymer, it may be possible that one enantiomer may be retained in preference to the other. However, after taking into consideration the initial loading of the polymer, together with the fact that only 2 mol % of the polymer is used, we have calculated that only the maximum of 7% of any potential aldol products formed could in theory stay bound on the polymer. This indicates that even if one enantiomer was favourably trapped, the *ee* values that we measured are unlikely to be significantly affected.

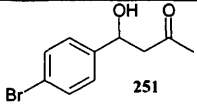
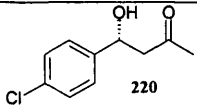
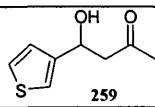
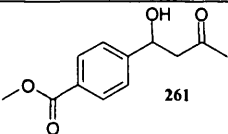
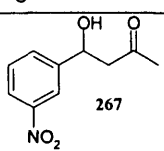
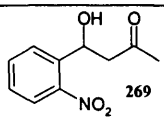
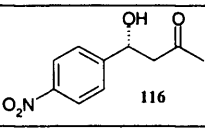
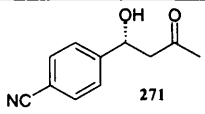
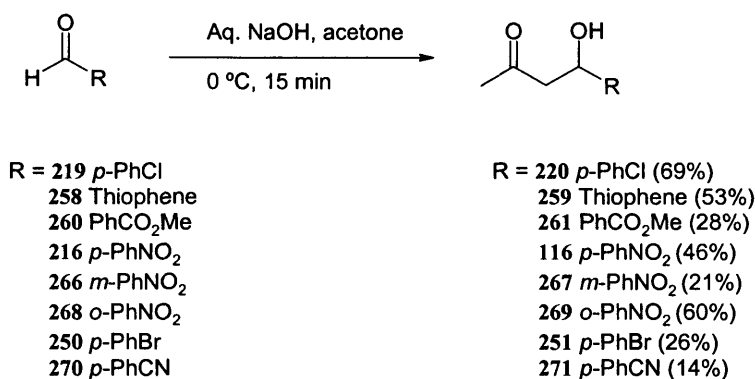
Entry	Aldol product favoured	ee (%)	$[\alpha]_D$ of enantiomeric mixture
1.	 251	0 ^a	0°
2.	 220	19 ^b	+13.5°
3.	 259	69 ^{a,c}	-6.8°
4.	 261	0 ^a	0°
5.	 267	0 ^a	0°
6.	 269	n.d. ^{c,d}	-13.8°
7.	 116	48 ^{a,b}	+23.7°
8.	 271	48 ^{a,b}	+40.8°

Table 3.4.5 Selectivity of aldol catalyst **238**. ^a Determined by chiral-phase HPLC analysis. ^b Determined by optical rotation and corresponding literature values. ^c Not a literature compound, hence the favoured enantiomer unknown. ^d *ee* not determined, enantiomers could not be separated on chiral-phase HPLC.

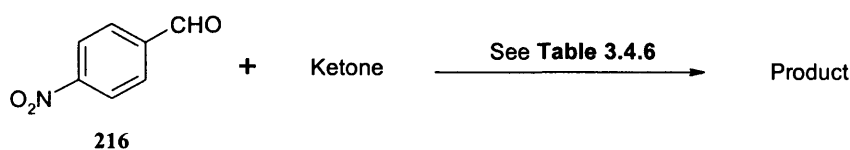
We note parenthetically that in order to carry out analysis by chiral HPLC, the corresponding racemates of the above products had to be synthesised. This was performed following the procedure of Schultz *et al.*, by treating the aldehyde in acetone as a solvent, with dropwise addition of aqueous sodium hydroxide at 0 °C (**Scheme 3.4.15**).¹²⁷



Scheme 3.4.15 Synthesis of racemic aldol product.

3.4.4.4 Aldol substrate specificity studies (Part 2)

A small number of screening reactions with ketones other than acetone were also investigated using catalyst **238** (Scheme 3.4.16 and Table 3.4.6). Our intention was only to observe whether the aldol reaction would proceed with these ketones and hence products were not isolated by purification. Thus, use of cyclopentanone (Table 3.4.6, entry 1) revealed encouraging results, whilst the corresponding reaction with cyclohexanone (Table 3.4.6, entry 2) was unsuccessful, with only a trace of desired product **222** and dehydrated product **281** detectable by NMR analysis. Using cyclobutanone as a ketone gave only 15% of the desired product by NMR analysis (entry 3), whereas 2-methyl cyclopentanone gave no product at all (entry 4).



Scheme 3.4.16 Reaction of 4-nitrobenzaldehyde with different ketones.

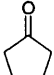
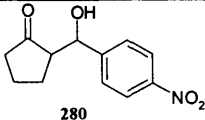
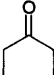
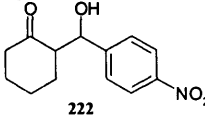
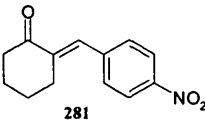
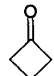
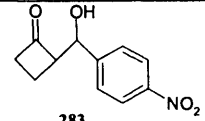
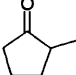
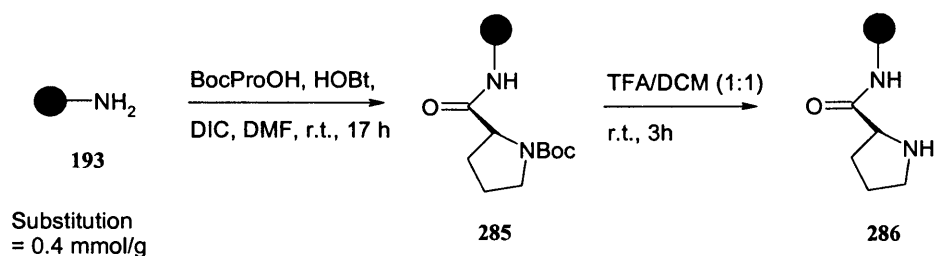
Entry	Ketone	Conditions	Product	Ratio of aldehyde to product ^a
1.	 66	Polymer 238 (4 mol%), <i>N</i> -methymorpholine, DCM, r.t., 18 h	 280	42
2.	 221	Polymer 238 (4 mol%), <i>N</i> -methymorpholine, DCM, r.t., 18 h	 222 +  281	Trace of mixed products observed
3.	 282	Polymer 238 (4 mol%), <i>N</i> -methymorpholine, DCM, r.t., 24 h	 283	15
4.	 284	Polymer 238 (4 mol%), <i>N</i> -methymorpholine, DCM, r.t., 18 h	-	-

Table 3.4.6 Reaction of 4-nitrobenzaldehyde with different ketones. ^a Molar ratio determined by NMR analysis of crude isolated material after 18 h.

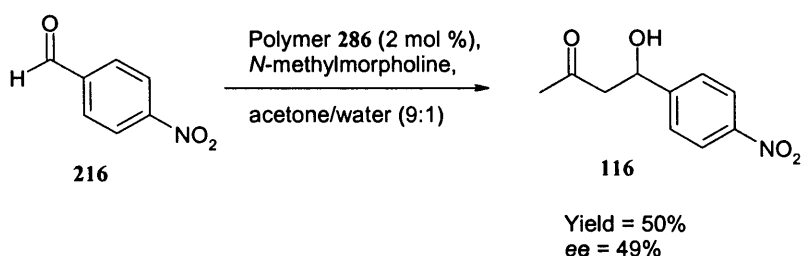
These preliminary results imply, that in principle, the activity of polymer **238** is not restricted to acetone. This presents the possibility that more elaborate systems could be investigated in future.

3.4.5 Development of alternative tentagel based catalysts

Since the reaction protocol adopted required the use of *N*-methymorpholine, it was not clear whether the presence of carboxylic acid in polymer **238** had any beneficial effect on the aldol reaction itself. Accordingly, the polymer containing only the proline residue was prepared (Scheme 3.4.17). Comparison of the activity of polymer **286** with polymer **238** in an aldol reaction (Scheme 3.4.18), revealed that there was no difference in terms of either conversion or enantiomeric excess. This indicates that the carboxylic acid attached to polymer **238** does not play a significant role within this particular system, in terms of activating the aldehyde as we had initially thought.

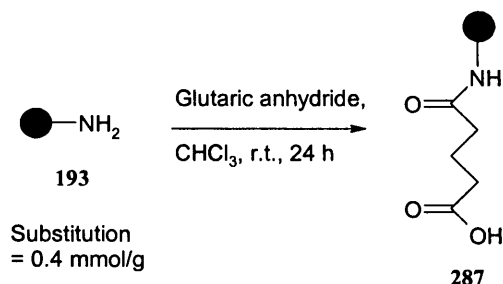


Scheme 3.4.17 Synthesis of aldol catalyst **286**.



Scheme 3.4.18 Aldol reaction catalysed by polymer **286**.

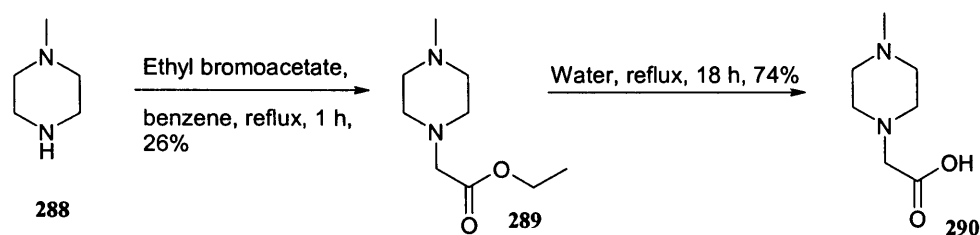
For comparison purposes, the resin containing only the carboxylic acid was also prepared (**Scheme 3.4.19**) and tested in the aldol reaction shown in **Scheme 3.4.19**. As expected, it was inactive and no product was isolated.



Scheme 3.4.19 Synthesis of polymer **287**.

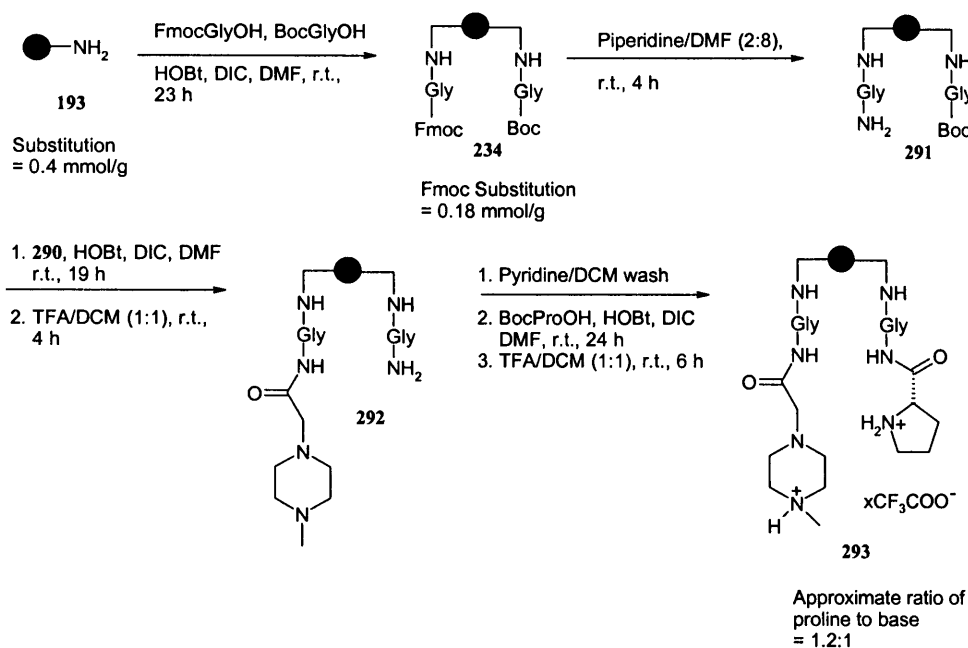
The third type of catalyst which we decided to examine was one which contained an internal base. As the use of *N*-methylmorpholine was required for all of our reactions, we wanted to see whether the introduction of an *N*-methylmorpholine analogue (to

mimic the base) as one strand of our polymer, would allow us to avoid the use of this base in solution.



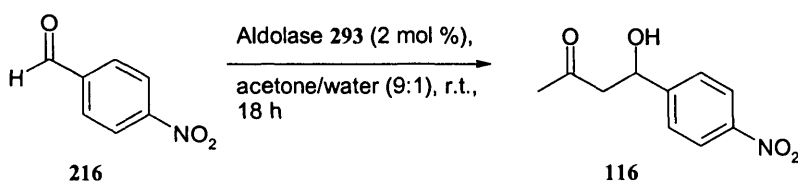
Scheme 3.4.20 Synthesis of **290**.

Ethyl bromoacetate was reacted with *N*-methyl piperazine, followed by hydrolysis with water to give **290** in 74% yield (**Scheme 3.4.20**). The acid **290** was then incorporated into the resin, using our previously established procedure to give the desired polymer **293** (**Scheme 3.4.21**).



Scheme 3.4.21 Synthesis of aldol catalyst **293** with incorporated internal base.

Initial testing of the aldolase **293** (Scheme 3.4.22), in the absence of *N*-methylmorpholine gave only recovered starting materials. Once again, the presence of the TFA salt of proline and of the *N*-methyl piperazine unit was probably undesirable, and hence the polymer was washed with a solution of triethylamine/DCM (2:8) in order to liberate the free amino groups. This was followed by extensive washings of the polymer with DCM and methanol, in order to remove any traces of triethylamine. Gratifyingly, the use of the free base polymer **293** as a catalyst resulted in a 100% conversion to product, determined by NMR analysis.

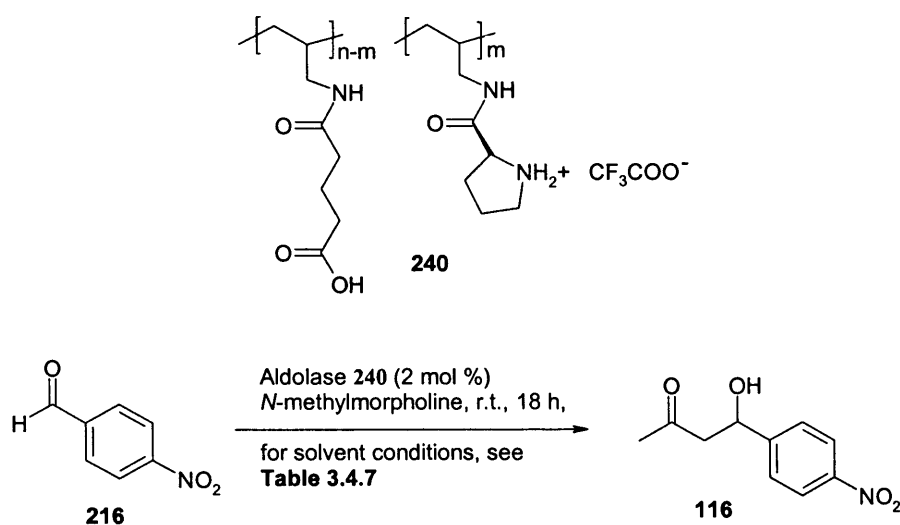


Scheme 3.4.22 Aldol reaction catalysed by polymer **293**.

The ability of the tertiary amine unit to mediate proton transfer is clearly a significant observation. It may be involved at several steps of the sequence, either as its free base or in its protonated form, to aid enamine formation or to deliver a proton to the initial aldol adduct.

3.4.6 Re-investigation of catalytic activity of polyallylamine catalyst **240**

In light of the results obtained with the tentagel based aldol catalysts, it was appropriate to revisit the polyallylamine based polymer **240**, synthesised previously (Section 3.4.2). Polymer **240** was tested on our model system (Scheme 3.4.23), under the conditions outlined in Table 3.4.7. From the Table, it can be seen that a mixture of acetone/water (entries 2 and 4) was shown to be the best solvent for the reaction. In contrast to the tentagel based resin an increase in the water content of the reaction (Table 3.4.7, entry 4) did not appear to have any adverse affect on conversion, possibly as a consequence of the better compatibility of polyallylamine with aqueous systems.



Scheme 3.4.23 Aldol reaction catalysed by polyallylamine based polymer **240**.

Entry	Solvent	Ratio of aldehyde to product ^a	Isolated yield (%) ^b
1.	Acetone/ DMSO (1 : 4)	No product observed	-
2.	Acetone/Water (4.5 : 0.5)	0:1	29
3.	Acetone/DMSO/Water (1 : 3.5 : 0.5)	2:1	-
4.	Acetone/Water (1 : 1)	0:1	-

Table 3.4.7 Reaction conditions attempted for the aldol reaction catalysed by polymer **240**. ^a Molar ratio determined by NMR analysis of crude isolated material after 18 h. ^b Isolated yield of product after column chromatography.

3.4.7 Development of a Merrifield resin based aldol catalyst

As previously mentioned (Section 3.4.3.1) the dipeptide **242** (**Figure 3.4.1**) was shown to catalyse aldol reactions by Li *et al.*¹²² We therefore questioned whether the catalytic properties of this dipeptide would change if we attached it to a solid support. Since the dipeptide does not contain any functional groups which would provide a suitable link to the resin, we decided to select the hydroxyproline version of the dipeptide (**294**, **Figure 3.4.1**) with the hydroxyl group of **294** providing a suitable point for attachment. Merrifield resin was chosen as our polymer backbone, since it has a chloro group which

can be easily displaced by a nucleophile. It should be noted that peptide **294** was also investigated by Li and co-workers in their aldol studies and they found it to have comparable catalytic properties to the proline derivative, peptide **242** (**Figure 3.4.1**).¹²²

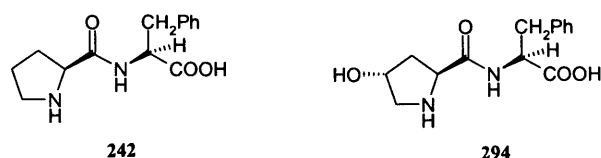
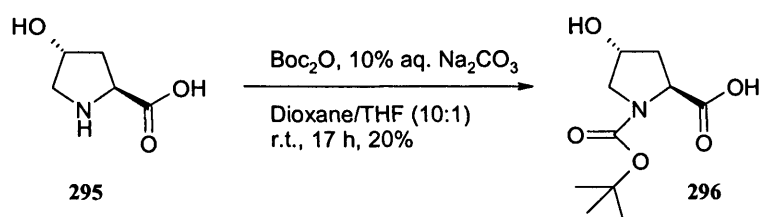


Figure 3.4.1 Aldol catalysts **242** and **294**, used by Li and co-workers in their studies.

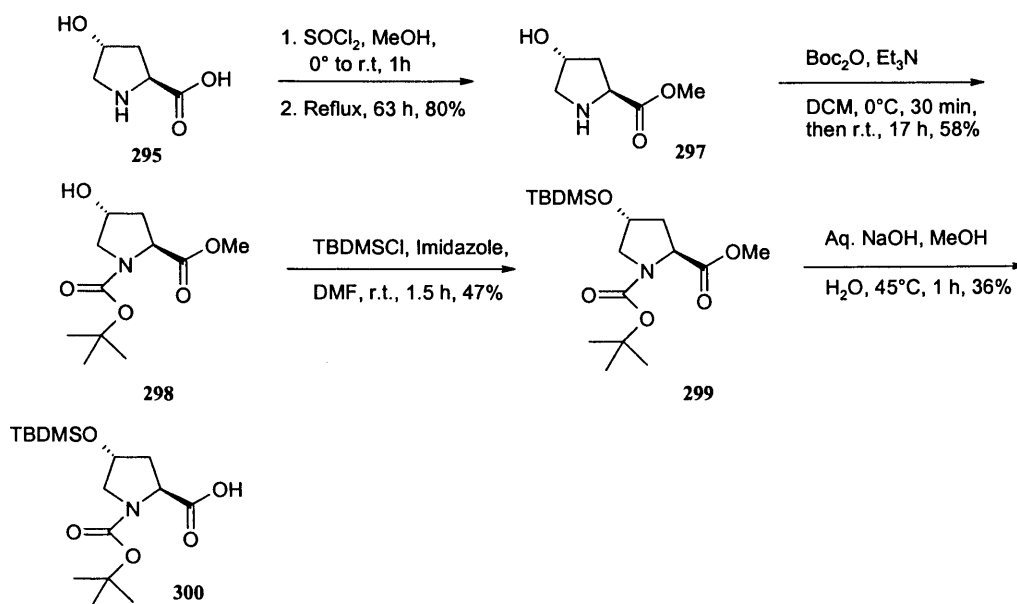
Before attachment to the resin, a suitably protected version of dipeptide **294** had to be synthesised (**Scheme 3.4.24**). Addition of Boc anhydride in the presence of aqueous sodium carbonate, gave compound **296** in only 20% yield. Attempting the same reaction, over 2 days, did not improve the yield.



Scheme 3.4.24 Synthesis of Boc protected hydroxy proline **296**.

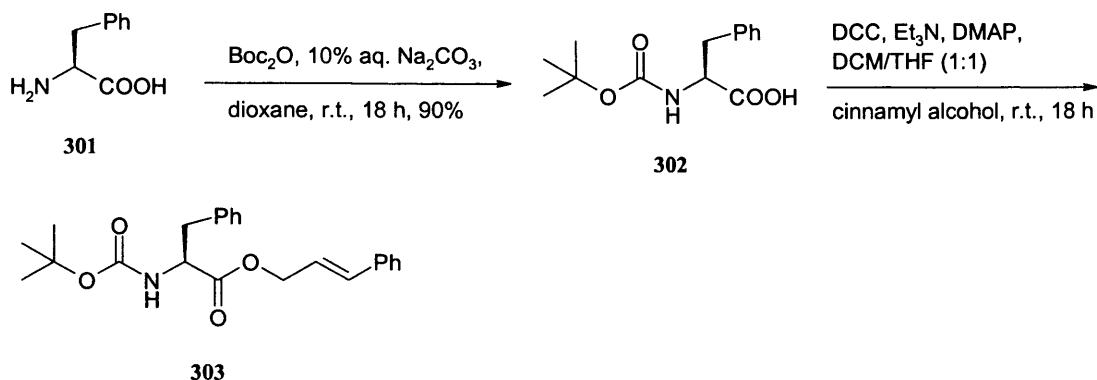
In order to improve the yield, the reaction was repeated using NaOH in THF/water, however the product was still isolated in a disappointing 20% yield.

One of the major problems encountered for the Boc protection was the solubility of hydroxyproline. We felt that if the methyl ester was prepared, this would be much more soluble and would allow Boc protection to proceed more easily. Reaction of hydroxyproline with thionyl chloride in methanol proceeded smoothly to generate ester **297** in 80% yield (**Scheme 3.4.25**). Subsequent Boc protection gave **298** in 58% yield.¹²⁸ Protection of the hydroxyl group with *tert*-butyl dimethyl silyl (TBDMS) chloride,¹²⁹ followed by cleavage of the ester with sodium hydroxide¹³⁰ gave the desired acid **300**, which was suitable for peptide coupling.



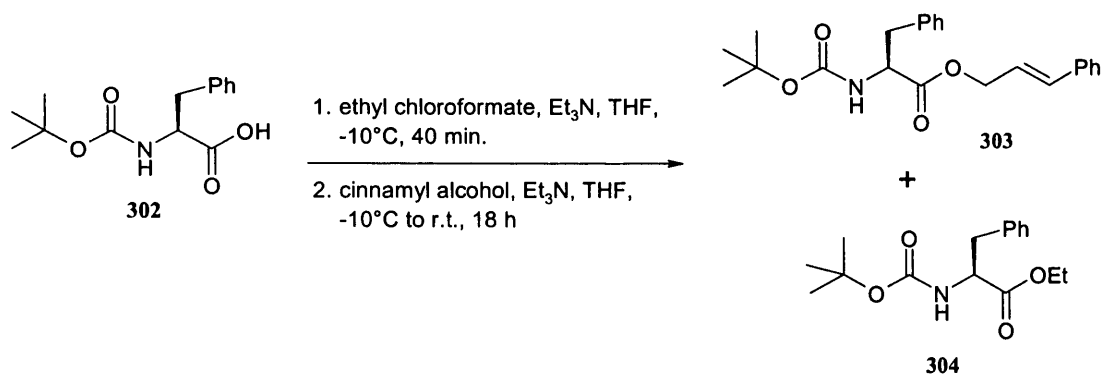
Scheme 3.4.25 Synthesis of protected hydroxyproline **300**.

The next step was to couple a protected version of phenylalanine to the protected hydroxyproline unit **300**. A requirement for the phenylalanine component was that it should also possess a UV active alcohol attached to it, since this would allow us eventually to measure the substitution of the dipeptide on the resin by simple cleavage of the alcohol in a manner similar to the procedure previously used for Fmoc substitution measurements (see Section 2.3.1). We felt that cinnamyl alcohol was a suitable choice, since it has good UV absorption. Phenylalanine was therefore protected with a Boc anhydride to form **302** (Scheme 3.4.26), followed by the coupling of cinnamyl alcohol using DCC. Some product was isolated in this case, however, it was very difficult to separate it from the urea by-product and hence alternative routes were explored.



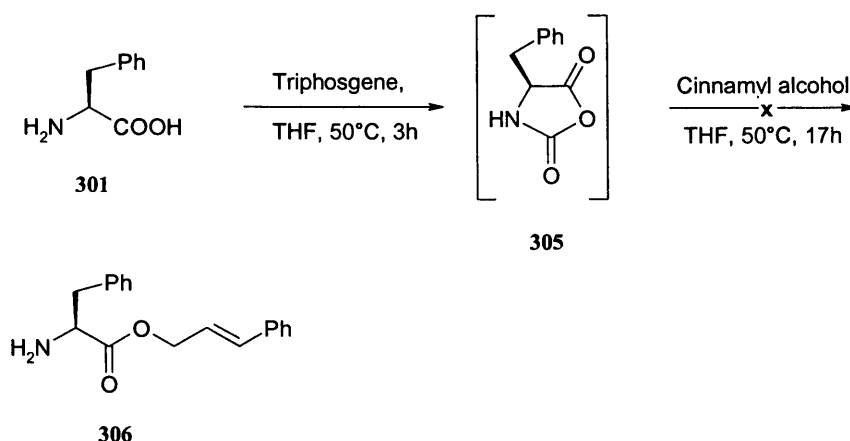
Scheme 3.4.26 Synthesis of protected phenylalanine ester **303**.

The use of EDCI, was next considered, since its urea by-product is soluble in water. However, in this reaction, only a trace of product was recovered. Ester formation *via* Mitsunobu conditions (PPh₃, DEAD) gave no desired product.¹³¹ Using the mixed anhydride method in the presence of ethyl chloroformate led to a mixture of the desired product **303** and the ethyl ester **304** (Scheme 3.4.27).¹²³ Unfortunately, these esters were inseparable by flash chromatography.



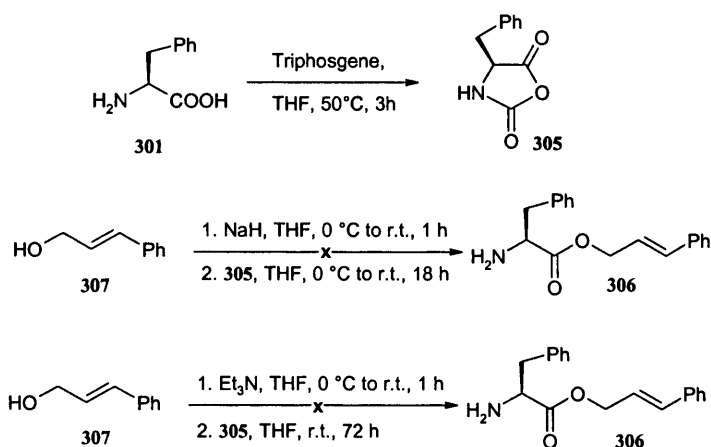
Scheme 3.4.27 Synthesis of protected phenylalanine ester **303**.

The final attempt was to couple the alcohol *via in situ* formation of the *N* – carboxyanhydride **305**, however no product was isolated in this case (Scheme 3.4.28).¹³²



Scheme 3.4.28 Attempted synthesis of phenylalanine ester **306**.

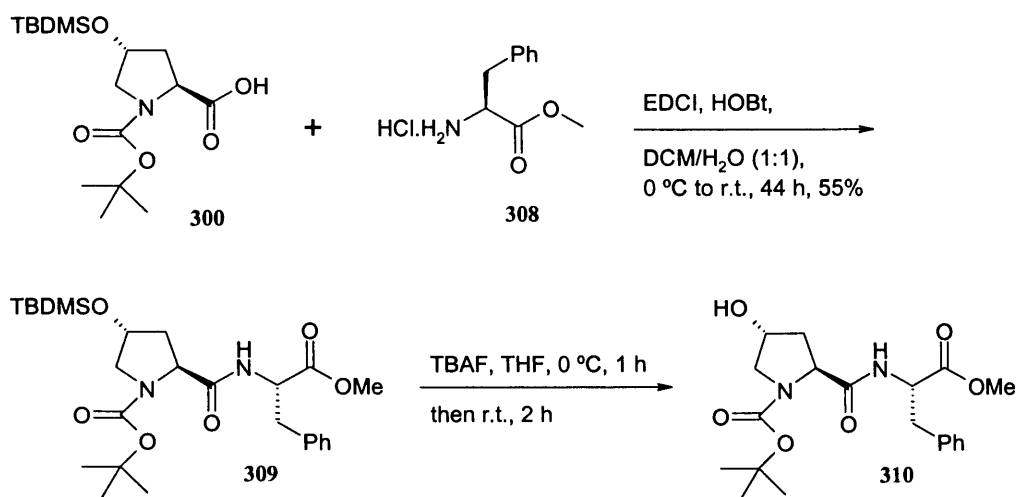
Alternatively, prior isolation of the *N*-carboxyanhydride (**Scheme 3.4.29**), followed by a subsequent reaction with the alcohol, in the presence of either sodium hydride or triethylamine as a base also failed to yield the desired product (**Scheme 3.4.29**).



Scheme 3.4.29 Attempted synthesis of phenylalanine ester **306**.

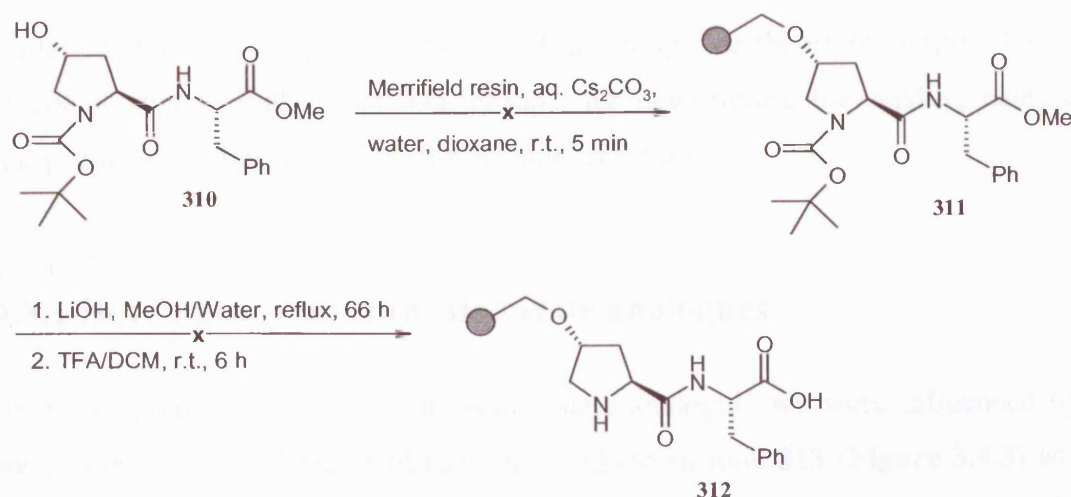
Due to the surprising lack of success in preparing the cinnamyl ester of phenylalanine, we decided to use the methyl ester as the protecting group instead, even though in this case we would not be able to estimate the substitution of dipeptide on the resin. An estimate of the approximate amount of dipeptide once it is attached to Merrifield resin was therefore used. Coupling of commercially available phenylalanine methyl ester hydrochloride with protected proline **300**, using EDCI, gave the dipeptide **309** (**Scheme**

3.4.30). Deprotection of the silyl protecting group with tetrabutyl ammonium fluoride (TBAF) yielded dipeptide **310**, together with an ammonium impurity, which could not be separated from **309**.



Scheme 3.4.30 Attempted synthesis of protected phenylalanine ester **310**.

Nonetheless, attachment of crude dipeptide **310** to Merrifield resin was attempted, using caesium carbonate (**Scheme 3.4.31**), followed by the hydrolysis of the ester moieties with lithium hydroxide.¹³³ At this point, the Malachite green test for the presence of carboxylic acids gave a negative result. This indicated either that the peptide had not coupled to the resin or that the hydrolysis step was not successful. Nevertheless, a small amount of the resin was carried through to the next step, which involved cleavage of the Boc groups using TFA/DCM solution to give **312**. The chloranil test for the presence of secondary amines indicated that proline was not coupled to the resin. This suggests that the initial attachment of hydroxyproline to the resin was unsuccessful. Nonetheless, we attempted to use the resin **312** as a catalyst in our model aldol reaction, in case the qualitative tests were giving us false negative results. Resin **312** did not exhibit any catalytic activity, thereby further implying that the peptide was not coupled in the first place.



Scheme 3.4.31 Attempted synthesis of polymer catalyst **312**.

3.4.8 Designing an aldol catalyst with improved selectivity

Even at this most simplistic first generation level, we have observed some encouraging results using the tentagel based aldolase **238**, with selectivities comparable to those previously reported.¹²² Accordingly, we were interested in developing this catalyst further, especially in terms of its stereoselectivity. In order to achieve this, the inclusion of both a chiral recognition group in conjunction with the catalytic proline group on the polymer backbone would be desirable (**Figure 3.4.2**).

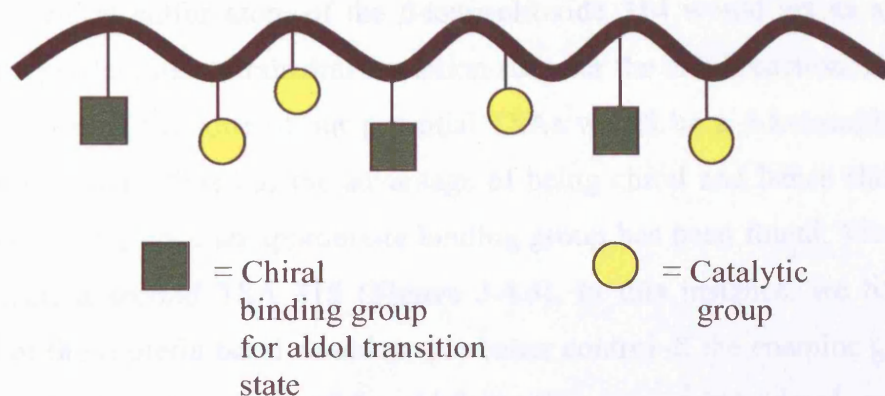


Figure 3.4.2 Representation of aldol catalyst with incorporated chiral binding group.

In order to find the most appropriate binding group, we therefore adapted the NMR protocol developed within our own group⁹⁶ for determining the binding energies of suitable transition state analogues for the aldol reaction.

3.4.8.1 Development of transition state analogues

In terms of preparing a suitable transition state analogue, we were influenced by the work of Lerner *et al.*¹³⁴ who had used the β -diketo-sulfone **313** (Figure 3.4.3) as their transition state analogue for generation of a library of catalytic aldolase antibodies. The tetrahedral geometry of sulfone moiety in **313** was considered to mimic the tetrahedral transition state in the carbon-carbon bond forming step of the aldol reaction.

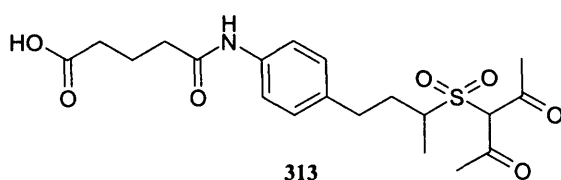


Figure 3.4.3 β -diketo-sulfone TSA.

More recently however, Domingo and co-workers conducted a number of comparative computational studies between the β -ketosulfoxide **314** (Figure 3.4.4) and the β -diketosulfone **313** (Figure 3.4.3).¹³⁵ They concluded that the pyramidal arrangement around the chiral sulfur atom of the β -ketosulfoxide **314** would act as a much better mimic of a product like tetrahedral transition state for the aldol reaction. Bearing this in mind, we decided that one of our potential TSAs would be a β -ketosulfoxide such as **314** (Figure 3.4.4). This has the advantage of being chiral and hence should facilitate enantioselectivity, once an appropriate binding group has been found. We also decided to synthesise a second TSA **315** (Figure 3.4.4). In this instance, we hoped that the presence of the E olefin bond would enable better control of the enamine geometry. The carbons in the transition state of the aldol reaction are sp^2 hybridised, and this planar TSA may be more representative of the aldol transition state.

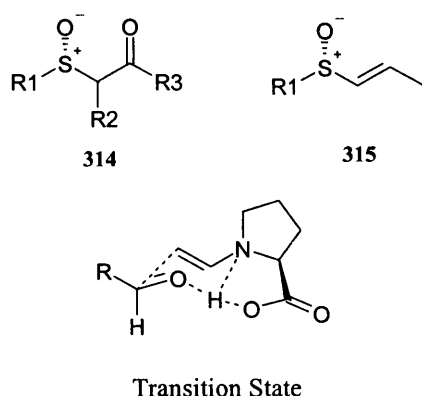


Figure 3.4.4 Sulfoxide TSAs (**314** and **315**) and representation of the aldol transition state.

3.4.8.2 Synthesis of sulfoxide transition state analogues

The transition state analogues we aimed to prepare are shown in **Figure 3.4.5**. Although our aldehyde substrates had different substituents attached to the benzene ring, our decision to use the *para*-toluene sulfoxide TSA was due to the fact that they are available using established methodology by Solladie.^{136;137}

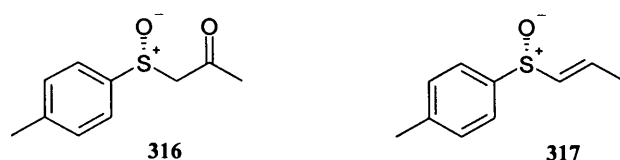
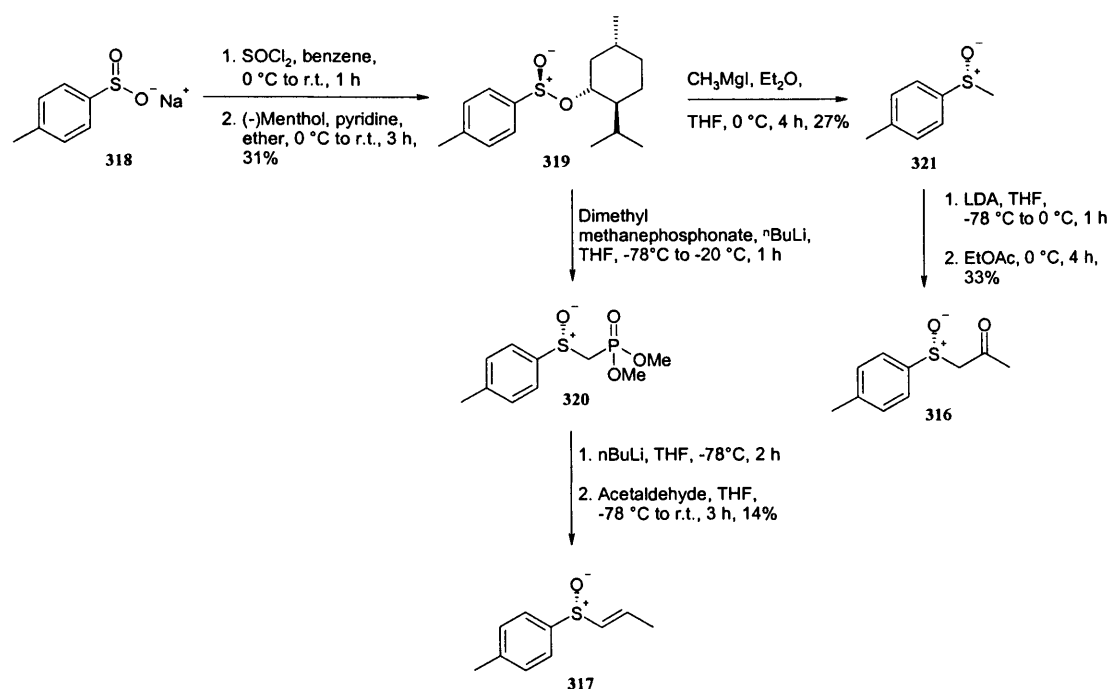


Figure 3.4.5 Target sulfoxide transition state analogues.

Starting from *p*-toluene sulfinic acid, chirality was introduced into the molecule using menthol to give **319** in a modest conversion of 31% (**Scheme 3.4.32**). Addition of dimethylmethanephosphonate led to inversion of configuration to afford **320** *in situ*, followed by a Wittig reaction to obtain the desired α,β -unsaturated sulfoxide **317** as the *trans* isomer.¹³⁸



Scheme 3.4.32 Synthesis of sulfoxide TSAs **316** and **317**.

The second route to the formation of the β -ketosulfoxide **316** involved treatment of **319** with methyl magnesium iodide to give **321** in 27% yield. Compound **321** was converted to the β -ketosulfoxide **316** using lithium diisopropylamine (LDA) and ethyl acetate in 33% yield.

3.4.8.3 Selecting a binding group for the transition state analogues

With the sulfoxide (**316** and **317**) TSAs in hand, we next turned our attention towards the selection of appropriate binding groups. A review of the literature indicated that carboxylic acids and hydroxyl groups have favourable binding interactions with sulfoxides.¹³⁹⁻¹⁴¹ This influenced us to select a small set of amino acid based potential binders, that contained a carboxylic acid functionality and were also chiral. We focused on the binding of the carboxylic acid moiety to the sulfoxides and therefore we had to cap the amino group. A number of Boc protected amino acids were selected as potential binders and these are shown in **Table 3.4.8**. Tryptophan and phenylalanine were chosen on the basis that they contained aromatic rings, which we were hoping would favour π – π stacking with the aromatic ring of the sulfoxides, in addition to the binding of the sulfoxide moiety with the carboxylic acid. Cysteine and serine were selected on the

basis of their hydroxyl and thiol group side chains which could potentially act as hydrogen bond donors. Finally, alanine was chosen as a control, since it is devoid of further functionality, allowing the potential binding contribution of the carboxylic acid group to binding to be estimated.

The PFG NMR binding studies were conducted using the previously established protocol.^{91;96} The studies were performed in chloroform solution with a 3 mM concentration of Boc protected amino acid and a 30 mM concentration of TSA. The results are presented in **Table 3.4.8**, which shows the change in diffusion coefficient as a percentage value.

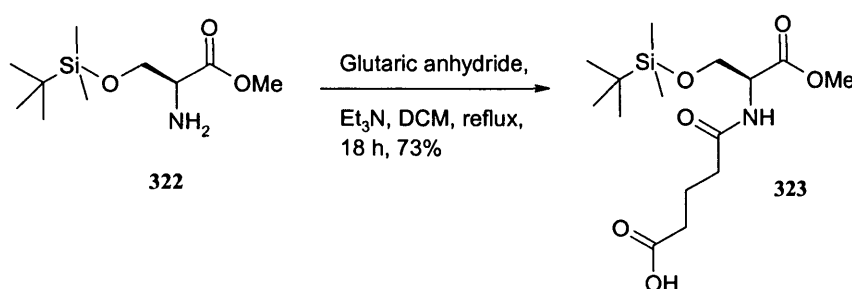
Entry	Amino Acid	D ($\times 10^{-10}$ m^2/s)	D' ($\times 10^{-10}$ m^2/s)	R _d with TSA 316 (%)	D'' ($\times 10^{-10}$ m^2/s)	R _d with TSA 317 (%)
1	BocSerOH	11.69	9.51	19	9.06	22
2	BocCysOH	11.85	10.42	12	9.56	22
3	BocAlaOH	12.02	11.43	5	11.10	8
4	BocPheOH	10.01	9.85	2	9.98	0
5	BocTrpOH	8.27	8.09	2	Not determined	Not determined

Table 3.4.8 Results of NMR binding studies between Boc protected amino acids and sulfoxide TSAs **316** and **317**. D is the diffusion coefficient for 3 mM solution of Boc amino acid in CDCl_3 . D' is the diffusion coefficient for mixtures containing Boc amino acid (3 mM) and TSA **316** (30 mM). D'' is the diffusion coefficient for mixtures containing Boc amino acid (3 mM) and TSA **317** (30 mM). R_d is the relative change in diffusion coefficient ($100(\text{D}-\text{D}')/\text{D}$ or $100(\text{D}-\text{D}'')/\text{D}$).

Serine and cysteine exhibited the most favourable binding towards both TSAs (biggest change in diffusion coefficient). Alanine demonstrated modest binding, however the aromatic amino acids phenylalanine and tryptophan had poor interactions with either sulfoxide TSA, possibly due to unfavourable steric constraints. Following the results outlined above, we decided to incorporate serine within our polymeric system as it demonstrated the best binding. Serine was chosen instead of cysteine due to the fact that cysteine can potentially form unfavourable disulfide bonds.

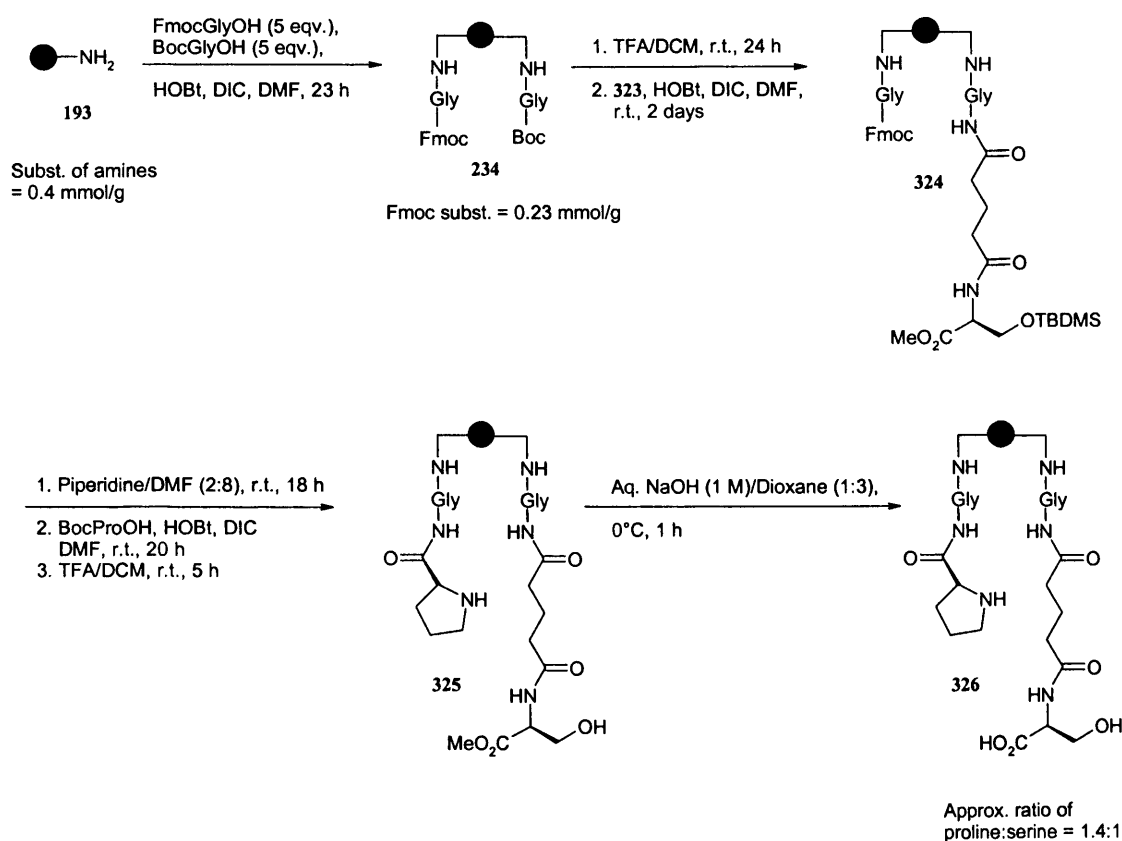
3.4.8.4 Synthesis of aldol catalyst containing a serine binding group

It was decided that the serine residue should be attached to the polymer *via a* suitable spacer. A polymeric system based upon tentagel resin was again used, to enable a more accurate comparison with catalyst **238**. Preparation of the spacer unit involved reacting TBDMS protected serine methyl ester¹⁴² with glutaric anhydride to afford the desired serine unit **323** in 73% yield (**Scheme 3.4.33**).



Scheme 3.4.33 Synthesis of serine derivative **323**.

The serine derivative **323** was incorporated onto the tentagel resin, together with the catalytic proline unit (**Scheme 3.4.34**). Following previously established procedures, Boc protected and Fmoc protected glycine were attached to tentagel to give **234**. Boc deprotection, followed by attachment of the serine derivative **323** gave resin **324**. The proline catalytic unit was incorporated by Fmoc deprotection of **324**, followed by treatment with Boc protected proline. Deprotection of both the Boc and TBDMS groups was achieved using TFA/DCM.¹⁴³ It was anticipated that the serine methyl ester **325** could moderate the aldol reaction, therefore a quantity was retained for testing. Hydrolysis of **325** with sodium hydroxide gave aldolase catalyst **326**.



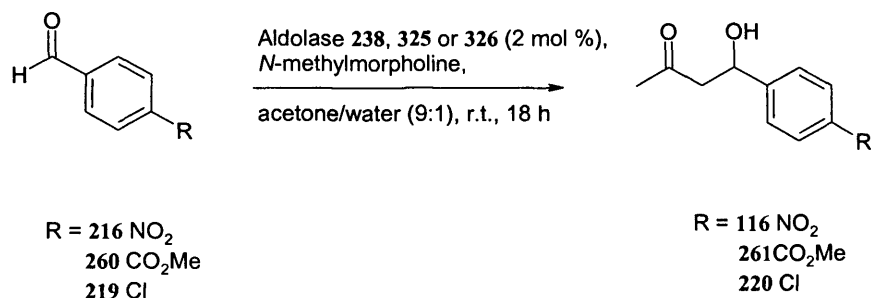
Scheme 3.4.34 Synthesis of aldolase catalyst **326** with incorporated serine binding group.

3.4.8.5 Activity of aldol catalyst **326** containing serine binding group

The serine based polymer **326** was examined for activity on three previously tested aldehydes. Additionally, the activity of the serine methyl ester catalyst **325** was also investigated. This was conducted in order to assess the contribution of the free carboxylic acid on selectivity and yield of conversion. The results are shown in **Table 3.4.9**, together with the results of the original polymer **238** (see Section 3.4.4.3) for comparison purposes.

The first reaction to be investigated was the model reaction, with 4-nitrobenzaldehyde (**Table 3.4.9**, entry 1). In this case, both the methyl ester **325** and the acid **326** had no effect on either the conversion or the enantiomeric excess. The second aldehyde, 4-carboxymethyl benzaldehyde (**Table 3.4.9**, entry 2), for which polymer **238** had previously displayed no enantioselection, also yielded racemic product with the methyl ester **325**. In sharp contrast however, use of the acid **326**, led to a preference for the *R*-

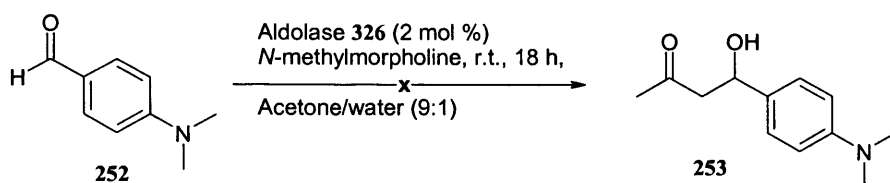
enantiomer ($ee = 33\%$). The aldol reaction with 4-chlorobenzaldehyde proceeded in moderate yield and gave an almost identical stereo-selectivity for both polymer **238** and serine methyl ester polymer **325** (Table 3.4.9, entry 3). Interestingly, the acid catalyst **326**, displayed a preference for the opposite enantiomer. It is difficult to speculate as to why different stereoselectivities were observed, and additional substrates would need to be studied in order to give us more insight into the behaviour of the catalyst. The differences between the catalysts containing the serine methyl ester unit (**325**) and the acid (**326**) (Table 3.4.9, entries 2 and 3), suggest that hydrogen bonding may play some role in altering the selectivity of the catalyst. In this case, the presence of particular groups on the benzene ring of the substrate aldehyde, such as the hydrogen bond acceptor in entry 2, may lead to a particularly favourable interaction with serine, and hence favour attack from proline from one side more than the other. Alternatively, the interactions of the substrates with the polymer may also be dependent on the size and shape of the substrate and this may affect how the substrate fits into the cavities of the polymer, once again leading to different selectivities.



Entry	Aldehyde	Favoured product with catalyst 238	Favoured product with catalyst 325	Favoured product with catalyst 326
1.	 216	 116 <i>ee</i> = 48% Yield = 30%	 116 <i>ee</i> = 48% Yield = 28%	 116 <i>ee</i> = 48% Yield = 33%
2.	 260	 261 <i>ee</i> = 0% Yield = 30%	 261 <i>ee</i> = 0% Yield = 31%	 261 <i>ee</i> = 33% Yield = 16%
3.	 219	 220 <i>ee</i> = 19% Yield = 30%	 220 <i>ee</i> = 22% Yield = 23%	 220 <i>ee</i> = 8% Yield = 21%

Table 3.4.9 Selectivity of the aldol catalyst **238**, **325** and **326**.

Finally, we attempted to use aldolase **326** containing the serine moiety to examine whether we can encourage one of the previously unsuccessful aldol reactions to proceed. However, aldehyde **252** (Scheme 3.4.35) was once again unreactive.



Scheme 3.4.35 Attempted aldol reaction using aldol catalyst 326.

3.5 Exploring artificial aldolases through supramolecular assembly

3.5.1 Introduction

The approach thus far described towards the construction of artificial enzymes is based on the facts that an enzyme can be considered to possess a binding region, a catalytically active functional group and the flexibility to achieve stereoelectronically favoured reaction pathways for attack on the bound substrate by the catalytic group. As we have seen, this strategy has provided evidence for the cooperativity between a binding site selected to recognise a designed transition state mimic and a catalytically active group in a flexible environment. However, as discussed in Section 2.9, each polymeric thread that has been produced by a random attachment of catalytic and binding groups forms a distinct molecular entity and this aspect is inherently undesirable. In order to address this problem, and in tandem with our studies on artificial aldolases we therefore conducted some very preliminary studies towards the formation of molecular assemblies, which could hopefully generate more defined molecular structures.

Our plan was to explore simple systems, based on triple hydrogen bond interactions as illustrated in **Figure 3.5.1**. This strategy involved the synthesis of complementary monomer units, which combine, to form a polymer consisting of a hydrogen bonded network, which should possess a more uniform structure. This approach should enable a rapid variation of the binding site and/or catalytic group if required.

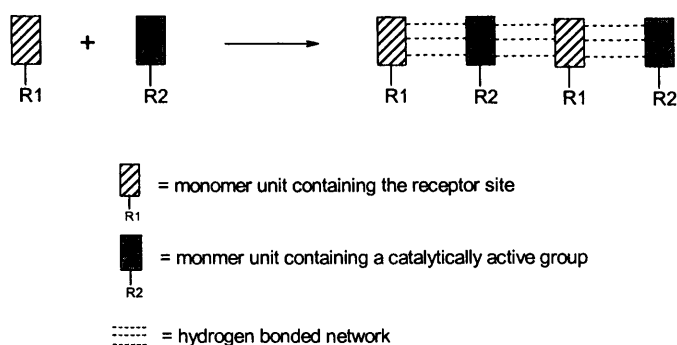


Figure 3.5.1 Representation of hydrogen bonded monomer units.

Recently, significant advances have been made in the formation of supramolecular polymers *via* complementary hydrogen bonding networks of two different monomers.¹⁴⁴⁻¹⁴⁷ These systems have been explored extensively by Lehn and some examples are illustrated in **Figure 3.5.2**.^{146;147}

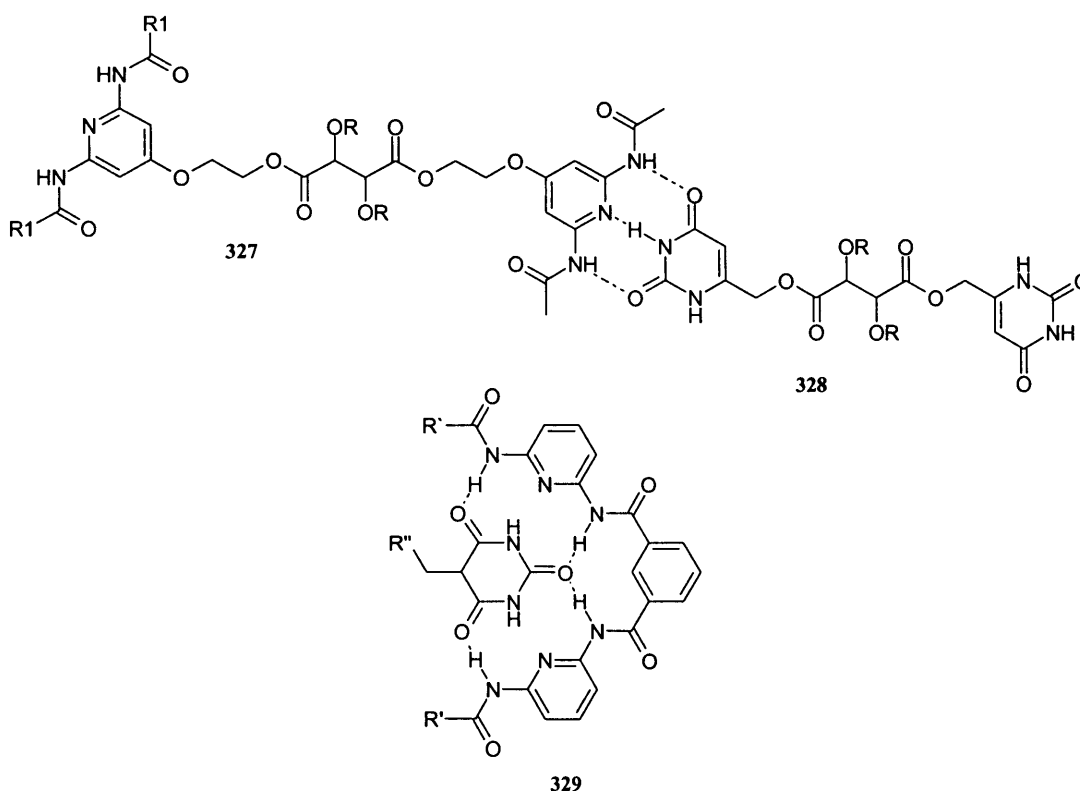


Figure 3.5.2 Hydrogen bonded dimers.

Initially, we wished to investigate a basic system consisting of a dimeric unit **332**, comprising of a 2,6-diaminopyridine **330** and a functionalised uracil counterpart **331**.

These units can form a triple hydrogen bonded interaction (**Figure 3.5.3**). Systems containing derivatives of diaminopyridine and uracil have been explored in the literature.¹⁴⁸ Our desire was to attach both catalytic and binding groups to the monomers and generate a supramolecular catalyst designed specifically for the aldol reaction.

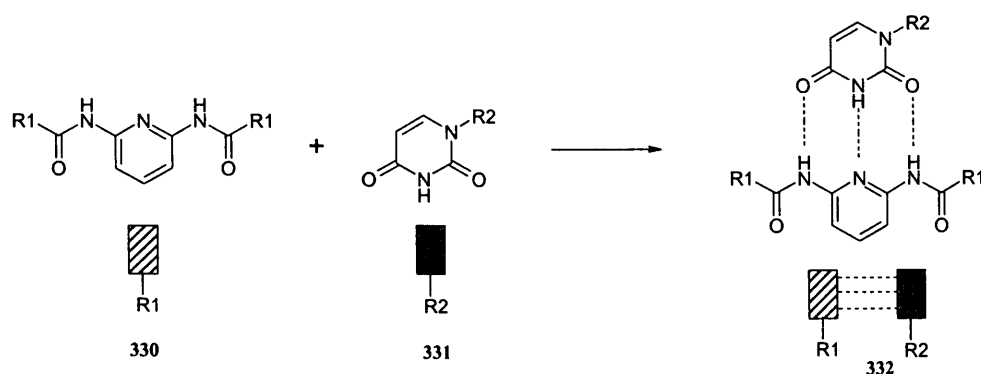


Figure 3.5.3 Target dimer unit.

Hence, one monomer would have proline attached, whilst the other would contain the carboxylic acid (**Figure 3.5.4**). Although we have previously established that the presence of a carboxylic acid was not necessary for the aldol reaction catalysed by our own polymeric system (Section 3.4.5), we decided to incorporate one within this system, due to the fact that the primary literature indicated its importance.^{115;126}

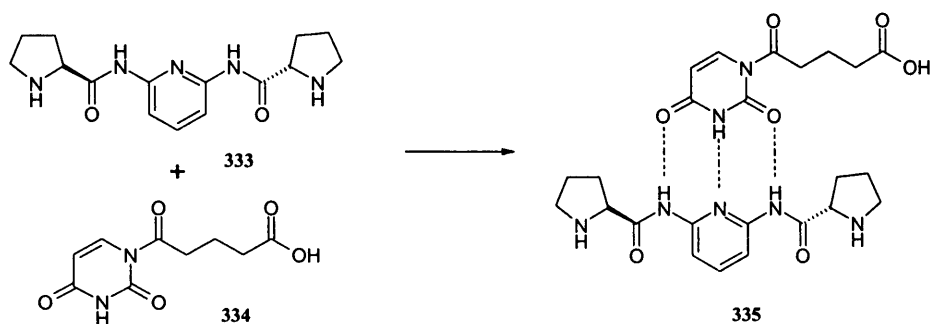
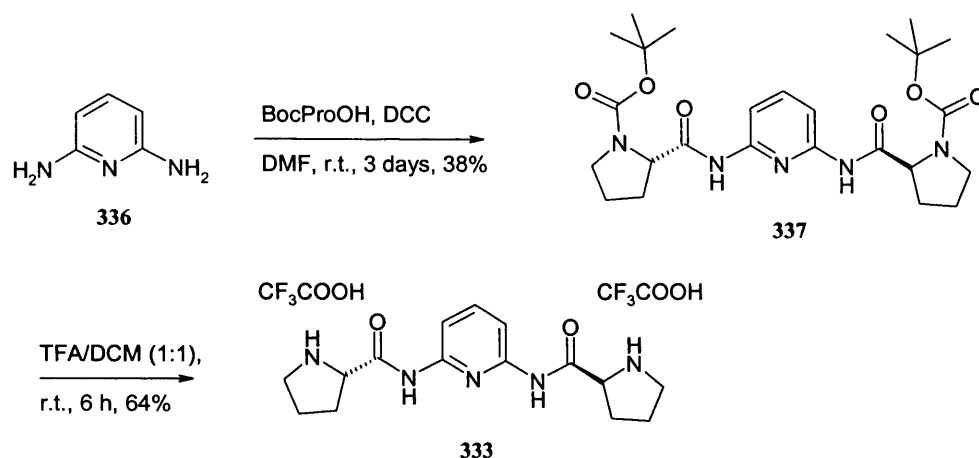


Figure 3.5.4 Target dimer unit consisting of proline catalytic group and carboxylic acid proton donor.

3.5.2 Synthesis of monomer units

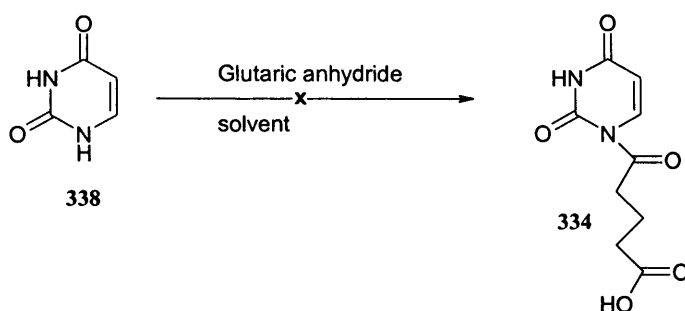
The synthesis of the diaminopyridine unit **333**, generated from 2,6-diaminopyridine, using Boc protected proline, in the presence of DCC (**Scheme 3.5.1**) gave **337** in 38%

yield. Deprotection was achieved using TFA/DCM mixture, and the desired product **333** isolated in 64% yield.



Scheme 3.5.1 Synthesis of diaminopyridine derivative **333**.

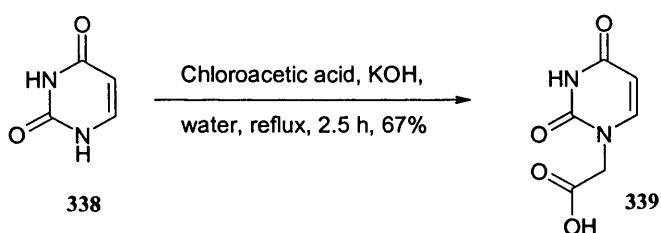
Our attention then focused upon preparation of the uracil monomer **334**. Reaction of uracil with glutaric anhydride was initially attempted using DMAP in chloroform (**Scheme 3.5.2**). However, after heating for 17 h, no product was observed. The coupling was repeated using a mixture of acetonitrile/pyridine to help aid solubilisation of uracil, but no acylated derivatives were isolated. Uracil was hence dissolved in DMSO and then treated with glutaric anhydride at 50 °C for 17 h, but once again no product formation was observed.



Scheme 3.5.2 Attempted synthesis of uracil derivative **334**.

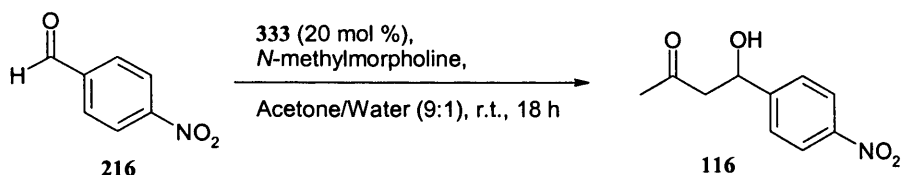
Attempts to introduce pentadioic acid were therefore put on hold and our attention turned to incorporation of acetic acid. Following previously established methodology, uracil was alkylated with chloroacetic acid to afford **339** in 67% yield (**Scheme**

3.5.3).¹⁴⁹ Since our aim was to include any carboxylic acid within our system, we did not feel that this slight modification would significantly impact on our design rational (**Figure 3.5.4**).



Scheme 3.5.3 Synthesis of uracil derivative **339**.

Before starting investigations into whether the two monomer units are able to form a dimer by hydrogen bonding, we first wished to assess whether the prolinylpyridine **333** could act as a catalyst for the aldol reaction. Indeed, we found that using 20 mol% of the diaminopyridine derivative **333** gave the aldol product **116** with 100% conversion by NMR analysis. The behaviour of the prolinyl pyridine derivative **333** as an organic catalyst is certainly a useful observation and worthy of further study in its own right.



Scheme 3.5.4 Aldol reaction using diaminopyridine derivative **333** as a catalyst.

The next step was to investigate if the two monomers could form a hydrogen bonded complex (**Figure 3.5.5**). Our intention was to study the formation of the dimer by NMR spectroscopy. Hydrogen bonding is ideally studied in chloroform solution,¹⁵⁰ however, the diaminopyridine derivative **333** was only soluble in methanol whereas the uracil derivative **339** was soluble in DMSO. This precluded us from studying this further, due to the insolubility of both monomer units in a chloroform solution.

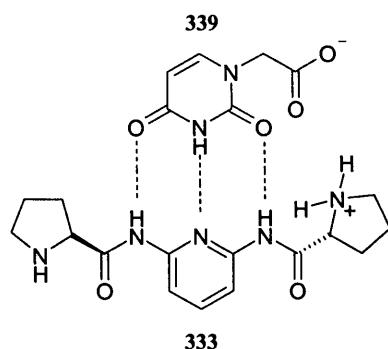
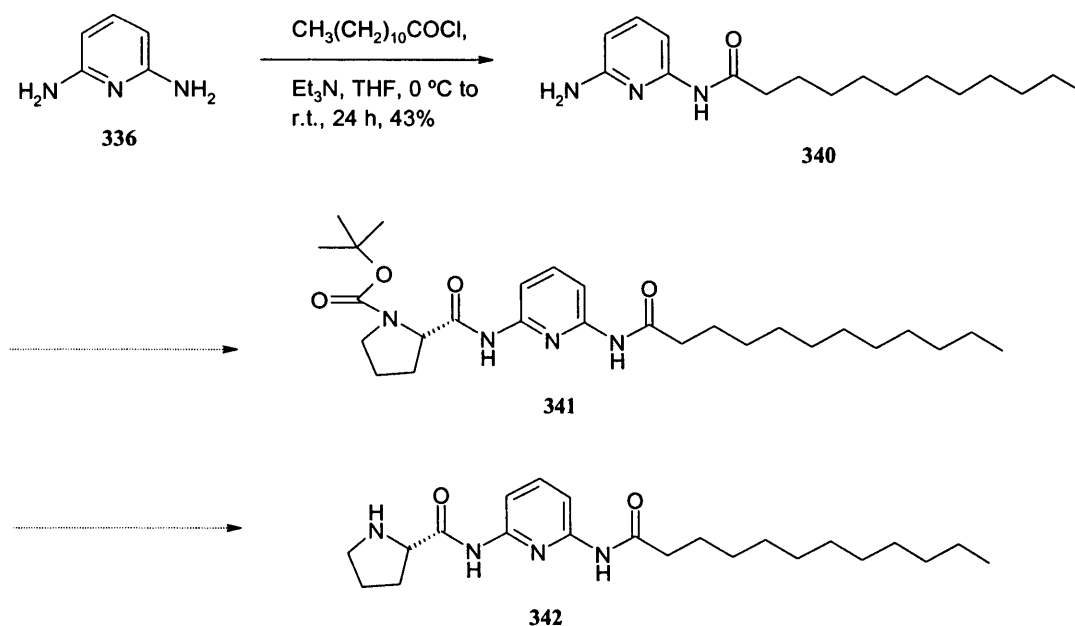


Figure 3.5.5 Example of a possible hydrogen bonded complex between **333** and **339**.

In an attempt to make both units more soluble in chloroform, we wanted to attach them to long alkyl chains. Starting from 2,6-diaminopyridine, lauryl chloride was successfully coupled using triethylamine in THF (**Scheme 3.5.5**).¹⁵¹

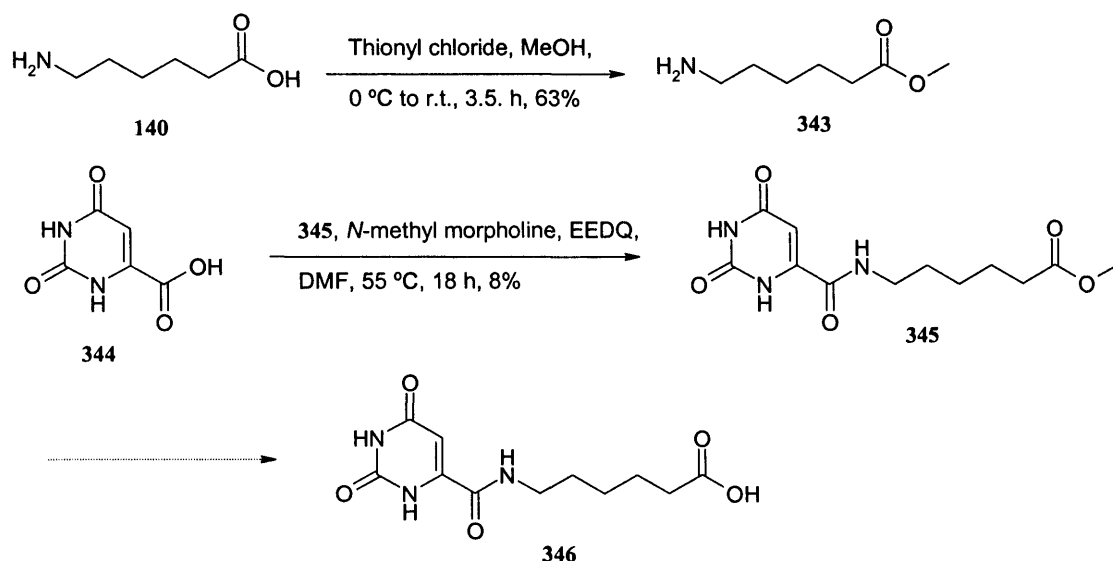


Scheme 3.5.5 Towards the synthesis of diaminopyridine derivative **342**.

Attachment of Boc proline and removal of the Boc protecting group could have been attempted to give the diaminopyridine derivative **342**, however, due to time constraints, the synthesis was not carried out.

In the case of the other monomer, we decided to utilise orotic acid **344** as an alternative to uracil, since it contained a suitable point of attachment for other functional groups.

Orotic acid **344** was attached to the methyl ester of caproic acid **343** to give **345** in a low yield of 8% (**Scheme 3.5.6**).¹⁵² However, once again time constraints prevented further work. It should be noted however, that **345** was not soluble in chloroform, which suggests that attachment of these particular alkyl chains would not necessarily have aided solubility of **346** or **342** in chloroform in this instance.



Scheme 3.5.6 Towards the synthesis of orotic acid derivative **346**.

3.6 Conclusions and Perspectives from the aldolase studies

Several aldol reactions have been successfully performed using tentagel resin containing proline and carboxylic acid, notably with polymer **238**. The activity demonstrated by polymer **286** implied that within our system, the presence of a carboxylic acid is not necessary for the reaction to proceed, under the specified conditions. Aromatic aldehydes that contain an electron withdrawing group were the substrates that were most likely to undergo an aldol reaction. Some selectivity was observed and we have demonstrated that by introducing a chiral binding group, the selectivity of the catalyst can be altered, although this was shown to be substrate dependent. We have also demonstrated that other polymers such as polyallylamine can also be successfully employed in our catalytic system. The advantages of using a polymer as a catalyst are that it can readily be removed at the end of reaction and that one can effortlessly incorporate any binding group into the polymer in order to modify

the selectivity of the catalyst. However, the disadvantage is the fact that isolated yields are low, possibly due to a lot of product remaining on the polymer after the reaction.

There are still a number of things that could be done with aldolases. More substrates could be studied, especially, aliphatic ones. A larger range of substrates should be studied with the aldolase containing serine, to obtain a better picture of its selectivity capabilities. Other binding groups could also be incorporated and alternative catalytic groups, such as various proline derivatives can be studied. The behaviour of the aldolases should be monitored as product formation against time as well as at different substrate concentrations to establish the kinetic behaviour of the aldolase catalysts. Other varieties of polymers should also be incorporated to see how the selectivity and kinetic behaviour of these may vary.

Although, we were not faced with problems of reproducibility with the aldolase system, possibly due to slightly more controlled attachment of functional groups to the resin, as discussed in the esterase section, synthesising artificial enzymes with a more precisely located binding and catalytic groups on a more defined polymeric strand would be desirable. Hence, the work initiated on supramolecular chemistry should be explored further. As demonstrated by our preliminary results, the diaminopyridine derivative **333** containing proline, has the ability to catalyse the aldol reaction. Once, the solubility problems of both diaminopyridine and uracil derivatives are resolved, the self assembly of the two monomer units, could provide us with a more efficient aldolase catalyst as well as initiating an interesting study to see whether extensive polymeric structures are really required for catalytic activity. In general, the synthesis of artificial enzymes through self-assembly, could incorporate all the essential features of our earlier models and as well as being more elegant, it provides potential for more rapid variation of both the catalytic and binding group. Through this systematic variation, one can hope that this approach might provide us with a better understanding of cooperativity effects between functional groups which are found in natural enzymes, as well as the synthesis of catalysts for a wide range of chemical transformations.

3.7 Final Remarks

The foregoing study has hopefully indicated that the simplistic concept of attaching different functionalised threads to a polymer backbone provides a simple and experimentally convenient method for exploring cooperativity and hence for generating catalysts which can be considered to function, at least to some degree, as artificial enzymes. The contribution of the PFG NMR method using transition state mimics to estimate selective binding efficiencies in “receptor sites” and the knowledge of commonly used catalytically active functional groups employed in enzymes can serve as the basis for the selection of two differing threads as in the esterase studies. By way of contrast, the aldol reaction, requiring both transition state recognition and controlled proton movement is a much more complex reaction and in this respect our studies using the most favourable electron deficient aldehydes as the carbonyl component must be regarded as a prelude to more advanced systems. The reversal of selectivity observed on the introduction of the binding unit using one enantiomer of the chiral sulfoxide serves to emphasise the subtlety of the overall process. As we have demonstrated throughout, the nature of the polymeric backbone is of course of crucial relevance in these studies, particularly in terms of solvents used.

In terms of future perspectives, a great body of work remains to be done, especially in terms of developing a general method which will ensure that each polymeric thread is identical. In this respect, the very preliminary results on the attempted construction of supramolecular threads (or even dimeric assemblies) may provide a way forward.

CHAPTER 4

EXPERIMENTAL

4.1 General Experimental

All chemicals were purchased from Sigma Aldrich, Avocado, Lancaster, BDH, Nova Biochem and Bachem and unless stated these were used without further purification unless otherwise stated.

^1H NMR spectra were recorded at 300 MHz on a Bruker AMX300 spectrometer, 400 MHz on a Bruker AMX400 spectrometer, or 500 MHz on a Bruker Avance DRX500 spectrometer. The chemical shift (δ) of each peak is given relative to tetramethylsilane (TMS), where $\delta \text{ TMS} = 0$ ppm. Chemical shifts are quoted using following abbreviations: s, singlet; d, doublet; t, triplet; q, quartet; dd, doublet of doublets; m, multiplet; br, broad.

^{13}C NMR spectra were recorded at 75 MHz on a Bruker AMX300 spectrometer, 100 MHz on a Bruker AMX400 spectrometer, or 125 MHz on a Bruker Avance DRX500 spectrometer. The chemical shift (δ) of each peak is given relative to the residual solvent peak. Solid state ^{13}C NMR spectra were recorded at 75 MHz on a Bruker MSL300 spectrometer.

IR spectra were obtained from a Shimadzu FTIR-8700 machine. Absorption maxima are reported in wavenumbers (cm^{-1}), using the following abbreviations: w, weak; m, medium; s, strong; br, broad. Only selected absorbencies are reported. Solid state IR was performed using Perkin Elmer Spectrum One machine. UV-vis spectra were recorded using Shimadzu UV-2401PC spectrophotometer.

Mass spectra were obtained using VG ZAB SE instrument.

Melting points were measured on a Reichert Hotstage apparatus, for all solids, where possible and are quoted to the nearest $^{\circ}\text{C}$ and are uncorrected.

Optical rotations were recorded using a POLAAR2000 photo polarimeter.

Analytical HPLC was carried out on Perkin Elmer Series 2000 lc pump, using Gilson 231 XL sampling injector, Gilson 401 C dilutor and Waters 486 tunable absorbance detector. The column used was Waters Symmetry C_{18} $5\mu\text{m}$ reverse phase (3.9 x 150

mm). Enantiomeric excess determination was carried out using a HPLC with Perkin Elmer Series 2000 lc pump, Gilson 231 XL sampling injector, Gilson 402 dilutor and Waters 486 tunable absorbance detector. The columns used were Chiralcel OD, Chiralpak AD or Chiralcel OB (Daicel Chemical Industries). All the HPLC data was monitored using Atlas Lab Systems 2000 software.

Scanning electron micrographs were obtained using a Hitachi s-570 machine.

Analytical thin layer chromatography (t.l.c.) was carried out on pre-coated, aluminium backed (Merck 60 F₂₅₄ silica) plates. T.l.c. visualising systems used were ultraviolet light (254 nm), potassium permanganate solution {KMnO₄ (1.25 g) and Na₂CO₃ (6.25 g) in water (250 ml)}, acidic vanillin {vanillin (15 g) and conc. H₂SO₄ (2.5 ml) in ethanol (250 ml)}, acidic anisaldehyde solution {anisaldehyde (15 g) and conc. H₂SO₄ (2.5 ml) in ethanol (250 ml)}, or bromocresol green solution {bromocresol green (40 mg) and NaOH solution (0.1 M) in ethanol (100 ml)}.

The qualitative tests¹³³ used to test the presence of certain functional groups on resins are:

Kaiser test {ninhydrin (5 g), phenol (80 g) and aqueous KCN solution (0.001 M, 2 ml) in ethanol (120 ml)} – the resin beads turn blue in the presence of primary amines.

Chloranil test {*p*-chloranil (2 g) in DMF (100 ml) and acetaldehyde (2 g) in DMF (100 ml)} – the resin beads turn blue/green in the presence of secondary amines.

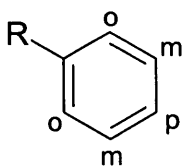
Malachite green test {malachite green oxalate (0.25 g) in ethanol (100 ml)} – the resin beads turn green in the presence of carboxylic acid groups.

Anhydrous tetrahydrofuran was distilled from sodium and benzophenone under nitrogen. Anhydrous dichloromethane was distilled from calcium hydride under nitrogen. Anhydrous methanol was distilled from a solution of methanol, magnesium turnings and iodine. Triethylamine and diisopropylamine were refluxed with potassium hydroxide, distilled and stored over potassium hydroxide pellets under nitrogen. Dimethylformamide was dried with MgSO₄ and then distilled and stored over Linde Type 4 Å molecular sieves under nitrogen. Brine refers to saturated sodium chloride solution.

The term *in vacuo* refers to the removal of solvents by means of evaporation at reduced pressure, provided by a water or air pump, using a Büchi rotary evaporator.

For all air and moisture sensitive reactions, glassware was dried at 120 °C and cooled under a flow of nitrogen.

The following assignement system will be used for mono substituted benzene rings:

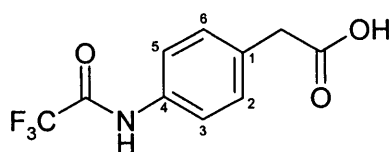


where o denotes *ortho*, m denotes *meta* and p denotes *para*.

4.2 Artificial Esterases

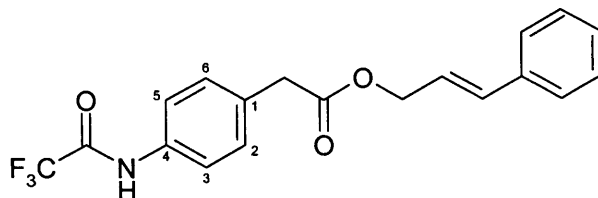
4.2.1 Synthesis of Ester Substrates

(4-Trifluoroacetylamido phenyl)-acetic acid (171)¹⁵³



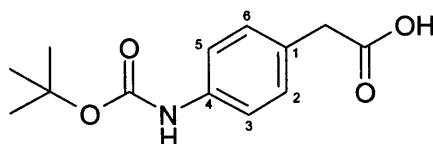
4-Aminophenylacetic acid (3.00 g, 20.0 mmol) was dissolved in acetonitrile (30 ml) and water (3.0 ml) and cooled to 0 °C. Sodium carbonate (4.21 g, 40.0 mmol) was added, followed by dropwise addition of trifluoroacetic anhydride (8.42 ml, 60.0 mmol). The reaction was allowed to warm to room temperature and stirred vigorously for 1 h. The volatiles were removed *in vacuo* and the resulting residue was partitioned between ethyl acetate (30 ml) and water (30 ml). The pH of the solution was adjusted to 2 using concentrated aqueous HCl solution and the layers were separated. The organic extract was washed with aqueous HCl (2 M, 2 x 20 ml), brine (20 ml), dried over MgSO₄ and the mixture concentrated until a brown precipitate appeared. The solid was collected by filtration to afford the product as a brown solid (2.41 g, 49%). **m.p.** 200 °C (lit. 175 °C¹⁵³); **R_f** = 0.65 (SiO₂; ethyl acetate) **¹H NMR** (300 MHz, CD₃OD) δ_{H} /ppm 3.56 (s, 2H, ArCH₂CO₂H), 7.26 (d, *J* = 8.5, 2H, H(3) and H(5)), 7.55 (d, *J* = 8.5, 2H, H(2) and H(6)); **¹³C NMR** (75 MHz, CD₃OD) δ_{C} /ppm 41.7 (ArCH₂CO₂H), 117.9 (q, *J*_{CF} = 285.9, C_{CF₃}-), 122.7 (C(2) and C(6)), 131.5 (C(3) and C(5)), 134.2 and 136.8 (C(1) and C(4)), 157.0 (q, CF₃C(O)NH-), 175.8 (-CO₂H); **¹⁹F NMR** (282 MHz, CD₃OD) δ_{F} /ppm -77.4 (CF₃-); ν_{max} (nujol/cm⁻¹) 1377 (s, C-F), 1703 (m, C=O), 2924 (s, C-H), 3250 (w, N-H); **m/z** (FAB) 248 (75%, [M + H]⁺).

(4-Trifluoroacetylaminophenyl)-acetic acid (2*E*,4*E*,6*Z*)-4-vinyl octa-2,4,6-trienyl ester (173)



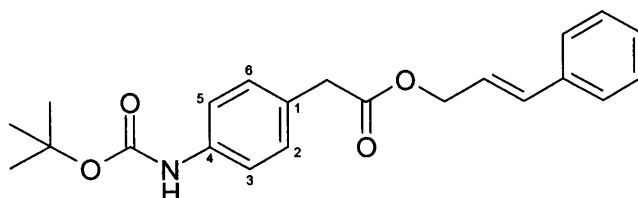
To a stirred suspension of carboxylic acid (**171**) (1.00 g, 4.05 mmol) in anhydrous dichloromethane (30 ml), under nitrogen, was added oxalyl chloride (0.47 ml, 5.40 mmol) and a few drops of dimethylformamide (*ca.* 100 μ l). The suspension was stirred for 4 h at room temperature, after which time, it became homogenous. Cinnamyl alcohol (0.81 g, 6.07 mmol) and triethylamine (1.69 ml, 12.00 mmol) were added and stirring was continued for 15 hours. Solvent was removed *in vacuo* to give a yellow residue, which was dissolved in ethyl acetate (200 ml) and the mixture was washed with aqueous HCl (0.5 M, 2 x 100 ml), saturated aqueous NaHCO₃ (2 x 100 ml), brine (100 ml), and dried over MgSO₄. The solvent was removed *in vacuo* to yield an orange oil, which was purified by flash chromatography (SiO₂; petroleum spirit/ethyl acetate; 2:1) to give **173** as a white solid (0.85 g, 58%). **m.p.** 143 °C; **R_f** = 0.50 (SiO₂; petroleum spirit/ethyl acetate; 2:1). **¹H NMR** (300 MHz, CDCl₃) δ_{H} /ppm 3.58 (s, 2H, ArCH₂CO₂-), 4.68 (d, *J* = 5.2, 2H, ArCH₂CO₂CH₂-), 6.18 (m, 1H, -CH=CHAr), 6.53 (d, *J* = 15.9, 1H, -CH=CHAr), 7.16 – 7.43 (m, 9H, ArH), 8.0 (s, br, 1H, -NH-); **¹³C NMR** (75 MHz, CDCl₃) δ_{C} /ppm 41.1 (ArCH₂CO₂-), 66.0 (ArCH₂CO₂CH₂-), 118.1 (F₃CC(O)NH-), 121.1 (C(3), C(5)), 123.2 (-CH=CHAr), 126.5 (*para* ArC), 128.6 and 128.8 (2 x *ortho* ArC and 2 x *meta* ArC), 130.6 and 130.7 (C(2), C(6)), 132.4 (quaternary ArC), 134.7(-CH=CHAr), 134.9 and 136.9 (C(1), C(4) and), 155.2 (F₃CC(O)NH-), 171.6 (ArCH₂CO₂-); **¹⁹F NMR** (282 MHz, CDCl₃) δ_{F} /ppm -76.1 (CF₃C(O)NH-); ν_{max} (DCM/cm⁻¹) 1346 (m, C-F), 1601 (m, Ar), 1703 (s, C=O (amide)), 1730 (s, C=O (ester)), 2900 (w, C-H), 3311 (w, N-H); **m/z** (FAB) 363 (27%, [M]⁺); **HRMS** found 363.1077, [M]⁺ (C₁₉H₁₆O₃NF₃) requires 363.1082; **Anal.** (C₁₉H₁₆O₃NF₃) found C, 62.89; H, 4.54; N, 3.88%; requires C, 62.81; H, 4.44; N, 3.85%.

4-*tert*-Butoxycarbonylamino phenyl acetic acid (176)¹⁵⁴



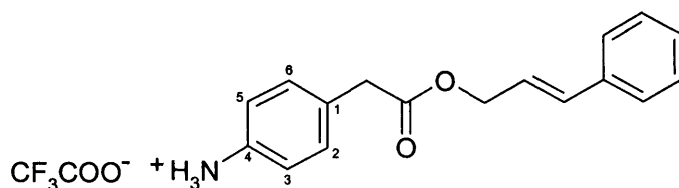
To 4-aminophenylacetic acid (1.00 g, 6.62 mmol) in dioxane (20 ml) and water (10 ml) was added triethylamine (1.38 ml, 9.93 mmol), followed by di-*tert*-butyl dicarbonate (2.17 g, 9.93 mmol) and the resulting mixture stirred at room temperature for 18 h. Aqueous sodium hydroxide (1 M, 50 ml) and ethyl acetate (50 ml) were added and the layers separated. The aqueous layer was acidified to pH 4 with concentrated aqueous HCl, and a brown precipitate formed. The product was extracted into ethyl acetate (3 x 50 ml), which was washed with brine (100 ml) and water (100 ml). The organic extracts were dried over MgSO₄ and concentrated *in vacuo* to afford the product as a brown solid (1.54 g, 94%). **m.p.** 158 °C (lit. 141.5 – 142.5 °C¹⁵⁴); **¹H NMR** (300 MHz, CD₃OD) δ_{H} /ppm 1.50 (s, 9H, -C(CH₃)₃), 3.46 (s, 2H, ArCH₂CO₂H), 7.15 (d, *J* = 8.5, 2H, H(3) and H(5)), 7.31 (d, *J* = 8.5, 2H, H(2) and H(6)); **¹³C NMR** (75 MHz, CD₃OD) δ_{C} /ppm 29.1 (-C(CH₃)₃), 41.7 (ArCH₂CO₂H), 81.3 (-C(CH₃)₃), 120.4 (ArC), 130.5 (ArC), 155.8 (ArNHCO₂-), 176.2 (ArCH₂CO₂H); ν_{max} (nujol/cm⁻¹) 1377 (m, C-(CH₃)₃), 1593 (m, Ar), 1701 (s, C=O), 3383 (m, NH); **m/z** (FAB) 252 (12%, [M + H]⁺), 251 (29%, [M]⁺), 196 (82%, [M - tBu + H]⁺), 152 (8%, [M - Boc]⁺).

(4-*tert*-Butoxycarbonylamino phenyl) acetic acid (*E*)-3-phenyl allyl ester (177)



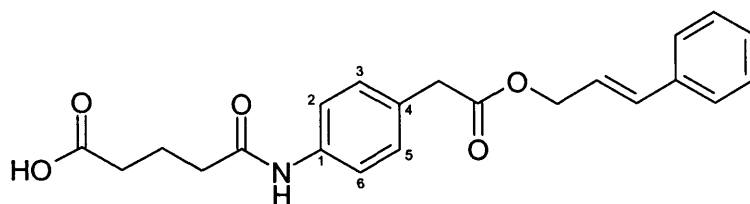
Carboxylic acid **176** (0.60 g, 2.39 mmol) was dissolved in anhydrous dichloromethane (10 ml) and tetrahydrofuran (10 ml). Cinnamyl alcohol (0.32 g, 2.39 mmol), dicyclohexylcarbodiimide (0.54 g, 2.63 mmol), 4,4-dimethylaminopyridine (0.01 g, 0.05 mmol) and triethylamine (0.66 ml, 4.78 mmol) were added to the mixture. The reaction was stirred for 40 h at room temperature. The urea by-product was then removed by filtration and the solvents removed *in vacuo*. The residue was dissolved in dichloromethane (20 ml) and the mixture was then washed with saturated aqueous NaHCO₃ solution (20 ml), aqueous HCl (1 M, 20 ml), brine (20 ml) and water (20 ml). The organic solution was dried over MgSO₄, filtered and concentrated *in vacuo* to afford the crude product as a brown oil. Purification by flash chromatography (SiO₂; petroleum spirit/ethyl acetate; 2:1) gave the product as a white solid (0.50 g, 57%). **m.p.** 108 °C; **R_f** = 0.76 (SiO₂; petroleum spirit/ethyl acetate; 1:1); **¹H NMR** (300 MHz, CDCl₃) δ_{H} /ppm 1.66 (s, 9H, -C(CH₃)₃), 3.89 (s, 2H, ArCH₂CO₂R), 4.88 (d, *J* = 5.0, 2H, -CO₂CH₂CH=CH-), 6.40 (m, 1H, -CH=CHAr), 6.68 (m, *J* = 15.0, 1H, -CH=CHAr) 7.44 (m, 9H, ArH); **¹³C NMR** (75 MHz, CDCl₃) δ_{C} /ppm 28.5 (-C(CH₃)₃), 40.9 (ArCH₂CO₂-), 65.5 (-CO₂CH₂CH=CH-), 80.6 (-C(CH₃)₃), 118.9 (C(3) and C(5)), 123.2 (-CH=CHAr), 126.8 (ArC), 128.1 and 128.6 (2 x ArC and 2 x ArC), 128.7 (C(2) and C(6)), 130.0 (1 x quaternary ArC), 134.3 (-CH=CHAr), 136.4 and 137.6 (C(1) and C(4)), 152.9 (ArNHCO₂-), 171.5 (ArCH₂CO₂-); ν_{max} (nujol/cm⁻¹) 1377 (s, C-(CH₃)₃), 1693 (s, C=O (amide)), 1732 (s, C=O (ester)), 2928 (s, C-H), 3369 (m, NH); **m/z** (FAB) 368 (5%, [M + H]⁺), 367 (11%, [M]⁺), 267 (3%, [M - Boc]⁺); **HRMS** found 390.1686, [M + Na]⁺ (C₂₂H₂₅NO₄Na) requires 390.1681; **Anal.** (C₂₂H₂₅NO₄) found C, 71.92; H, 7.31; N, 3.82%; requires C, 71.91; H, 6.86; N, 3.81%.

(4-Ammonium phenyl)-acetic acid (*E*)-3-phenyl-allyl ester trifluoroacetate (178)



Ester **177** (2.06 g, 3.00 mmol) was stirred in trifluoroacetic acid (4 % v/v in anhydrous dichloromethane) at room temperature for 5 h under nitrogen. The mixture was concentrated *in vacuo* to give a brown oil, which was purified by flash chromatography (SiO₂; petroleum spirit/ethyl acetate; 2:1) to give the desired product as a brown oil (0.81 g, 54%). *R_f* = 0.33 (SiO₂; petroleum spirit/ethyl acetate, 2:1); ¹H NMR (300 MHz, CDCl₃) δ_H/ppm 3.30 (s, br, 3H, ArNH₃⁺), 3.56 (s, 2H, ArCH₂CO₂-), 4.74 (d, *J* = 6.0, 2H, ArCH₂CO₂CH₂-), 6.27 (m, 1H, -CH=CHAr), 6.60 (d, *J* = 12, 1H, -CH=CHAr), 6.69 (m, 2H, H(2) and H(6)), 7.11 (m, 2H, H(3) and H(5)), 7.25 – 7.39 (m, 5H, ArH); ¹³C NMR (75 MHz, CDCl₃) δ_C/ppm 39.6 (ArCH₂CO₂-), 64.2 (ArCH₂CO₂CH₂-), 114.3 (C(3) and C(5)), 122.3 (-CH=CHAr), 122.9 (C(1)), 125.6 (ArC), 127.0 and 127.6 (4 x ArC), 128.0 (C(2) and C(6)), 133.0 (-CH=CHAr), 135.3 (quaternary ArC), 144.4 (C(4)), 170.9 (ArCH₂CO₂-); ν_{max} (film/cm⁻¹) 1150 (s, C-OR), 1740 (s, C=O), 3370 (s, NH); *m/z* (FAB) 382 (35%, [M + H]⁺), 267 (100%, [M – TFA]⁺).

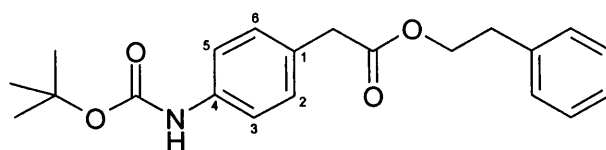
4-[4-((2*E*,4*E*,6*Z*)-4-Vinylocta-2,4,6-trienyloxycarbonylmethyl) phenylcarbamoyl] butyric acid (169)



Glutaric anhydride (0.13 g, 1.17 mmol) was added to a stirred solution of triethylamine (0.28 ml, 2.04 mmol) and amine salt **178** (0.37 g, 0.97 mmol) in anhydrous dichloromethane (12 ml), under nitrogen. The solution was heated at reflux for 19 h.

After cooling, dichloromethane (30 ml) was added and the solution was washed with aqueous HCl (2 M, 50 ml) and brine (50 ml). The organic extract was dried over MgSO₄ and concentrated *in vacuo*. Purification by recrystallisation from water/acetonitrile yielded the product as a brown solid (0.36 g, 53%). **m.p.** 145 °C; **R_f** = 0.80 (SiO₂; methanol/ethyl acetate, 9:1); **¹H NMR** (300 MHz, CD₃OD) δ_{H} /ppm 2.03 (m, 2H, HO₂CCH₂CH₂-), 2.46 (m, 4H, HO₂CCH₂CH₂CH₂-), 3.71 (s, 2H, ArCH₂CO₂-), 4.78 (d, 2H, ArCH₂CO₂CH₂-), 6.34 (m, 1H, -CH=CHAr), 6.63 (d, *J* = 16.0, 1H, -CH=CHAr), 7.27 – 7.81 (m, 9H, ArH); **¹³C NMR** (75 MHz, CD₃OD) δ_{C} /ppm 22.1 (HO₂CCH₂CH₂-), 34.1 (HO₂C(CH₂)₂CH₂-), 36.9 (HO₂CCH₂-), 41.5 (ArCH₂CO₂-), 66.3 (ArCH₂CO₂CH₂-), 121.3 (C(2) and C(6)), 124.2 (-CH=CHAr), 127.6 (*para* ArC), 129.0 and 129.6 (*ortho* ArC and *meta* ArC), 130.8 (C(3) and C(5)), 131.3 (1 x quaternary ArC), 134.9 (-CH=CHAr), 137.7 and 138.9 (C(1) and C(4)), 173.3 (ArCH₂CO₂-), 173.7 (ArNHC(O)-), 176.8 (HO₂C-); ν_{max} (nujol/cm⁻¹) 1529 (s, C=O (amide)), 1728 (s, C=O (ester)), 2920 (s, C-H), 3279 (m, N-H); **m/z** (CI⁺) 382 (80%, [M + H]⁺), 381 (16%, [M]⁺), 266 (7%, [M – alcohol + H]⁺); **HRMS** found 382.1649, [M + H]⁺ (C₂₂H₂₄NO₅) requires 382.1654; **Anal.** (C₂₂H₂₃NO₅) found C, 69.61; H, 6.42; N, 3.65%; requires C, 69.28; H, 6.08; N, 3.67%.

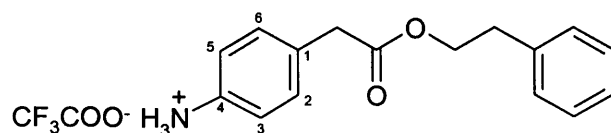
(4-*tert*-Butoxycarbonylamino phenyl) acetate-2-phenethyl ester (179)



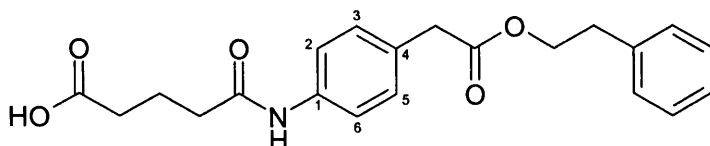
(4-*tert*-Butoxycarbonylamino-phenyl) acetic acid **176** (3.00 g, 12.0 mmol) was dissolved in anhydrous tetrahydrofuran/dichloromethane (1:1, 40 ml), under nitrogen. 2-Phenyl ethanol (1.43 ml, 12.0 mmol), dicyclohexylcarbodiimide (2.71 g, 13.0 mmol), 4,4-dimethylaminopyridine (0.03 g, 0.24 mmol) and triethylamine (3.32 ml, 23.0 mmol) were added and the solution was stirred at room temperature for 22 h. The urea by-product was filtered off and the resulting filtrate was concentrated *in vacuo*. The residue was dissolved in dichloromethane (50 ml) and washed with aqueous saturated NaHCO₃ (50 ml), aqueous HCl (1 M, 50 ml), water (50 ml) and brine (50 ml) and then dried over MgSO₄. The solvents were removed *in vacuo*, which afforded the crude product as a

brown oil. Purification by flash chromatography (SiO₂; gradient; petroleum spirit/ethyl acetate, (7:3) to petroleum spirit/ethyl acetate (1:2)) gave the title product as a white solid (4.24, 54%). **m.p.** 60 °C; **R_f** = 0.73 (SiO₂; petroleum spirit/ethyl acetate; 1:1); **¹H NMR** (300 MHz, CDCl₃) δ_{H} /ppm 1.53 (s, 9H, C(CH₃)₃), 2.91 (t, *J* = 7.0, 2H, -CH₂CH₂Ar), 3.54 (s, 2H, ArCH₂CO₂-), 4.30 (t, *J* = 7.0, 2H, -CH₂CH₂Ar), 7.14 – 7.33 (m, 9H, ArH); **¹³C NMR** (75 MHz, CDCl₃) δ_{C} /ppm 28.4 (C(CH₃)₃), 35.1 (-CH₂CH₂Ph), 40.8 (ArCH₂CO₂-), 65.3 (-CH₂CH₂Ar), 80.5 (C(CH₃)₃), 118.7 (C(3) and C(5)), 126.6 (*para* ArC), 128.5 and 128.6 (2 x *ortho* ArC and 2 x *meta* ArC), 128.9 (C(2) and C(6)), 129.9 (1 x quaternary ArC), 137.5 and 137.7 (C(1) and C(4)), 152.8 (-CONH-), 171.6 (-CH₂CO₂-); ν_{max} (nujol/cm⁻¹) 1370 (m, C-(CH₃)₃), 1593 (m, Ar), 1716 (s, C=O), 2921 (s, CH), 3356 (s, NH); **m/z** (FAB) 355 (48%, [M]⁺), 255 (22%, [M – Boc]⁺); **HRMS** found 355.1790, [M]⁺ (C₂₁H₂₅NO₄) requires 355.1784; **Anal.** (C₂₁H₂₅NO₄) found C, 71.09; H, 7.58; N, 4.07%; requires C, 70.96; H, 7.09; N, 3.94%.

(4-Ammonium-phenyl)-acetate-2-phenethyl ester trifluoroacetate (347)

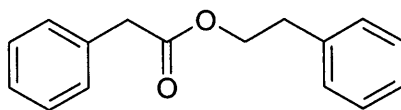


(4-*tert*-Butoxycarbonylamino-phenyl) acetate phenethyl ester **179** (0.30 g, 0.80 mmol) was dissolved in anhydrous dichloromethane (4 ml), under nitrogen. Trifluoroacetic acid (4 ml) was added and the mixture was stirred for 2.5 h at room temperature. The volatiles were removed under reduced pressure and the desired product was isolated as a brown oil (0.31 g, 100%). **R_f** = 0.23 (SiO₂; petroleum spirit/ethyl acetate; 1:1); **¹H NMR** (300 MHz, CDCl₃) δ_{H} /ppm 2.99 (t, *J* = 7.0 2H, -CH₂CH₂Ar), 3.62 (s, 2H, ArCH₂CO₂-), 4.33 (t, *J* = 6.9, 2H, -CH₂CH₂Ar), 7.14 – 7.26 (m, 9H, ArH); **¹³C NMR** (75 MHz, CDCl₃) δ_{C} /ppm 34.8 (-CH₂CH₂Ar), 40.4 (ArCH₂CO₂-), 66.2 (-CH₂CH₂Ar), 115.3 (q, CF₃CO₂-), 123.1 (*para* ArC), 126.7 (2 x *meta* ArC), 128.6, 128.9 (2 x *ortho* ArC, C(2), C(6)), 131.0 (C(3), C(5)), 135.2, 137.3 (C(4), 1 x quaternary ArC and C(1)), 160.9 (q, *J*_{CF} = 39.5, CF₃CO₂-), 172.5 (-CH₂CO₂-); ν_{max} (neat/cm⁻¹) 1142 (s, C-F), 1720 (s, C=O), 2951 (s, C-H), 3425 (m, NH); **m/z** (FAB) 256 (6%, [M + H – TFA]⁺), 255 (17%, [M – TFA]⁺); **HRMS** found 256.1334, [M + H – TFA]⁺ (C₁₆H₁₈NO₂) requires

4-(4-Phenethyloxycarbonylmethyl phenylcarbamoyl) butyric acid (127)⁹⁰

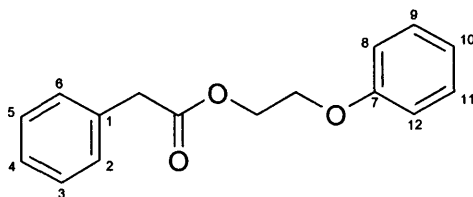
(4-Ammonium phenyl) acetate-2-phenethyl ester trifluoroacetate **347** (2.51 g, 6.80 mmol) was dissolved in anhydrous dichloromethane (40 ml) under nitrogen. Glutaric anhydride (0.93 g, 8.16 mmol) and triethylamine (1.18 ml, 8.50 mmol) were added and the mixture was heated at reflux for 17 h. After cooling, the solvents were removed under reduced pressure. The crude product was dissolved in ethyl acetate (100 ml) and then washed with aqueous HCl (2 M, 100 ml), water (100 ml) and brine (100 ml) and dried over MgSO₄. The solvents were removed *in vacuo* and the desired product was isolated as a yellow solid (1.20 g). **m.p.** = 106 °C (lit. 105 - 107 °C⁹⁰); ¹H NMR (300 MHz, CD₃CN) δ_H/ppm 1.95 (m, 2H, -CH₂CH₂CH₂-), 2.36 (m, 4H, -CH₂CH₂CH₂C(O)N-), 2.88 (t, *J* = 6.7, 2H, -CH₂CH₂Ar), 3.53 (s, 2H, ArCH₂CO₂-), 4.26 (t, *J* = 6.7, 2H, -CH₂CH₂Ar), 7.12 – 7.30 (m, 7H, ArH), 7.47 (d, *J* = 8.4, 2H, ArH), 8.40 (s, 1H, -C(O)NH-); ¹³C NMR (75 MHz, CD₃CN) δ_C/ppm 21.6 (-CH₂CH₂CH₂-), 33.6 (CO₂CH₂CH₂CH₂-), 35.7 (-CH₂CH₂Ar), 36.7 (-CH₂CH₂CH₂NH-), 41.2 (ArCH₂CO₂-), 66.1 (-CH₂CH₂Ar), 120.7, 127.4, 129.5, 130.0 and 130.7 (9 x ArC), 130.8 (1 x quaternary ArC), 138.8 and 139.4 (C(1) and C(4)), 172.3 (ArCH₂CO₂-), 172.5 (-CONH-), 175.2 (-CO₂H); ν_{max} (nujol/cm⁻¹) 1526 (m, Ar), 1652 (s, C=O (amide)), 1730 (s, C=O (acid and ester)), 2923 (s, CH), 3312 (w, NH); **m/z** (FAB) 370 (48%, [M + H]⁺); **HRMS** found 370.1661, [M + H]⁺ (C₂₁H₂₄NO₅) requires 370.1655.

Phenyl-acetate-2-phenyl ester (199)¹⁵⁵



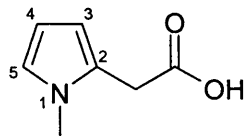
Phenylacetic acid (1.50 g, 11.0 mmol) was dissolved in anhydrous tetrahydrofuran/dichloromethane (1:1, 20 ml) under nitrogen. 2-Phenylethanol (1.32 ml, 11.0 mmol), dicyclohexylcarbodiimide (2.50 g, 12.0 mmol), 4,4-dimethylaminopyridine (27.0 mg, 0.22 mmol) and triethylamine (3.07 ml, 22.0 mmol) were added and the reaction stirred at room temperature for 18 h. The urea by-product was removed by filtration and the filtrate was concentrated. The crude product was dissolved in dichloromethane (70 ml) and washed with saturated aqueous Na₂CO₃ (50 ml), aqueous HCl (1 M, 50 ml), water (50 ml) and brine (50 ml), dried over MgSO₄ and concentrated. Purification by flash chromatography (SiO₂; gradient; ethyl acetate/petroleum spirit (3:7) to ethyl acetate/petroleum spirit (1:1)) gave the desired product as a colourless oil (0.80 g, 30%). **R_f** = 0.63 (SiO₂; petroleum spirit/ethyl acetate; 1:1); **¹H NMR** (300 MHz, CDCl₃) δ_H/ppm 2.96 (t, *J* = 7.0, 2H, -CH₂CH₂Ar), 3.64 (s, 2H, ArCH₂CO₂-), 4.35 (t, *J* = 7.0, 2H, -CH₂CH₂Ar), 7.18 – 7.36 (m, 10H, ArH); **¹³C NMR** (75 MHz, CDCl₃) δ_C/ppm 35.0 (-CH₂CH₂Ar), 41.5 (ArCH₂CO₂-), 65.4 (-CH₂CH₂Ar), 126.6, 126.8, 127.1, 128.5, 128.6, 129.0 and 129.4 (10 x ArC), 134.0 and 137.8 (2 x quaternary ArC), 171.5 (ArCH₂CO₂-); **ν_{max}** (neat/cm⁻¹) 1584 and 1604 (m, Ar), 1732 (s, C=O), 2854 and 2931 (s, CH); **m/z** (FAB) 263 (100%, [M + Na]⁺), 241 (3%, [M + H]⁺); **HRMS** found 241.1224, [M + H]⁺ (C₁₆H₁₇O₂) requires 241.1229.

Phenyl-acetic acid 2-phenoxy-ethyl ester (200)



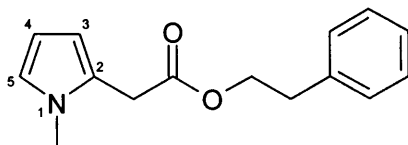
Ethylene glycol phenyl ether (1.38 ml, 11.0 mmol) and phenyl acetic acid (1.50 g, 11.0 mmol) were dissolved in a mixture of anhydrous dichloromethane/tetrahydrofuran (1:1, 30 ml) under nitrogen. Dicyclohexylcarbodiimide (2.50 g, 12.0 mmol) followed by 4,4-dimethylaminopyridine (27.0 mg, 0.20 mmol) and triethylamine (3.07 ml, 22.0 mmol) were then added and the reaction was stirred for 18 h. The urea by-product was filtered off and solvents removed under reduced pressure. The crude material was dissolved in dichloromethane (50 ml) and washed with saturated aqueous NaHCO₃ (50 ml), aqueous HCl (1 M, 50 ml), brine (50 ml) and water (50 ml) and dried over MgSO₄ and solvent removed under reduced pressure. Purification by flash chromatography (SiO₂; gradient; petroleum spirit/ethyl acetate (4:1) to petroleum spirit/ethyl acetate (2:1)) afforded the desired product as a yellow liquid (2.06 g, 73%). R_f = 0.76 (SiO₂; ethyl acetate/petroleum spirit; 1:1); ¹H NMR (300 MHz, CDCl₃) δ_H /ppm 3.67 (s, 2H, ArCH₂CO₂-), 4.14 (m, 2H, -CH₂OAr), 4.46 (m, 2H, -CH₂CH₂OAr), 7.03 (m, 3H, ArH), 7.30 (m, 7H, ArH); ¹³C NMR (75 MHz, CDCl₃) δ_C /ppm 41.2 (ArCH₂CO₂-), 63.3 (-CH₂CH₂OAr), 65.8 (-CH₂CH₂OAr), 114.7, 121.3, 127.1, 128.6, 129.3, 129.6 (ArC), 133.9 (C(1)), 158.6 (C(7)), 171.6 (-CH₂CO₂-); ν_{max} (DCM/cm⁻¹) 1088 (m, C-O), 1593 (w, Ar), 1740 (m, C=O), 2924 (s, C-H); m/z (FAB) 257 (33%, [M + H]⁺), 256 (17%, [M]⁺); HRMS found 257.1181, [M + H]⁺ (C₁₆H₁₇O₃) requires 257.1178.

(1-Methyl-1H-pyrrol-2-yl) acetic acid (348)¹⁵⁶



A solution of potassium hydroxide (3.89 g, 70.0 mmol) in water (40 ml) was added to a stirred solution of methyl 1-methyl-2-pyrroleacetate (5.00 ml, 35.0 mmol) in ethanol (80 ml). The resulting solution was stirred at room temperature for 3 days. Ethanol was removed under reduced pressure and the resulting aqueous solution was washed with diethyl ether (50 ml). The aqueous layer was then acidified to approximately pH 2 using concentrated aqueous HCl and a brown precipitate formed, which was extracted into ethyl acetate (3 x 50 ml). The combined organic extracts were washed with brine (200 ml), dried over MgSO₄ and concentrated *in vacuo*. The desired product was isolated as a beige solid (4.40 g, 91%). **m.p.** 126 °C (lit. 135 °C¹⁵⁶); **¹H NMR** (300 MHz, CDCl₃) δ_{H} /ppm 3.58 (s, 3H, -CH₃), 3.67 (s, 2H, -CH₂CO₂H), 6.10 (m, 2H, H(3), H(4)), 6.61 (m, 1H, H(5)); **¹³C NMR** (75 MHz, CDCl₃) δ_{C} /ppm 32.6 (-CH₂CO₂H), 34.2 (-NCH₃), 107.5 (C(3)), 109.4 (C(4)), 123.1 (C(5)), 124.3 (C(2)), 177.4 (-CO₂H); ν_{max} (nujol/cm⁻¹) 1645 (m, C=O), 2937 (s, C-H); **m/z** (Cl⁺) 137 (100%, [M-2H]⁺).

(1-Methyl-1H-pyrrol-2-yl) acetic acid phenethyl ester (202)

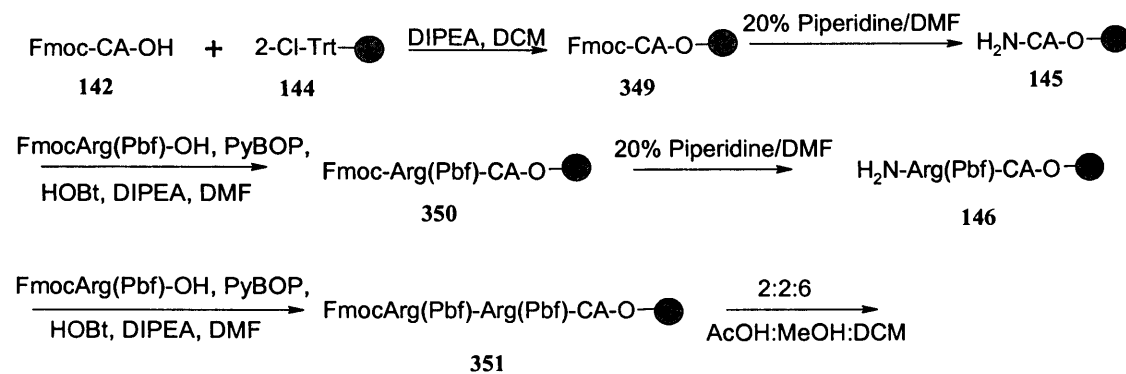


(1-Methyl-1H-pyrrol-2-yl)-acetic acid **348** (3.00 g, 20.0 mmol) was dissolved in anhydrous dichloromethane (35 ml) and anhydrous tetrahydrofuran (35 ml) under nitrogen. 2-Phenyl ethanol (2.58 ml, 10.0 mmol), dicyclohexylcarbodiimide (4.89 g, 24.0 mmol), 4,4-dimethylaminopyridine (0.05 g, 0.43 mmol) and triethylamine (6.00 ml, 43.0 mmol) were added and the resulting solution was stirred at room temperature for 18 h. The urea by-product was then removed by filtration and the filtrate was

concentrated *in vacuo*. The residue was dissolved in dichloromethane (100 ml) and washed with saturated aqueous NaHCO₃ (100 ml), aqueous HCl (1 M, 100 ml), brine (100 ml) and water (100 ml). The chlorinated layer was dried over MgSO₄ and concentrated *in vacuo*. Purification by flash chromatography (SiO₂; petroleum spirit/ethyl acetate; 3:1) afforded the desired product as a brown oil (2.70 g, 52%). **m.p.** 86 °C; **R_f** = 0.33 (SiO₂; petroleum spirit/ethyl acetate; 1:1) **¹H NMR** (300 MHz, CDCl₃) δ_{H} /ppm 3.01 (m, 2H, -CH₂CH₂Ar), 3.52 (s, 3H, -CH₃), 3.67 (s, 2H, -CH₂CO₂-), 4.40 (m, 2H, -CH₂CH₂Ar), 6.14 (m, 2H, H(3), H(4)), 6.65 (m, 1H, H(5)), 7.23 – 7.31 (m, 5H, ArH); **¹³C NMR** (75 MHz, CDCl₃) δ_{C} /ppm 32.7, 33.9 and 35.0 (-C(2)CH₂-, -NCH₃ and -CH₂Ar), 65.5 (-CH₂CH₂Ar), 107.1 and 108.9 (C(3) and C(4)), 122.6 (C(5)), 124.9 (C(2)), 127.2, 128.6 and 129.1 (5 x ArC), 137.9 (1 x quaternary ArC), 170.6 (-CO₂-); ν_{max} (DCM/cm⁻¹) 1678 (s, C=O), 2922 (w, C-H) **m/z** (CI⁺) 244 (3%, [M+H]⁺), 243 (10%, [M]⁺); **HRMS** found 244.1341, [M + H]⁺ (C₁₅H₁₈NO₂) requires 244.1338.

4.2.2 Synthesis of Binding Units

Synthesis of FmocArg(Pbf)Arg(Pbf)-CA-OH Binding Unit 131



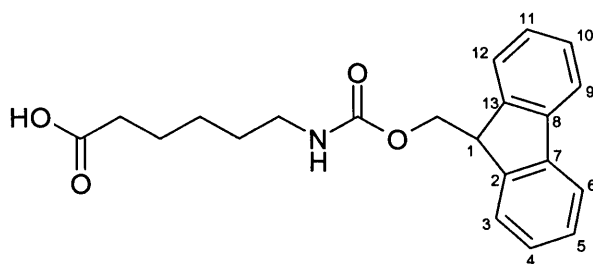
FmocArg(Pbf)-Arg(Pbf)-CA-OH

131

● = 2-chlorotrityl resin

CA = $\text{-HN(CH}_2)_5\text{CO}_2\text{H}$

6-(9H-Fluoren-9-ylmethoxycarbonylamino)-hexanoic acid (142)¹⁵⁷



A stirred solution of 6-aminocaproic acid (3.00 g, 23.0 mmol) in 10% aqueous sodium carbonate solution (6.09 g in 60 ml of water, 57.0 mmol) was cooled to 0 °C, whereupon 9-fluorenylmethyl chloroformate (5.92 g, 23.0 mmol) in dioxane (30 ml) was added. The solution was stirred for 10 min, after which time a white precipitate had formed. The solution was allowed to warm to room temperature and stirred for 4 h. The mixture was diluted with water (500 ml) and washed with ether (2 x 100 ml). The pH of the aqueous layer was adjusted to pH 1 (using concentrated aqueous HCl) and a white

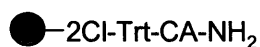
precipitate formed. The mixture was extracted with ethyl acetate (3 x 200 ml). The combined organic extracts were dried over MgSO_4 and concentrated *in vacuo* to afford a white solid, which was purified by flash chromatography (SiO_2 ; ethyl acetate). The desired product was isolated as a white solid (6.23 g, 77%). **m.p.** 109 °C (lit. 116 °C¹⁵⁷); **R_f** = 0.57 (SiO_2 ; ethyl acetate); **¹H NMR** (300 MHz, CDCl_3) δ_{H} /ppm 1.37 (m, 2H, $\text{HO}_2\text{CH}_2\text{CH}_2\text{CH}_2-$), 1.53 (m, 2H, $-\text{CH}_2\text{CH}_2\text{NHC(O)}-$), 1.64 (m, 2H, $\text{HO}_2\text{CCH}_2\text{CH}_2-$), 2.35 (t, $J = 7.2$, 2H, HO_2CCH_2-), 3.19 (br, m, $-\text{CH}_2\text{NHC(O)}-$), 4.21 (m, 1H, H(1)), 4.41 (d, $J = 6.0$, 2H, H(1) CH_2-), 4.76 (br, s, 1H, $\text{CH}_2\text{NHC(O)}$), 7.31 (m, 2H, H(4) and H(11)), 7.40 (m, 2H, H(5) and H(10)), 7.58 (d, $J = 7.3$, 2H, H(3) and H(12)), 7.76 (d, $J = 7.4$, 2H, H(6) and H(9)); **¹³C NMR** (75 MHz, CDCl_3) δ_{C} /ppm 24.3, 26.2, 29.7 (3 x CH_2 , $\text{HO}_2\text{CH}_2\text{CH}_2\text{CH}_2\text{CH}_2-$), 33.8 ($-\text{CH}_2\text{NHC(O)}-$), 40.9 (HO_2CCH_2-), 47.4 (C(1)), 66.6 (C(1) HCH_2-), 120.0, 125.0, 127.1, 127.7 (C(3), C(4), C(5), C(6), C(9), C(10), C(11) and C(12)), 141.4 (C(2) and C(13)), 144.1 (C(7) and C(8)), 156.6 ($-\text{NHC(O)}-$), 178.6 ($\text{HO}_2\text{C}-$); ν_{max} (nujol/ cm^{-1}) 1686 (s, C=O (carbamate)), 2928 (s, C-H), 3342 (s, N-H); **m/z** (FAB) 376 (4%, $[\text{M} + \text{Na}]^+$), 354 (33%, $[\text{M} + \text{H}]^+$).

Resin 349



Diisopropylethylamine (1.97 ml, 11.3 mmol) was added to a stirred solution of Fmoc-6-aminocaproic acid **142** (1.00 g, 2.83 mmol) in anhydrous dichloromethane (20 ml) under nitrogen. The mixture was stirred for an additional 10 min. The resulting solution was added to 2-chlorotrityl resin (1.69 g, 1.40 mmol/g) and the mixture agitated by sonication at room temperature for 3 h. The resin was filtered and washed sequentially with methanol (3 x 40 ml), methanol/dichloromethane /diisopropylethylamine (2:17:1, 3 x 40 ml), dichloromethane (3 x 40 ml), dimethylformamide (3 x 40 ml) and dichloromethane (3 x 40 ml). The resin was dried under vacuum overnight to afford the desired product (2.75 g). Fmoc substitution = 0.95 mmol/g.

Resin 145



The resin **349** (2.75 g) was suspended in piperidine/dimethylformamide solution (2:8, 20 ml) and sonicated at room temperature for 3 h. The resin was filtered and washed with dimethylformamide (5 x 30 ml) and dichloromethane (5 x 25 ml). The resin was dried under vacuum to give the deprotected resin **145** (1.90 g).

Resin 350



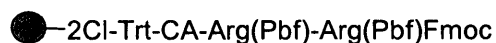
Fmoc-Arg(Pbf)-OH (3.49 g, 5.38 mmol), PyBOP (2.80 g, 5.38 mmol) and HOBt (0.73 g, 5.38 mmol) were dissolved in anhydrous dimethylformamide (30 ml) under nitrogen. Diisopropylethylamine (1.04 ml, 5.96 mmol) was added and the resulting solution was immediately added to the resin **145** (1.90 g, 0.95 mmol/g). The resulting suspension was agitated by sonication at room temperature for 4 h. The Kaiser test indicated the reaction was completed. The resin was then filtered and washed sequentially with dimethylformamide (4 x 50 ml), dichloromethane (3 x 50 ml), dimethylformamide (2 x 25 ml) and dichloromethane (2 x 50 ml). The resin was dried under vacuum to afford **350** (3.04 g). Fmoc substitution = 0.47 mmol/g.

Resin 146



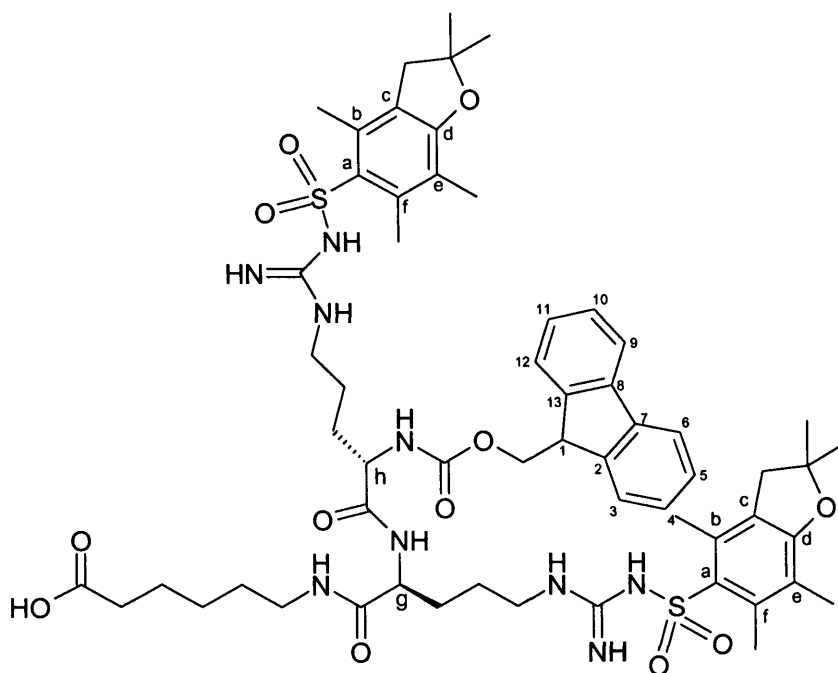
The resin **350** (3.04 g) was suspended in piperidine/dimethylformamide (2:8, 30 ml) and the mixture was sonicated at room temperature for 3 h. The resin was filtered and washed with dimethylformamide (5 x 30 ml) and dichloromethane (5 x 25 ml) and dried under vacuum to give the product **146** (2.58 g).

Resin 351



Fmoc-Arg(Pbf)-OH (3.02 g, 4.66 mmol), PyBOP (2.42 g, 4.66 mmol) and HOBt (0.63 g, 4.66 mmol) were dissolved in anhydrous dimethylformamide (30 ml) under nitrogen. Diisopropylethylamine (0.67 ml, 3.85 mmol) was added and the mixture added immediately to the resin **146** (2.58 g, 0.47 mmol/g). The suspension was agitated by sonication at room temperature for 4 h. The Kaiser test indicated the reaction was completed. The resin was then filtered and washed sequentially with dimethylformamide (4 x 50 ml), dichloromethane (3 x 50 ml), dimethylformamide (2 x 25 ml) and dichloromethane (2 x 50 ml). The resin was then dried under vacuum to give the product **351** (3.74 g). Fmoc substitution = 0.29 mmol/g.

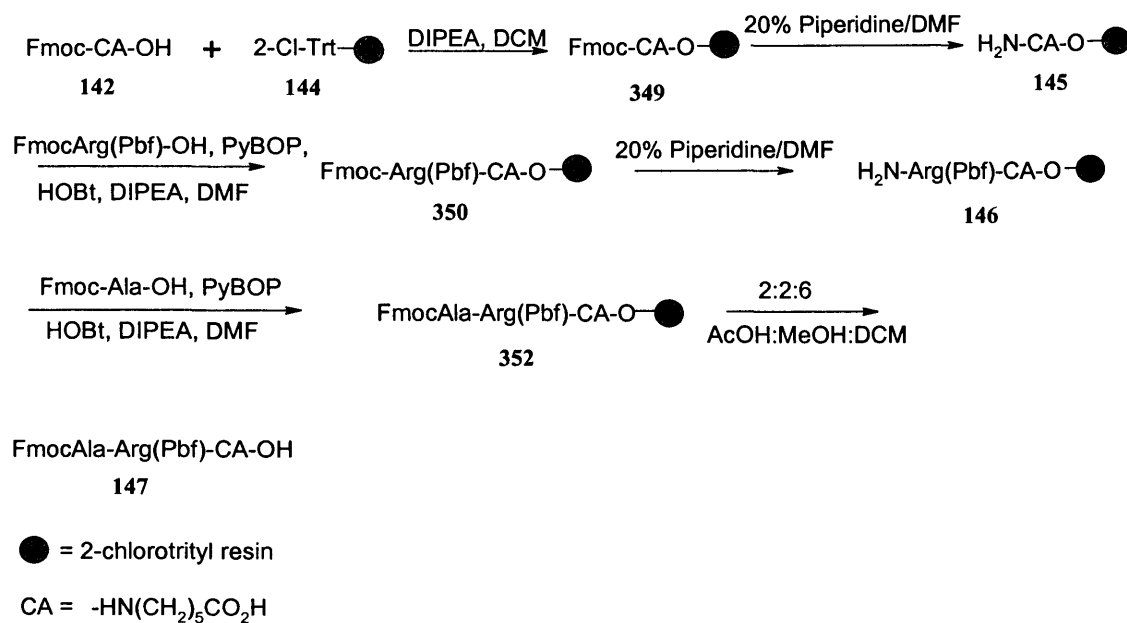
FmocArg(Pbf)Arg(Pbf)CA-OH (131)⁹⁰



The resin **351** (3.74 g, 0.29 mmol/g) in a solution of acetic acid/trifluoroethanol/dichloromethane (2:2:6, 20 ml) was sonicated at room temperature for 3 h. The resin was subsequently filtered and washed with acetic acid/trifluoroethanol/dichloromethane (2:2:6, 40 ml), dichloromethane (40 ml), methanol (20 ml) and dichloromethane (40 ml). The filtrate was concentrated *in vacuo* to afford a brown coloured oil. Purification by flash chromatography (SiO₂; methanol/ethyl acetate; 2:8), gave the product as a white solid (0.64 g, 19% over six steps). **m.p.** 134 °C (lit. 135 – 137 °C⁹⁰); **R_f** = 0.58 (SiO₂; methanol/ethyl acetate; 2:8); **¹H NMR** (300 MHz, CD₃OD) δ_H/ppm 1.25 – 1.60 (m, 14H, HO₂CCH₂CH₂CH₂CH₂- and 2 x (-CH₂CH₂CH₂NHC(NH)NH-), 1.44 (s, 12H, 2 x (-CH₂C(CH₃)₂O-), 1.96 (s, 6H, 2 x C(e)CH₃), 2.21 (m, 2H, HO₂CCH₂-), 2.52 (s, 3H, C(f)CH₃), 2.54 (s, 3H, C(f)CH₃), 2.59 (s, 3H, C(b)CH₃), 2.61 (s, 3H, C(b)CH₃), 2.97 (s, 2H, -CH₂C(CH₃)₂O-), 2.98 (s, 2H, -CH₂C(CH₃)₂O-), 3.22 (m, 6H, -CH₂NHC(O)- and 2 x (-CH₂NHC(NH)NH-), 3.75 (m, 1H, H(h)), 4.13 (m, 1H, H(1)), 4.21 (m, 1H, H(g)), 4.42 (m, 2H, H(1)CH₂-), 7.31 (m, 2H, (H(4) and H(11)), 7.39 (m, 2H, H(5) and H(10)), 7.65 (m, 2H, H(3) and H(12)), 7.79 (d, *J* = 7.4, 2H, H(6) and H(9)); **¹³C NMR** (100 MHz, CD₃OD, 320 K)

δ_c /ppm 13.2 (C(e)CH₃), 19.0, 20.2 (C(b)CH₃ and C(f)CH₃), 26.4, 27.5, 28.1 (HO₂CCH₂CH₂CH₂CH₂-), 29.3 (2 x -CH₂C(CH₃)₂O-), 30.5, 31.1 (2 x -CH₂CH₂CH₂NH(=NH)-), 35.8 (HO₂CCH₂-), 40.9, 42.1 (2 x -CH₂NH(C=NH) and -CH₂NHC(O)CH(g)-), 44.6 (2 x -CH₂C(CH₃)₂O-), 49.1 (C(1)), 55.0 (C(g)), 57.0 (C(h)), 68.7 (C(1)HCH₂-), 88.3 (2 x -CH₂C(CH₃)₂O-), 119.1 (2 x C(e)), 121.6 (C(6) and C(9)), 126.8 (C(3) and C(12)), 128.8 (C(4) and C(11)), 129.4 (C(5) and C(10)), 134.2 (2 x C(b) and 2 x C(f)), 135.1 (2 x C(a)), 140.0 (C(7) and C(8)), 143.2 (C(2) and C(13)), 145.9 (2 x C(c)), 158.7 (2 x C(d)), 160.5 (-NHC(O)O-) and 2 x -NH(C=NH)-, 174.2, 178.4 (2 x -C(O)NH- and -CO₂H); ν_{\max} (nujol/cm⁻¹) 1377 (s, -SO₂-N), 1535 (w, C=O (amide)), 1636 (w, C=O (acid)), 2853 (s, C-H), 3333 (w, N-H); m/z (FAB) 1170 (44%, [M + H]⁺); $[\alpha]_D + 9.0^\circ$ (c 0.20, MeOH).

Synthesis of FmocAla-Arg(Pbf)-CA-OH Binding Unit 147

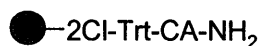


Resin 349



Diisopropylethylamine (1.97 ml, 11.3 mmol) was added to a stirred solution of Fmoc-6-aminocaproic acid **142** (1.00 g, 2.83 mmol) in anhydrous dichloromethane (20 ml) under nitrogen. The mixture was stirred for an additional 10 min. The resulting solution was added to 2-chlorotrityl resin (1.69 g, 1.40 mmol/g) and the mixture agitated by sonication at room temperature for 3 h. The resin was filtered and washed sequentially with methanol (3 x 40 ml), methanol/dichloromethane /diisopropylethylamine (2:17:1, 3 x 40 ml), dichloromethane (3 x 40 ml), dimethylformamide (3 x 40 ml) and dichloromethane (3 x 40 ml). The resin was dried under vacuum overnight to afford the desired product (2.41 g). Fmoc substitution = 1.26 mmol/g.

Resin 145



The resin **349** (2.41 g) was suspended in piperidine/dimethylformamide solution (2:8, 20 ml) and sonicated at room temperature for 3 h. The resin was filtered and washed with dimethylformamide (5 x 30 ml) and dichloromethane (5 x 25 ml). The resin was dried under vacuum to give the deprotected resin **145** (1.90 g).

Resin 350



Fmoc-Arg(Pbf)-OH (4.64 g, 7.14 mmol), PyBOP (3.71 g, 7.14 mmol) and HOBt (0.96 g, 7.14 mmol) were dissolved in anhydrous dimethylformamide (30 ml) under nitrogen. Diisopropylethylamine (2.48 ml, 14.3 mmol) was added and the resulting solution was immediately added to the resin **145** (1.89 g, 1.26 mmol/g). The resulting suspension was agitated by sonication at room temperature for 4 h. The Kaiser test indicated the reaction was completed. The resin was then filtered and washed sequentially with dimethylformamide (4 x 50 ml), dichloromethane (3 x 50 ml), dimethylformamide (2 x 25 ml) and dichloromethane (2 x 50 ml). The resin was dried under vacuum to afford **350** (3.22 g). Fmoc substitution = 0.77 mmol/g.

Resin 146



The resin **350** (3.22 g) was suspended in piperidine/dimethylformamide (2:8, 30 ml) and the mixture was sonicated at room temperature for 3 h. The resin was filtered and washed with dimethylformamide (5 x 30 ml) and dichloromethane (5 x 25 ml) and dried under vacuum to give the product **146** (2.58 g).

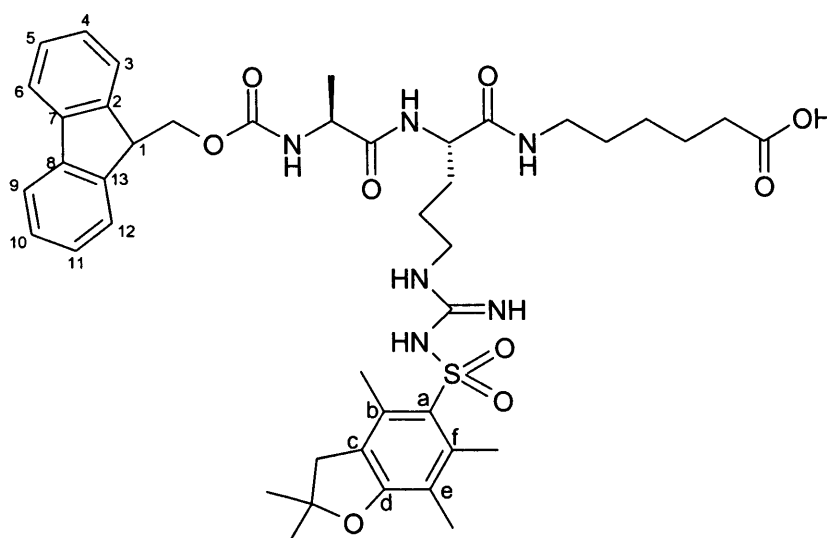
Resin 352



Diisopropylethylamine (2.20 ml, 12.6 mmol) was added to a stirred solution of Fmoc-alanine (1.97 g, 6.33 mmol), PyBOP (3.29 g, 6.33 mmol) and HOBt (0.85 g, 6.33 mmol) in anhydrous dimethylformamide (30 ml), under nitrogen. The resulting mixture was added immediately to the resin **146** (2.74 g, 0.77 mmol/g) and the suspension was agitated by sonication at room temperature for 4 h. The Kaiser test indicated the

reaction was completed. The resin was filtered and washed sequentially with dimethylformamide (4 x 50 ml), dichloromethane (3 x 50 ml), dimethylformamide (2 x 25 ml) and dichloromethane (2 x 50 ml). The resin was dried under vacuum to give the product **352** (3.16 g). Fmoc substitution = 0.49 mmol/g.

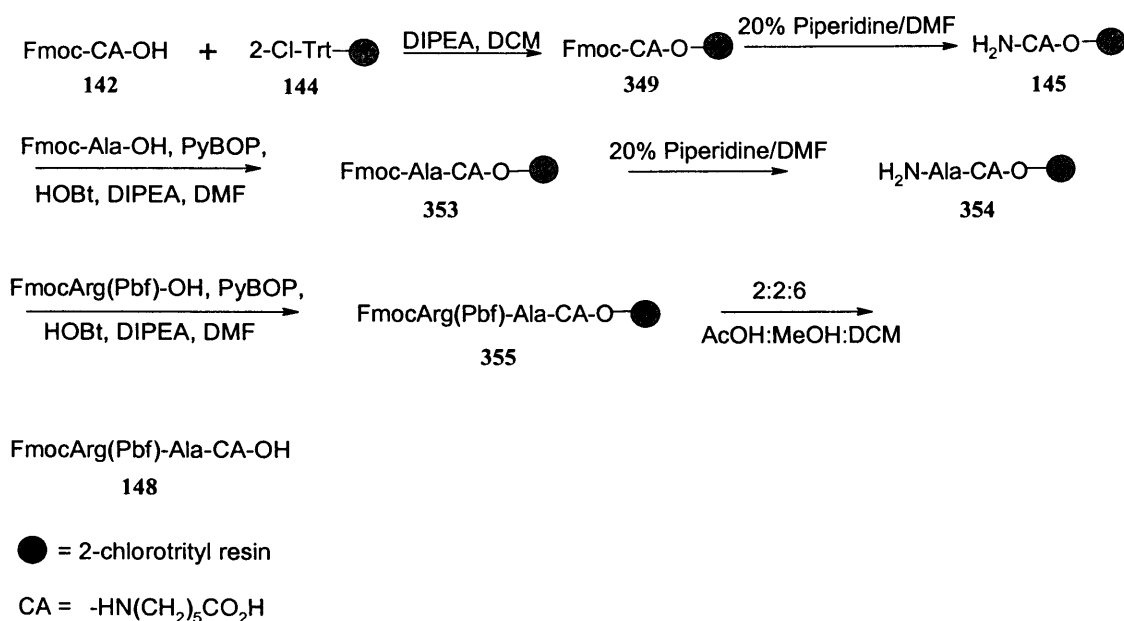
FmocAla-Arg(Pbf)-CA-OH (147)



A suspension of the resin **352** (3.16 g, 0.49 mmol/g) in a solution of acetic acid/trifluoroethanol/dichloromethane (2:2:6, 20 ml) was sonicated at room temperature for 3 h. The resin was filtered and washed sequentially with acetic acid/trifluoroethanol/dichloromethane (2:2:6, 40 ml), dichloromethane (40 ml), methanol (20 ml) and dichloromethane (40 ml). The filtrate was concentrated *in vacuo* to afford a brown coloured oil. Purification by flash chromatography (SiO₂; methanol/ethyl acetate; 2:8) gave the product as a white solid (0.50 g, 21% over six steps). **m.p.** 135 °C; **R_f** = 0.51 (SiO₂; methanol/ethyl acetate; 2/8); **¹H NMR** (500 MHz, CD₃OD) δ_{H} /ppm 1.31 (m, 6H, -CH₂CH₂CH₂NHC(NH)NH- and HO₂CCH₂CH₂CH₂-), 1.39 (s, 6H, -CH₂C(CH₃)₂O-), 1.46 – 1.57 (m, 7H, HO₂CCH₂CH₂CH₂CH₂- and -HNC(O)CHC(CH₃)-), 2.03 (s, 3H, C(e)CH₃), 2.24 (m, 2H, HO₂CCH₂-), 2.48 (s, 3H, C(f)CH₃), 2.55 (s, 3H, C(b)CH₃), 2.92 (s, 2H, -CH₂C(CH₃)₂O-), 3.12 (m, 4H, -

$\text{CH}_2\text{NHC(O)-}$ and $-\text{CH}_2\text{NHC(NH)NH-}$, 4.09 (m, 1H, $-\text{HNC(O)CH}(\text{CH}_3)-$), 4.17 (m, 1H, $\underline{\text{H}}(1)$), 4.32 (m, 3H, $-\text{HNC(O)CHNHC(O)-}$ and $\text{H}(1)\text{CH}_2-$), 7.28 (m, 2H, $\underline{\text{H}}(4)$ and $\underline{\text{H}}(11)$), 7.34 (m, 2H, $\underline{\text{H}}(5)$ and $\underline{\text{H}}(10)$), 7.63 (m, 2H, $\underline{\text{H}}(3)$ and $\underline{\text{H}}(12)$), 7.75 (d, $J = 6.9$, 2H, $\underline{\text{H}}(6)$ and $\underline{\text{H}}(9)$); ^{13}C NMR (125 MHz, CD_3OD) δ_c/ppm 12.5 ($\text{C}(\text{e})\underline{\text{C}}\text{H}_3$), 18.0 ($\text{C}(\text{b})\underline{\text{C}}\text{H}_3$), 18.4 ($\text{C}(\text{f})\underline{\text{C}}\text{H}_3$), 19.6 ($-\text{C}(\text{O})\text{CH}(\underline{\text{C}}\text{H}_3)\text{NH-}$), 25.7 ($\text{HO}_2\text{CCH}_2\text{CH}_2\underline{\text{C}}\text{H}_2-$), 27.4 ($\text{HO}_2\text{CCH}_2\underline{\text{C}}\text{H}_2-$), 28.7 ($-\text{CH}_2\underline{\text{C}}(\text{CH}_3)_2\text{-O-}$), 29.9, 30.3, 33.0 ($-\underline{\text{C}}\text{H}_2\text{CH}_2\text{NHC(O)-}$ and $-\underline{\text{C}}\text{H}_2\text{CH}_2\text{NHC(NH)NH-}$), 34.9 ($\text{HO}_2\text{C}\underline{\text{C}}\text{H}_2-$), 40.2 ($-\underline{\text{C}}\text{H}_2\text{NHC(O)-}$), 43.9 ($-\underline{\text{C}}\text{H}_2\text{NHC(NH)NH-}$), 52.3 ($-\text{C}(\text{O})\text{NH}\underline{\text{C}}\text{H}(\text{CH}_3)\text{C}(\text{O})-$), 54.2 ($-\text{C}(\text{O})\underline{\text{C}}\text{H}\text{NHC(O)-}$), 68.0 ($\text{C}(1)\underline{\text{C}}\text{H}_2-$), 87.6 ($-\text{CH}_2\underline{\text{C}}(\text{CH}_3)_2\text{-O-}$), 118.4 ($\underline{\text{C}}(\text{e})$), 120.9 ($\underline{\text{C}}(6)$ and $\underline{\text{C}}(9)$), 126.2 ($\underline{\text{C}}(3)$ and $\underline{\text{C}}(12)$), 128.2 ($\underline{\text{C}}(4)$ and $\underline{\text{C}}(11)$), 128.8 ($\underline{\text{C}}(5)$ and $\underline{\text{C}}(10)$), 133.5 ($\underline{\text{C}}(\text{c})$), 134.3 ($\underline{\text{C}}(\text{b})$), 139.4 ($\underline{\text{C}}(7)$ and $\underline{\text{C}}(8)$), 142.5 ($\underline{\text{C}}(2)$ and $\underline{\text{C}}(13)$), 145.1 ($\underline{\text{C}}(\text{a})$), 145.3 ($\underline{\text{C}}(\text{f})$), 158.1 ($\underline{\text{C}}(\text{d})$), 158.5 ($\text{C}(1)\text{CH}_2\underline{\text{C}}\text{O}_2-$), 159.8 ($-\text{HNC}(\text{NH})\text{NH-}$), 173.7, 175.7, 177.6 ($\text{HO}_2\underline{\text{C}}-$, $-\text{NHC}(\text{O})\text{CHNH-}$ and $-\text{NHC}(\text{O})\text{CH}(\text{CH}_3)\text{NH-}$); ν_{max} (nujol/ cm^{-1}) 1377 (s, $\text{SO}_2\text{-N}$), 1542 (br, C=O (amide)), 1708 (w, C=O (acid)), 2922 (s, C-H), 3376 (w, N-H); m/z (FAB) 833 (69%, $[\text{M}]^+$); HRMS found 833.3870, $[\text{M}]^+$ ($\text{C}_{43}\text{H}_{56}\text{N}_6\text{O}_9\text{S}$) requires 833.3908; $[\alpha]_{\text{D}} + 3.1^\circ$ (c 0.26, MeOH).

Synthesis of FmocArg(Pbf)-Ala-CA-OH Binding Unit 148



Resin 349



Diisopropylethylamine (1.38 ml, 7.93 mmol) was added to a stirred solution of Fmoc-6-aminocaproic acid **142** (0.70 g, 1.98 mmol) in anhydrous dichloromethane (20 ml) under nitrogen. The mixture was stirred for an additional 10 min. The resulting solution was added to 2-chlorotrityl resin (1.18 g, 1.40 mmol/g) and the mixture agitated by sonication at room temperature for 3 h. The resin was filtered and washed sequentially with methanol (3 x 40 ml), methanol/dichloromethane /diisopropylethylamine (2:17:1, 3 x 40 ml), dichloromethane (3 x 40 ml), dimethylformamide (3 x 40 ml) and dichloromethane (3 x 40 ml). The resin was dried under vacuum overnight to afford the desired product (1.70 g). Fmoc substitution = 0.97 mmol/g.

Resin 145



The resin **349** (1.70 g) was suspended in piperidine/dimethylformamide solution (2:8, 20 ml) and sonicated at room temperature for 3 h. The resin was filtered and washed with dimethylformamide (5 x 30 ml) and dichloromethane (5 x 25 ml). The resin was dried under vacuum to give the deprotected resin **145** (1.16 g).

Resin 353



Diisopropylethylamine (1.17 ml, 6.75 mmol) was added to a stirred solution of Fmoc-alanine (1.05 g, 3.38 mmol), PyBOP (1.76 g, 3.38 mmol) and HOBt (0.46 g, 3.38 mmol) in anhydrous dimethylformamide (15 ml), under nitrogen. The resulting mixture was added immediately to the resin **145** (1.16 g, 0.97 mmol/g) and the suspension was agitated by sonication at room temperature for 4 h. The Kaiser test indicated the reaction was completed. The resin was filtered and washed with dimethylformamide (4 x 50 ml), dichloromethane (3 x 50 ml), dimethylformamide (2 x 25 ml) and dichloromethane (2 x 50 ml). The resin was dried under vacuum to give the product **353** (1.38 g). Fmoc substitution = 0.57 mmol/g.

Resin 354



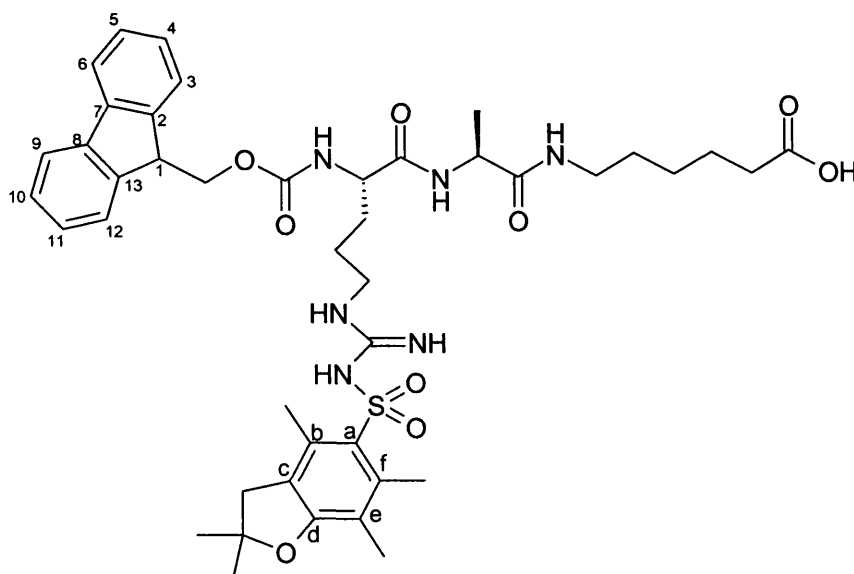
A suspension of the resin **353** (1.38 g) in piperidine/dimethylformamide solution (2:8, 20 ml) was sonicated at room temperature for 3 h. The resin was filtered and washed with dimethylformamide (5 x 30 ml) and dichloromethane (5 x 25 ml) and dried under vacuum to give **354** (1.13 g).

Resin 355



Diisopropylethylamine (0.67 ml, 3.86 mmol) was added to a stirred solution of Fmoc-Arg(Pbf)-OH (1.25 g, 1.93 mmol), PyBOP (1.00 g, 1.93 mmol) and HOBt (0.26 g, 1.93 mmol) in anhydrous dimethylformamide (20 ml) under nitrogen. The resulting mixture was immediately added to the resin **354** (1.13 g, 0.57 mmol/g) and the suspension was agitated by sonication at room temperature for 4 h. The Kaiser test indicated the reaction was completed. The resin was filtered and washed with dimethylformamide (4 x 50 ml), dichloromethane (3 x 50 ml), dimethylformamide (2 x 25 ml) and dichloromethane (2 x 50 ml). The resin was dried under vacuum to give **354** (1.75 g). Fmoc substitution = 0.38 mmol/g.

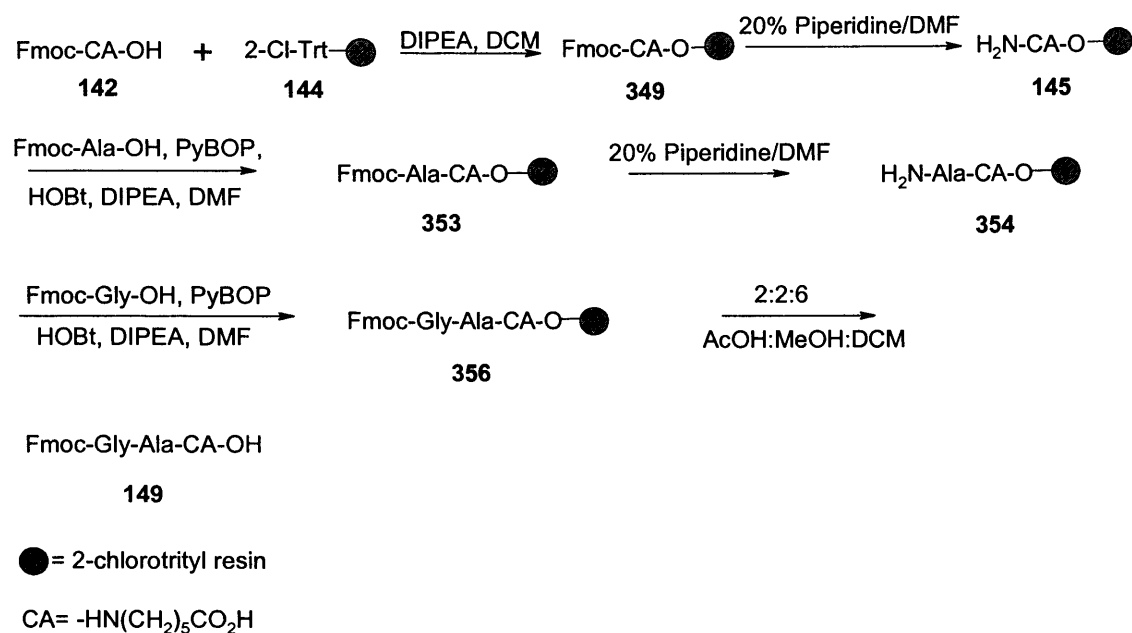
FmocArg(Pbf)-Ala-CA-OH 148



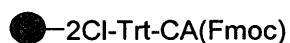
Resin **355** (1.75 g, 0.38 mmol/g) in a solution of acetic acid/trifluoroethanol/dichloromethane (2:2:6, 15 ml) was sonicated at room temperature for 3 h. The resin was filtered and washed with acetic acid/trifluoroethanol/dichloromethane (2:2:6, 40 ml), dichloromethane (40 ml),

methanol (20 ml) and dichloromethane (40 ml). The filtrate was concentrated *in vacuo* to afford a brown oil. Purification by flash chromatography (SiO₂; methanol/ethyl acetate; 20:80) gave the product as a white solid (0.55 g, 33% over six steps). **m.p.** 150 °C; **R_f** = 0.45 (SiO₂; MeOH/EtOAc; 2:8); **¹H NMR** (500 MHz, CD₃OD) δ_{H} /ppm 1.30 (m, 4H, HO₂CCH₂CH₂CH₂-, -CH₂CH₂CH₂NHC(NH)NH-), 1.40 (s, 6H, -CH₂C(CH₃)₂C(O)-), 1.46 – 1.57 (m, 9H, HO₂CCH₂CH₂CH₂CH₂-, -HNC(O)CH(CH₃)- and -CH₂CH₂NHC(NH)NH-), 2.04 (s, 3H, C(e)CH₃), 2.20 (m, 2H, HO₂CCH₂-), 2.50 (s, 3H, C(f)CH₃), 2.57 (s, 3H, C(b)CH₃), 2.93 (s, 2H, -CH₂C(CH₃)₂-O-), 3.15 (m, 4H, -CH₂NHC(O)CH(CH₃)- and -CH₂NHC(NH)NH-), 4.05 (m, 1H, -HNC(O)CH(CH₃)), 4.19 (m, 1H, H(1)), 4.29 – 4.41 (m, 3H, -NHC(O)CHNHCO₂- and H(1)CH₂-), 7.25 (m, 2H, H(4) and H(11)), 7.26 (m, 2H, H(5) and H(10)), 7.62 (m, 2H, H(3) and H(12)), 7.75 (d, *J* = 7.6, 2H, H(6) and H(9)); **¹³C NMR** (125 MHz, CD₃OD) δ_{C} /ppm 12.5 (C(e)CH₃), 18.2 (C(b)CH₃), 18.4 (C(f)CH₃), 19.6 (-C(O)CH(CH₃)NH-), 26.3 (HO₂CCH₂CH₂CH₂-), 27.5 (HO₂CCH₂CH₂-), 28.7 (-CH₂C(CH₃)₂-O-), 30.0, 30.2, 30.7 (-CH₂CH₂NHC(O)- and -CH₂CH₂NHC(NH)NH-), 36.6 (HO₂CCH₂-), 40.2 (-CH₂NHC(O)-), 43.9 (-CH₂NHC(NH)NH-) 48.5 (C(1)), 48.8 (-CH₂C(CH₃)₂-O-), 50.5 (-C(O)CH(CH₃)NH-), 56.1 (-C(O)CHNHHC(O)-), 67.9 (C(1)HCH₂-), 87.6 (-CH₂C(CH₃)₂-O-), 118.4 (C(e)), 120.9 (C(6) and C(9)), 126.2 (C(3) and C(12)), 128.2 (C(4) and C(11)), 128.8 (C(5) and C(10)), 133.5 (C(c)), 134.4 (C(b)), 139.4 (C(7) and C(8)), 142.6 (C(2) and C(13)), 145.1 (C(a)), 145.3 (C(f)), 158.2 (C(d)), 158.6 (C(1)CH₂OC(O)-), 159.8 (-NHC(NH)NH-), 174.4, 174.7, 180.3 (HO₂C-, -NHC(O)C(CH₃)NHC(O)-); ν_{max} (nujol/cm⁻¹) 1377 (s, SO₂-N), 1552 (br, C=O (amide)), 1645 (br, C=O (amide)), 1708 (w, C=O (acid)), 2854, 2923 (s, C-H), 3322 (w, N-H); **m/z** (FAB) 834 (35%, [M + H]⁺), 833 (65%, [M]⁺); **HRMS** found 833.3964, [M]⁺ (C₄₃H₅₆N₆O₉S) requires 833.3908.

Synthesis of FmocGly-Ala-CA-OH Binding Unit 149

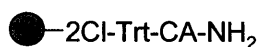


Resin 349



Diisopropylethylamine (1.38 ml, 7.93 mmol) was added to a stirred solution of Fmoc-6-aminocaproic acid **142** (0.70 g, 1.98 mmol) in anhydrous dichloromethane (20 ml) under nitrogen. The mixture was stirred for an additional 10 min. The resulting solution was added to 2-chlorotrityl resin (1.18 g, 1.40 mmol/g) and the mixture agitated by sonication at room temperature for 3 h. The resin was filtered and washed sequentially with methanol (3 x 40 ml), methanol/dichloromethane /diisopropylethylamine (2:17:1, 3 x 40 ml), dichloromethane (3 x 40 ml), dimethylformamide (3 x 40 ml) and dichloromethane (3 x 40 ml). The resin was dried under vacuum overnight to afford the desired product (2.48 g). Fmoc substitution = 0.91 mmol/g.

Resin 145



The resin **349** (2.48 g) was suspended in piperidine/dimethylformamide solution (2:8, 20 ml) and sonicated at room temperature for 3 h. The resin was filtered and washed with dimethylformamide (5 x 30 ml) and dichloromethane (5 x 25 ml). The resin was dried under vacuum to give the deprotected resin **145** (1.94 g).

Resin 353



Diisopropylethylamine (1.84 ml, 10.6 mmol) was added to a stirred solution of Fmoc-alanine (1.65 g, 5.30 mmol), PyBOP (2.75 g, 5.30 mmol) and HOBt (0.71 g, 5.30 mmol) in anhydrous dimethylformamide (15 ml), under nitrogen. The resulting mixture was added immediately to the resin **145** (1.94 g, 0.91 mmol/g) and the suspension was agitated by sonication at room temperature for 4 h. The Kaiser test indicated the reaction was completed. The resin was filtered and washed with dimethylformamide (4 x 50 ml), dichloromethane (3 x 50 ml), dimethylformamide (2 x 25 ml) and dichloromethane (2 x 50 ml). The resin was dried under vacuum to give the product **353** (2.64 g). Fmoc substitution = 0.76 mmol/g.

Resin 354



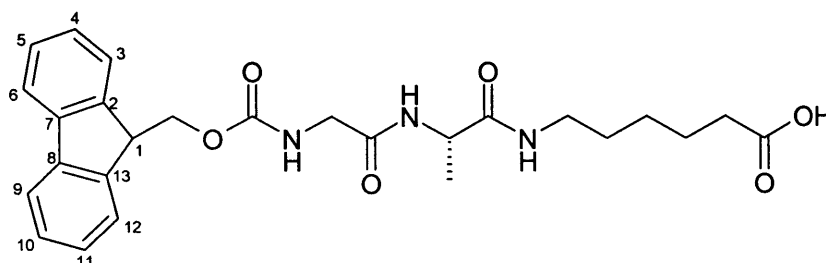
A suspension of the resin **353** (2.64 g) in piperidine/dimethylformamide solution (2:8, 20 ml) was sonicated at room temperature for 3 h. The resin was filtered and washed with dimethylformamide (5 x 30 ml) and dichloromethane (5 x 25 ml) and dried under vacuum to give **354** (2.01 g).

Resin 356



Diisopropylethylamine (1.59 ml, 9.17 mmol) was added to a stirred mixture of Fmoc-glycine (1.36 g, 4.58 mmol), PyBOP (2.38 g, 4.58 mmol) and HOBT (0.62 g, 4.58 mmol) in anhydrous dimethylformamide (20 ml), under nitrogen. The resulting mixture was then added immediately to the resin **354** (2.01 g, 0.76 mmol/g) and the suspension was agitated by sonication at room temperature for 4 h. The Kaiser test indicated the reaction was completed. The resin was filtered and washed with dimethylformamide (4 x 50 ml), dichloromethane (3 x 50 ml), dimethylformamide (2 x 25 ml) and dichloromethane (2 x 50 ml). The resin was dried under vacuum to give **356** (2.62 g). Fmoc substitution = 0.40 mmol/g.

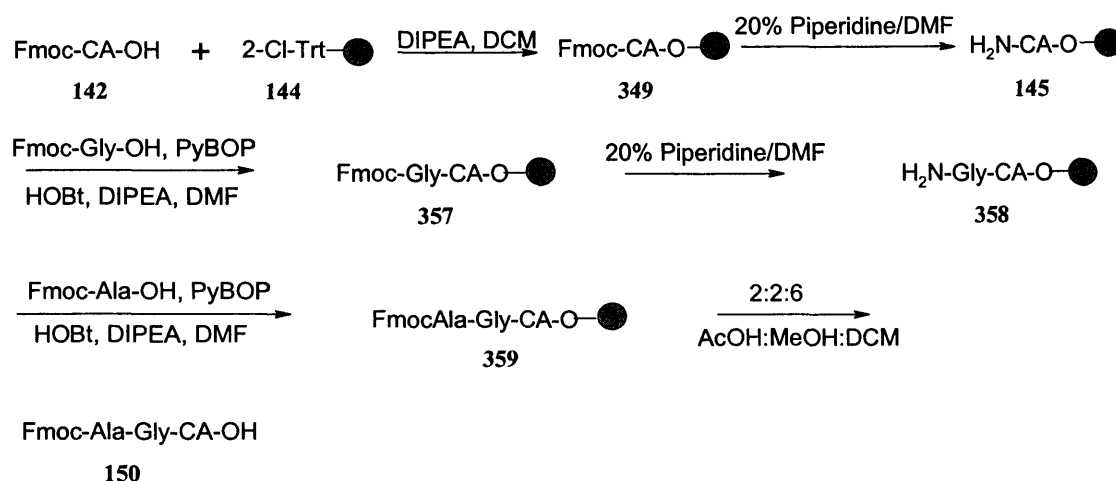
FmocGly-Ala-CA-OH (149)



The resin **356** (2.62 g, 0.40 mmol) was sonicated in a solution of acetic acid/trifluoroethanol/dichloromethane (2:2:6, 20 ml) at room temperature for 3 h. The resin was filtered and washed with acetic acid/trifluoroethanol/dichloromethane (2:2:6, 40 ml), dichloromethane (40 ml), methanol (20 ml) and dichloromethane (40 ml). The filtrate was concentrated *in vacuo* to afford a brown oil. Purification by flash chromatography (SiO₂; methanol/ethyl acetate; 2:8) gave the desired the product as a beige solid (0.62 g, 46% over six steps). **m.p.** 110 °C; **R_f** = 0.48 (SiO₂; methanol/ethyl acetate; 2:8); ¹H NMR (500 MHz, CD₃OD) δ_H/ppm 1.33 (m, 5H, HO₂CCH₂CH₂CH₂- and -HNC(O)C(CH₃)-), 1.48 (m, 2H, -CH₂CH₂NHC(O)-), 1.57 (m, 2H, HO₂CCH₂CH₂-), 2.24 (t, *J* = 7.4, 2H, HO₂CCH₂-), 3.14 (m, 2H, -CH₂CH₂NHC(O)-), 3.74, 3.79 (AB q,

$J = 16.7$, 2H, $-\text{HNC}(\text{O})\text{CH}_2\text{NH}-$), 4.20 (m, 1H, $\underline{\text{H}}(1)$), 4.32 – 4.38 (m, 3H, $\text{H}(1)\text{CH}_2-$ and $-\text{NHC}(\text{O})\text{CH}(\text{CH}_3)-$), 7.28 (m, 2H, $\underline{\text{H}}(4)$ and $\underline{\text{H}}(11)$), 7.36 (m, 2H, $\underline{\text{H}}(5)$ and $\underline{\text{H}}(10)$), 7.61 (d, $J = 7.4$, 2H, $\underline{\text{H}}(3)$ and $\underline{\text{H}}(12)$), 7.75 (d, $J = 7.5$, 2H, $\underline{\text{H}}(6)$ and $\underline{\text{H}}(9)$); ^{13}C NMR (125 MHz, CD_3OD) δ_c/ppm 18.3 ($-\text{HNC}(\text{O})\text{CH}(\underline{\text{C}}\text{H}_3)-$), 25.7 ($\text{HO}_2\text{CCH}_2\text{CH}_2\underline{\text{C}}\text{H}_2-$), 27.4 ($\text{HO}_2\text{CCH}_2\underline{\text{C}}\text{H}_2-$), 30.0 ($-\underline{\text{C}}\text{H}_2\text{CH}_2\text{NHC}(\text{O})-$), 35.1 ($\text{HO}_2\text{C}\underline{\text{C}}\text{H}_2-$), 40.4 ($-\text{CH}_2\underline{\text{C}}\text{H}_2\text{NHC}(\text{O})-$), 45.2 ($-\text{HNC}(\text{O})\underline{\text{C}}\text{H}_2\text{NH}-$), 48.9 ($\underline{\text{C}}(1)$), 50.4 ($-\text{HNC}(\text{O})\underline{\text{C}}\text{H}(\text{CH}_3)$), 68.3 ($\text{C}(1)\text{H}\underline{\text{C}}\text{H}_2-$), 120.9 ($\underline{\text{C}}(6)$ and $\underline{\text{C}}(9)$), 126.1 ($\underline{\text{C}}(3)$ and $\underline{\text{C}}(12)$), 128.1 ($\underline{\text{C}}(4)$ and $\underline{\text{C}}(11)$), 128.8 ($\underline{\text{C}}(5)$ and $\underline{\text{C}}(10)$), 142.6 ($\underline{\text{C}}(7)$ and $\underline{\text{C}}(8)$), 145.3 ($\underline{\text{C}}(2)$ and $\underline{\text{C}}(13)$), 171.7, 174.6, 177.8 ($\text{HO}_2\underline{\text{C}}\text{H}_2-$, $-\text{HNC}(\text{O})\text{CH}(\text{CH}_3)-$ and $-\text{HNC}(\text{O})\text{CH}_2\text{NH}-$); ν_{max} ($\text{KBr}/\text{cm}^{-1}$) 1538 (br, $\text{C}=\text{O}$ (amide)), 1645 (br, $\text{C}=\text{O}$ (amide)), 1708 (br, $\text{C}=\text{O}$ (acid)), 2936 (s, C-H), 3069 (s, C-H), 3308 (s, N-H); m/z (FAB) 482 (100%, $[\text{M} + \text{H}]^+$); **HRMS** found 504.2117, $[\text{M} + \text{Na}]^+$ ($\text{C}_{26}\text{H}_{31}\text{N}_3\text{O}_6\text{Na}$) requires 504.2110; **Anal.** ($\text{C}_{26}\text{H}_{31}\text{N}_3\text{O}_6 \cdot \text{H}_2\text{O}$) found C, 61.66; H, 6.69; N, 8.31%; requires C, 62.51; H, 6.66; N, 8.41%.

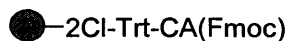
Synthesis of FmocAla-Gly-CA-OH Binding Unit 150



● = 2-chlorotrityl resin

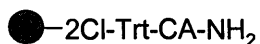
CA = $-\text{HN}(\text{CH}_2)_5\text{CO}_2\text{H}$

Resin 349



Diisopropylethylamine (1.97 ml, 11.3 mmol) was added to a stirred solution of Fmoc-6-aminocaproic acid **142** (1.00 g, 2.83 mmol) in anhydrous dichloromethane (20 ml) under nitrogen. The mixture was stirred for an additional 10 min. The resulting solution was added to 2-chlorotrityl resin (1.69 g, 1.40 mmol/g) and the mixture agitated by sonication at room temperature for 3 h. The resin was filtered and washed sequentially with methanol (3 x 40 ml), methanol/dichloromethane /diisopropylethylamine (2:17:1, 3 x 40 ml), dichloromethane (3 x 40 ml), dimethylformamide (3 x 40 ml) and dichloromethane (3 x 40 ml). The resin was dried under vacuum overnight to afford the desired product (2.40 g). Fmoc substitution = 0.97 mmol/g.

Resin 145



The resin **349** (2.40 g) was suspended in piperidine/dimethylformamide solution (2:8, 20 ml) and sonicated at room temperature for 3 h. The resin was filtered and washed with dimethylformamide (5 x 30 ml) and dichloromethane (5 x 25 ml). The resin was dried under vacuum to give the deprotected resin **145** (1.84 g).

Resin 357



To a stirred solution of Fmoc-Glycine (1.59 g, 5.35 mmol), PyBOP (2.78 g, 5.35 mmol) and HOBt (0.72 g, 5.35 mmol) in anhydrous dimethylformamide (20 ml), diisopropylethylamine (1.86 ml, 10.7 mmol) was added. The resulting solution was immediately added to the resin **145** (1.84 g, 0.97 mmol/g). The suspension was agitated by sonication at room temperature for 4 h. The Kaiser test indicated the reaction was

completed. The resin was filtered and washed sequentially with dimethylformamide (4 x 50 ml), dichloromethane (3 x 50 ml), dimethylformamide (2 x 25 ml) and dichloromethane (2 x 50 ml). The resin was dried under vacuum to give product **357** (2.40 g). Fmoc substitution = 0.82 mmol/g.

Resin 358



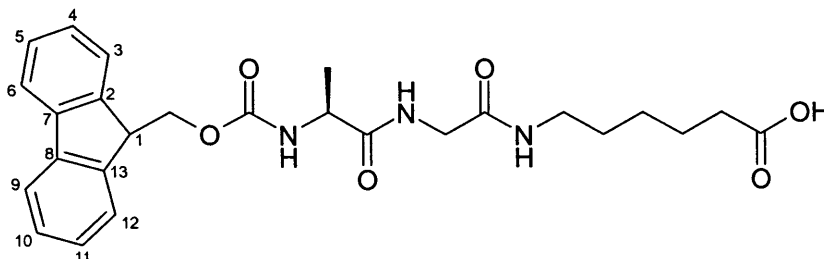
The resin **357** (2.40 g) was suspended in piperidine/dimethylformamide solution (2:8, 20 ml) and sonicated at room temperature for 3 h. The resin was filtered and washed with dimethylformamide (5 x 30 ml) and dichloromethane (5 x 25 ml), and dried under vacuum to give product **358** (1.87 g).

Resin 359



To a stirred solution of Fmoc-Alanine (1.43 g, 4.60 mmol), PyBOP (2.39 g, 4.60 mmol) and HOBt (0.62 g, 4.60 mmol) in anhydrous dimethylformamide (20 ml), diisopropylethylamine (1.60 ml, 9.20 mmol) was added. The solution was then added immediately to the resin **358** (1.87 g, 0.82 mmol/g). The suspension was agitated by sonication at room temperature for 4 h. The Kaiser test indicated the reaction was completed. The resin was filtered and washed sequentially with dimethylformamide (4 x 50 ml), dichloromethane (3 x 50 ml), dimethylformamide (2 x 25 ml) and dichloromethane (2 x 50 ml). The resin was dried under vacuum to give the product **359** (2.56 g). Fmoc substitution = 0.58 mmol/g.

FmocAla-Gly-CA-OH 150

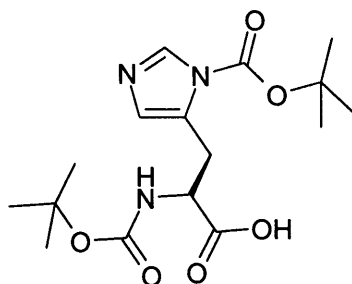


A suspension of resin **359** (2.56 g, 0.58 mmol/g) in acetic acid/trifluoroethanol/dichloromethane (2:2:6, 20 ml) was sonicated at room temperature for 3 h. The resin was then filtered and washed sequentially with acetic acid/trifluoroethanol/dichloromethane (2:2:6, 40 ml), dichloromethane (40 ml), methanol (20 ml) and dichloromethane (40 ml). The filtrate was concentrated *in vacuo* to afford a brown coloured oil. Purification by flash chromatography (SiO₂; methanol/ethyl acetate; 2:8) gave the product as a white solid (0.44 g, 32% yield over six steps). **m.p.** 104 °C; **R_f** = 0.52 (SiO₂; chloroform/methanol/acetic acid; 80:20:0.1); **¹H NMR** (500 MHz, CD₃OD) δ_{H} /ppm 1.26 (m, 2H, HO₂CCH₂CH₂CH₂-), 1.33 (m, 3H, -NHC(O)CH(CH₃)NH-), 1.46 (m, 2H, CH₂CH₂NHC(O)-), 1.53 (m, 2H, HO₂CCH₂CH₂-), 2.17 (m, 2H, HO₂CCH₂-), 3.12 (m, 2H, -CH₂CH₂NHC(O)-), 3.74, 3.85 (AB q, *J* = 16.9, 2H, -HNC(O)CH₂NH-), 4.04 (m, 1H, -HNC(O)CH(CH₃)HN-), 4.21 (m, 1H, H(1)CH₂-), 4.38 (m, 2H, H(1)CH₂-), 7.29 (m, 2H, H(4) and H(11)), 7.37 (m, 2H, H(5) and H(10)), 7.64 (m, 2H, H(3) and H(12)), 7.76 (d, *J* = 7.4, 2H, H(9) and H(6)); **¹³C NMR** (125 MHz, CD₃OD) δ_{C} /ppm 17.4 (-HNC(O)CH(CH₃)NH-), 26.1 (-HO₂CCH₂CH₂CH₂-), 27.5 (HO₂CCH₂CH₂-), 29.9 (-CH₂CH₂NHCO-), 36.2 (HO₂CCH₂-), 40.3 (-CH₂CH₂NHC(O)-), 43.6 (-HNC(O)CH₂NHC(O)-), 48.7 (C(1)), 52.6 (-C(O)CH(CH₃)NHC(O)-), 68.0 (C(1)CH₂-), 121.0 (C(6) and C(9)), 126.2 (C(3) and C(12)), 128.2 (C(4) and C(11)), 128.8 (C(5) and C(10)), 142.6 (C(7) and C(8)), 145.2 (C(2) and C(13)), 158.7 (C(1)CH₂CO₂NH-), 171.4, 176.3, 179.7 (HO₂CCH₂CH₂-, -CH₂NHC(O)CH₂- and -HNC(O)CH(CH₃)-); ν_{max} (nujol/cm⁻¹) 1560 (br, C=O (amide)), 1647 (br, C=O (amide)), 1694 (br, C=O (acid)), 2853 (s, C-H), 3295 (N-H); **m/z** (FAB) 504 (49%, [M + Na]⁺), 482 (29%, [M + H]⁺); **HRMS** found 482.2285, [M + H]⁺ (C₂₆H₃₂N₃O₆) requires 482.2291; **Anal.** (C₂₆H₃₁N₃O₆·H₂O) found C, 61.94; H, 6.36; N,

8.45%; requires C, 62.51; H, 6.66; N, 8.41%; $[\alpha]_D + 1.8^\circ$ (c 0.34, MeOH).

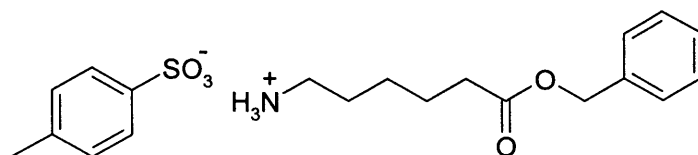
Synthesis of BocHis(Boc)-CA-OH Catalytic Unit 190

5-(2-*tert* Butoxycarbonylamino-2-carboxy ethyl) imidazole-1-carboxylic acid *tert* butyl ester (188)¹⁵⁸



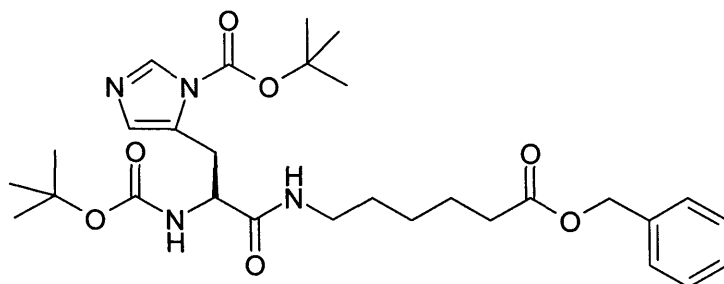
L-Histidine (0.30 g, 1.94 mmol) was dissolved in methanol (7.5 ml) and triethylamine (0.25 ml, 4.26 mmol) followed by di-*tert*-butyl dicarbonate (0.93 g, 1.76 mmol) were added and the reaction was stirred at room temperature for 23 h. The solvents were removed *in vacuo* and the resulting residue was partitioned between water (20 ml) and diethyl ether (30 ml). The layers were separated and the aqueous layer was then acidified to pH 4 with aqueous HCl (1 M) and subsequently extracted with ethyl acetate (3 x 20 ml). The combined ethyl acetate layers were dried over MgSO₄ and concentrated *in vacuo*, which provided a sticky white solid. The solid was dissolved in methanol/dichloromethane (1:1) and then precipitated by the addition of hexane. The desired product was isolated as a white solid (0.34 g, 50%). **m.p.** 109 °C; **¹H NMR** (300 MHz, CDCl₃) δ_H /ppm 1.41 (s, 9H, -C(CH₃)₃), 1.58 (s, 9H, -C(CH₃)₃), 3.16 (br m, 2H, -CH₂-), 4.48 (br m, 1H, -NHCHCO₂H), 5.44 (br s, 1H, -C(O)NH-), 7.14 (s, 1H, -C=CH), 8.13 (s, 1H, N=CHN-); **¹³C NMR** (75 MHz, CDCl₃) δ_C /ppm 27.8 and 28.4 (2 x -C(CH₃)₃), 29.7 (-CH₂-), 52.8 (-NHCHCO₂H), 79.6 and 86.4 (2 x -C(CH₃)₃), 115.6 (-C=CH-), 136.5 (-C=CH-), 137.0 (-N=CHN), 146.3 (Im-NC(O)O-), 155.2 (-NHC(O)O-), 173.0 (-CO₂H); ν_{\max} (DCM/cm⁻¹) 1366 (s, -C(CH₃)₃), 1707, 1763 (s, C=O), 2476 (w, C=N), 2970 (m, C-H), 3447 (w, N-H); **m/z** (Cl⁺) 356 (48%, [M + H]⁺).

6-Ammonium-hexanoic acid benzyl ester *p*-toluene sulfonate (185)¹⁵⁹



6-Aminocaproic acid (2.00 g, 15.0 mmol), benzyl alcohol (16 ml, 150 mmol) and *para*-toluene sulfonic acid (3.19 g, 17.0 mmol) were dissolved in toluene and heated at 120 °C (Dean-Stark conditions) for 5 h. After cooling, diethyl ether (70 ml) was added and the mixture cooled (*ca.* 4 °C), the resulting white solid was isolated by filtration. The filter cake was washed with diethyl ether and dried under vacuum to yield the desired product as a white solid (5.10 g, 81%). **m.p.** 110 °C; **R_f** = 0.41 (SiO₂; ethyl acetate/methanol; 4:1); **¹H NMR** (300 MHz, CDCl₃) $\delta_{\text{H/ppm}}$ 1.23 (m, 2H, H₃NCH₂CH₂CH₂-), 1.46 (m, 4H, -H₃NCH₂CH₂CH₂-), 2.19 (m, 2H, H₃NCH₂-), 2.30 (s, 3H, CH₃Ar-), 2.73 (s, 2H, -CH₂CO₂-), 5.07 (s, 2H, -CH₂Ar), 7.14 (d, 2H, *J* = 7.8, tosyl ArH), 7.33 (m, 5H, ArH), 7.66 (br s, 3H, -NH₃), 7.72 (d, *J* = 8.0, 2H, -tosyl ArH); **¹³C NMR** (75 MHz, CDCl₃) $\delta_{\text{C/ppm}}$ 21.3 (CH₃Ar), 24.2, 25.8 and 27.0 (H₃NCH₂CH₂CH₂CH₂-), 33.8 (H₃NCH₂-), 39.7 (-CH₂CO₂), 66.2 (-CO₂CH₂Ar), 125.9, 128.2, 128.6 and 129.1 (9 x ArC), 136.0, 140.9 and 141.1 (3 x quaternary ArC), 173.2 (-CO₂CH₂-); ν_{max} (nujol/cm⁻¹) 1621 (w, Ar), 1725 (s, C=O), 2855 (s, CH); **m/z** (FAB) 222 (67%, [M + H⁺ - [MeArSO₃]⁻], 244 (36%, [M + Na⁺ - MeArSO₃]⁻); **HRMS** found 244.1315, [M + Na⁺ - MeArSO₃]⁻ (C₁₃H₁₉NO₂Na) requires 244.1313.

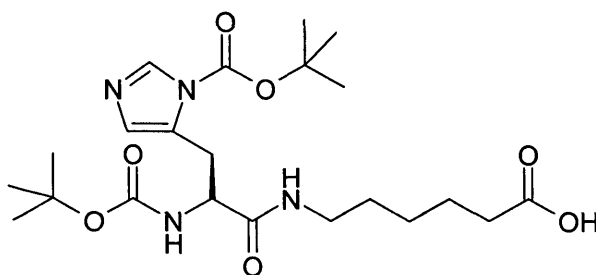
5-[2-(5-Benzoyloxycarbonyl-pentylcarbamoyl)-2-*tert*-butoxycarbonylamino-ethyl]-imidazole-1-carboxylic acid *tert*-butyl ester (189)



A solution of BocHis(Boc)OH **188** (9.50 g, 27.0 mmol) and anhydrous *N*-methyl morpholine (6.44 ml, 59.0 mmol) in anhydrous dichloromethane (150 ml) was cooled to $-15\text{ }^{\circ}\text{C}$ under nitrogen. Isobutyl chloroformate (4.07 ml, 31.0 mol) was added dropwise and the solution was stirred at $-15\text{ }^{\circ}\text{C}$ for 20 min.. 6-Ammonium-hexanoic acid benzyl ester *p*-toluene sulfonate **186** (11.0 g, 27.0 mmol) was added and the mixture was allowed to warm to room temperature and stirring was continued for 20 h. The solvent was removed in *vacuo* and the residue was partitioned between ethyl acetate (80 ml) and water (80 ml). The layers were separated and the organic layer was washed with aqueous KHSO_4 (10% v/v, 100 ml), brine (100 ml), aqueous NaHCO_3 (10% v/v, 100 ml), brine (100 ml), dried over MgSO_4 and solvents removed. Purification by flash chromatography (SiO_2 ; gradient; petroleum spirit/ethyl acetate (3:1) to petroleum spirit/ethyl acetate (1:3)) gave the product as a brown oil (2.97 g, 19%). $R_f = 0.27$ (SiO_2 ; ethyl acetate/petroleum spirit; 3:1); $^1\text{H NMR}$ (400 MHz, CDCl_3) δ_{H} /ppm 0.93 (m, 3H, $-\text{CH}_2\text{CH}(\text{H})\text{CH}_2\text{CO}_2-$), 1.38 (m, 10H, $-\text{C}(\text{CH}_3)_3$ and $-\text{CH}_2\text{CH}(\text{H})\text{CH}_2\text{CO}_2-$), 1.58 (m, 11H, $-\text{C}(\text{CH}_3)_3$ and $-\text{CH}_2(\text{CH}_2)_3\text{CO}_2-$), 2.32 (m, 2H, $-\text{CH}_2\text{CO}_2-$), 2.91 (m, 1H, $-\text{NHC}(\text{O})\text{CHCH}(\text{H})-$), 3.10 (m, 1H, $\text{NHC}(\text{O})\text{CHCH}(\text{H})-$), 3.15 (m, 2H, $-\text{CH}_2(\text{CH}_2)_4\text{CO}_2-$), 4.38 (br m, 1H, $-\text{NHC}(\text{O})\text{CH}-$), 5.09 (s, 2H, $-\text{CH}_2\text{Ar}$), 6.07 (br m, 1H, NHCO_2-), 6.69 (br m, 1H, $\text{NHC}(\text{O})\text{CH}-$), 7.29 (m, 6H, ArH and $-\text{CH}=\text{C}-$), 7.98 (s, 1H, $-\text{N}=\text{CH}-\text{N}-$); $^{13}\text{C NMR}$ (75 MHz, CDCl_3) δ_{C} /ppm 24.3 ($-\text{CH}_2\text{CH}_2\text{CH}_2\text{CO}_2-$), 26.0 ($-\text{CH}_2\text{CH}_2\text{CO}_2-$), 27.6 and 27.9 ($-\text{C}(\text{CH}_3)_3$), 28.9 ($-\text{CH}_2(\text{CH}_2)_3\text{CO}_2-$), 30.9, 33.8 ($-\text{CH}_2\text{CO}_2-$ and $-\text{NHC}(\text{O})\text{CHCH}_2-$), 38.9 ($-\text{C}(\text{O})\text{NCH}_2-$), 54.0 ($-\text{NHC}(\text{O})\text{CH}-$), 65.8 ($-\text{CH}_2\text{Ar}$), 79.2 and 85.2 (2 x $-\text{C}(\text{CH}_3)_3$), 114.5 ($-\text{CH}=\text{C}-$), 126.7, 128.1, 128.3 (ArC), 136.0 (quaternary

ArC), 136.5 (-CH=C-), 139.3 (-N=CHN-), 146.7 (Im-NC(O)O-), 155.5 (-NHCO₂C(CH₃)₃), 171.4 (-NHC(O)CH-), 173.0 (-CO₂CH₂Ar); **m/z** (CI⁺) 559 (23%, [M + H]⁺); **HRMS** found 559.31383, [M + H]⁺ (C₂₉H₄₃N₄O₇) requires 559.31316; [α]_D +16.3 ° (c 0.40, MeOH).

5-[2-*tert* Butoxycarbonylamino-2-(5-carboxy pentylcarbamoyl) ethyl] imidazole-1 carboxylic acid *tert*-butyl ester (190)

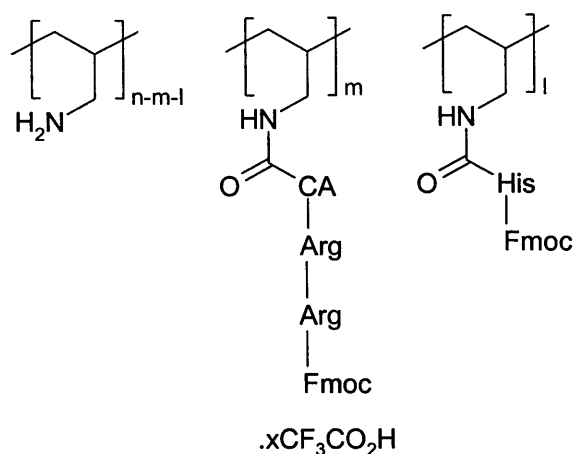


To a stirred solution of **189** (0.50 g, 0.87 mmol) in ethanol (10 ml) was added palladium on carbon (10%, 0.50 g) and 1, 4-cyclohexadiene (0.83 ml, 8.70 mmol) under nitrogen. The mixture was stirred at room temperature for 19 h. The mixture was filtered through a plug of Celite and the filter cake was washed with ethanol (3 x 10 ml). The filtrate was concentrated *in vacuo* and the crude product was triturated with dichloromethane/hexane which gave the product as a white solid (0.38 g, 90%). **m.p.** 72 °C; **R_f** = 0.10 (SiO₂; ethyl acetate/petroleum spirit; 1:1); **¹H NMR** (300 MHz, CDCl₃) δ _H/ppm 1.25 (m, 13H, -C(CH₃)₃ and -CH₂CH₂CH₂CO₂-), 1.48 (m, 11H, -C(CH₃)₃ and -CH₂(CH₂)₃CO₂-), 2.18 (m, 2H, -CH₂CO₂-), 2.71 (m, 1H, -NHC(O)CHCH(H)-), 2.78 (m, 1H, NHC(O)CHCH(H)-), 3.09 (m, 2H, -CH₂(CH₂)₄CO₂-), 4.33 (br m, 1H, -NHC(O)CH-), 5.83 (br m, 1H, NHCO₂-), 7.08 (m, 1H, NHC(O)CH-), 7.18 (m, 1H, -CH=C-), 7.94 (s, 1H, -N=CH-N-); **¹³C NMR** (75 MHz, CDCl₃) δ _C/ppm 22.5 (-CH₂CH₂CH₂CO₂-), 26.0 (-CH₂CH₂CO₂-), 27.8, 28.2 (-C(CH₃)₃), 28.8 (-CH₂(CH₂)₃CO₂-), 31.2 (-NHC(O)CHCH₂-), 34.0 (-CH₂CO₂-), 39.0 (-CH₂(CH₂)₄CO₂-), 54.3 (-NHC(O)CH-), 79.7, 85.7 (2 x -C(CH₃)₃), 114.8 (-CH=C-), 136.6 (-CH=C-), 139.1 (-N=CH-N-), 146.6 (Im-NC(O)O-), 155.6 (-NHCO₂C(CH₃)₃), 171.3 (-NHC(O)CH-),

177.0 ($-\underline{\text{CO}}_2\text{H}$); ν_{max} (DCM/ cm^{-1}) 1390 (s, C(CH₃)₃), 1664 (s, C=O (amide)), 1710 (s, C=O (acid and Boc)), 2924 (s, C-H), 3437 (s, N-H); m/z (Cl^+) 469 (8%, $[\text{M} + \text{H}]^+$), 369 (75%, $[\text{M} + \text{H} - \text{Boc}]^+$); **HRMS** found 469.26474, $[\text{M} + \text{H}]^+$ ($\text{C}_{22}\text{H}_{37}\text{N}_4\text{O}_7$) requires 469.26621; **Anal.** ($\text{C}_{19}\text{H}_{26}\text{N}_2\text{O}_5 \cdot \frac{1}{2}\text{H}_2\text{O}$) found C, 55.47; H, 7.74; N, 11.57%; requires C, 55.33; H, 7.81; N, 11.73%; $[\alpha]_{\text{D}} +10.4^\circ$ (c 0.28, MeOH).

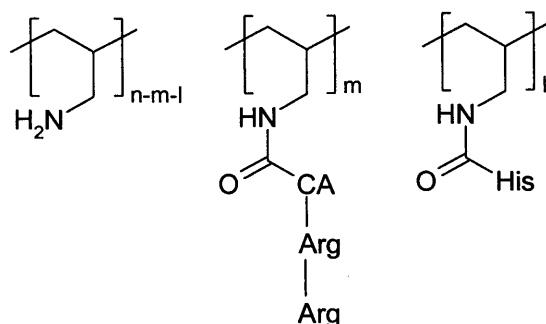
6.90 – 7.76 (br, ArH of Fmoc, Trityl and histidine groups).

Polymer 360



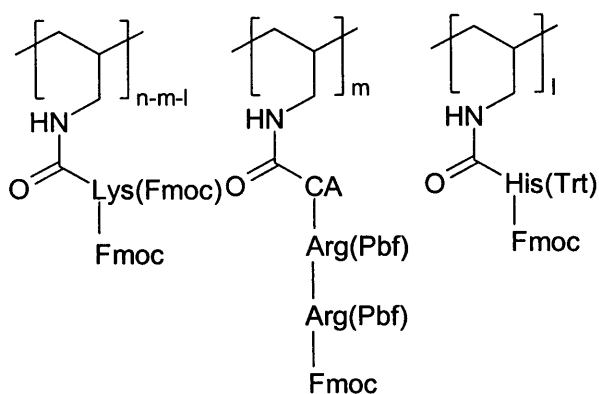
A suspension of polymer (**167**) (252 mg) in trifluoroacetic acid/ triisopropylsilane/water (95:2.5:2.5, 20 ml) was sonicated at room temperature for 3 h. Water (5 ml) was added to the mixture which formed a cream coloured gum, which was isolated by filtration. The gum was washed with dichloromethane (3 x 30 ml), then dried under vacuum to yield the product as a cream coloured gum (233 mg). ¹H NMR (500 MHz, CD₃OD) δ_H/ppm 1.17 – 1.96 (br, CH₂ of polyallylamine and amino acids), 2.45, 3.15 and 3.36 (br, CH of polyallylamine, -CH₂N- of amino acids and polyallylamine), 4.06 – 4.32 (br, αH of amino acids and -NHCO₂CH₂- of Fmoc group), 7.25 – 7.72 (br, H of Fmoc groups and histidine).

Polymer 168



A suspension of polymer **360** (205 mg) in piperidine/anhydrous dimethylformamide (15 ml, 2:8) was sonicated at room temperature for 3.5 h. The mixture was filtered and the resulting solid washed with dimethylformamide (5 x 20 ml), dichloromethane (5 x 20 ml) and dried under vacuum. The desired product was isolated as a white solid (154 mg). ^1H NMR (300 MHz, D_2O) δ_{H} /ppm 1.25 – 1.83 (br, CH_2 of polyallylamine and amino acids), 2.27 – 3.39 (br, CH of polyallylamine, $-\text{CH}_2\text{N}-$ of amino acids and polyallylamine, $-\text{CH}_2-$ of histidine), 3.68 – 4.30 (br, αH of amino acids), 6.96 and 7.70 (br, $-\text{CH}=\text{C}-$ and $\text{N}=\text{CH}-\text{N}$ of histidine).

Polymer 157

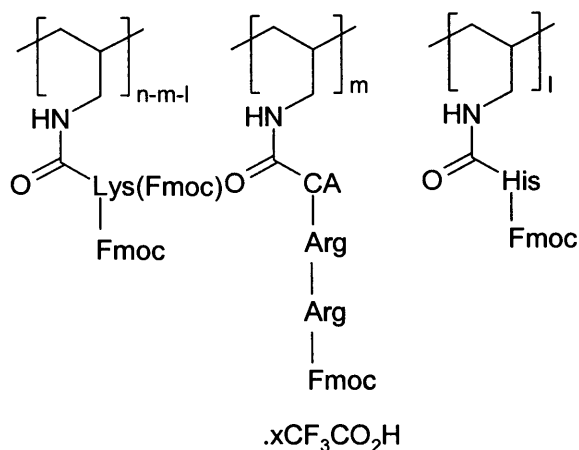


Polyallylamine hydrochloride (50.0 mg, 0.54 mmol) was treated with potassium hydroxide (35.0 mg, 0.62 mmol) in methanol (10 ml) at room temperature for 16 h. The solvent was removed under reduced pressure and ethanol (15 ml) was added to the residue. The resulting white precipitate was removed by filtration and the filtrate was

concentrated *in vacuo* to leave approximately 10 ml of solvent.

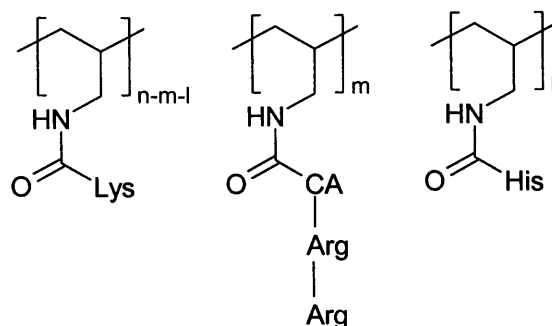
FmocArg(Pbf)Arg(Pbf)-CA-OH (**131**) (180 mg, 0.15 mmol), FmocHis(Trt)OH (100 mg, 0.15 mmol), *N,N'*-diisopropylcarbodiimide (0.05 ml, 0.32 mmol) and *N*-hydroxysuccinimide (50.0 mg, 0.43 mmol) were dissolved in chloroform (20 ml) and stirred at room temperature for 3 h. This solution was added to the solution of polyallylamine in ethanol (above) and the resulting mixture was then stirred at room temperature for 2 h. Concurrently, FmocLys(Fmoc)-OH (0.16 g, 0.27 mmol), *N,N'*-diisopropylcarbodiimide (0.05 g, 0.32 mmol) and *N*-hydroxysuccinimide (0.04 g, 0.38 mmol) were dissolved in chloroform (20 ml) and stirred at room temperature for 2 h. This solution was then added to the solution containing polyallylamine and stirring was continued for 24 h. The reaction mixture was concentrated to approximately 20 ml and the crude product was precipitated by the addition of methanol. The precipitate was purified by trituration from chloroform/methanol and the resulting solid was dried under vacuum. The desired polymer was isolated as a white gum. (100 mg). ¹H NMR (300 MHz, CDCl₃) δ_H/ppm 1.23 – 1.50 (br, CH₂ of polyallylamine and amino acids), 2.00 (br, ArCH₃ of Pbf), 2.52 (br, CH of polyallylamine, -CH₂N- of amino acids and polyallylamine), 3.69 – 4.40 (br, αH of amino acids and -NHCO₂CH₂- of Fmoc group), 7.12 – 7.75 (br, ArH of Fmoc, Trityl and histidine groups).

Polymer 162



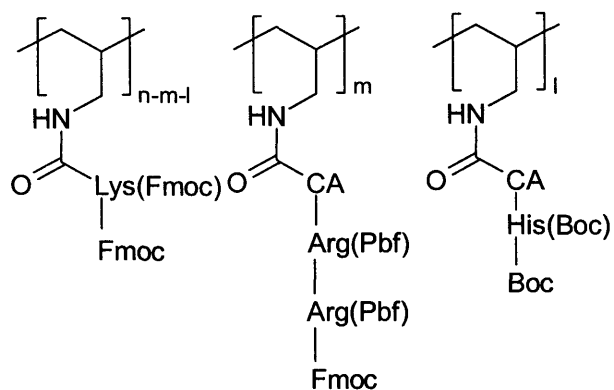
A suspension of polymer (157) (91.0 mg) in trifluoroacetic acid/triisopropylsilane/water (95:2.5:2.5, 10 ml) was sonicated at room temperature for 3 h. Water (5 ml) was added to the mixture which formed a white gum, which was isolated by filtration. The gum was washed with water (2 x 30 ml), trifluoroacetic acid (40 ml) and water (40 ml), then dried under vacuum to yield the product as a yellow gum (87 mg). ¹H NMR (300 MHz, CD₃OD) δ_H/ppm 1.16 – 1.79 (br, CH₂ of polyallylamine and amino acids), 2.52 and 3.12 (br, CH of polyallylamine, -CH₂N- of amino acids and polyallylamine), 4.09 – 4.30 (br, αH of amino acids and -NHCO₂CH₂- of Fmoc group), 7.23 – 7.67 (br, H of Fmoc groups and histidine).

Polymer 132



A suspension of polymer **162** (54.0 mg) in piperidine/anhydrous dimethylformamide (15 ml, 2:8) was sonicated at room temperature for 3.5 h. The mixture was filtered and the resulting solid washed with dimethylformamide (5 x 20 ml), dichloromethane (5 x 20 ml) and dried under vacuum. The desired product was isolated as a white solid (31.0 mg). ^1H NMR (300 MHz, D_2O) δ_{H} /ppm 1.37 – 2.16 (br, CH_2 of polyallylamine and amino acids), 2.31 – 3.52 (br, CH of polyallylamine, $-\text{CH}_2\text{N}-$ of amino acids and polyallylamine, $-\text{CH}_2-$ of histidine), 3.89 – 4.34 (br, αH of amino acids), 6.97 and 7.74 (br, $-\text{CH}=\text{C}-$ and $\text{N}=\text{CH}-\text{N}$ of histidine); ν_{max} (solid state/ cm^{-1}) 1559 (s, $\text{C}=\text{O}$ (amide), 2175 (m, $\text{C}=\text{N}$), 3228 (w, $\text{N}-\text{H}$).

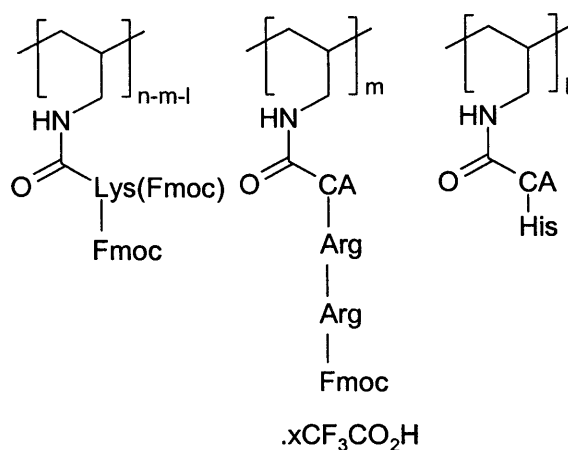
Polymer 192



Polyallylamine hydrochloride (100 mg, 1.08 mmol) was treated with potassium hydroxide (70.0 mg, 1.24 mmol) in methanol (15 ml) at room temperature for 16 h. The solvent was removed under reduced pressure and ethanol (25 ml) was added to the residue. The resulting white precipitate was removed by filtration and the filtrate was concentrated *in vacuo* to leave approximately 10 ml of solvent.

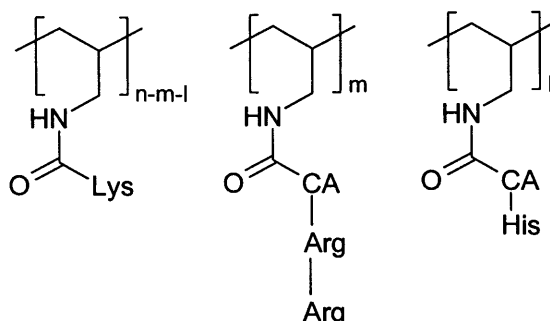
FmocArg(Pbf)Arg(Pbf)-CA-OH **131** (350 mg, 0.30 mmol), BocHis(Boc)-CA-OH **190** (150 mg, 0.31 mmol), *N,N'*-diisopropylcarbodiimide (0.12 ml, 0.74 mmol) and *N*-hydroxysuccinimide (100 mg, 0.86 mmol) were dissolved in chloroform (20 ml) and stirred at room temperature for 4 h. This solution was added to the solution of polyallylamine in ethanol (above) and the resulting mixture was stirred at room temperature for 2 h. Concurrently, FmocLys(Fmoc)-OH (320 mg, 0.54 mmol), *N,N'*-diisopropylcarbodiimide (0.10 ml, 0.64 mmol) and *N*-hydroxysuccinimide (80.0 mg, 0.70 mmol) were dissolved in chloroform (10 ml) and stirred at room temperature for 5 h. This solution was then added to the solution containing polyallylamine and stirring was continued for 22 h. The solvent was removed *in vacuo* and the residue was dissolved in chloroform (10 ml) with the aid of sonication. Methanol (*ca.* 30 ml) was added, until a white precipitate formed. The precipitate was isolated and then washed with methanol (3 x 20 ml) and dried under vacuum. The desired polymer was isolated as a white solid (50.0 mg) ν_{\max} (solid state/cm⁻¹) 1062 (s, C-O (Pbf groups)), 1331 (m, SO₂ (Pbf groups)), 1496 (s, Ar (Pbf groups)), 1675 (m, C=O (amides, Boc and Fmoc groups)), 2891 (m, C-H), 3043 (m, [-NH₃]⁺), 3347 (N-H (amides)), 3492 (N-H (amines)).

Polymer 361



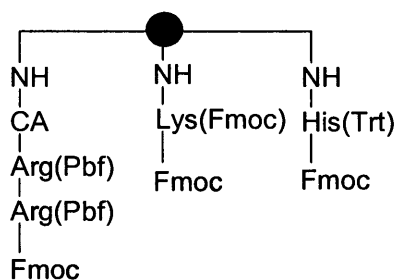
A suspension of polymer **192** (50 mg) in trifluoroacetic acid/triisopropylsilane/water (95:2.5:2.5, 10 ml) was sonicated at room temperature for 4 h. The polymer was isolated by filtration and washed with chloroform (2 x 50 ml), then dried under vacuum to yield a waxy solid (55 mg). ¹³C NMR (75 MHz, solid state) δ_c/ppm 17.9 – 68.7 (br, CH₂ of polyallylamine and amino acids), 115.4, 118.6 and 128.2 (br, ArC of imidazole and Fmoc groups), 141.8 (br, ArC of Fmoc groups) 158.4 (br, -NHC(NH)NH-), 162.3 (-NHC(O)₂- of Fmoc groups), 175.0 (br, -C(O)NH-).

Polymer 181



A suspension of polymer **361** (79.0 mg) in piperidine/anhydrous dimethylformamide (2:8, 15 ml) was shaken at room temperature for 4 h. The polymer was filtered and washed sequentially with dimethylformamide (3 x 30 ml), dichloromethane (3 x 30 ml), dimethylformamide (2 x 10 ml) and dichloromethane (3 x 30 ml). The polymer was dried under vacuum to yield the desired product as a brown solid (52.0 mg). ^{13}C NMR (75 MHz, solid state) δ_c /ppm 15.0 – 55.6 (br, CH_2 of polyallylamine and CH and CH_2 of amino acids), 109.8, 127.4, 137.1 (br, ArC of imidazole), 158.5 and 163.9 (br, $-\text{NHC}(\text{NH})\text{NH}-$), 175.6 (br, $-\text{C}(\text{O})\text{NH}-$).

Resin 195



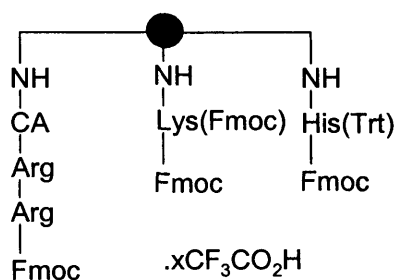
Tentagel resin (3.00 g, 0.40 mmol/g) was swelled in dimethylformamide for 30 min. and then filtered.

HOBt (0.10 g, 0.72 mmol) was added to a solution of tripeptide **131** (0.42 g, 0.36 mmol), FmocHis(Trt)OH (0.22 g, 0.36 mmol) and diisopropylcarbodiimide (0.16 ml,

1.00 mmol) in dimethylformamide (20 ml). The solution was stirred for 10 min. and then added to tentagel resin (above) and subsequently shaken for 3 h.

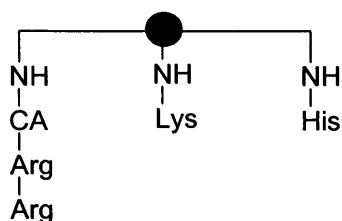
To a solution of FmocLys(Fmoc)OH (0.35 g, 0.60 mmol) and diisopropylcarbodiimide (0.13 ml, 0.84 mmol) in dimethylformamide (20 ml), HOBt (81.0 mg, 0.60 mmol) was added. The solution was stirred for 10 min. and then added to the above solution of resin and the mixture shaken for further 24 h. The resin was filtered and washed with dimethylformamide (200 ml), dichloromethane (200 ml), dimethylformamide (100 ml) and dichloromethane (100 ml) and dried under vacuum to yield the desired product (3.65 g).

Resin 362



A solution of trifluoroacetic acid/triisopropylsilane/water (95:2.5:2.5, 50 ml) was added to the resin **195** (3.59 g) and the mixture shaken at room temperature for 6 h. The resin was then filtered and washed with dichloromethane (4 x 50 ml) and dried under vacuum to give **362** (5.73 g).

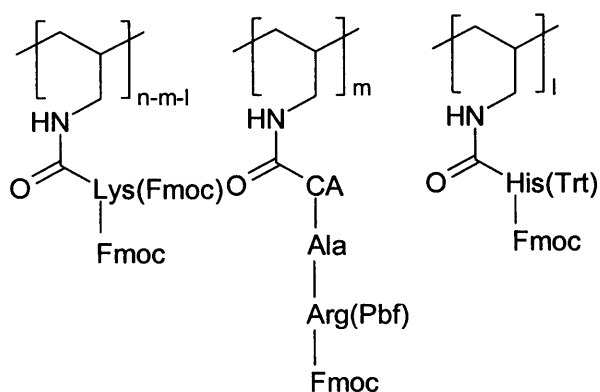
Resin 196



A solution of piperidine/dimethylformamide (2:8, 30 ml) was added to resin **362** (5.69 g) and the mixture shaken at room temperature for 6 h. The resin was filtered and washed sequentially with dimethylformamide (200 ml), dichloromethane (200 ml), dimethylformamide (100 ml) and dichloromethane (100 ml). The resin was dried under vacuum to give **196** (2.79 g).

Synthesis of Artificial Esterases containing Ala-Arg Binding Unit

Polymer 159

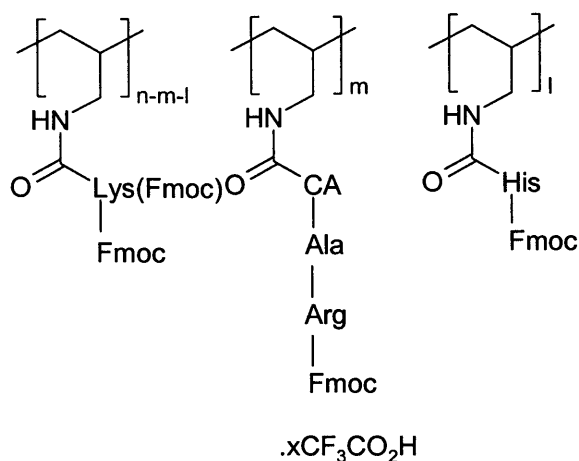


Polyallylamine hydrochloride (100 mg, 1.08 mmol) was treated with potassium hydroxide (70.0 mg, 1.24 mmol) in methanol (15 ml), at room temperature for 16 h. The mixture was concentrated under reduced pressure, and ethanol (25 ml) was added to the

residue. The resulting white precipitate was removed by filtration, and the filtrate was then concentrated *in vacuo*, to leave approximately 10 ml of solvent.

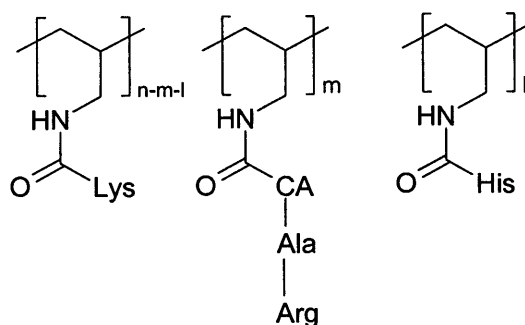
FmocArg(Pbf)Ala-CA-OH **148** (270 mg, 0.32 mmol), FmocHis(Trt)OH (200 mg, 0.32 mmol), *N,N'*-diisopropylcarbodiimide (0.23 ml, 1.45 mmol) and *N*-hydroxysuccinimide (100 mg, 0.88 mmol) were dissolved in chloroform (40 ml), and stirred at room temperature for 4 h. This solution was added to the solution of polyallylamine in ethanol (above), and the resulting mixture stirred at room temperature for 2 h. Concurrently, FmocLys(Fmoc)-OH (320 mg, 0.54 mmol), *N,N'*-diisopropylcarbodiimide (110 mg, 0.70 mmol) and *N*-hydroxysuccinimide (90.0 mg, 0.75 mmol) were dissolved in chloroform (35 ml), and stirred at room temperature for 2 h. This solution was then added to the solution containing polyallylamine (above). The resulting mixture was stirred for 24 h. The reaction mixture was concentrated to a volume of 20 ml. The crude product was precipitated by the addition of methanol. The resulting solid was washed with chloroform (50 ml) and methanol (50 ml), and then dried under vacuum to afford a yellow gum (270 mg). ¹H NMR (400 MHz, CDCl₃) δ_{H} /ppm 1.27 – 1.70 (br, CH₂ of polyallylamine and amino acids), 2.00 (br, ArCH₃ of Pbf), 2.54 (br, CH of polyallylamine, -CH₂N- of amino acids and polyallylamine), 3.83 – 4.60 (br, α H of amino acids), 6.99 – 7.63 (br, ArH of Fmoc, Trityl groups and histidine).

Polymer 164



A suspension of polymer **159** (270 mg) in trifluoroacetic acid/triisopropylsilane/water (95:2.5:2.5, 10 ml) was sonicated at room temperature for 3 h. Water (5 ml) was added to the mixture to form a yellow gum. The gum was isolated by filtration and washed with water (2 x 30 ml), trifluoroacetic acid (1 x 40 ml), water (1 x 40 ml) and dried under vacuum to yield the desired product as a yellow gum (180 mg). ¹H NMR (400 MHz, CDCl₃) δ_H/ppm 1.19 – 1.78 (br, CH₂ of polyallylamine and amino acids), 2.92 (br, CH of polyallylamine, -CH₂N- of amino acids and polyallylamine), 4.08 and 4.29 (br, αH of amino acids), 7.54 – 7.68 (br, ArH of Fmoc group and histidine).

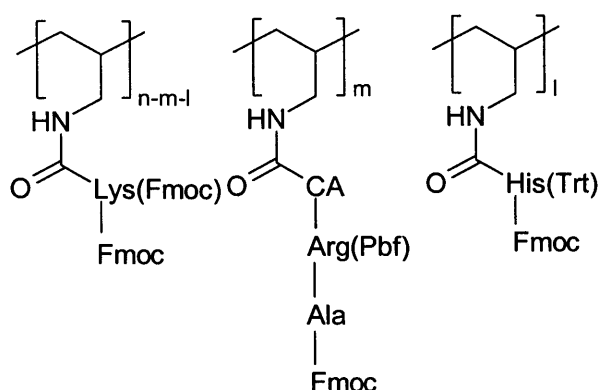
Polymer 137



A suspension of polymer **164** (180 mg) in piperidine/anhydrous DMF solution (2:8, 15 ml) was sonicated at room temperature for 3 h, under nitrogen. The mixture was filtered

and the resulting solid washed with dimethylformamide (3 x 30 ml), water (2 x 40 ml) and dichloromethane (2 x 40 ml). The polymer was dried under vacuum to yield an off white gum (100 mg). ν_{\max} (solid state/cm⁻¹) 1670 (s, C=O (amide)), 2938 (m, C-H), 3426 (m, N-H).

Polymer 158

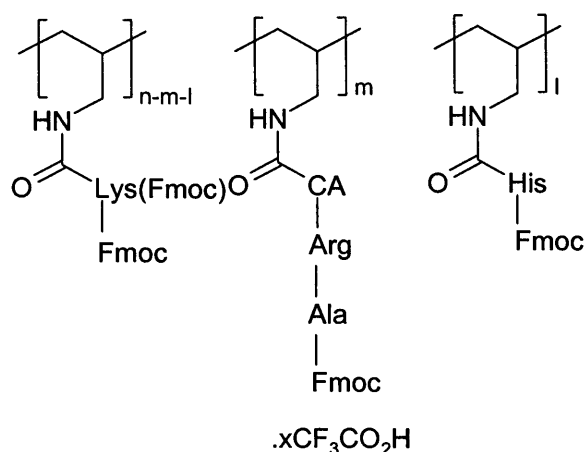


Polyallylamine hydrochloride (100 mg, 1.08 mmol) was treated with potassium hydroxide (70.0 mg, 1.24 mmol) in methanol (15 ml) at room temperature for 16 h. The solvent was removed under reduced pressure and ethanol (25 ml) was added to the residue. The resulting white precipitate was removed by filtration and the filtrate was concentrated *in vacuo* to leave approximately 10 ml of solvent.

FmocAla-Arg(Pbf)-CA-OH **147** (270 mg, 0.32 mmol), FmocHis(Trt)OH (200 mg, 0.32 mmol), *N,N'*-diisopropylcarbodiimide (0.23 ml, 1.45 mmol) and *N*-hydroxysuccinimide (100 mg, 0.88 mmol) were dissolved in chloroform (30 ml) and stirred at room temperature for 4 h. This solution was added to the solution of polyallylamine in ethanol (above) and the resulting mixture stirred at room temperature for 2 h. Concurrently, FmocLys(Fmoc)-OH (320 mg, 0.54 mmol), *N,N'*-diisopropylcarbodiimide (110 mg, 0.70 mmol) and *N*-hydroxysuccinimide (90 mg, 0.75 mmol) were dissolved in chloroform (35 ml) and stirred at room temperature for 2 h. The resulting mixture was then added to the solution containing polyallylamine and stirring was continued for 24 h. The reaction mixture was concentrated to approximately 20 ml and the crude product

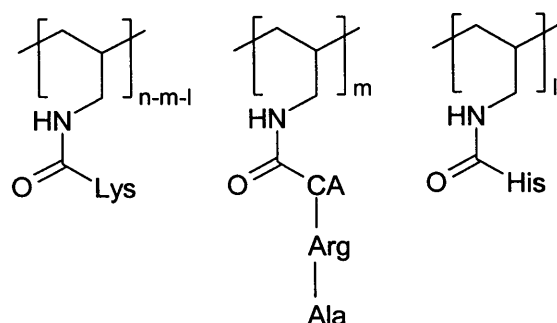
was precipitated by the addition of methanol. The precipitate was purified by trituration from chloroform/methanol and the resulting solid was dried under vacuum. The desired polymer was isolated as a beige solid (276 mg). $^1\text{H NMR}$ (300 MHz, CDCl_3) $\delta_{\text{H}}/\text{ppm}$ 1.12 – 1.50 (br, CH_2 of polyallylamine and amino acids), 2.00 (br, ArCH_3 of Pbf group), 2.54 (br, CH of polyallylamine and $-\text{CH}_2\text{N}-$ of amino acids and polyallylamine), 3.86 – 4.60 (br, αH of amino acids and $-\text{NHCO}_2\text{CH}_2-$ of Fmoc group), 7.25 – 7.57 (br, ArH of Fmoc and Trityl groups and histidine).

Polymer 163



A suspension of polymer **158** (269 mg) in trifluoroacetic acid/triisopropylsilane/water (95:2.5:2.5, 10 ml) was sonicated at room temperature for 6 h. Water (5 ml) was added to the mixture which formed a yellow gum. The gum was purified by trituration from a mixture of chloroform and water. The resulting solid was then washed with chloroform (2 x 50 ml) and then dried under vacuum. The desired polymer was isolated as a cream coloured gum (160 mg). $^1\text{H NMR}$ (300 MHz, CD_3OD) $\delta_{\text{H}}/\text{ppm}$ 1.26 – 1.71 (br, CH_2 of polyallylamine and amino acids), 3.11 (br, CH of polyallylamine, $-\text{CH}_2\text{N}-$ of amino acids and polyallylamine), 4.07 and 4.30 (br, αH of amino acids and $-\text{NHCO}_2\text{CH}_2-$ of Fmoc group), 7.16 – 7.70 (br, ArH of Fmoc groups and histidine).

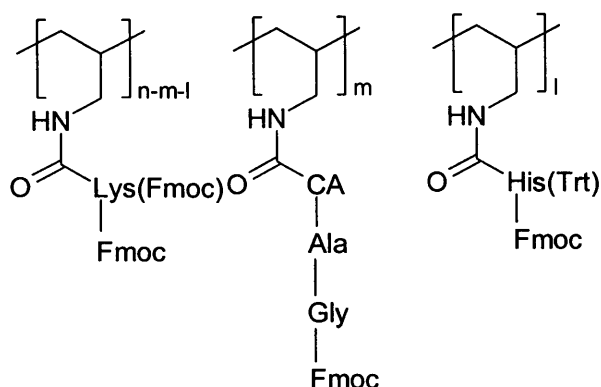
Polymer 136



A suspension of polymer **163** (149 mg) in piperidine/anhydrous dimethylformamide (1:1, 20 ml) was shaken at room temperature for 4.5 h. A precipitate was formed by the addition of petroleum spirit/ethyl acetate (1:1), which was filtered and dried under vacuum. The desired product was isolated as a white solid (113 mg). ν_{\max} (solid state/cm⁻¹) 1558 (m, C=O), 1709 (C=O), 2136 (w, C=N), 2920 (m, C-H), 3384 (s, N-H).

Synthesis of Artificial Esterases containing Ala-Gly Binding Unit

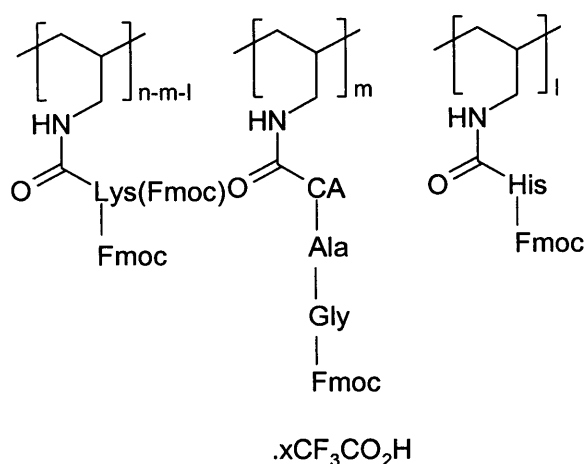
Polymer 160



Polyallylamine hydrochloride (100 mg, 1.08 mmol) was treated with potassium hydroxide (70.0 mg, 1.24 mmol) in methanol (15 ml) at room temperature for 16 h. The solvent was removed under reduced pressure and ethanol (25 ml) was added to the residue. The resulting white precipitate was removed by filtration and the filtrate was then concentrated *in vacuo* to leave approximately 10 ml of solvent.

FmocGly-Ala-CA-OH **149** (150 mg, 0.32 mmol), FmocHis(Trt)OH (190 mg, 0.31 mmol), *N,N'*-diisopropylcarbodiimide (0.23 ml, 1.45 mmol) and *N*-hydroxysuccinimide (190 mg, 1.69 mmol) were all dissolved in chloroform (40 ml) and stirred at room temperature for 4 h. This solution was added to the solution of polyallylamine in ethanol (above) and the resulting mixture was then stirred at room temperature for 2 h. Concurrently, FmocLys(Fmoc)-OH (320 mg, 0.54 mmol), *N,N'*-diisopropylcarbodiimide (110 mg, 0.70 mmol) and *N*-hydroxysuccinimide (90.0 mg, 0.81 mmol) were dissolved in chloroform (35 ml) and stirred at room temperature for 2 h. This solution was then added to the solution containing polyallylamine and stirring was continued for 24 h. The reaction mixture was concentrated to a volume of 20 mL and the crude product was precipitated by the addition of methanol. The precipitate was purified by trituration from chloroform/methanol and the resulting solid was dried under vacuum. The desired polymer was isolated as a white solid (123 mg). ¹H NMR (300 MHz, CDCl₃) δ_H/ppm 1.10 – 1.50 (br, CH₂ of polyallylamine and amino acids), 2.51 - 3.10 (br, CH of polyallylamine, -CH₂N- of amino acids and polyallylamine), 3.41 - 4.41 (br, αH of amino acids and -NHCO₂CH₂- of Fmoc group), 7.09 – 7.70 (br, ArH of Fmoc and Trityl groups and histidine);

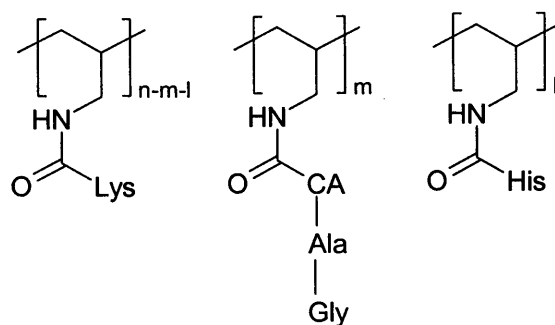
Polymer 165



A suspension of polymer **160** (119 mg) in trifluoroacetic acid/triisopropylsilane/water (95:2.5:2.5, 10 ml) was sonicated at room temperature for 3 h. Water (5 ml) was added

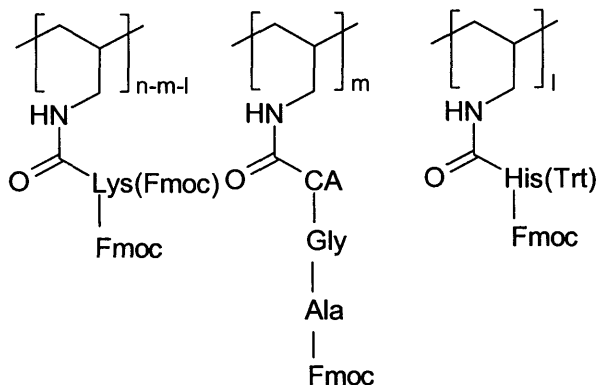
to the mixture which formed a white precipitate, which was isolated by filtration and washed with water (2 x 30 ml). The resulting crude solid was then triturated from a mixture of chloroform and water, which afforded a white gum. The gum was then washed with chloroform (5 x 30 ml) and dried under vacuum, which gave the product as a white gum (102 mg). ^1H NMR (300 MHz, CD_3OD) $\delta_{\text{H}}/\text{ppm}$ 1.13 – 1.42 (br, CH_2 of polyallylamine and amino acids), 2.42 - 3.06 (br, CH of polyallylamine, $-\text{CH}_2\text{N}-$ of amino acids and polyallylamine), 3.77 - 4.21 (br, αH of amino acids and $-\text{NHCO}_2\text{CH}_2$ of Fmoc group), 7.23 – 7.65 (br, ArH of Fmoc groups and histidine).

Polymer 138



A suspension of polymer **165** (95.0 mg) in piperidine/anhydrous dimethylformamide solution (2:8, 15 ml) was sonicated at room temperature for 3 h under nitrogen. Water was then added until a precipitate formed, which was isolated by filtration. The resulting solid was washed with dimethylformamide (5 x 30 ml), dichloromethane (5 x 30ml) and dried under vacuum to yield a beige solid (50.0 mg). ^{13}C NMR (75 MHz, solid state) $\delta_{\text{C}}/\text{ppm}$ 36.6 (br, CH and CH_2 of polyallylamine and amino acids), 125.2 (br, carbons of imidazole), 160.5, 174.2 (br, carbons of amides); ν_{max} (solid state/ cm^{-1}) 1543 (s, $-\text{C}(\text{O})\text{NH}$), 2135 (w, $\text{C}=\text{N}$), 2921 (m, CH), 3214 (m, $\text{C}(\text{O})\text{NH}$), 3348 (m, NH).

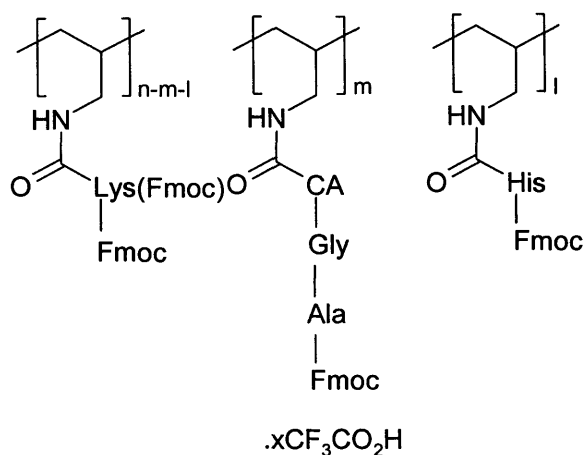
Polymer 161



Polyallylamine hydrochloride (100 mg, 1.08 mmol) was treated with potassium hydroxide (70.0 mg, 1.24 mmol) in methanol (15 ml) at room temperature for 16 h. The solvent was removed under reduced pressure and ethanol (25 ml) was added to the residue. The resulting white precipitate was removed by filtration and the filtrate was concentrated *in vacuo* to leave approximately 10 ml of solvent.

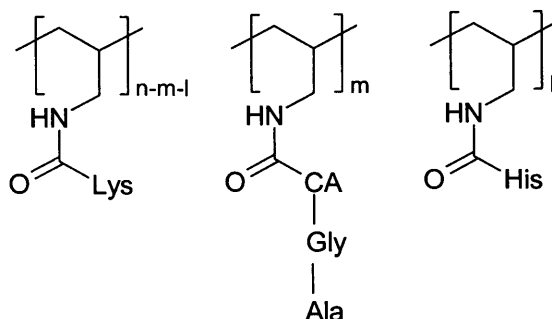
FmocAla-Gly-CA-OH **150** (150 mg, 0.31 mmol), FmocHis(Trt)OH (190 mg, 0.31 mmol), *N,N'*-diisopropylcarbodiimide (0.23 ml, 1.45 mmol) and *N*-hydroxysuccinimide (190 mg, 1.69 mmol) were dissolved in chloroform (25 ml) and stirred at room temperature for 4 h. This solution was added to the solution of polyallylamine in ethanol (above) and the resulting mixture stirred at room temperature for 2 h. Concurrently, FmocLys(Fmoc)-OH (320 mg, 0.54 mmol), *N,N'*-diisopropylcarbodiimide (110 mg, 0.70 mmol) and *N*-hydroxysuccinimide (90.0 mg, 0.80 mmol) were dissolved in chloroform (25 ml) and stirred at room temperature for 2 h. This solution was then added to the solution containing polyallylamine and stirring was continued for 24 h. The reaction mixture was concentrated to approximately 20 ml and the crude product was precipitated by the addition of methanol. The precipitate was purified by trituration from chloroform/methanol and the resulting solid was dried under vacuum. The desired polymer was isolated as a white gum (119 mg). ¹H NMR (400 MHz, CDCl₃) δ_H/ppm 1.10 – 1.52 (br, CH₂ of polyallylamine and amino acids), 2.51, 3.05 and 3.19 (br, CH of polyallylamine, -CH₂N- of amino acids and polyallylamine), 3.43, 3.81, 4.14 and 4.34 (br, αH of amino acids), 7.10 – 7.55 (br, ArH of Fmoc and Trityl groups and histidine);

Polymer 166



A suspension of polymer **161** (113 mg) in trifluoroacetic acid/triisopropylsilane/water (95:2.5:2.5, 10 ml) was sonicated at room temperature for 3 h. Water (5 ml) was added to the mixture which formed a yellow gum. The gum was isolated by filtration and then washed with water (2 x 30 ml). The resulting crude solid was then triturated from a mixture of chloroform and water and then washed with chloroform (5 x 30 ml). The desired polymer was isolated as a yellow gum (105 mg). ¹H NMR (500 MHz, CD₃OD) δ_H/ppm 1.05 – 1.31 (br, CH₂ of polyallylamine and amino acids), 2.43 and 3.09 (br, CH of polyallylamine, -CH₂N- of amino acids and polyallylamine), 3.56, 3.77, 4.04 and 4.29 (br, αH of amino acids), 7.08 – 7.68 (br, ArH of Fmoc groups and histidine).

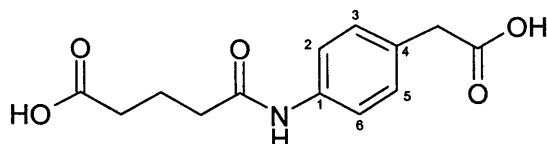
Polymer 139



A suspension of polymer **166** (99.0 mg) in piperidine/anhydrous dimethylformamide (2:8, 20 ml) was sonicated at room temperature for 7 h. The volatiles were removed under reduced pressure and the residue was washed sequentially with dimethylformamide (50 ml), water (50 ml), dichloromethane (50 ml), chloroform (50 ml), methanol (50 ml) and chloroform (50 ml). The resulting solid was dried under vacuum, which gave the desired product as a beige solid (62.0 mg). **¹H NMR** (500 MHz, CD₃OD) δ_{H} /ppm 1.33 – 1.69 (br, CH₂ of polyallylamine and amino acids), 2.49 – 3.17 (br, CH of polyallylamine, -CH₂N- of amino acids and polyallylamine), 3.30 – 4.11 (br, α H of amino acids), 6.95 – 7.70 (br, ArH of histidine); ν_{max} (solid state/cm⁻¹) 1556 (w, C=O (amide)), 2165 (w, C=N), 2925 (m, C-H), 3278 (w, N-H).

4.2.4 Synthesis of Acid Product For Use as a Standard in HPLC

4-(Ethanoic Acid-Phenylcarbamoyl)-Butyric Acid (129)⁹⁰



4-Aminophenylacetic acid (1.20 g, 7.95 mmol) was suspended in DCM (60 ml). Glutaric anhydride (1.09 g, 9.54 mmol) and triethylamine (2.43 ml, 17.5 mmol) were added and the mixture was stirred at reflux for 18 h. The mixture was then cooled and diluted with water (100 ml) and the organic layer was separated. The pH of the aqueous layer was adjusted to 1, using aq. HCl (2 M), and then extracted with ethyl acetate (2 x 120 ml). The organic layers were combined and dried over MgSO₄ and then concentrated *in vacuo*. The titled product was isolated as a cream solid (1.39 g, 66%). **m.p.** 150 °C (lit. 168 - 169 °C⁹⁰); **¹H NMR** (300 MHz, CD₃OD) δ_{H} /ppm 1.96 (m, 2H, CH₂CH₂CH₂), 2.38 (m, 4H, CH₂CH₂CH₂), 3.55 (s, 2H, ArCH₂COOH), 7.20 (d, *J* = 8.6, 2H, C(3)H, C(5)H), 7.48 (d, *J* = 8.6, 2H, C(2)H, C(6)H); **¹³C NMR** (75 MHz, CD₃OD) δ_{C} /ppm 22.1 (HO₂CCH₂CH₂), 34.1 (HO₂CCH₂CH₂CH₂-), 36.9 (HO₂CCH₂-), 41.3 (ArCH₂CO₂-), 121.3 (C(3) and C(5)), 130.8 (C(2) and C(6)), 131.8 (C(4)), 138.7 (C(1)), , 173.7 (ArNHC(O)-), 175.6, 176.8 (ArCH₂CO₂- and HO₂C-); ν_{max} (nujol/cm⁻¹) 1593 (m, Ar), 1695 (s, C=O), 2854 (s, C-H), 3307 (m, N-H) ; **m/z** (FAB) 288 (23%, [M + Na]⁺); **HRMS** found 288.0848, [M + Na]⁺ (C₁₃H₁₅NO₅Na) requires 288.0848;

4.2.5 Calibration of HPLC by the External Standard Method¹⁶⁰

The compounds used as standards were synthesised as described previously.

HPLC conditions: Reverse phase C18 column, elution of acetonitrile/water (0.05 % TFA). Solvent gradient 100% water to 95:5 acetonitrile/water. Flow rate 1ml/min, UV detection at 254nm.

Calibration of Acid Product 129

Different concentrations of acid 129 were prepared in phosphate buffer (Table 4.2.1). The area of peak at $R_t = 7.59$ was measured.

Concentration of acid 129 (mM)	Area of acid peak
0.2	1306
0.4	2165
0.6	2791
0.8	3714
1.0	4338

Table 4.2.1

A plot of the area of the peak against the concentration was made and linear regression analysis performed (Equation 4.2.1):

$$y = 4596x$$

Equation 4.2.1

where y is the area of the acid and x is the concentration.

Calibration of Ester 127

Different concentrations of ester **127** were prepared in phosphate buffer (**Table 4.2.2**).

The area of peak at $R_t = 11.90$ was measured.

Concentration of ester 127 (mM)	Area of ester peak
0.2	13679
0.4	20725
0.6	28734
0.8	36299

Table 4.2.2

A plot of the area of the peak against the concentration was made and linear regression analysis performed (**Equation 4.2.2**):

$$y = 47755x$$

Equation 4.2.2

where y is the area of the acid and x is the concentration.

Calibration of Ester 169

Different concentrations of ester **169** were prepared in a 1:1 mixture of acetonitrile/phosphate buffer (**Table 4.2.3**). The area of peak at $R_t = 12.32$ was measured.

Concentration of ester 169 (mM)	Area of ester peak
0.02	6844
0.04	9373
0.06	11610
0.08	13943
0.10	16769

Table 4.2.3

A plot of the area of the peak against the concentration was made and linear regression analysis performed (**Equation 4.2.3**):

$$y = 181856x$$

Equation 4.2.3

where y is the area of the acid and x is the concentration.

Calibration of Cinnamyl alcohol 180

Different concentrations of cinnamyl alcohol were prepared in a 1:1 mixture of acetonitrile/phosphate buffer (**Table 4.2.4**). The area of peak at $R_t = 10.44$ was measured.

Concentration of alcohol 180 (mM)	Area of alcohol peak
0.02	2801
0.04	4301
0.06	6721
0.08	8249
0.10	8936

Table 4.2.4

A plot of the area of the peak against the concentration was made and linear regression analysis performed (**Equation 4.2.4**):

$$y = 107604x$$

Equation 4.2.4

where y is the area of the acid and x is the concentration.

4.2.6 General Procedures for Ester Hydrolysis with Polymers

Control Reaction

A solution of ester in aqueous buffer (0.5 mM) was stirred at room temperature. The change in ester concentration and acid product formation was monitored by HPLC at time $t = 0$, $t = 5$, $t = 8$, $t = 12$, $t = 15$, $t = 20$ min and then every 30 min thereafter for 5 h, and then at 24 h.

General Procedure using buffers

Polymer (10 mg) was added to a solution of ester in aqueous buffer (0.5 mM, 1 ml) and the mixture stirred at room temperature. The change in ester concentration and acid product formation was monitored by HPLC at time $t = 0$, $t = 5$, $t = 8$, $t = 12$, $t = 15$, $t = 20$ min and then every 30 min thereafter for 5 h, and then at 24 h. The results are presented in Chapter 2.

Ester hydrolysis experiments at different ester concentrations (0.25 mM, 0.5 mM, 1 mM and 2 mM) were conducted using the above general procedure.

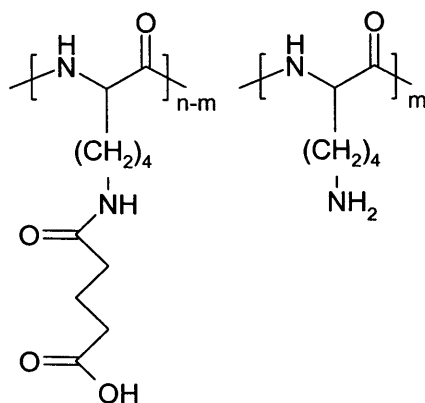
General Procedure using a mixture of organic solvent and buffer

Polymer (10 mg) was added to a stirred solution of ester dissolved in a mixture of aqueous buffer/solvent (1 ml) (ester concentration of 0.5 mM) and the mixture stirred at room temperature. The change in ester concentration and acid product formation was monitored by HPLC at time $t = 0$, $t = 5$, $t = 8$, $t = 12$, $t = 15$, $t = 20$ min and then every 30 min thereafter for 5 h, and then at 24 h. The results are presented in Chapter 2.

4.3 Artificial Aldolases

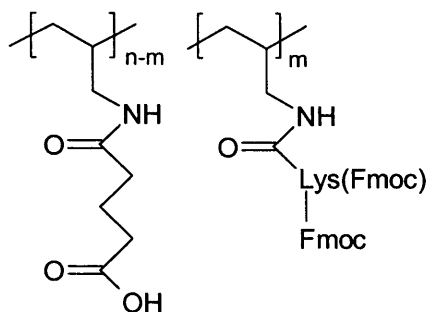
4.3.1 Synthesis of Artificial Aldolases With Incorporated Lysine

Polymer 207



Polylysine hydrobromide (50.0 mg, 0.24 mmol) was suspended in a mixture of anhydrous dimethylformamide (0.96 ml) and 2,6-lutidine (0.24 ml, 2.06 mmol) under nitrogen. After stirring at room temperature for 5 min., the solution turned homogenous. The mixture was then cooled to 0 °C and glutaric anhydride (14 mg, 0.12 mmol) dissolved in dimethylformamide (0.24 ml) was added dropwise. The mixture was then stirred at 0 °C for 1 h and room temperature for 24 h. Dropwise addition of diethyl ether/ethanol (1:1, 10 ml) to the stirring reaction mixture, resulted in the appearance of a white precipitate. The solid was filtered, washed with diethyl ether/ethanol (1:1, 3 x 20 ml) and dried under vacuum. The desired polymer was isolated as a white solid (72 mg). ^1H NMR (300 MHz, DMSO) δ_{H} /ppm 1.33 (br, CH_2 of polylysine), 1.55 (br, CH_2 of polylysine), 1.66 (br, $-\text{CH}_2\text{CH}_2\text{CH}_2\text{CO}_2\text{H}$), 2.16 (br, $-\text{CH}_2\text{CH}_2\text{CH}_2\text{CO}_2\text{H}$), 2.77 (br, CH_2N of polylysine), 4.24 (br, αH of polylysine), 8.04 (br, $-\text{NH}_2$);

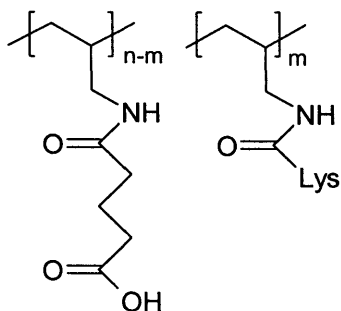
Polymer 210



Polyallylamine hydrochloride (100 mg, 1.08 mmol) was treated with potassium hydroxide (70.0 mg, 1.24 mmol) in methanol (20 ml) at room temperature for 16 h. The solvent was removed under reduced pressure and ethanol (25 ml) was added to the residue. The resulting white precipitate was removed by filtration and the filtrate was concentrated *in vacuo* to leave approximately 10ml of solvent.

FmocLys(Fmoc)OH (320 mg, 0.54 mmol), *N,N'*-diisopropylcarbodiimide (0.10 ml, 0.65 mmol) and *N*-hydroxysuccinimide (90.0 mg, 0.75 mmol) were dissolved in chloroform (20 ml) and stirred at room temperature for 5 h. This solution was added to the solution of polyallylamine in ethanol (above). Glutaric anhydride (60.0 mg, 0.54 mmol) was then added and the mixture was stirred at room temperature for 3 days. The solvents were removed under vacuum and the remaining white residue was triturated from chloroform/methanol (1:1, 40 ml). The isolated solid was washed with methanol (3 x 20 ml) and dried under vacuum to yield the product as a white solid (140 mg). ν_{\max} (solid state/cm⁻¹) 1539 (s, Ar (Fmoc groups)), 1711 (m, C=O (amides and carboxylic acid)), 2930 (s, C-H), 3306 (s, N-H).

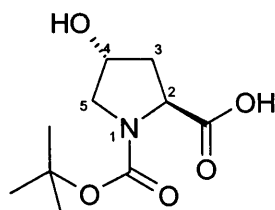
Polymer 211



A solution of piperidine/dimethylformamide (2:8, 15 ml) was added to the polymer **210** (120 mg) and the flask shaken for 20 h. The polymer was isolated by filtration and washed with dimethylformamide (3 x 20 ml) and dichloromethane (3 x 20 ml). The white solid was dried under vacuum to yield the desired product (80.0 mg). ^{13}C NMR (75 MHz, solid state) δ_c /ppm 23.6 – 53.1 (br, CH and CH_2 of polyallylamine, lysine and butyric acid), 175.4 (br, $-\text{C}(\text{O})\text{NH}-$), 181.0 (br, $-\text{C}(\text{O})\text{OH}$); ν_{max} (solid state/ cm^{-1}) 1558 (s, $\text{C}=\text{O}$ (amides)), 1693 (s, $\text{C}=\text{O}$ (carboxylic acid)), 2485 (s, $\text{O}-\text{H}$ (carboxylic acid)), 2940 (m, $\text{C}-\text{H}$), 3074 (m, $[-\text{NH}_3]^+$), 3397 (m, $\text{N}-\text{H}$).

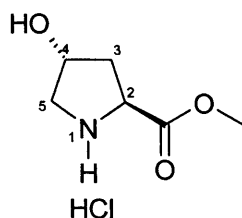
4.3.2 Synthesis of Catalytic Units Containing Proline for Artificial Aldolase Catalysts

(2S,4R)-4-Hydroxy pyrrolidine-1,2-dicarboxylic acid 1-*tert* butyl ester (296)¹⁶¹



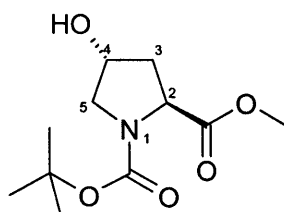
A solution of *trans*-4-hydroxyproline (3.00 g, 23.0 mmol) in aqueous sodium carbonate (10% w/v, 24 ml) was added dropwise to a stirred mixture of di-*tert*-butyl dicarbonate (4.74 g, 22.0 mmol) in tetrahydrofuran/dioxane (11 ml, 1:10). The mixture was then stirred at room temperature for 17 h. Diethyl ether (100 ml) was added and the phases were separated. The aqueous phase was cooled to 0 °C and then acidified to pH 3 using concentrated HCl. The acidic solution was extracted with ethyl acetate (3 x 70 ml). The combined organic extracts were dried over MgSO₄ and concentrated *in vacuo* to yield the product as a viscous colourless oil (1.06 g, 20%). ¹H NMR (300 MHz, CDCl₃) δ_H/ppm 1.37 (m, 9H, -C(CH₃)₃), 2.04 – 2.32 (m, 2H, H(3)), 3.38 – 3.54 (m, 2H, H(5)), 4.29 – 4.41 (m, 2H, H(2), H(4)); ¹³C NMR (75 MHz, CDCl₃) δ_C/ppm 28.4 and 28.6 (rotamers, -CH₃), 38.1 and 39.0 (rotamers, C(3)), 54.6 and 54.8 (rotamers, C(2)), 57.8 and 58.1 (rotamers, C(5)), 69.4 and 69.9 (rotamers, C(4)), 81.2 (-C(CH₃)₃), 154.6 and 155.7 (rotamers, -NCO₂-), 175.8 and 177.3 (rotamers, -CO₂H); ν_{max} (DCM/cm⁻¹) 1636 (s, C=O (Boc group)), 1672 (s, C=O (carboxylic acid)), 2980 (w, C-H), 3055 (w, O-H), 3423 (s, N-H); m/z (FAB) 254 (12%, [M + Na]⁺); HRMS found 254.1008, [M + Na]⁺ (C₁₀H₁₇NO₅Na) requires 254.1004; [α]_D - 38.8 ° (c 0.16, EtOH).

(2S,4R)-4-Hydroxy-2-methoxycarbonyl pyrrolidinium chloride (297)¹⁶²



Thionyl chloride (0.62 ml, 8.55 mmol) was added dropwise to a stirred solution of *trans*-4-hydroxyproline (1.00 g, 7.63 mmol) in methanol (14 ml) at 0 °C. The reaction was allowed to warm to room temperature and then stirred for 1 h. The mixture was then heated at reflux for 63 h. The resulting solution was concentrated and the residue was azeotroped with methanol to yield the product as a white solid (1.10 g, 80%). **m.p.** 162 °C (lit. 162-164 °C¹⁶²); **¹H NMR** (300 MHz, CD₃OD) δ_{H} /ppm 2.23 (m, 1H, H(3)), 2.41 (m, 1H, H(3)), 3.33 (m, 1H, H(5)), 3.51 (m, 1H, H(5)), 3.86 (s, 3H, -CO₂CH₃), 4.61 (m, 2H, H(2) and H(4)); **¹³C NMR** (75 MHz, CDCl₃) δ_{C} /ppm 39.5 (C(3)), 54.9 (-CH₃), 55.8 (C(5)), 60.3 (C(2)), 71.4 (C(4)), 171.3 (-CO₂CH₃); ν_{max} (nujol/cm⁻¹) 1742 (m, C=O), 2855, 2924 (s, C-H), 3323 (m, N-H); **m/z** (Cl⁺) 147 (45%, [M - Cl + 2H]⁺), 146 (100%, [M - Cl + H]⁺); **HRMS** found 147.0891, [M - Cl + 2H]⁺ (C₆H₁₃NO₃) requires 147.0895; **[α]_D** - 17.7 ° (*c* 0.90, EtOH), lit. - 24.3 ° (*c* 1.05, MeOH).¹⁶²

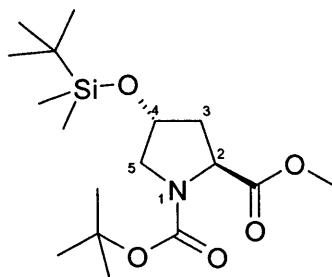
(2S,4R)-4-Hydroxy pyrrolidine-1,2-dicarboxylic acid 1-*tert* butyl ester-2-methyl ester (298)¹⁶³



To a stirred solution of *trans*-hydroxyproline methyl ester **297** (0.50 g, 2.75 mmol) dissolved in dichloromethane (4 ml), triethylamine (1.15 ml, 8.26 mmol) was added. The mixture was cooled to 0 °C and di-*tert*-butyl dicarbonate (0.66 g, 3.03 mmol) was added and the mixture was stirred for 30 min.. The mixture was warmed to room

temperature and stirring was continued for 17 h. Dichloromethane (30 ml) was added and the mixture was washed with aqueous HCl (1 M, 50 ml), saturated aqueous NaHCO₃ (50 ml), water (50 ml) and brine (50 ml). The chlorinated layer was dried over MgSO₄ and the solvent removed to give a colourless oil (0.39 g, 58%). R_f = 0.46 (SiO₂; ethyl acetate); $^1\text{H NMR}$ (300 MHz, CDCl₃) δ_{H} /ppm 1.20 and 1.25 (s, 9H, -C(CH₃)₃), 1.83 (m, 1H, H(3)), 1.98 (m, 1H, H(3)), 3.35 (m, 2H, H(5)), 3.43 (s, 3H, -CO₂CH₃), 4.18 (m, 2H, H(2) and H(4)); $^{13}\text{C NMR}$ (75 MHz, CDCl₃) δ_{C} /ppm 28.1 and 28.3 (rotamers, -C(CH)₃), 38.3 and 39.0 (rotamers, C(3)), 52.0 and 52.1 (-CO₂CH₃), 54.4 and 54.6 (rotamers, C(5)), 57.6 and 58.0 (rotamers, C(2)), 68.9 and 69.5 (rotamers, C(4)), 80.2 and 80.3 (rotamers, -C(CH₃)₃), 154.0 and 154.6 (-NCO₂-), 173.5 and 173.8 (-CO₂CH₃); ν_{max} (DCM/cm⁻¹) 1367 (s, C-(CH₃)₃), 1682 (s, C=O (Boc group)), 1747 (s, C=O (ester)), 2978 (s, C-H), 3435 (s, N-H); m/z (CI⁺) 246 (6%, [M + H]⁺), 146 (99%, [M - Boc + H]⁺); **HRMS** found 246.1337, [M + H]⁺ (C₁₁H₂₀NO₅) requires 246.1341; $[\alpha]_{\text{D}}$ - 56.3 ° (c 0.80, CHCl₃), lit. - 40.5 ° (c 0.80, CHCl₃).¹⁶³

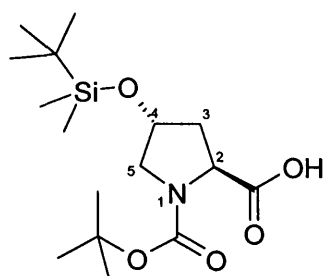
(2S,4R)-4-(*tert*-Butyl dimethyl silanyloxy) pyrrolidine-1,2-dicarboxylic acid 1-*tert* butyl ester 2-methyl ester (299)¹²⁹



The alcohol **298** (0.39 g, 1.59 mmol) was dissolved in dimethylformamide (0.5 ml) and imidazole (0.23 g, 3.34 mmol) and *tert*-butylchlorodimethylsilane (0.26 g, 1.75 mmol) were added. The mixture was stirred at room temperature for 1.5 h. The resulting solution was diluted with diethyl ether (10 ml) and washed with water (10 ml), aqueous HCl (1 M, 10 ml) and saturated aqueous NaHCO₃ (10 ml). The ether layer was dried over MgSO₄ and solvents removed to give the product as colourless oil (0.27 g, 47%). R_f = 0.84 (SiO₂; ethyl acetate); $^1\text{H NMR}$ (400 MHz, CDCl₃, 325 K) δ_{H} /ppm 0.03 (s, 6H, -Si(CH₃)₂-), 0.83 (s, 9H, -SiC(CH₃)₃), 1.41 (s, 9H, -NCO₂C(CH₃)₃), 1.97 (m, 1H, H(3)), 2.12 (m, 1H, H(3)), 3.33 (m, 1H, H(5)), 3.48 (m, 1H, H(5)), 3.66 (s, 3H, -CO₂CH₃),

4.31 and 4.37 (m, 2H, $\underline{\text{H}}(2)$ and $\underline{\text{H}}(4)$); ^{13}C NMR (100 MHz, CDCl_3 , 328 K) δ_c/ppm – 4.6 ($-\text{Si}(\underline{\text{C}}\text{H}_3)_2$), 18.2 ($-\text{Si}\underline{\text{C}}(\text{CH}_3)_3$), 26.0 ($-\text{Si}\underline{\text{C}}(\underline{\text{C}}\text{H}_3)_3$), 28.6 ($-\text{CO}_2\text{C}(\underline{\text{C}}\text{H}_3)_3$), 40.4 ($\underline{\text{C}}(3)$), 52.1 ($-\text{CO}_2\underline{\text{C}}\text{H}_3$), 55.0 ($\underline{\text{C}}(5)$), 58.4 ($\underline{\text{C}}(2)$), 70.4 ($\underline{\text{C}}(4)$), 80.2 ($-\text{CO}_2\underline{\text{C}}(\text{CH}_3)_3$), 173.7 ($-\underline{\text{C}}\text{O}_2\text{CH}_3$); ν_{max} ($\text{DCM}/\text{cm}^{-1}$) 1096 (w, Si-O), 1256 (w, Si-CH₃), 1366 (m, C-(CH₃)₃), 1705 (s, C=O (Boc group)), 1755 (s, C=O (ester)), 2932 (s, C-H); m/z (Cl^+) 360 (12%, $[\text{M} + \text{H}]^+$); **HRMS** found 360.2211, $[\text{M} + \text{H}]^+$ ($\text{C}_{17}\text{H}_{33}\text{NO}_5\text{Si}$) requires 360.2206; $[\alpha]_{\text{D}} - 19.3^\circ$ (c 0.11, CHCl_3). **Anal.** ($\text{C}_{17}\text{H}_{33}\text{NO}_5\text{Si}$) found C, 57.19; H, 9.69; N, 3.85%; requires C, 56.79; H, 9.25; N, 3.90%.

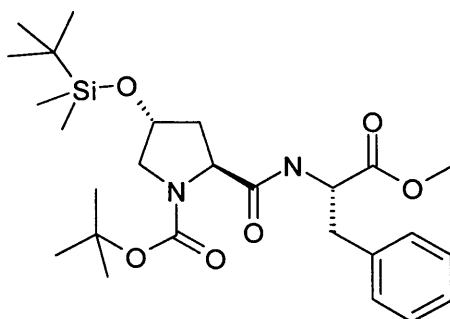
(2S,4R)-4-(*tert* Butyl dimethyl silanyloxy) pyrrolidine-1,2-dicarboxylic acid 1-*tert* butyl ester (300)



To a solution of ester **299** (0.27 g, 0.75 mmol) in methanol (1.4 ml) was added a mixture of NaOH (45.0 mg, 1.13 mmol) in water (0.5 ml). The reaction was then heated to 45 °C, and stirred for 1 h. The solution was cooled to 0 °C and then acidified with aqueous HCl (5% v/v) to ~ pH 4. The acidic solution was extracted with diethyl ether (3 x 5 ml). The combined organic extracts were dried over MgSO_4 and concentrated *in vacuo* to yield the desired acid as a clear oil (90.0 mg, 36%). $R_f = 0.53$ (SiO_2 ; petroleum spirit/ethyl acetate; 1:1); ^1H NMR (300 MHz, CDCl_3) $\delta_{\text{H}}/\text{ppm}$ 0.03 (s, 6H, $-\text{Si}(\underline{\text{C}}\text{H}_3)_2-$), 0.81 (s, 9H, $-\text{Si}\underline{\text{C}}(\text{CH}_3)_3$), 1.36 and 1.41 (s, 9H, $-\text{NCO}_2\text{C}(\underline{\text{C}}\text{H}_3)_3$), 2.02 (m, 2H, $\underline{\text{H}}(3)$), 3.28 – 3.58 (m, 2H, $\underline{\text{H}}(5)$), 4.28 – 4.39 (m, 2H, $\underline{\text{H}}(2)$ and $\underline{\text{H}}(4)$); ^{13}C NMR (75 MHz, CDCl_3) δ_c/ppm – 4.6 and – 3.5 (rotamers, $-\text{Si}(\underline{\text{C}}\text{H}_3)_2$), 18.2 ($-\text{Si}\underline{\text{C}}(\text{CH}_3)_3$), 25.9 and 26.0 (rotamers, $-\text{Si}\underline{\text{C}}(\underline{\text{C}}\text{H}_3)_3$), 28.5 and 28.6 (rotamers, $-\text{CO}_2\text{C}(\underline{\text{C}}\text{H}_3)_3$), 38.5 and 40.0 (rotamers, $\underline{\text{C}}(3)$), 54.8 and 55.1 (rotamers, $\underline{\text{C}}(5)$), 58.1 and 58.2 (rotamers $\underline{\text{C}}(2)$), 70.0 and 70.4 (rotamers, $\underline{\text{C}}(4)$), 80.9 and 81.3 (rotamers, $-\text{CO}_2\underline{\text{C}}(\text{CH}_3)_2$), 154.3 and 156.1 (rotamers, $-\text{N}\underline{\text{C}}\text{O}_2-$), 176.7 and 178.7 (rotamers, $-\underline{\text{C}}\text{O}_2\text{H}$); ν_{max} ($\text{DCM}/\text{cm}^{-1}$) 1096 (w, Si-

O), 1256 (w, Si-CH₃), 1682 (s, C=O (Boc group)), 1736 (s, C=O (ester)), 2932 (s, C-H); **m/z** (CI⁺) 346 (12%, [M + H]⁺), 246 (100%, [M – Boc + H]⁺); **HRMS** found 346.2053, [M + H]⁺ (C₁₆H₃₂NO₅Si) requires 346.2050; **Anal.** (C₁₆H₃₁NO₅Si.½H₂O) found C, 54.61; H, 9.52; N, 4.04%; requires C, 54.21; H, 9.10; N, 3.95%; [α]_D - 25.3 ° (c 0.32, MeOH).

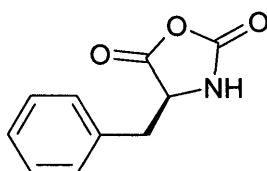
(2S,4R)-4-(*tert* Butyl dimethyl silanyloxy)-2-((S)-1-methoxycarbonyl-2-phenyl ethylcarbamoyl) pyrrolidine-1-carboxylic acid *tert* butyl ester (311)



Triethylamine (0.08 ml, 0.58 mmol), water (5 ml), **300** (200 mg, 0.58 mmol) and HOBT (80 mg, 0.58 mmol) were added sequentially to a solution of L-phenylalanine methyl ester (130 mg, 0.58 mmol) in dichloromethane (5 ml). The mixture was then cooled to 0 °C and EDCI (120 mg, 0.64 mmol) was added. The solution was stirred for 15 min. and warmed to room temperature, and subsequently stirred for 44 h. The mixture was diluted with dichloromethane (20 ml) and organic layer washed with aqueous HCl (0.5 M, 20 ml), followed by saturated aqueous NaHCO₃ (20 ml) and brine (20 ml). The organic extracts were dried over MgSO₄ and solvents removed to give the product as a white solid (160 mg, 55%). **m.p.** 57 °C; ¹H NMR (300 MHz, CDCl₃) δ _H/ppm 0.01 (s, 6H, -Si(CH₃)₂), 0.81 (s, 9H, -SiC(CH₃)₃), 1.38 (m, 9H, -CO₂C(CH₃)₃), 1.78 (m, 1H, H(3)) 2.09 (m, 1H, H(3)), 2.96 (dd, *J* = 7.1, *J* = 13.9, 1H, -NHCHCH(H)Ph), 3.13 (dd, *J* = 5.6, *J* = 13.9, 1H, -NHCHCH(H)Ph), 3.24 (m, 1H, H(5)), 3.50 (m, 1H, H(5)), 3.65 (s, 3H, -CO₂CH₃), 4.17 (m, 2H, H(2) and H(4)), 4.79 (m, 1H, -NHCHCO₂CH₃), 7.06 (m, 2H, ArH), 7.20 (m, 3H, ArH), 7.31 (m, 1H, NH); ¹³C NMR (75 MHz, CDCl₃, 328 K) δ _C/ppm – 4.5 (-SiC(CH₃)₂), 18.2 (-SiC(CH₃)₃), 26.0 (-SiC(CH₃)₃), 28.6 (-CO₂C(CH₃)₃), 38.6 (-NHCHCH₂Ph and C(3)), 52.3 (-CO₂CH₃), 53.4 (-NHCHCO₂CH₃), 55.1 (C(5)), 60.2 (C(2)), 70.6 (C(4)), 80.9 (-CO₂C(CH₃)₃), 127.2, 128.7 and 129.5 (5 x ArC), 136.5

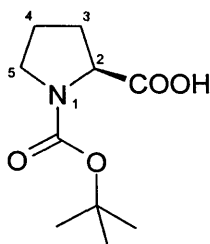
(1 x quaternary ArC), 156.4 (-NCO₂C(CH₃)₃), 171.9 (-CO₂CH₃ and -C(O)NH-); ν_{\max} (DCM/cm⁻¹) 1024 (m, Si-O), 1265 (s, Si-CH₃), 1500 (w, Ar), 1678 (s, C=O (amide)), 1744 (m, C=O (ester)), 2856 and 2932 (m, C-H), 3414 (s, N-H); **m/z** (CI⁺) 507 (8%, [M + H]⁺), 393 (80%, [M - Boc - Me + H]⁺); **HRMS** found 507.2897, [M + H]⁺ (C₂₆H₄₃N₂O₆Si) requires 507.2890; **Anal.** (C₂₆H₄₂N₂O₆Si) found C, 61.24; H, 8.50; N, 5.43%; requires C, 61.24; H, 8.50; N, 5.43%.

4-Benzyl oxazolidine-2,5-dione (305)¹³²



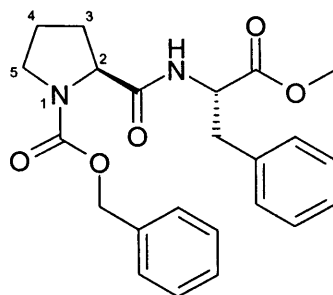
A solution of triphosgene (2.10 g, 7.00 mmol) in anhydrous tetrahydrofuran (20 ml) was added to a solution of L-phenylalanine (3.16 g, 19.0 mmol) in tetrahydrofuran (40 ml) under nitrogen. The resulting solution was heated to 50 °C and stirred at this temperature until the phenylalanine dissolved (*ca.* 3 h). After cooling, the solvent was removed under reduced pressure, to half of its original volume. Hexane was then added until a white precipitate formed. The white precipitate was isolated by filtration and washed with cold hexane (3 x 40 ml), and then dried under vacuum. The desired product was isolated as a white solid (2.65 g, 72%). **m.p.** > 230 °C; **¹H NMR** (300 MHz, CDCl₃) δ_{H} /ppm 3.01(m, 1H, -CH(H)Ph) and 3.22 (m, 1H, -CH(H)Ph), 4.53 (m, 1H, -NHCHCO₂-), 7.16 – 7.34 (m, 5H, ArH); **¹³C NMR** (75 MHz, CDCl₃) δ_{C} /ppm 37.7 (-CH₂Ph), 59.1 (-NHCHCO₂-), 128.1, 129.3 and 129.7 (5 x ArC), 134.1 (1 x quaternary ArC), 152.7 (-NHCO₂-), 169.3 (-NHCHCO₂-); ν_{\max} (DCM/cm⁻¹) 1653 (m, Ar), 1782 (s, C=O), 1850 (m, C=O), 3304 (m, N-H); **m/z** (CI⁺) 192 (8%, [M + H]⁺); **HRMS** found 192.0662, [M + H]⁺ (C₁₀H₁₀NO₃) requires 192.0660.

Pyrrolidine-1,2-dicarboxylic acid 1-*tert* butyl ester (230)¹³³



To L-proline (2.00 g, 17.0 mmol) in dioxane/water (2:1, 90 ml) was added triethylamine (3.63 ml, 26.0 mmol) and di-*tert*-butyl dicarbonate (5.69 g, 26.0 mmol) and the mixture stirred at room temperature for 24 h. Aqueous sodium hydroxide (1 M, 100 ml) and ethyl acetate (100 ml) were added and the layers were separated. The aqueous layer was acidified to pH 4 with concentrated aqueous HCl, and then extracted with ethyl acetate (3 x 50 ml). The combined organic extracts were washed with water (100 ml) and brine (100 ml), dried over MgSO₄ and concentrated *in vacuo* to yield a clear oil. Hot ethyl acetate was added to the oil and the flask left in the fridge overnight. This gave a white solid (di-*tert*-butyl dicarbonate), which was filtered off. Ethyl acetate was then removed from the filtrate to afford the product as a white solid (1.63 g, 44%). **m.p.** 133 °C; **¹H NMR** (300 MHz, CD₃OD) δ_{H} /ppm 1.45 (d, $J = 10.1$, 9H, -C(CH₃)₃), 1.96 and 2.26 (m, 4H, H(3), H(4)), 3.43 (m, 2H, H(5)), 4.20 (m, 1H, H(2)), 5.11 (br s, 1H, -CO₂H); **¹³C NMR** (75 MHz, CD₃OD) δ_{C} /ppm 25.4 and 26.0 (rotamers, -C(CH₃)₃), 29.4 and 29.6 (rotamers, C(4)), 31.8 and 32.6 (rotamers, C(3)), 48.3 and 48.6 (rotamers, C(5)), 61.0 and 61.3 (rotamers, C(2)), 82.0 and 82.2 (rotamers, -C(CH₃)₃), 156.7 and 157.0 (rotamers, -NC(O)₂-), 177.1 and 177.5 (rotamers, -CO₂H) ν_{max} (DCM/cm⁻¹) 1123 (m, C-O), 1693 (s, C=O), 2581 (w, OH (carboxylic acid)), 2970 (m, C-H), 3495 (s, OH); **m/z** (FAB) 216 (19%, [M + H]⁺);

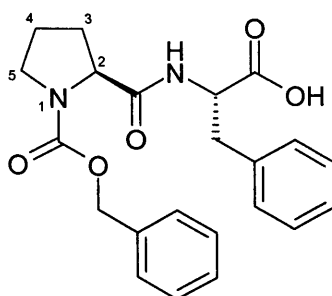
(S)-2-(S)-(1-Methoxycarbonyl-2-phenyl ethylcarbamoyl) pyrrolidine-1-carboxylic acid benzyl ester (244)¹⁶⁴



Ethyl chloroformate (0.15 ml, 1.61 mmol) in tetrahydrofuran (1 ml) was added dropwise to a stirred solution of Cbz-proline (0.50 g, 2.01 mmol) and anhydrous triethylamine (0.28 ml, 2.01 mmol) in anhydrous tetrahydrofuran (6 ml) at $-10\text{ }^{\circ}\text{C}$. The resulting suspension was stirred at $-10\text{ }^{\circ}\text{C}$ for 40 min.. Concurrently, to phenylalanine methyl ester hydrochloride (0.35 g, 1.61 mmol) in tetrahydrofuran/dichloromethane (1:1, 10 ml), triethylamine (0.22 ml, 1.61 mmol) was added and the solution was stirred at room temperature for 30 min.. The mixture was then added to the above solution containing Cbz-proline, at $-10\text{ }^{\circ}\text{C}$, and the mixture was allowed to warm room temperature. Stirring was then continued for 17 h at room temperature. The solvents were then removed under reduced pressure and the residue was dissolved in dichloromethane (25 ml). The mixture was washed with aqueous HCl (0.5 M, 2 x 25 ml), saturated aqueous NaHCO_3 (2 x 25 ml), water (2 x 25 ml) and brine (2 x 25 ml). The chlorinated extract was dried over MgSO_4 , filtered and concentrated *in vacuo*. The desired dipeptide was isolated as a colourless oil (0.50 g, 61%). $R_f = 0.59$ (SiO_2 ; ethyl acetate); $^1\text{H NMR}$ (400 MHz, CDCl_3) $\delta_{\text{H}}/\text{ppm}$ 1.73 (br m, 2H, H(4)), 1.89 (br m, 1H, H(3)), 2.12 (br m, 1H, H(3)), 2.94 (dd, $J = 7.0$, $J = 13.9$, 1H, -NHCHCH(H)Ph), 3.10 (dd, $J = 5.8$, $J = 13.9$, 1H, -NHCHCH(H)Ph), 3.36 (m, 2H, H(5)), 3.62 (s, 3H, - CO_2CH_3), 4.27 (m, 1H, H(1)), 4.79 (m, 1H, -NHCHC O_2Me), 5.09 (s, 2H - $\text{CO}_2\text{CH}_2\text{Ph}$), 7.03 – 7.30 (m, 10H, ArH); $^{13}\text{C NMR}$ (75 MHz, CDCl_3) $\delta_{\text{C}}/\text{ppm}$ 24.5 and 23.7 (rotamers, C(4)), 27.9 and 30.8 (rotamers, C(3)), 37.9 (-NHCHC H_2Ph), 46.8 and 47.1 (rotamers, C(5)), 52.3 and 53.5 (rotamers, -C H_3), 52.7 and 53.2 (-NHCHC(O)-), 60.2, 60.6 (C(2)), 67.3 (- $\text{NCO}_2\text{CH}_2\text{Ph}$), 126.9-129.3 (10 x ArC), 136.0 and 136.4 (2 x quaternary ArC), 155.1 (- NCO_2CH_2), 171.5 (-NHC(O)-), 171.7 (- CO_2CH_3); ν_{max}

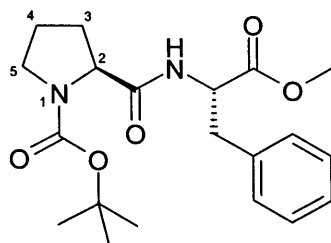
(neat/cm⁻¹) 1497 (m, Ar), 1651 (s, C=O (amide)), 1711 (s, C=O from (ester)), 2953 (s, C-H), 3323 (s, N-H); *m/z* (FAB) 411 (12%, [M + H]⁺); [α]_D – 42.0 ° (*c* 1.0, MeOH), lit. – 36.2 ° (*c* 1.0, MeOH)¹⁶⁵.

**(S)-2-(S)-(1-Carboxy-2-phenyl ethylcarbamoyl) pyrrolidine-1-carboxylic acid
benzyl ester (245)** ¹⁶⁶



Dipeptide **244** (1.37 g, 3.34 mmol) was dissolved in dioxane (11 ml) and water (11 ml). Aqueous sodium hydroxide (4 M, 4 ml) was added dropwise and the mixture was stirred for 2.5 h. The organics were removed *in vacuo* and the resulting aqueous residue was acidified with concentrated HCl (pH 2). The product was extracted with ethyl acetate (3 x 15 ml) and the combined organic extracts were washed with water (30 ml) and brine (30 ml). The organic layer was dried over MgSO₄, filtered and concentrated to yield the desired product as a colourless oil (1.08 g, 82%). *R_f* = 0.59 (SiO₂; ethyl acetate); ¹H NMR (400 MHz, CDCl₃, 328 K) δ _H/ppm 1.72 (br m, 2H, H(4)), 1.91 (br m, 1H, H(3)), 1.99 (br m, 1H, H(3)), 2.98 (dd, *J* = 7.1, *J* = 14.0, 1H, NHCHCHH(H)Ph), 3.18 (dd, *J* = 5.6, *J* = 14.0, 1H, -NHCHCHH(H)Ph), 3.34 (br m, 2H, H(5)), 4.27 (m, 1H, H(2)), 4.80 (m, 1H, -NHCHCCO₂H), 5.08 (s, 2H, -CO₂CH2Ph), 6.93 – 7.28 (m, 10H, ArH); ¹³C NMR (75 MHz, CDCl₃) δ _C/ppm 23.2 and 24.3 (rotamers, C(4)), 28.5 and 30.9 (rotamers, C(3)), 37.4 (-NHCHCH₂Ph), 46.9 and 47.4 (rotamers, C(5)), 52.9 and 53.2 (rotamers, -NHCHC(O)-), 60.4 (C(2)), 67.6 (-NCO₂CH2Ph), 127.1 - 129.4 (10 x ArC), 136.2 (2 x quaternary ArC), 155.6 and 156.2 rptamers, -NCO₂CH₂-), 171.9 and 17.6 (-NHC(O)-), 173.8 (-CO₂H); ν _{max} (DCM/cm⁻¹) 1499 (m, Ar), 1641 (s, C=O (amide)), 1701 (s, C=O (carboxylic acid)), 2968 (w, C-H), 3061 (w, O-H), 3321 (w, N-H); *m/z* (FAB) 419 (2%, [M + Na]⁺, 397 (12%, [M + H]⁺); [α]_D - 38.0 ° (*c* 2.0, CHCl₃), lit. - 49.0 ° (*c* 2.0, CHCl₃).¹⁶⁶

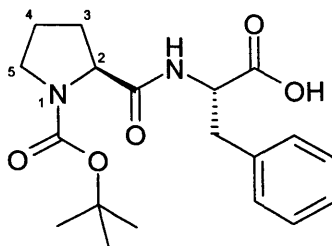
(S)-2-((S)-1-Methoxycarbonyl-2-phenyl ethylcarbamoyl) pyrrolidine-1-carboxylic acid *tert* butyl ester (246)¹⁶⁷



Ethyl chloroformate (0.36 ml, 3.72 mmol) in anhydrous tetrahydrofuran (3 ml) was added dropwise to a stirred mixture of Boc-proline **230** (1.00 g, 4.65 mmol) and anhydrous triethylamine (0.65 ml, 4.65 mmol) in tetrahydrofuran (14 ml) at $-10\text{ }^{\circ}\text{C}$, under nitrogen. The resulting suspension was stirred at $-10\text{ }^{\circ}\text{C}$ for 40 min. Concurrently, triethylamine (0.51 ml, 0.80 mmol) was added to a stirred mixture of phenylalanine methyl ester (0.80 g, 0.80 mmol) in tetrahydrofuran/dichloromethane (2:1, 15 ml) at $-10\text{ }^{\circ}\text{C}$. The mixture was stirred for 30 min. The mixture was then added to the above solution containing Boc-proline, at $-10\text{ }^{\circ}\text{C}$. The resulting mixture was allowed to warm to room temperature and stirring was continued for 17 h. The solvents were removed under reduced pressure and resulting the residue was dissolved in dichloromethane (50 ml). The mixture was washed with aqueous HCl (0.5 M, 2 x 50 ml), saturated aqueous NaHCO_3 (2 x 50 ml), water (2 x 50 ml) and brine (2 x 50 ml). The chlorinated extract was dried over MgSO_4 , filtered and concentrated *in vacuo* to yield the desired product as a white solid (1.64 g, 94%). **m.p.** $44\text{ }^{\circ}\text{C}$ (lit. $71\text{ }^{\circ}\text{C}^{167}$); **R_f** = 0.59 (SiO_2 ; ethyl acetate); **¹H NMR** (400 MHz, CDCl_3 , 328 K) δ_{H} /ppm 1.37 (s, 9H, $-\text{C}(\text{CH}_3)_3$), 1.74 (br m, 2H, $\text{H}(4)$), 1.87 (br m, 1H, $\text{H}(3)$), 2.00 (br m, 1H, $\text{H}(3)$), 2.93 (dd, $J = 6.9$, $J = 13.9$, 1H, $-\text{NHCHCH}(\text{H})\text{Ph}$), 3.09 (dd, $J = 5.8$, $J = 13.9$, 1H, $-\text{NHCHCH}(\text{H})\text{Ph}$), 3.22 (m, 2H, $\text{H}(5)$), 3.62 (s, 3H, $-\text{CO}_2\text{CH}_3$), 4.14 (m, 1H, $\text{H}(2)$), 4.76 (m, 1H, $-\text{NHCHCO}_2\text{Me}$), 7.02 – 7.20 (m, 5H, ArH); **¹³C NMR** (100 MHz, CDCl_3 , 328 K) δ_{C} /ppm 24.1 ($\text{C}(4)$), 25.7 ($\text{C}(3)$), 28.4 ($-\text{C}(\text{CH}_3)_3$), 38.3 ($-\text{CHCH}_2\text{Ph}$), 47.1 ($\text{C}(5)$), 52.1 ($-\text{CH}_3$), 53.2 ($-\text{NHCHC}(\text{O})-$), 59.2 ($\text{C}(2)$), 80.5 ($-\text{C}(\text{CH}_3)_3$), 127.0, 128.6 and 129.3 (ArC), 136.4 (quaternary ArC), 171.8 and 172.0 ($-\text{CO}_2\text{CH}_3$, $-\text{NC}(\text{O})_2-$ and $-\text{NHC}(\text{O})-$); **ν_{max}** (DCM/ cm^{-1}) 1367 (w, $\text{C}-(\text{CH}_3)_3$), 1529 (m, Ar), 1682 (s, $\text{C}=\text{O}$ (amide)), 1746 (s, $\text{C}=\text{O}$ (ester)), 2976 (s, C-H), 3321 (s, N-H); **m/z** (FAB) 377 (24%, $[\text{M} + \text{H}]^+$); **$[\alpha]_{\text{D}}$** -52.9 ° (c 1.4,

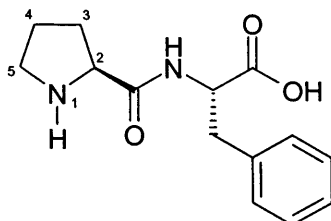
MeOH), lit. - 50.4 ° (*c* 1.4, MeOH).¹⁶⁸

(S)-2-((S)-1-Carboxy-2-phenyl ethylcarbamoyl) pyrrolidine-1-carboxylic acid *tert* butyl ester (247)



Dipeptide **246** (1.43 g, 3.81 mmol) was dissolved in dioxane (24 ml) and water (24 ml) and aqueous sodium hydroxide (4 M, 4.5 ml) was added dropwise. The mixture was then stirred at room temperature for 2 h. The solvents were removed *in vacuo* and the resulting aqueous residue was acidified with concentrated aqueous HCl to pH 4. The acidic solution was extracted with ethyl acetate (3 x 15 ml). The organic extracts were then washed with water (30 ml) and brine (30 ml) and dried over MgSO₄. The solvent was removed *in vacuo* to yield a colourless oil. The oil was then taken up into dichloromethane and the desired product was precipitated by the addition of hexane. The desired acid was isolated as white solid (1.38 g, 79%). **m.p.** 48 °C; **¹H NMR** (400 MHz, CDCl₃, 328 K) δ_{H} /ppm 1.34 and 1.38 (s, 9H, -C(CH₃)₃), 1.65 – 1.94 (br m, 4H, H(3) and H(4)), 2.97 (dd, *J* = 7.0, *J* = 14.0, 1H, -NHCHCH(H)Ph), 3.20 (br m, 3H, -NHCHCH(H)Ph and H(5)), 4.17 (m, 1H, H(2)), 4.79 (m, 1H, -NHCHC(O)CH₃), 7.08 – 7.19 (m, 5H, ArH); **¹³C NMR** (100 MHz, CDCl₃, 328 K) δ_{C} /ppm 23.8 (C(4)), 28.5 (-C(CH₃)₃), 37.8 (-CHCH₂Ph), 47.0 (C(5)), 53.1 (-NHCHC(O)-), 59.1 (C(2)), 81.1 (-C(CH₃)₃), 127.0, 128.5 and 129.5 (ArC), 136.5 (quaternary ArC), 155.4 (-NC(O)₂-), 172.8 (-NHC(O)-), 173.3 (-CO₂OH); ν_{max} (DCM/cm⁻¹) 1367 (w, C-(CH₃)₃), 1499 (w, Ar), 1736 (s, C=O), 2978 (s, C-H), 3333 (s, N-H); **m/z** (FAB) 363 (12%, [M + H]⁺), 263 (100%, [M + H - Boc]⁺); **HRMS** found 363.1923, [M + H]⁺ (C₁₉H₂₇N₂O₅) requires 363.1920; [α]_D -37.5 ° (*c* 0.8, MeOH); **Anal.** (C₁₉H₂₆N₂O₅·H₂O) found C, 60.10; H, 7.79; N, 8.13%; requires C, 59.99; H, 7.42; N, 7.36%.

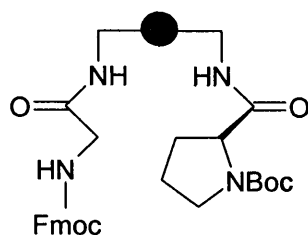
(S)-2-((S)-1-Carboxy-2-phenyl-ethylcarbamoyl)-pyrrolidinium trifluoroacetate
(242)¹²⁵



Dipeptide **247** (0.87 g, 2.40 mmol) in trifluoroacetic acid/dichloromethane (1:1, 20 ml) was stirred at room temperature for 3.5 h. The solvents were removed under reduced pressure to yield a brown oil. The oil was dissolved in ethanol and neutralised (pH 7) with aqueous NaOH (10 M) and sodium acetate, until a white precipitate appeared. The solution was left in the fridge over 72 h. The solid was filtered off and washed with cold water, cold methanol and cold ether and then dried under vacuum to give the product as a white solid (0.27 g, 43%). **m.p.** > 220 °C (lit. 244-246 °C¹²⁵); ¹H NMR (400 MHz, DMSO, 353 K) δ_{H} /ppm 1.53 and 1.88 (br m, 4H, H(3) and H(4)), 2.66 (br m, 1H, H(5)), 2.84 (br m, 1H, H(5)), 2.97 (br m, 1H, -NHCHCHH(H)Ph), 3.10 (br m, 1H, -NHCHCH(H)Ph), 3.55 (br m, 1H, H(2)), 4.54 (br m, 1H, -NHCHCCO₂H), 7.17 – 7.25 (m, 5H, ArH); ν_{max} (nujol/cm⁻¹) 1572 (m, Ar), 1676 (m, C=O), 2923 (s, C-H), 3194 (w, O-H), 3400 (w, N-H); **m/z** (FAB) 263 (9%, [M + H]⁺); [α]_D - 38.0 ° (c 2.0, aq. HCl (2 M)), lit. - 39.2 ° (c 4.9, aq. HCl (6 M))¹²⁵.

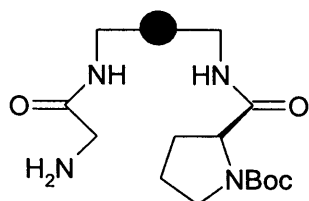
4.3.3 Synthesis of Artificial Aldolases With Incorporated Proline

Resin 231



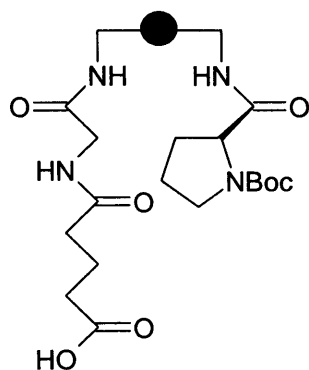
Tentagel resin (300 mg, 0.40 mmol/g) was swelled in anhydrous dimethylformamide (40 ml) for 1 h and the solvent was then filtered. To Boc-proline (130 mg, 0.60 mmol) in anhydrous dimethylformamide (3 ml), under nitrogen, was sequentially added HATU (230 mg, 0.60 mmol) and *N*-ethyldiisopropylamine (0.21 ml, 1.20 mmol). Concurrently, Fmoc-Glycine (180 mg, 0.60 mmol) was dissolved in anhydrous dimethylformamide (3 ml), under nitrogen, followed by the sequential addition of HATU (230 mg, 0.60 mmol) and *N*-ethyldiisopropylamine (0.21 ml, 1.20 mmol). Both solutions were then stirred at room temperature for 5 min., then combined, and added to the tentagel resin. The resulting mixture was shaken at room temperature for 18 h. The Kaiser test indicated the reaction was complete. Therefore the resin was filtered and washed with dimethylformamide (2 x 30 ml), dichloromethane (2 x 30 ml), dimethylformamide (20 ml), dichloromethane (20 ml) and then dried under vacuum. The desired resin was isolated as a solid (407 mg). The level of Fmoc substitution was calculated to be 0.24 mmol/g. This therefore indicated that the substitution of proline on the resin is 0.16 mmol/g.

Resin 363



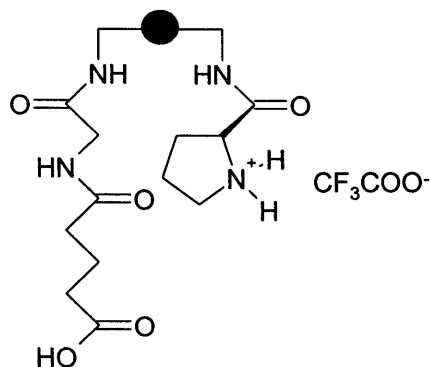
The resin **231** (400 mg, 0.24 mmol/g) was shaken in a mixture of piperidine/dimethylformamide (2:8, 6 ml) at room temperature for 2 h. The Kaiser test was negative. The resin was therefore filtered and treated with a further 6 ml of piperidine/DMF (2:8) and shaken for a further 5 min.. This procedure was then repeated once more, after which time the Kaiser test indicated complete reaction. The resin was filtered and washed with dimethylformamide (3 x 10 ml) and dichloromethane (3 x 10ml) and dried under vacuum. The desired resin was isolated as a solid (242 mg).

Resin 232



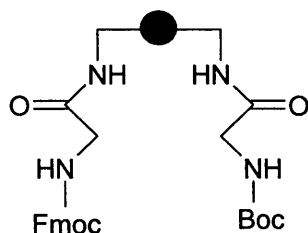
Resin **363** (230 mg, 0.24 mmol/g) was swelled in dichloromethane (40 ml) for 1 h. The resin was then filtered and washed with dichloromethane (2 x 10 ml). Glutaric anhydride (60.0 mg, 0.55 mmol) in anhydrous dichloromethane (5 ml) was added to the resin under nitrogen. The resulting mixture was shaken at room temperature for 19 h, after which time, the Kaiser test indicated the reaction was complete. The resin was then filtered and washed with dichloromethane (100 ml) and then dried under vacuum. The desired resin was isolated as a solid (253 mg).

Resin 233



The resin **232** (250 mg, 0.16 mmol/g) was added to a mixture of trifluoroacetic acid/dichloromethane (1:1, 6 ml). The mixture was shaken at room temperature for 2 h, after which time, the chloronil test indicated the reaction was complete. The resin was filtered and washed with dichloromethane (5 x 20 ml) and then dried under vacuum. The desired resin was isolated as a solid (253 mg). ν_{max} (solid state/cm⁻¹) 1558 (w, Ar (tentagel)), 1602 (w, Ar (tentagel)), 1688 (m, C=O (amide)), 1782 (s, C=O (carboxylic acid)), 2554 (w, OH (carboxylic acid)), 2913 (s, C-H), 3389 (s, N-H);

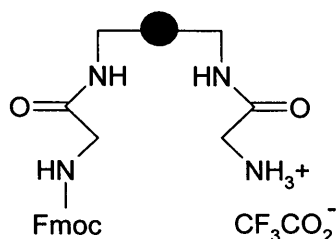
Resin 234



Tentagel resin (3.00 g, 0.50 mmol/g) was swelled in dimethylformamide for 30 min. and then filtered. Boc-glycine (1.31 g, 7.50 mmol) and Fmoc-glycine (2.23 g, 7.50 mmol) were dissolved in dimethylformamide (30 ml) and to this solution was added diisopropylcarbodiimide (3.28 ml, 21.0 mmol) followed by HOBt (2.03 g, 15.0 mmol). This mixture was then immediately added to the resin and the mixture shaken at room temperature for 23 h. After this time, the Kaiser indicated the reaction was complete. The resin was filtered and washed with dimethylformamide (100 ml), dichloromethane

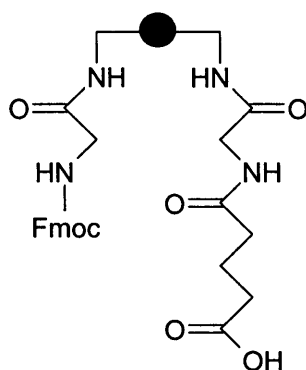
(100 ml), dimethylformamide (100 ml) and dichloromethane (150 ml), then dried under vacuum to yield the desired resin (2.77 g). Fmoc substitution = 0.18 mmol/g.

Resin 235



Resin **234** (2.77 g, 0.32 mmol/g) was swelled in DCM (25 ml) for 30 minutes and then filtered. A solution of trifluoroacetic acid/dichloromethane (1:1, 50 ml) was added to the resin and the mixture was shaken at room temperature for 24 h. After this time, the Kaiser test indicated the reaction was complete. The resin was filtered and washed with dichloromethane (5 x 30 ml), then dried under vacuum to yield the desired product (2.72 g).

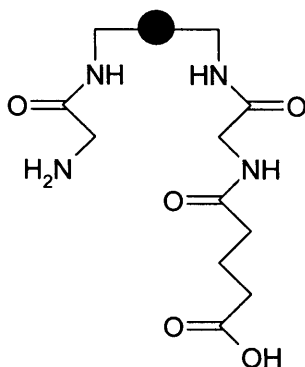
Resin 236



The resin **235** (2.77 g, 0.32 mmol/g) was washed with pyridine/dichloromethane (2:8, 50 ml) and dichloromethane (3 x 50 ml), and then filtered. Glutaric anhydride (0.57 g, 5.00 mmol) dissolved in chloroform (30 ml) was then added, and the flask was shaken at room temperature for 63 h. After this time, the Kaiser test indicated incomplete reaction. The resin was filtered, washed with dichloromethane (200 ml) and re-treated with glutaric anhydride (0.57 g, 5.00 mmol) dissolved in chloroform (30 ml) for an

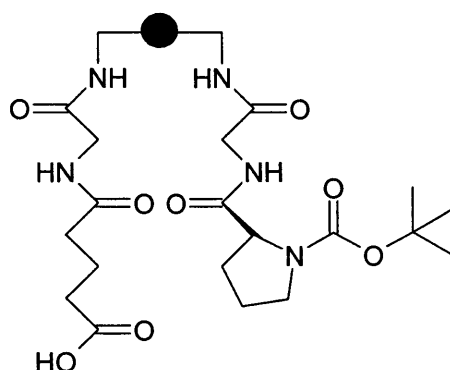
additional 1.5 h. After which time, the Kaiser test indicated complete reaction. The resin was filtered, washed with dichloromethane (5 x 30 ml) and dried under vacuum to give the desired product (2.95 g). Fmoc substitution = 0.12 mmol/g.

Resin 237



The resin **236** (3.00 g, 0.12 mmol/g) was treated with piperidine/dimethylformamide (2:8, 50 ml) and then shaken at room temperature for 4 h. After this time, the Kaiser test indicated the reaction was complete. The resin was washed with dimethylformamide (200 ml), dichloromethane (200 ml), dimethylformamide (100 ml), dichloromethane (100 ml) and then dried under vacuum to afford the desired product (2.44 g).

Resin 364

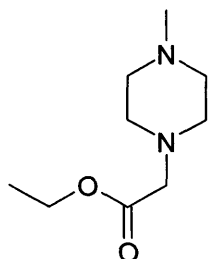


Resin **237** (2.40 g, 0.12 mmol/g) was swelled in dimethylformamide for 30 min. and then filtered. To Boc-proline (0.31 g, 1.44 mmol) in dimethylformamide (5 ml) was added HOBt (0.19 g, 1.44 mmol) followed by diisopropylcarbodiimide (0.32 ml, 2.02

Resin 238

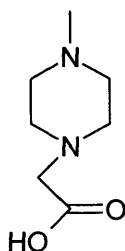
The chemical structure of Resin 238 is a macrocyclic polyamide. It features a large ring with alternating amide and amine groups. The ring is substituted with a 2,2,2-trifluoroethyl group (represented as CF_3) and a carboxylic acid group (COOH). The structure is shown with a repeating unit indicated by a dot and a subscript x . The carboxylic acid group is labeled with a subscript x and the formula $\text{CF}_3\text{CO}_2\text{H}$.

(4-Methyl-piperazin-1-yl)-acetic acid ethyl ester (289)



To *N*-methyl piperazine (2.34 ml, 21.0 mmol) in benzene (5 ml), a solution of ethyl bromoacetate (1.17 ml, 11.0 mmol) in benzene (5 ml) was added dropwise. The solution was then heated at reflux for 1 h. After cooling, a precipitate was removed by filtration and the resulting filtrate was concentrated *in vacuo* to yield the product as a pale yellow oil (1.02 g, 26%). $R_f = 0.17$ (SiO₂; petroleum spirit/ethyl acetate; 1:1) $^1\text{H NMR}$ (300 MHz, CDCl₃) δ_H /ppm 1.18 (m, 3H, -CH₂CH₃), 2.21 (s, 3H, -NCH₃), 2.41 (br m, 4H, 2 x -CH₂NCH₃), 2.54 (br m, 4H, 2 x -CH₂CH₂NCH₃), 3.13 (s, 2H, -NCH₂CO₂-), 4.10 (q, $J = 7.1$, 2H, -CH₂CH₃); $^{13}\text{C NMR}$ (75 MHz, CDCl₃) δ_C /ppm 13.6 (-CH₂CH₃), 45.4 (-NCH₃), 52.3 (2 x -CH₂NCH₃), 54.2 (2 x -CH₂CH₂NCH₃), 58.7 and 59.7 (-NCH₂CO₂CH₂-), 169.3 (-CO₂-); ν_{max} (neat/cm⁻¹) 1747 (s, C=O), 2795 (s, N-CH₂), 2937 (s, C-H); m/z (CI⁺) 187 (88%, [M + H]⁺), 186 (36%, [M]⁺); **HRMS** found 187.1448, [M + H]⁺ (C₉H₁₉N₂O₂) requires 187.1447; **Anal.** (C₉H₁₈N₂O₂·H₂O) found C, 52.52; H, 9.34; N, 13.95%, requires C, 52.92; H, 9.87; N, 13.71%;

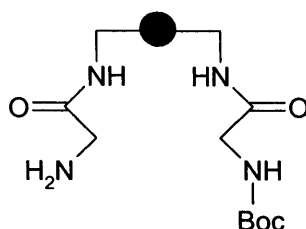
(4-Methyl-piperazin-1-yl)-acetic acid (290)¹⁶⁹



Compound **289** (0.36 g, 1.93 mmol) was dissolved in water (10 ml) and heated at reflux for 18 h. The solvents were removed *in vacuo* to yield the product as a white solid (0.23 g, 74%). **m.p.** 163 °C (lit. 160-161 °C¹⁶⁹); $^1\text{H NMR}$ (300 MHz, CD₃OD) δ_H /ppm 2.32

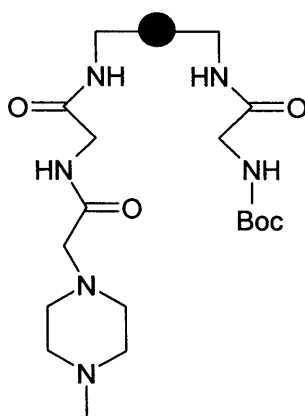
(s, 3H, -NCH₃), 2.73 (br m, 8H, 2 x -CH₂NCH₃ and 2 x -CH₂CH₂NCH₃), 3.01 (s, 2H, -NCH₂-); ¹³C NMR (75 MHz, CD₃OD) δ_c/ppm 44.7 (-NCH₃), 52.3 (2 x -CH₂NCH₃), 54.1 (2 x -CH₂CH₂NCH₃), 61.4 (-NCH₂-), 174.5 (-CO₂H); ν_{max} (nujol/cm⁻¹) 1641 (w, C=O), 2852 and 2937 (s, C-H); m/z (CI⁺) 159 (100%, [M + H]⁺), 158 (7%, [M]⁺); HRMS found 159.1133, [M + H]⁺ (C₇H₁₅N₂O₂) requires 159.1133.

Resin 291



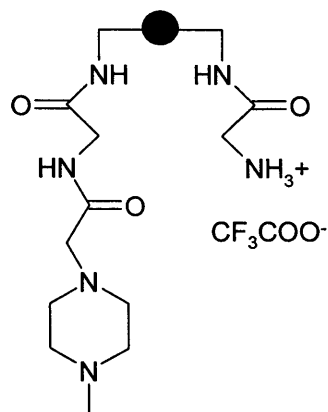
Resin **234** (4.41 g, 0.18 mmol/g) was swelled in dimethylformamide for 30 min. and then filtered. To the resin was added a solution of piperidine/dimethylformamide (2:8, 50 ml) and the mixture was shaken for 7 h. The Kaiser test indicated the reaction was complete. The resin was filtered and washed with dimethylformamide (200 ml), dichloromethane (200 ml), dimethylformamide (100 ml), dichloromethane (200 ml) and dried under vacuum to yield the desired product (4.22 g). ν_{max} (solid state/cm⁻¹) 1678 (s, C=O (amide)), 1715 (s, C=O (Boc)), 2904 (s, C-H), 3345 (w, N-H).

Resin 365



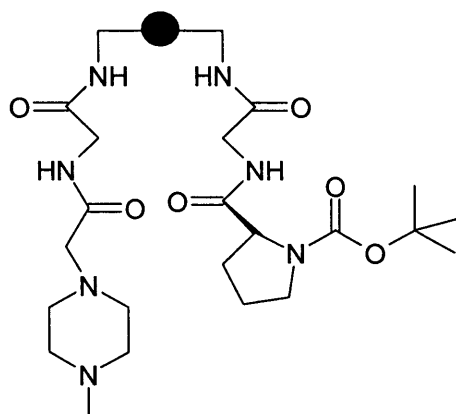
To compound **290** (0.22 g, 1.39 mmol) in dimethylformamide (20 ml), HOBt (0.19 g, 1.39 mmol) followed by diisopropylamine (0.30 ml, 1.94 mmol) were added. The solution was stirred at room temperature for 20 min. and then added to the resin **291** (1.54 g, 0.18 mmol/g) which was previously swelled in dimethylformamide for 30 min.. The reaction mixture was shaken at room temperature for 19 h. The Kaiser test indicated the reaction was complete. The resin was filtered and washed with dimethylformamide (100 ml), dichloromethane (100 ml), dimethylformamide (100 ml), dichloromethane (100 ml) and dried under vacuum to give product **365** (1.63 g). ν_{\max} (solid state/ cm^{-1}) 1674 (s, C=O (amide)), 1715 (s, C=O (Boc group)), 2878 (s, C-H), 3348 (m, N-H).

Resin 292



Resin **365** (1.37 g, 0.18 mmol/g) was swelled in dichloromethane for 30 min. and then filtered. The resulting resin was treated with trifluoroacetic acid/dichloromethane (1:1, 30 ml) and the mixture shaken for 4 h. The Kaiser test indicated the reaction was complete. The resin was filtered and washed with dichloromethane (5 x 50 ml) and dried under vacuum to give the product **292** (1.92 g). ν_{max} (solid state/ cm^{-1}) 1692 (s, C=O (amide)), 1782 (s, C=O (TFA salt)), 2921 (s, C-H), 3373 (m, N-H).

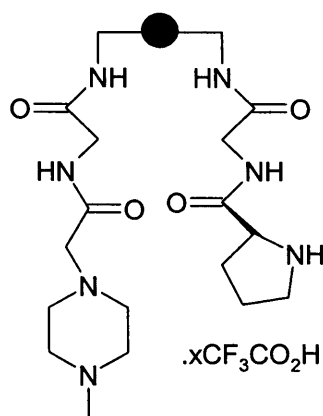
Resin 366



Resin **292** (1.92 g, 0.22 mmol/g) was washed with a pyridine/dichloromethane solution (1:1, 100 ml) and then dichloromethane (5 x 40 ml).

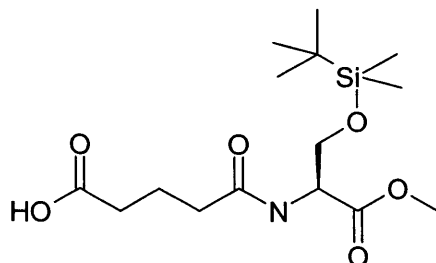
Boc-Proline (0.45 g, 2.10 mmol) was dissolved in dimethylformamide (20 ml), HOBt (0.29 g, 2.10 mmol) followed by diisopropylcarbodiimide (0.46 ml, 2.96 mmol) were added. The resulting mixture was stirred for 30 min. at room temperature and then added to the resin (above). The mixture was shaken at room temperature for 24 h. The Kaiser test indicated the reaction was complete. The resin was filtered and washed with dimethylformamide (3 x 30 ml), dichloromethane (3 x 30 ml), dimethylformamide (50 ml) and then dichloromethane (100 ml) and dried under vacuum to give product **366** (2.21 g).

Resin 293



Resin **366** (1.10 g, 0.22 mmol/g) was swelled in dichloromethane for 30 min. and then filtered. The resin was then treated with trifluoroacetic acid/dichloromethane (1:1, 30 ml) and the mixture shaken for 6 h. The Kaiser test indicated the reaction was complete. The resin was filtered and washed with dichloromethane (5 x 50 ml) and dried under vacuum to give the product **293** (1.15 g).

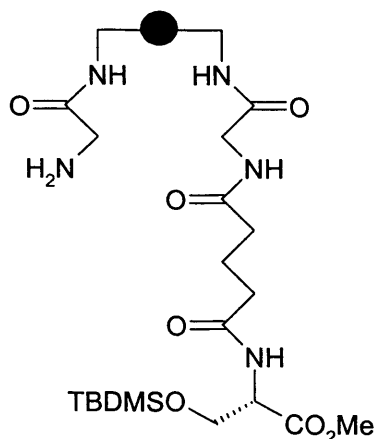
4-[(S)-2-(*tert*-Butyl-dimethyl-silanyloxy)-1-methoxycarbonyl-ethylcarbamoyl]-butyric acid (323)



TBDMS-Serine methyl ester **322** (200 mg, 0.86 mmol) was dissolved in anhydrous dichloromethane (4 ml). Triethylamine (0.15 ml, 1.08 mmol) and glutaric anhydride (120 mg, 1.03 mmol) were added and the mixture was heated at reflux for 18 h. After cooling, the solution was concentrated *in vacuo*. The crude residue was dissolved in ethyl acetate (30 ml) and washed with aqueous HCl (2M, 30 ml), water (30 ml) and brine (30 ml) and dried over MgSO₄. The solvent was removed *in vacuo* to yield the product as a clear oil (210 mg, 73%). ¹H NMR (300 MHz, CDCl₃) δ_H/ppm –0.05 (s, 6H, -Si(CH₃)₂), 0.74 (s, 9H, -C(CH₃)₃), 1.90 (m, 3H, CO₂CH(H)CH₂CH₂-), 2.29 (m, 3H, CO₂CH(H)CH₂CH₂-), 3.63 (s, 3H, -CO₂CH₃), 3.71 (dd, *J* = 3.2, *J* = 10.1, 1H, -CH(H)OSi-), 3.94 (dd, *J* = 2.9, *J* = 10.1, 1H, -CH(H)OSi-), 4.60 (m, 1H, -NHCHCO-), 6.70 (m, 1H, NH); ¹³C NMR (75 MHz, CDCl₃) δ_C/ppm – 5.4 (-Si(CH₃)₂), 18.2 (-SiC(CH₃)₃), 20.7 (-NHC(O)CH₂CH₂-), 25.8 (-SiC(CH₃)₃), 33.0 (O₂CCH₂CH₂CH₂-), 35.1 (O₂C(CH₂)₂CH₂-), 52.5 (-CH₃), 54.4 (-NHCHCO₂-), 63.6 (-CH₂OSi-), 171.2 (-NHC(O)-), 172.8 (-CO₂CH₃), 177.2 (-CO₂H); ν_{max} (neat/cm⁻¹) 1060 (s, Si-O), 1653 (s, C=O (amide)), 1740 (s, C=O (acid and ester)), 2949 (s, C-H), 3333 (s, N-H); m/z (CI⁺) 348 (100%, [M + H]⁺); HRMS found 348.1834, [M + H]⁺ (C₁₄H₂₈NO₆Si) requires 348.1842; [α]_D + 28.6 ° (c 0.44, MeOH).

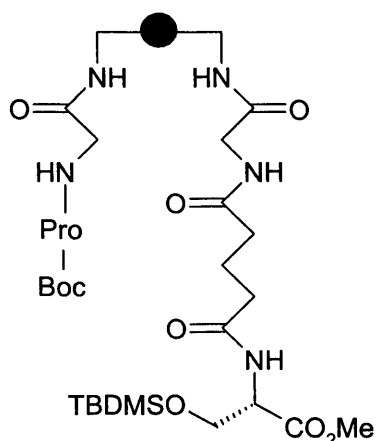
Acid **323** (1.00 g, 2.88 mmol) was dissolved in dimethylformamide (7 ml) and HOBT (0.39 g, 2.88 mmol), followed by diisopropylcarbodiimide (0.63 ml, 4.06 mmol) were added. The solution was stirred for 5 min. and then added to the resin (above), and the resulting mixture was shaken at room temperature for 2 days. The Kaiser test indicated the reaction was completed. The resin was filtered and washed sequentially with dimethylformamide (3 x 40 ml), dichloromethane (3 x 40 ml), dimethylformamide (50 ml) and dichloromethane (100 ml). The resin was dried under vacuum to give product **324** (2.23 g). Fmoc substitution = 0.23 mmol/g.

Resin 367



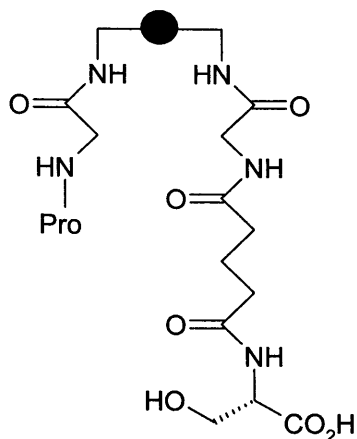
A solution of piperidine/dimethylformamide (2:8, 30 ml) was added to resin **324** (2.15 g, 0.23 mmol/g) and the mixture was shaken at room temperature for 18 h. The Kaiser test indicated the reaction was complete. The resin was filtered and washed sequentially with dimethylformamide (200 ml), dichloromethane (200 ml), dimethylformamide (100 ml) and dichloromethane (100 ml). The resin was dried under vacuum to give product **367** (2.05 g).

Resin 368



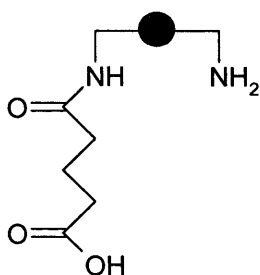
Resin **367** (1.94 g, 0.23 mmol/g) was swelled in dimethylformamide for 30 min. and then filtered. To Boc-Proline (0.35 g, 1.65 mmol) in dimethylformamide (10 ml), HOBT (0.22 g, 1.65 mmol) followed by diisopropylcarbodiimide (0.36 ml, 2.31 mmol) were added. The mixture was stirred for 5 min. and this solution was then added to the resin.

Resin 326



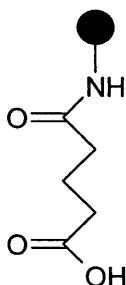
Resin **325** (1.00 g, 0.17 mmol/g) was swelled in dioxane for 30 min. and then filtered. To the resin, a cooled solution ($\sim 0^{\circ}\text{C}$) of aqueous NaOH (1M)/dioxane (1:3, 20 ml) was added. The reaction mixture was left to stand at 0°C for 1 h. Malachite green test indicated the reaction was completed. The resin was filtered and washed sequentially with water (3 x 50 ml), dioxane (50 ml), methanol (50 ml) and dichloromethane (3 x 50 ml). The resin was dried under vacuum to give product **326** (0.83 g).

Resin 212



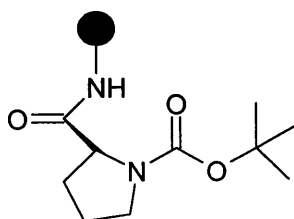
Tentagel resin (0.50 g, 0.40 mmol/g) was washed with dichloromethane (3 x 10 mL) using a Merrifield bubbler. A mixture of glutaric anhydride (11.0 mg, 0.10 mmol) in anhydrous dichloromethane (8 ml) was added under nitrogen and the Merrifield bubbler shaken at room temperature for 24 h. The resin was filtered and washed sequentially with dichloromethane (2 x 10 ml), tetrahydrofuran (2 x 10 ml), methanol (2 x 10 ml) and dichloromethane (2 x 10 ml) and then dried under vacuum to give the resin (0.54 g).

Resin 287



Tentagel resin (0.57 g, 0.40 mmol/g) was swelled in chloroform for 30 min. and then filtered. A solution of glutaric anhydride (0.26 g, 2.28 mmol) in chloroform (4 ml) was then added and the mixture was shaken at room temperature for 24 h. After this time, the Kaiser test indicated complete reaction. The resin was then filtered, and washed with chloroform (10 x 10 ml) and dried under vacuum to yield the desired product (0.70 g). ν_{max} (solid state/ cm^{-1}) 1669 (m, C=O (amide)), 1729 (m, C=O (carboxylic acid)), 2867 (s, C-H), 3512 (m, N-H).

Resin 285

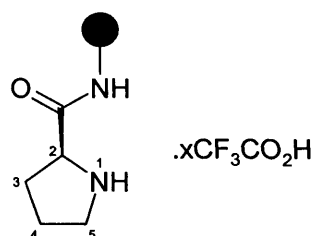


Tentagel resin (1.05 g, 0.40 mmol/g) was swelled in dimethylformamide for 30 min. and then filtered.

Boc-Proline (0.45 g, 2.10 mmol) was dissolved in dimethylformamide (5 ml) and HOBT (0.28 g, 2.10 mmol) followed by diisopropylcarbodiimide (0.46 ml, 2.94 mmol) were

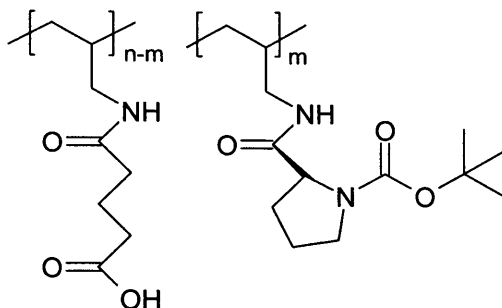
added. The solution was immediately added to the resin and the mixture shaken at room temperature for 17 h. After this time, the Kaiser test indicated incomplete reaction. The resin was filtered, washed with dimethylformamide (3 x 40 ml) and then re-treated with the above reagents. The mixture was subsequently shaken for an additional 2 h, after which time, the Kaiser test indicated complete reaction. The resin was then filtered and washed with dimethylformamide (2 x 30 ml), dichloromethane (2 x 30 ml), dimethylformamide (50 ml) and dichloromethane (100 ml). The resin was dried under vacuum to yield the desired product (1.30 g).

Resin 286



A mixture of trifluoroacetic acid/dichloromethane (1:1, 40 ml) was added to resin **285** (1.10 g, 0.40 mmol/g) and the resulting mixture shaken at room temperature for 3 h. After this time, the chloronil test indicated completion of the reaction. The resin was then washed with a mixture of trifluoroacetic acid/dichloromethane (1:1, 40 ml), dichloromethane (7 x 10 ml) and dried under vacuum to yield the desired product (1.13 g); ¹H NMR (400 MHz, solid state) δ_H/ppm 1.00 – 2.45 (br, H(3) and H(4)), 3.25 – 3.90 (br, H(5) and H of polyethylene glycol (tentagel)), 4.15 – 4.45 (br, H(2)), 6.20 – 8.60 (ArH of polystyrene (tentagel)); ν_{max} (solid state/cm⁻¹) 1687 (w, C=O), 2914 (s, C-H), 3391 (s, N-H).

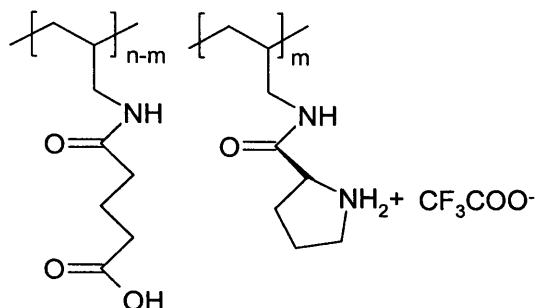
Polymer 239



Polyallylamine hydrochloride (0.18 g, 3.16 mmol) was treated with potassium hydroxide (0.13 mg, 2.32 mmol) in methanol (40 ml) at room temperature for 16 h. The solvent was removed under reduced pressure and ethanol (35 ml) was added to the residue. The resulting white precipitate was removed by filtration and the filtrate was concentrated *in vacuo* to leave approximately 10 ml of solvent. To the mixture was added chloroform (10 ml), followed by glutaric anhydride (0.18 g, 1.58 mmol) and the reaction mixture was stirred for 6 h at room temperature.

Concurrently, diisopropylcarbodiimide (0.32 ml, 2.05 mmol), followed by *N*-hydroxysuccinimide (0.27 g, 2.37 mmol) were added to a solution of Boc-proline (0.34 g, 1.58 mmol) in chloroform (10 ml). The resulting solution was stirred at room temperature for 6 h. The mixture was then added to the solution containing polyallylamine (above) and stirring was continued for 18 h. The solvents were removed under reduced pressure and the residue was washed with chloroform (3 x 20 ml), methanol (3 x 20 ml) and chloroform (2 x 20 ml). The resulting solid was dried under vacuum to give the desired product as a white powder (430 mg). ^{13}C NMR (75 MHz, solid state) δ_c /ppm 23.5 and 25.4 (br, $-\text{C}(\underline{\text{C}}\text{H}_3)_3$), 28.9 – 49.9 (br, $\underline{\text{C}}\text{H}$ and $\underline{\text{C}}\text{H}_2$ of polyallylamine, $\underline{\text{C}}\text{H}_2$ of butyric acid and $\underline{\text{C}}\text{H}$ and $\underline{\text{C}}\text{H}_2$ of proline), 80.5 (br, $-\underline{\text{C}}(\text{CH}_3)_3$), 158.2 (br, $-\text{N}\underline{\text{C}}(\text{O})\text{OC}(\text{CH}_3)_3$), 174.9 (br, $-\underline{\text{C}}(\text{O})\text{NH}-$ and $-\underline{\text{C}}\text{OOH}$);

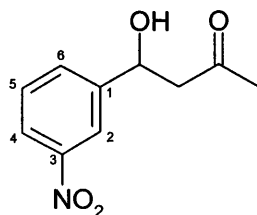
Polymer 240



A mixture of polymer **239** (400 mg) and trifluoroacetic acid/dichloromethane (1:1, 20 ml) was shaken at room temperature for 2.5 h. The polymer was filtered, washed with dichloromethane (5 x 30 ml) and then dried under vacuum. The desired polymer was isolated as a white powder (470 mg). ^{13}C NMR (75 MHz, solid state) δ_c/ppm 22.1 – 43.3 (br, $\underline{\text{CH}}$ and $\underline{\text{CH}_2}$ of polyallylamine, $\underline{\text{CH}_2}$ of butyric acid and $\underline{\text{CH}}$ and $\underline{\text{CH}_2}$ of proline), 115.4 – 118.6 (br, $-\underline{\text{CF}_3\text{COO}^-}$), 162.2 ($-\text{C}(\text{O})\text{NH}-$ (proline)), 176.0 (br, $-\underline{\text{C}}(\text{O})\text{NHCH}_2-$ and $-\underline{\text{COOH}}$); ν_{max} (solid state/ cm^{-1}) 1378, 1238 (s, C-F), 1693 (m, C=O (amides and carboxylic acid)), 2913 (m, C-H), 3072 (m, O-H (carboxylic acid)), 3367 (m, N-H);

4.3.4 Synthesis of Racemic Aldol Products

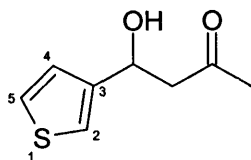
4-Hydroxy-4-(3-nitro-phenyl)-butan-2-one (267)



To a stirred solution of 3-nitrobenzaldehyde (3.00 g, 20.0 mmol) in acetone (38 ml), aqueous NaOH (1% w/v, 3.80 ml) was added dropwise at 0 °C. Stirring was continued

at this temperature for an additional 15 min.. The solution was then neutralised (pH 7; by addition of aqueous HCl (0.5 M)) and concentrated *in vacuo*. The residue was suspended in water (40 ml) and extracted with diethyl ether (3 x 40 ml). The combined organic extracts were washed with brine (100 ml), dried over MgSO₄, and evaporated *in vacuo*. Purification by flash chromatography (SiO₂; gradient; petroleum spirit/ethyl acetate (3:1) to petroleum spirit/ethyl acetate (1:2)) gave the desired product as a brown oil (0.87 g, 21%). R_f = 0.41 (SiO₂; petroleum spirit/ethyl acetate; 1:1); ¹H NMR (300 MHz, CDCl₃) δ_H /ppm 2.21 (s, 3H, -CH₃), 2.80 (m, 2H, -CH₂C(O)CH₃), 3.73 (m, 1H, OH), 5.18 (m, 1H, -ArCH(OH)-), 7.51, 7.68, 8.09 and 8.21 (m, 4H, ArH); ¹³C NMR (75 MHz, CDCl₃) δ_C /ppm 31.0 (-CH₃), 51.8 (-CH₂C(O)CH₃), 69.1 (-ArCH(OH)-), 121.0, 122.8, 129.8 and 132.1 (4 x ArC), 145.2 and 148.6 (C(1) and C(3)), 208.9 (-CH₂C(O)CH₃); ν_{max} (neat/cm⁻¹) 1070 (s, C-O), 1500 (w, Ar), 1522 (s, N=O), 1601 (w, Ar), 1709 (s, C=O), 2907 (m, C-H), 3427 (s, O-H); m/z (CI⁺) 192 (68%, [M - H₂O]⁺).

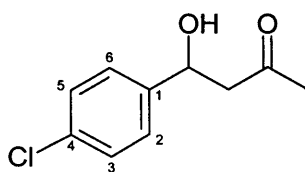
4-Hydroxy-4-(thiophen-3-yl)-butan-2-one (259)



To a stirred solution of 3-thiophenecarboxaldehyde (3.00 ml, 33.0 mmol) in acetone (62 ml), aqueous NaOH (1% w/v, 6.2 ml) was added dropwise at 0 °C. Stirring was continued at this temperature for an additional 15 min.. The solution was then neutralised (pH 7; by addition of aqueous HCl (0.5 M)) and concentrated *in vacuo*. The residue was suspended in water (30 ml) and extracted with diethyl ether (3 x 30 ml). The combined organic extracts were washed with brine (100 ml), dried over MgSO₄, and evaporated *in vacuo*. Purification by flash chromatography (SiO₂; gradient; petroleum spirit/ethyl acetate (3:1) to petroleum spirit/ethyl acetate (1:1)) gave the desired product as a brown liquid (2.96 g, 53%). R_f = 0.49 (SiO₂; petroleum spirit:ethyl acetate; 1:1); ¹H NMR (300 MHz, CDCl₃) δ_H /ppm 2.10 (s, 3H, -CH₃), 2.79 (m, 2H, -CH₂C(O)CH₃), 3.74 (m, 1H, OH), 5.15 (m, 1H, -ArCH(OH)-), 6.99 (m, 1H, H(4)), 7.12

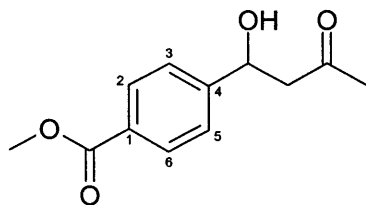
(m, 1H, H(2)), 7.23 (m, 1H, H(5)); ¹³C NMR (75 MHz, CDCl₃) δ_c/ppm 30.8 (-CH₃), 51.3 (-CH₂C(O)CH₃), 66.3 (-ArCH(OH)-), 120.9, 125.6 and 126.3 (C(4), C(5) and C(2)), 144.5 (C(3)), 208.9 (-CH₂C(O)CH₃); ν_{max} (neat/cm⁻¹) 1070 (s, C-O), 1705 (s, C=O), 2901 (m, C-H), 3416 (s, O-H); m/z (EI) 170 (42%, [M]⁺); HRMS found 170.0389, [M]⁺ (C₈H₁₀O₂S) requires 170.0396.

4-(4-Chloro-phenyl)-4-hydroxy-butan-2-one (220)¹⁷⁰



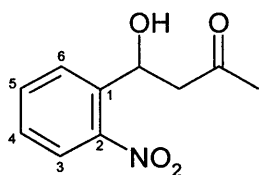
To a stirred solution of 4-chlorobenzaldehyde (3.00 g, 21.0 mmol) in acetone (38 ml), aqueous NaOH (1% w/v, 3.8 ml) was added dropwise at 0 °C. Stirring was continued at this temperature for an additional 15 min.. The solution was then neutralised (pH 7; by addition of aqueous HCl (0.5 M)) and concentrated *in vacuo*. The residue was suspended in water (30 ml) and then extracted with diethyl ether (3 x 30 ml). The combined organic extracts were washed with brine (100 ml), dried over MgSO₄ and evaporated *in vacuo*. Purification by flash chromatography (SiO₂; gradient; petroleum spirit/ethyl acetate (3:1) to petroleum spirit/ethyl acetate (1:1)) gave the desired product as a yellow oil (2.91 g, 69%). R_f = 0.50 (SiO₂; petroleum spirit/ethyl acetate; 1:1); ¹H NMR (300 MHz, CDCl₃) δ_H/ppm 2.01 (s, 3H, -CH₃), 2.58 (m, 2H, -CH₂C(O)CH₃), 3.98 (m, 1H, OH), 4.94 (m, 1H, -ArCH(OH)-), 7.15-7.18 (m, 4H, ArH); ¹³C NMR (75 MHz, CDCl₃) δ_c/ppm 30.6 (-CH₃), 51.8 (-CH₂C(O)CH₃), 68.9 (-ArCH(OH)-), 127.1 (C(3) and C(5)), 128.4 (C(2) and C(6)), 132.9 (C(4)), 141.8 (C(1)), 208.5 (-CH₂C(O)CH₃); ν_{max} (DCM/cm⁻¹) 1076 (s, C-O), 1497 (s, Ar), 1601 (s, Ar), 1709 (s, C=O), 2905 (m, C-H), 3427 (s, O-H); m/z (EI) 198 (25%, [M]⁺); HRMS found 198.0442, [M]⁺ (C₁₀H₁₁ClO₄) requires 198.0442.

4-(1-Hydroxy-3-oxo-butyl)-benzoic acid methyl ester (261)



To a stirred solution of 4-acetoxybenzaldehyde (3.00 g, 18.0 mmol) in acetone (33 ml), aqueous NaOH (1% w/v, 3.3 ml) was added dropwise at 0 °C. Stirring was continued at this temperature for an additional 15 min.. The solution was neutralised (pH 7; by addition of aqueous HCl (0.5 M)) and then concentrated *in vacuo*. The residue was suspended in water (30 ml) and extracted with diethyl ether (3 x 30 ml). The combined organic extracts were washed with brine (100 ml), dried over MgSO₄, and evaporated *in vacuo*. Purification by flash chromatography (SiO₂; gradient; petroleum spirit/ethyl acetate (3:1) to petroleum spirit/ethyl acetate (2:1)) gave the desired product as a white solid (1.13 g, 28%). **m.p.** 60 °C; **R_f** = 0.42 (SiO₂; petroleum spirit/ethyl acetate; 1:1); **¹H NMR** (300 MHz, CDCl₃) δ_{H} /ppm 2.14 (s, 3H, -CH₃), 2.75 (m, 2H, -CH₂C(O)CH₃), 3.72 (m, 1H, OH), 3.84 (s, 3H, -CO₂CH₃), 5.15 (m, 1H, -ArCH(OH)-), 7.37 (d, *J* = 8.4, 2H, H(3) and H(5)), 7.93 (d, *J* = 8.4, 2H, H(2) and H(6)); **¹³C NMR** (75 MHz, CDCl₃) δ_{C} /ppm 40.0 (-CH₃), 52.0 (-CH₂C(O)CH₃), 52.3 (-CO₂CH₃), 69.6 (-ArCH(OH)-), 125.8 (2 x ArC), 130.0 (C(1)), 130.3 (2 x ArC), 148.3 (C(4)), 167.1 (-CO₂CH₃), 208.8 (-CH₂C(O)CH₃); ν_{max} (DCM/cm⁻¹) 1074 (s, C-O), 1502 and 1611 (s, Ar), 1693 (s, C=O), 2951 (w, C-H), 3493 (s, O-H); **m/z** (EI) 222 (64%, [M]⁺); **HRMS** found 222.08901, [M]⁺ (C₁₂H₁₄O₄) requires 222.08866.

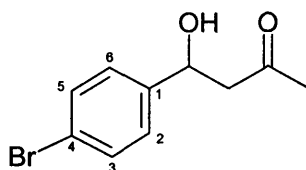
4-Hydroxy-4-(2-nitro-phenyl)-butan-2-one (269)¹⁷¹



To a stirred solution of 2-nitrobenzaldehyde (3.00 g, 20.0 mmol) in acetone (38 ml), aqueous NaOH (1% w/v, 3.8 ml) was added dropwise at 0 °C. Stirring was continued at

this temperature for an additional 15 min.. The solution was then neutralised (pH 7; by addition of aqueous HCl (0.5 M)) and concentrated *in vacuo*. The residue was suspended in water (30 ml) and extracted with diethyl ether (3 x 30 ml). The combined organic extracts were washed with brine (100 ml), dried over MgSO₄ and evaporated *in vacuo*. Purification by flash chromatography (SiO₂; gradient; petroleum spirit/ethyl acetate (3:1) to petroleum spirit/ethyl acetate (1:2)) gave the desired product as a brown oil (2.49 g, 60%). **R_f** = 0.43 (SiO₂; petroleum spirit/ethyl acetate; 1:1); **¹H NMR** (300 MHz, CDCl₃) δ_{H} /ppm 2.14 (s, 3H, -CH₃), 2.68 (m, 1H, -CH(H)C(O)CH₃), 2.98 (m, 1H, -CH(H)C(O)CH₃), 3.93 (m, 1H, OH), 5.61 (m, 1H, -ArCH(OH)-), 7.38 (m, 1H, ArH), 7.60 (m, 1H, ArH), 7.84 (m, 2H, ArH); **¹³C NMR** (75 MHz, CDCl₃) δ_{C} /ppm 30.5 (-CH₃), 51.4 (-CH₂C(O)CH₃), 65.6 (-ArCH(OH)-), 124.5 (C(3)), 128.3 and 128.4 (C(4) and C(6)), 133.9 (C(5)), 138.8 (C(1)), 147.2 (C(2)), 208.7 (-CH₂C(O)CH₃); ν_{max} (neat/cm⁻¹) 1043 (m, C-O), 1526, 1574 and 1611 (m, Ar), 1701 (s, C=O), 2860 (w, C-H), 2947 (w, C-H), 3416 (s, O-H); **m/z** (CI) 210 (48%, [M + H]⁺); **HRMS** found 210.0756, [M + H]⁺ (C₁₀H₁₂NO₄) requires 210.0761.

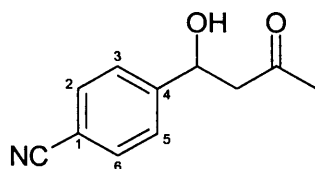
4-(4-Bromo-phenyl)-4-hydroxy-butan-2-one (251)¹⁷⁰



To a stirred solution of 4-bromobenzaldehyde (3.00 g, 32.0 mmol) in acetone (60 ml), aqueous NaOH (1% w/v, 6.00 ml) was added dropwise at 0 °C. The mixture was then stirred for 20 min.. The solution was then neutralised (pH 7; by addition of aqueous HCl (0.5 M)) and concentrated *in vacuo*. The resulting brown residue was suspended in water (50 ml) and extracted with ethyl acetate (3 x 70 ml). The combined organic extracts were dried over MgSO₄, filtered and concentrated. Purification by flash chromatography (SiO₂; gradient; petroleum spirit/ethyl acetate (3:1) to petroleum spirit/ethyl acetate (1:1)) gave the desired product as a brown oil (3.94 g, 26%). **R_f** = 0.50 (SiO₂; petroleum spirit/ethyl acetate; 1:1); **¹H NMR** (300 MHz, CDCl₃) δ_{H} /ppm 2.18 (s, 3H, -CH₃), 2.80 (m, 2H, -CH₂C(O)CH₃), 3.45 (s, 1H, OH), 5.12 (m, 1H, -

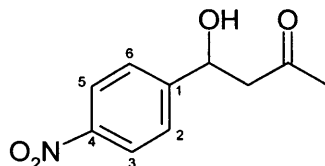
ArCH(OH)-), 7.25 (m, 2H, H(3) and H(5)), 7.39 (m, 2H, H(2) and H(6)); ¹³C NMR (75 MHz, CDCl₃) δ_c/ppm 31.1 (-CH₃), 52.1 (-CH₂C(O)CH₃), 69.5 (-ArCH(OH)-), 121.7 (C(4)), 127.7 (C(3) and C(5)), 132.0 (C(2) and C(6)), 142.1 (C(1)), 209.2 (-CH₂C(O)CH₃); ν_{max} (neat/cm⁻¹) 1020 (s, C-O), 1491 (s, Ar), 1709 (s, C=O), 2885 (w, C-H), 3427 (s, O-H); ⁺; m/z (Cl⁺) 243 (12%, [M + H]⁺), 187 (96%, [M - (CH₂C(O)CH₃)]⁺); HRMS found 243.0016, [M + H]⁺ (C₁₀H₁₂BrO₂) requires 243.0020.

4-(1-Hydroxy-3-oxo-butyl)-benzonitrile (271)¹⁷⁰



To a stirred solution of 4-cyanobenzaldehyde (4.00 g, 31.0 mmol) in acetone (48 ml), aqueous NaOH (1% w/v, 5.70 ml) was added dropwise at 0 °C. The mixture was then stirred for 15 min.. The solution was then neutralised (pH 7; by addition of aqueous HCl (0.5 M)) and concentrated *in vacuo*. The resulting brown residue was suspended in water (50 ml) and extracted with diethyl ether (3 x 80 ml). The combined organic extracts were dried over MgSO₄, filtered and concentrated. Purification by flash chromatography (SiO₂; gradient; petroleum spirit/ethyl acetate (3:1) to petroleum spirit/ethyl acetate (1:2)) gave the desired product as a white solid (0.81 g, 14%). **m.p.** 90 °C; **R_f** = 0.26 (SiO₂; petroleum spirit/ethyl acetate; 1:1); ¹H NMR (300 MHz, CDCl₃) δ_H/ppm 2.18 (s, 3H, -CH₃), 2.80 (d, *J* = 6.2, 2H, -CH₂C(O)CH₃), 3.68 (br s, 1H, OH), 5.18 (m, 1H, -ArCH(OH)-), 7.45 (d, *J* = 8.3, 2H, H(3) and H(5)), 7.60 (d, *J* = 8.4, 2H, H(2) and H(6)); ¹³C NMR (75 MHz, CDCl₃) δ_c/ppm 30.7 (-CH₃), 51.6 (-CH₂C(O)CH₃), 69.0 (-ArCH(OH)-), 111.3 (C(1)), 118.8 (-CN), 126.4 (C(3), C(5)), 132.4 (C(2) and C(6)), 148.2 (C(4)), 208.5 (-CH₂C(O)CH₃); ν_{max} (DCM/cm⁻¹) 1076 (s, C-O), 1504 and 1609 (m, Ar), 1709 (s, C=O), 2230 (s, C≡N), 2897 (w, C-H), 3435 (s, O-H); m/z (Cl⁺) 190 (100%, [M + H]⁺); HRMS found 190.0869, [M + H]⁺ (C₁₁H₁₁NO₂) requires 190.0868.

4-Hydroxy-4-(4-nitro phenyl) butan-2-one (116)¹²⁷



To a stirred solution of 4-nitrobenzaldehyde (4.00 g, 26.0 mmol) in acetone (48 ml), aqueous NaOH (1% w/v, 4.80 ml) was added at 0 °C. Stirring was continued for 15 min., at which point a black solution formed. The mixture was then neutralised (pH 7; by addition of aqueous HCl (0.5 M)) and concentrated *in vacuo*. The resulting brown residue was suspended in water (50 ml) and extracted with diethyl ether (3 x 80 ml). The combined organic layers were dried over MgSO₄ and concentrated to give the crude product as a brown solid. Purification by flash chromatography (SiO₂; gradient; petroleum spirit/ethyl acetate (3:1) to petroleum spirit/ethyl acetate (1:1)) gave the desired product as a yellow solid (2.54 g, 46%). **m.p.** 59 °C (lit. 59-61 °C¹²⁷); **R_f** = 0.26 (SiO₂; petroleum spirit/ethyl acetate; 1:1); **¹H NMR** (300 MHz, CDCl₃) δ_{H} /ppm 2.18 (s, 3H, -CH₂C(O)CH₃), 2.81 (d, *J* = 6.2, 2H, -CH₂C(O)CH₃), 3.79 (br s, 1H, -ArCH(OH)-), 5.22 (t, *J* = 6.1, 1H, -ArCH(OH)-), 7.49 (d, *J* = 7.0, 2H, H(3) and H(5)), 8.13 (d, *J* = 7.0, 2H, H(2) and H(6)); **¹³C NMR** (75 MHz, CDCl₃) δ_{C} /ppm 30.9 (-CH₂C(O)CH₃), 51.8 (-CH₂C(O)CH₃), 69.1 (-ArCH(OH)-), 123.9 (C(3) and C(5)), 126.7 (C(2) and C(6)), 147.4 (C(4)), 150.5 (C(1)), 208.8 (-CH₂C(O)CH₃); ν_{max} (DCM/cm⁻¹) 1078 (s, C-O), 1340 (s, NO₂), 1518 (s, NO₂), 1600 (s, Ar), 1710 (s, C=O), 2907 (m, C-H), 3447 (s, O-H); **m/z** (Cl⁻) 210 (82%, [M + H]⁺); **HRMS** found 210.0770, [M + H]⁺ (C₁₀H₁₂NO₄) requires 210.0766.

4.3.5 General Procedures for Aldol Reactions

General Procedure for the Formation of Aldol Products with Resins

Control Reaction

Aldehyde (10 mg, 1 eqv.) was added to a stirred solution of tentagel resin (2 mol%) and *N*-methylmorpholine (1.52 eqv.) in ketone (1 ml). The reaction was stirred at room temperature for 18 h. Ethyl acetate (5 ml) was added to the mixture and the resin filtered and washed with ethyl acetate (2 x 5 ml). The combined organic filtrate was washed with aqueous saturated ammonium chloride (2 x 15 ml), followed by brine (2 x 15 ml). The organic extracts were dried over MgSO₄ and evaporated *in vacuo*.

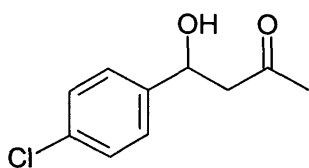
General Procedure

Aldehyde (10 mg, 1 eqv.) was added to a stirred solution of resin (2 mol%) and *N*-methylmorpholine (1.52 eqv.) in ketone (1 ml) and the reaction stirred at room temperature for 18 h. Ethyl acetate (5 ml) was added to the mixture and the resin was filtered and then washed with ethyl acetate (2 x 5 ml). The combined organic filtrate was washed with aqueous saturated ammonium chloride (2 x 15 ml), followed by brine (2 x 15 ml). The organic extracts were dried over MgSO₄ and evaporated *in vacuo*. The purification procedure is the same as for the corresponding aldol product racemates in Chapter 4.

$[\alpha]_D$ Values for the Enantiomeric Mixtures of the Aldol Products with Aldol Catalyst 238

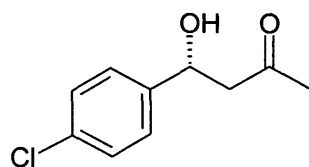
All the other analytical data for the products below, matched the data for the corresponding racemates in Chapter 4.

4-(4-Chloro-phenyl)-4-hydroxy-butan-2-one 220



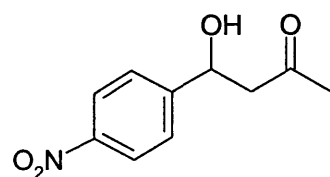
$[\alpha]_D + 13.5^\circ$ (*c* 0.48, CHCl₃)

Literature value:



$[\alpha]_D + 70.5^\circ$ (*c* 0.50, CHCl₃)¹⁷⁰

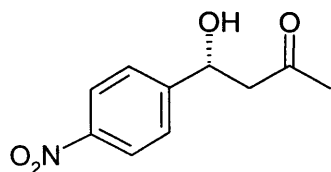
4-Hydroxy-4-(4-nitro-phenyl)-butan-2-one 116



$[\alpha]_D + 23.7^\circ$ (*c* 0.51, CHCl₃)

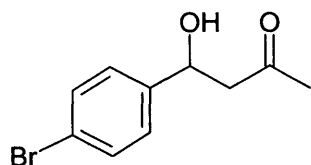
Chiral HPLC (OB, 80:20 Heptane/Isopropanol, 0.25 ml/min), *R_t* = 33.61 min (74%, Enantiomer A), *R_t* = 36.54 min (26%, Enantiomer B), *ee* = 48%.

Literature value:



$[\alpha]_{\text{D}} + 61.6^{\circ}$ (*c* 0.51, CHCl_3)¹¹⁸

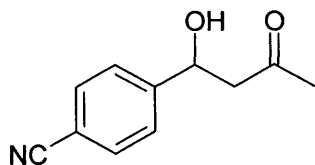
4-(4-Bromo-phenyl)-4-hydroxy-butan-2-one 251



$[\alpha]_{\text{D}} 0.0^{\circ}$

Chiral HPLC (OD, 95:5 Heptane/EtOH, 1 ml/min), $R_t = 2.80$ min (50%, Enantiomer A), $R_t = 3.10$ min (50%, Enantiomer B).

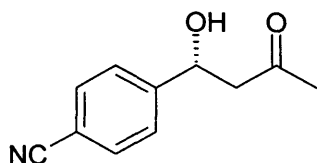
4-(1-Hydroxy-3-oxo-butyl)-benzonitrile 271



$[\alpha]_{\text{D}} + 40.8^{\circ}$ (*c* 0.48, CHCl_3)

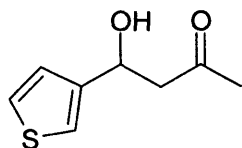
Chiral HPLC (OB, 90:10 Heptane/EtOH, 0.25 ml/min), $R_t = 12.43$ min (76%, Enantiomer A), $R_t = 15.50$ min (24%, Enantiomer B), *ee* = 51%.

Literature value:



$[\alpha]_{\text{D}} + 74.3^{\circ}$ (*c* 0.48, CHCl_3)¹⁷⁰

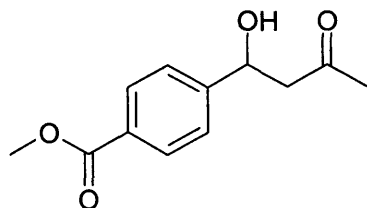
4-Hydroxy-4-(thiophen-3-yl)-butan-2-one 259



$[\alpha]_{\text{D}} - 6.8^{\circ}$ (*c* 0.88, CHCl_3)

Chiral HPLC (OB, 95:5 Heptane/EtOH, 1 ml/min), $R_t = 2.78$ min (15%, Enantiomer A), $R_t = 3.15$ min (85%, Enantiomer B), *ee* = 69%.

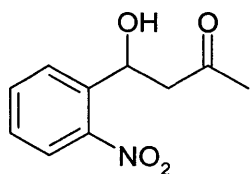
4-(1-Hydroxy-3-oxo-butyl)-benzoic acid methyl ester 261



$[\alpha]_{\text{D}} 0.0^{\circ}$

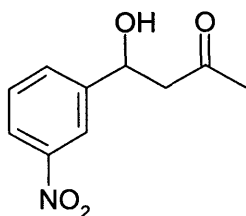
Chiral HPLC (OB, 95:5 Heptane/Isopropanol, 1 ml/min), $R_t = 2.83$ min (50%, Enantiomer A), $R_t = 3.14$ min (50%, Enantiomer B).

4-Hydroxy-4-(2-nitro-phenyl)-butan-2-one 269



$[\alpha]_D - 13.8^\circ$ (*c* 0.94, CHCl₃)

4-Hydroxy-4-(3-nitro-phenyl)-butan-2-one 267

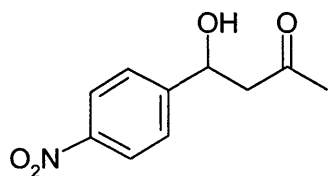


$[\alpha]_D 0.0^\circ$

Chiral HPLC (OB, 94:6 Heptane/Isopropanol, 1 ml/min), *R_t* = 2.79 min (15%, Enantiomer A), *R_t* = 3.11 min (85%, Enantiomer B).

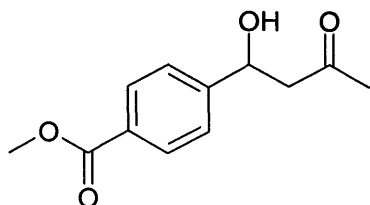
$[\alpha]_D$ Values for the Enantiomeric Mixtures of the Aldol Products with Aldolase Catalyst 325

4-Hydroxy-4-(4-nitro-phenyl)-butan-2-one 116



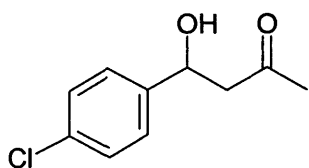
$[\alpha]_D + 23.7^\circ$ (*c* 0.51, CHCl₃)

4-(1-Hydroxy-3-oxo-butyl)-benzoic acid methyl ester 261



$[\alpha]_{\text{D}} 0.0^{\circ}$

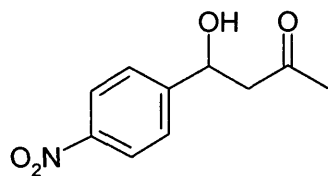
4-(4-Chloro-phenyl)-4-hydroxy-butan-2-one 220



$[\alpha]_{\text{D}} + 15.4^{\circ}$ (*c* 0.48, CHCl₃)

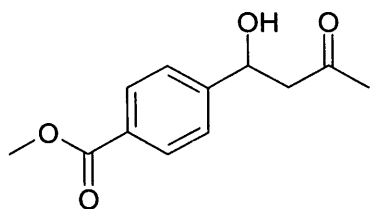
$[\alpha]_{\text{D}}$ Values for the Enantiomeric Mixtures of the Aldol Products with Aldolase Catalyst 326

4-Hydroxy-4-(4-nitro-phenyl)-butan-2-one 116



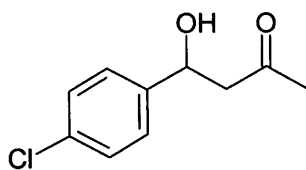
$[\alpha]_{\text{D}} + 23.5^{\circ}$ (*c* 0.51, CHCl₃)

4-(1-Hydroxy-3-oxo-butyl)-benzoic acid methyl ester 261



$[\alpha]_{\text{D}} + 7.8^{\circ}$ (*c* 0.41, CHCl₃)

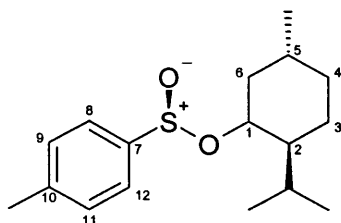
4-(4-Chloro-phenyl)-4-hydroxy-butan-2-one 220



$[\alpha]_{\text{D}} - 6.5^{\circ}$ (*c* 0.48, CHCl₃)

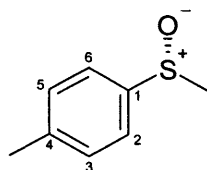
4.3.6 Synthesis of Sulfoxide Transition State Analogues

(S)-(-)-Menthyl *p*-toluenesulfinate (319)¹³⁶



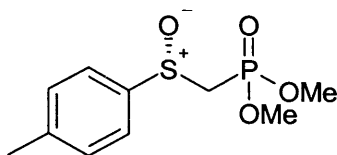
para-Toluene sulfinic acid (2.00 g, 11.0 mmol) was added portionwise to a solution of thionyl chloride (4.10 ml, 56.0 mmol) in benzene at 0 °C. The mixture was then allowed to warm to room temperature and then the volatiles were removed under reduced pressure. The residue was dissolved in anhydrous ether (20 ml) and cooled to 0 °C under nitrogen. A solution of (-)-menthol (1.93 g, 12.0 mmol) in pyridine (2 ml) was then added dropwise. After the addition was complete, the mixture was stirred for 3 h at room temperature. Water (20 ml) was added and the layers were separated. The organic layer was washed with aqueous HCl (10 % v/v, 20 ml) and brine (20 ml) and dried over MgSO₄. The solvent was evaporated and the remaining residue dissolved in acetone (8 ml) and five drops of concentrated aqueous HCl were added. The mixture was allowed to stand in the freezer (-18 °C) for 2 days. The resulting solid was isolated and then recrystallised from acetone and dried under vacuum. The desired product was isolated as a white crystalline solid (1.02 g, 31%). **m.p.** 106 °C (lit. 110 °C¹³⁶); **R_f** = 0.83 (SiO₂; ethyl acetate/petroleum spirit; 1:1); **¹H NMR** (300 MHz, CDCl₃) δ_H/ppm 0.71 (d, *J* = 6.9, 3H, H(5)CH₃), 0.85 (d, *J* = 7.1, 3H, -CHCH₃), 0.95 (d, *J* = 6.5, 3H, -CHCH₃), 1.01 – 1.46 (m, 5H, H(2), H(3), HH(6) and H(5)), 1.67 (m, 2H, H(4)), 2.14 (m, 1H, -CH(CH₃)₂), 2.27 (m, 1H, HH(6)), 2.40 (s, 3H, ArCH₃), 4.10 (m, 1H, H(1)), 7.30 (d, *J* = 8.0, 2H, H(9) and H(11)), 7.59 (d, *J* = 8.1, 2H, H(8) and H(12)); **¹³C NMR** (75 MHz, CDCl₃) δ_C/ppm 15.8 (C(5)CH₃), 21.1, 21.7, 22.3 (ArCH₃ and CH(CH₃)₂), 23.5 (C(3)), 25.6 (-CH(CH₃)₂), 32.0 (C(5)), 34.4 (C(4)), 43.3 (C(6)), 48.2 (C(2)), 80.3 (C(1)), 125.3 (C(8) and C(12)), 129.9 (C(9) and C(11)), 142.6, 143.6 (C(7) and C(10)); **ν_{max}** (DCM/cm⁻¹) 1040 (w, S=O), 1495 (s, Ar), 1593 (s, Ar), 2924 (s, C-H); **m/z** (FAB) 295 (19%, [M + H]⁺); **[α]_D** - 207 ° (c 2.0, acetone), lit. - 201 ° (c 2.0, acetone).¹³⁶

(+)-1-Methanesulfinyl-4-methyl benzene (321)¹³⁶



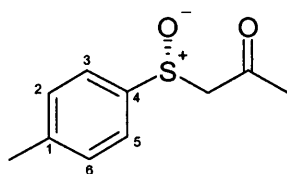
Methyl magnesium iodide in diethyl ether (1.7 M, 1.50 ml, 2.49 mmol) was added dropwise to a stirred mixture of (-)-(S)-menthyl-*p*-toluenesulfinate **319** (0.50 g, 1.78 mmol) in anhydrous ether (3.5 ml) and tetrahydrofuran (1.5 ml) at 0 °C under nitrogen. After the addition, the mixture was allowed to warm to room temperature and stirring was continued for 4 h. The reaction was quenched by the addition of saturated aqueous ammonium chloride solution (5 ml) and the resulting layers were separated. The organic layer was washed with brine (5 ml), dried over MgSO₄, and solvents removed under reduced pressure. The oily residue was suspended in hot hexane, until the formation of a yellow precipitate was observed. After cooling at 4 °C for 18 h, the resulting solid was isolated and recrystallised from ether/hexane. The desired sulfoxide was isolated as a white solid (70.0 mg, 27%). **m.p.** 73 °C (lit. 73 - 74 °C¹³⁶); **R_f** = 0.40 (SiO₂; petroleum spirit/ethyl acetate; 1:2); **¹H NMR** (300 MHz, CDCl₃) δ_{H} /ppm 2.38 (s, 3H, CH₃Ar-), 2.68 (s, 3H, ArS(O)CH₃), 7.24 (d, *J* = 6.5, H(3) and H(5)), 7.51 (d, *J* = 7.4, 2H, H(2) and H(6)); **¹³C NMR** (75 MHz, CDCl₃) δ_{C} /ppm 21.3 (CH₃Ar-), 44.0 (ArS(O)CH₃), 123.6 (C(2) and C(6)), 130.0 (C(3) and C(5)), 141.5 (C(4)), 142.6 (C(1)); ν_{max} (DCM/cm⁻¹) 1036 (s, S=O), 1599 (w, Ar), 2914 (w, C-H); **m/z** (CI⁺) 155 (100%, [M + H]⁺); **[α]_D** + 194 ° (c 1.5, CHCl₃), lit. + 145 ° (c 1.5, CHCl₃).¹⁷²

Dimethylphosphorylmethyl *p*-tolyl sulfoxide (320)¹³⁷



Dimethyl methanephosphonate (0.38 ml, 3.56 mmol) in anhydrous tetrahydrofuran (6 ml) was stirred at -78°C under nitrogen. *n*-Butyllithium in hexanes (2.32 M, 1.69 ml, 3.91 mmol) was added dropwise and stirring was continued for 30 min.. (-)-(S)-Menthyl *p*-toluenesulfinate **321** (0.50 g, 1.78 mmol) dissolved in THF (3.5 ml) was added and stirring was continued at -78°C for a further 15 min.. The mixture was then warmed to -20°C and the reaction quenched by the addition of saturated aqueous ammonium chloride (10 ml). The volatiles were removed *in vacuo* and the resulting aqueous mixture was washed with petroleum spirit (25 ml) and then extracted with chloroform (3 x 15 ml). The chloroform extracts were combined, dried over MgSO_4 and concentrated under reduced pressure to yield the crude material as a colourless oil, which was used immediately in the next step without further purification.

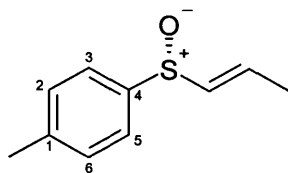
(+)-1-(Toluene-4-sulfinyl)-propan-2-one (316)¹⁷³



Diisopropylamine (0.42 ml, 2.99 mmol) in anhydrous tetrahydrofuran (23 ml) was cooled to -78°C under nitrogen. *n*-Butyllithium in hexanes (2.17 M, 1.31 ml, 2.84 mmol) was added and the reaction was stirred for 15 min.. The solution was warmed to 0°C and stirred at this temperature for 30 min. The mixture was then re-cooled to -78°C and the sulfoxide **321** (230 mg, 1.49 mmol) in tetrahydrofuran (5 ml) was added dropwise. After the addition, the mixture was allowed to warm up to 0°C and stirred for

1 h. Ethyl acetate (0.22 ml, 2.24 mmol) was then added and stirring was continued for 2 h. The reaction was quenched by the addition of saturated aqueous ammonium chloride (30 ml) and the resulting organic layer was separated. The aqueous layer was then acidified with aqueous HCl (10% v/v) to ~ pH4 and extracted with dichloromethane (30 ml). The organic extracts were combined and dried over MgSO₄. The solvents were removed *in vacuo* to yield the product as a yellow solid (97.6 mg, 33%). **m.p.** 33 °C (lit. 38 °C¹⁷³); **R_f** = 0.21 (SiO₂; ethyl acetate/petroleum spirit; 1:1); **¹H NMR** (300 MHz, CDCl₃) δ_{H} /ppm 2.05 (s, 3H, CH₃Ar-), 2.24 (s, 3H, -CH₂C(O)CH₃), 3.75 (s, 2H, -CH₂C(O)-), 7.16 (d, *J* = 8.1, 2H, H(2) and H(6)), 7.38 (d, *J* = 8.1, 2H, H(3) and H(5)); **¹³C NMR** (75 MHz, CDCl₃) δ_{C} /ppm 20.9 (CH₃Ar-), 31.5 (-C(O)CH₃), 68.3 (-CH₂C(O)CH₃), 123.7 (C(3) and C(5)) and 129.8 (C(2) and C(6)), 139.1 and 140.8 (2 x quaternary ArC), 199.3 (-CH₂C(O)CH₃); ν_{max} (DCM/cm⁻¹) 1042 (s, S=O), 1597 (w, Ar), 1711 (s, C=O), 2924 (m, C-H); **m/z** (Cl⁺) 197 (36%, [M + H]⁺), 139 (100%, [M - (CH₂C(O)CH₃)]⁺); **HRMS** found 197.0633, [M + H]⁺ (C₁₀H₁₃O₂S) requires 197.0636; **[α]_D** + 267 ° (*c* 1.0, acetone), lit. + 255 ° (*c* 1.0, acetone).¹⁷³

1-Methyl-4-[(*E*)-prop-1-ene-1-sulfinyl]-benzene (317)¹⁷⁴



To a crude mixture of **320** (4.05 g, 15.0 mmol) dissolved in anhydrous tetrahydrofuran (50 ml), *n*-butyllithium in hexanes (1.80 M, 16.1 ml, 29.0 mmol) was added at -78 °C, under nitrogen. Stirring was continued for 90 min. and the mixture was then warmed 0 °C, and stirred for an additional 30 min.. The mixture was cooled to -78 °C and a solution of acetaldehyde (1.46 ml, 26.0 mmol) in tetrahydrofuran (15 ml) was added dropwise. After the addition, the mixture was then warmed to room temperature and stirred for 3 h. Water (50 ml) was added and the organics were removed under reduced pressure. The aqueous residue was extracted with chloroform (3 x 50 ml) and the organic extracts were washed with water (150 ml) and dried over MgSO₄, filtered and concentrated. Purification by flash chromatography (SiO₂; gradient; petroleum spirit/ethyl acetate (3:1) to ethyl acetate/methanol (8:2)) yielded the product as a clear

oil (0.40 g, 14%). $R_f = 0.53$ (SiO₂; ethyl acetate); $^1\text{H NMR}$ (300 MHz, CDCl₃) δ_{H} /ppm 1.75 (m, 3H, -CH=CHCH₃), 2.26 (s, 3H, CH₃Ar-), 6.12 (m, 1H, -S(O)CH-), 6.45 (m, 1H, -CHCH₃), 7.17 (d, $J = 8.1$, 2H, H(2) and H(6)), 7.37 (d, $J = 8.1$, 2H, H(3) and H(5)); $^{13}\text{C NMR}$ (75 MHz, CDCl₃) δ_{C} /ppm 17.7 (-CHCHCH₃), 21.3 (CH₃Ar-), 124.4 (C(3) and C(5)) and 129.9 (C(2) and C(6)), 136.0 (-CHCHCH₃), 136.4 (C(1)), 141.2 (-CHCHCH₃), 141.4 (C(4)); ν_{max} (neat/cm⁻¹) 1042 (s, S=O), 1493, 1595 (m, Ar), 1632 (m, C=C), 2918 (m, C-H); m/z (CI⁺) 181 (100%, [M + H]⁺); **HRMS** found 181.0688, [M + H]⁺ (C₁₀H₁₃OS) requires 181.0687; $[\alpha]_{\text{D}} + 285.3^\circ$ (c 0.03, CHCl₃), lit. + 198° (c not stated, EtOH).¹⁷⁴

4.3.7 NMR Binding Studies

Measurement of Diffusion Coefficient of Sulfoxide TSAs (316 and 317) and Amino Acids Using Pulsed Field Gradient Techniques

The diffusion coefficients were measured according to the literature procedure.⁹⁶

3 mM solutions of each Boc protected amino acid and 30 mM solutions of each TSA (316 and 317) were prepared in CDCl₃ (0.5 mL) and diffusion coefficients measured using PFG-NMR spectroscopy.

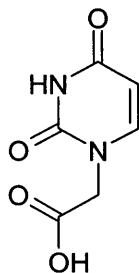
Sample mixtures containing one protected amino acid and one TSA were also prepared, where the concentration of the amino acid was 3 mM and that of the TSA 30 mM. Diffusion coefficients were then measured using PFG-NMR spectroscopy.

All of the diffusion measurements were performed at 298 K.

The results are presented in Chapter 3.

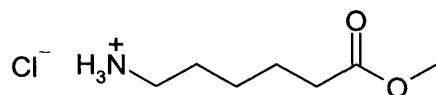
4.3.8 Supramolecular Chemistry

(2,4-Dioxo-3,4-dihydro-2H-pyrimidin-1-yl) acetic acid (339)¹⁷⁵



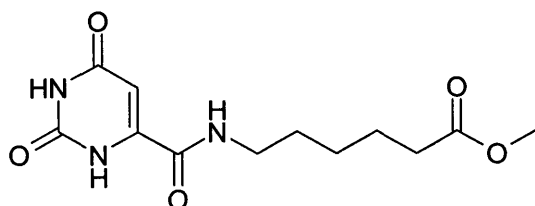
Uracil (0.25 g, 2.23 mmol), chloroacetic acid (0.38 g, 3.97 mmol) and potassium hydroxide (0.55 g, 9.80 mmol) were added to water (5 ml) and the mixture was heated at reflux for 2.5 h. After cooling, the resulting solution was acidified to pH 2 with concentrated aqueous HCl. The solution was left to stand in the fridge for 3 days, after which time, a white solid had precipitated. The solid was isolated by filtration, then washed with dichloromethane, and dried under vacuum to give the product as a white solid (0.20 g, 67%). **m.p.** > 230 °C (lit. 292-293 °C¹⁷⁶); **¹H NMR** (300 MHz, DMSO) δ_{H} /ppm 4.44 (s, 2H, -CH₂CO₂H), 5.62 (d, J = 7.7, 1H, -C(O)CH=CH-), 7.63 (d, J = 7.8, 1H, -C(O)CH=CH-); **¹³C NMR** (75 MHz, DMSO) δ_{C} /ppm 49.8 (-CH₂CO₂H), 102.0 (-C(O)CH=CH-), 147.3 (-NHC(O)CH=CH-), 152.2 (-NHC(O)N-), 165.1 and 170.8 (-C(O)CH=CH- and -CO₂H); ν_{max} (DCM/cm⁻¹) 1688 (m, C=O), 2853 and 2916 (s, C-H); **m/z** (Cl⁺) 171 (75%, [M + H]⁺), 170 (5%, [M]⁺); **HRMS** found 171.0406, [M + H]⁺ (C₆H₇N₂O₄) requires 171.0406.

5-Methoxycarbonyl pentyl ammonium chloride (343)



Thionyl chloride (3.64 ml, 50.0 mmol) was added to methanol (25 ml) at 0 °C and the solution was stirred at this temperature for 20 min.. To this solution 6-aminocaproic acid (3.00 g, 23.0 mmol) was then added. The solution was allowed to warm to room temperature and stirred for 3.5 h. The volatiles were removed under reduced pressure and the resulting solid was recrystallised from hexane/ethyl acetate and a few drops of methanol to obtain the final product as a white solid (2.09 g, 63%). **m.p.** 79 °C (EtOAc/hexane/MeOH); **¹H NMR** (300 MHz, CDCl₃) δ_{H} /ppm 1.35 (m, 2H, H₂NCH₂CH₂CH₂-), 1.56 (m, 2H, H₂NCH₂CH₂-), 1.72 (m, 2H, H₂N(CH₂)₃CH₂-), 2.24 (t, *J* = 7.2, 2H, H₂N(CH₂)₄CH₂-), 2.94 (br m, 2H, H₂NCH₂-), 3.56 (s, 3H, -CH₃), 8.05 (br s, 3H, -NH₃⁺); **¹³C NMR** (75 MHz, CDCl₃) δ_{C} /ppm 24.0 (H₂NCH₂CH₂CH₂-), 25.7 (H₂NCH₂CH₂-), 26.9 (H₂N(CH₂)₃CH₂-), 33.4 (H₂N(CH₂)₄CH₂-), 39.6 (H₂NCH₂-), 51.4 (-CH₃), 173.8 (-CO₂CH₃); ν_{max} (DCM/cm⁻¹) 1728 (s, C=O), 2852 (s, C-H), 3447 (w, N-H); **m/z** (Cl⁺) 146 (63%, [M - Cl]⁺); **HRMS** found 146.1791, [M - Cl]⁺ (C₇H₁₆NO₂) requires 146.1181.

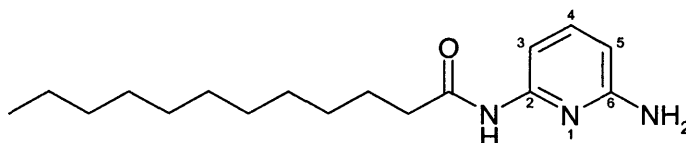
6-[(2,6-Dioxo-1,2,3,6-tetrahydro-pyrimidine-4-carbonyl)-amino]-hexanoic acid methyl ester (345)



A solution of orotic acid (0.50 g, 3.21 mmol), 6-amino-hexanoic acid methyl ester **343** (0.46 g, 3.21 mmol), *N*-methyl morpholine (0.35 ml, 3.21 mmol) and 1-(ethoxycarbonyl)-2-ethoxy-1, 2-dihydroquinoline (0.79 g, 3.21 mmol) in anhydrous dimethylformamide (7 ml) was stirred at 55 °C for 18 h. The reaction mixture was

concentrated *in vacuo* and the resulting residue was triturated with water, followed by ethyl acetate. The isolated solid was recrystallized from methanol to yield the desired product as a brown solid (74 mg, 8%). **m.p.** > 200 °C; **R_f** = 0.10 (SiO₂; petroleum spirit/ethyl acetate; 1:1); **¹H NMR** (300 MHz, CD₃OD) δ_{H} /ppm 1.37 (m, 2H, -NHCH₂CH₂CH₂-), 1.61 (m, 4H, -NHCH₂CH₂CH₂CH₂-), 2.33 (m, 2H, -NH(CH₂)₄CH₂-), 3.30 (m, 3H, -NHCH₂ and -NH-), 3.64 (s, 3H, -CH₃), 6.07 (s, 1H, -C(O)CH=C-); **¹³C NMR** (125 MHz, CD₃OD) δ_{C} /ppm 26.4 (-NHCH₂CH₂CH₂-), 28.2 and 30.5 (-NHCH₂CH₂CH₂CH₂-), 35.5 (-NH(CH₂)₄CH₂-), 41.7 (-NHCH₂-), 52.9 (-CH₃), 101.6 (-C(O)CH=C-), 147.8 (-C(O)CH=C-), 153.6 (-NHC(O)NH-), 162.7 (-CH=CC(O)NH-), 167.8 (-C(O)CH=C-), 176.8 (-CO₂CH₃); ν_{max} (nujol/cm⁻¹) 1651 (s, C=C), 1732 (s, C=O), 2853 and 2932 (s, C-H), 3306 (m, N-H); **m/z** (CI⁺) 284 (100%, [M + H]⁺); **HRMS** found 284.1246, [M + H]⁺ (C₁₂H₁₈N₃O₅) requires 284.1246. **Anal.** (C₁₂H₁₇N₃O₅) found C, 50.34; H, 5.98; N, 14.58%; requires C, 50.88; H, 6.05; N, 14.83%.

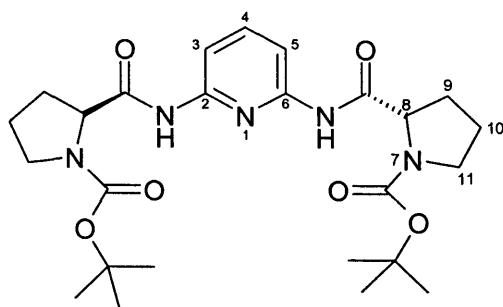
Dodecanoic acid (6-amino-pyridin-2-yl) amide (340)¹⁷⁷



2, 6 – Diaminopyridine (1.00 g, 9.17 mmol) and triethylamine (1.28 ml, 9.17 mmol) were dissolved in anhydrous tetrahydrofuran (15 ml) and the solution cooled to 0 °C. A solution of lauroyl chloride (2.29 ml, 9.63 mmol) in tetrahydrofuran (1.5 ml) was added dropwise and the solution stirred for 50 min.. The mixture was then warmed to room temperature and stirring was continued for 24 h. The reaction mixture was filtered and evaporated to dryness. Purification by flash chromatography (SiO₂; gradient; petroleum spirit/ethyl acetate, (3:1) to petroleum spirit/ethyl acetate, (1:2)) gave the product as a white solid (1.14 g, 43%). **m.p.** 51 °C; **R_f** = 0.41 (SiO₂; ethyl acetate/petroleum spirit; 1:1); **¹H NMR** (300 MHz, CDCl₃) δ_{H} /ppm 0.82 (m, 3H, CH₃-), 1.19 (m, 16H, CH₃(CH₂)₈-), 1.57 (m, 2H, -NHC(O)CH₂CH₂-), 2.24 (m, 2H, -NHC(O)CH₂-), 4.48 (br

s, 2H, -NH₂), 6.16 (d, $J = 8.0$, 1H, H(5)), 7.32 (m, 1H, H(3)), 7.47 (m, 1H, H(4)), 8.34 (br s, 1H, N-H); ¹³C NMR (75 MHz, CDCl₃) δ_c /ppm 14.3 (CH₃-), 22.9, 25.7, 29.4 and 29.8 (peaks overlap, CH₃(CH₂)₈-), 32.1 (-NHC(O)CH₂CH₂), 37.8 (-NHC(O)CH₂-), 103.4 and 104.3 (C(5) and C(3)), 140.3 (C(4)), 150.3 (C(2)), 157.4 (C(6)), 172.2 (-NHC(O)-); ν_{\max} (DCM/cm⁻¹) 1533 (s, Ar), 1574 (s, Ar), 1620 (s, Ar), 1682 (s, C=O), 2852 and 2924 (s, C-H); m/z (Cl⁺) 292 (100%, [M + H]⁺); HRMS found 292.2385, [M + H]⁺ (C₁₇H₃₀N₃O) requires 292.2389.

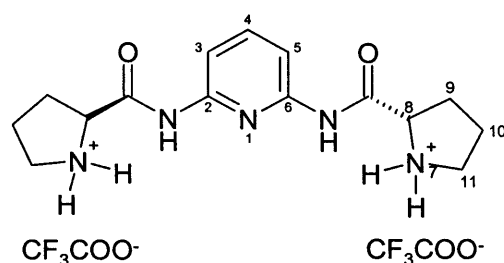
**(2, 6-Amino-pyridin-2-ylcarbamoyl)-pyrrolidine-1-carboxylic acid tert-butyl ester
(337)**



Dicyclohexylcarbodiimide (2.27 g, 11.0 mmol) was added to a solution of 2, 6-diaminopyridine (0.25 g, 2.30 mmol) and Boc-proline (2.47 g, 11.5 mmol) in dimethylformamide (10 ml). The resulting mixture was stirred at room temperature for 72 h. The urea by-product was filtered off and ethyl acetate (50 ml) was added to the filtrate. The resulting solution was washed with aqueous HCl (1 M, 2 x 50 ml), saturated aqueous Na₂CO₃ (4 x 50 ml) and brine (2 x 50 ml) and then dried over MgSO₄. The solvents were removed *in vacuo* and the resulting brown foam was purified by flash chromatography (SiO₂; gradient; petroleum spirit/ethyl acetate, (3:1) to ethyl acetate/methanol, (8:2)) to yield the desired product as a white solid (0.44 g, 38%). **m.p.** > 230 °C; **R_f** = 0.25 (SiO₂; petroleum spirit/ethyl acetate; 1:1) ¹H NMR (400 MHz, CDCl₃, 328 K) δ_H /ppm 1.39 (s, 18H, 2 x -C(CH₃)₃), 1.85 (m, 4H, 2 x H(10)), 2.05 (br m, 2H, H(9)), 2.23 (br m, 2H, H(9)), 3.43 (m, 4H, 2 x H(11)), 4.32 (m, 2H, 2 x H(8)), 7.58 (m, 1H, H(4)), 7.79 (d, $J = 6.0$, 2H, H(3), H(5)), 8.61 (br s, 2H, 2 x N-H); ¹³C NMR (100 MHz, CDCl₃, 328 K) δ_c /ppm 24.4 (2 x C(9), 2 x C(10)), 28.6 (2 x

-C(CH₃)₃), 47.4 (2 x C(11)), 61.7 (2 x C(8)), 81.0 (2 x -C(CH₃)₂), 109.6 (C(3), C(5)), 140.5 (C(4)), 149.9 (2 x quaternary ArC), 155.0 (2 x -CO₂C(CH₃)₃), 171.0 (2 x -NHC(O)-); ν_{\max} (DCM/cm⁻¹) 1522 and 1585 (m, Ar), 1693 (s, C=O), 2980 (m, C-H), 3418 (s, N-H); m/z (CI⁺) 504 (5%, [M + H]⁺), 503 (10%, [M]⁺); **HRMS** found 504.2827, [M + H]⁺ (C₂₅H₃₈N₅O₆) requires 504.2821; [α]_D + 235 ° (c 0.02, MeOH).

Pyrrolidinium-2-carboxylic acid (2, 6-methylamino-pyridin-2-yl) amide di-trifluoroacetate (333)



Compound **337** (79.0 mg, 0.16 mmol) was dissolved in a solution of trifluoroacetic acid/dichloromethane (1:1, 5 ml) and then stirred at room temperature for 6 h. The volatiles were removed under reduced pressure to yield the product as a clear oil (53.0 mg, 64%). ¹H NMR (300 MHz, CD₃OD) δ_{H} /ppm 1.73 (m, 6H, H(9) and 2 x H(10)), 2.16 (m, 2H, H(9)), 3.02 (m, 4H, 2 x H(11)), 4.13 (m, 2H, 2 x H(8)), 7.41 (m, 3H, H(3), H(4) and H(5)); ¹³C NMR (75 MHz, CD₃OD) δ_{C} /ppm 25.9 (2 x C(10)), 31.9 (2 x C(9)), 48.4 (2 x C(11)), 62.6 (2 x C(8)), 112.4 (C(3) and C(5)), 118.1 (CF₃COO-), 142.5 (C(4)), 151.8 (2 x quaternary ArC), 161.9 (q, CF₃COO-), 169.4 (-NHC(O)-); ν_{\max} (DCM/cm⁻¹) 1589 (m, Ar), 1674 (s, C=O), 2989 (w, C-H), 3447 (w, N-H); m/z (CI⁺) 306 (10%, [M - 2TFA + H]⁺), 305 (93%, [M - 2TFA]⁺); **HRMS** found 306.1935, [M - 2TFA + H]⁺ (C₁₅H₂₄N₅O₂) requires 306.1930; [α]_D + 205 ° (c 0.02, MeOH).

REFERENCES

Reference List

- (1) Voet, D.; Voet, J. G. *Biochemistry, John Wiley and Sons, Second Edition* **1994**.
- (2) Copeland, R. A. *Enzymes, 2nd Edn, Wiley-VCH, Inc.* **2000**.
- (3) Pauling, L. *Nature* **1948**, *161*, 707-709.
- (4) Davis, A. M.; Teague, S. J. *Angewandte Chemie International Edition* **1999**, *38*, 736-749.
- (5) Mader, M. M.; Bartlett, P. A. *Chemical Reviews* **1997**, *97*, 1281-1301.
- (6) Heginbotham, L.; Mackinnon, R. *Neuron* **1992**, *8*, 483-491.
- (7) Motherwell, W. B.; Bingham, M. J.; Six, Y. *Tetrahedron* **2001**, *57*, 4663-4686.
- (8) Fersht, A. R.; Shi, J. P.; Knilljones, J.; Lowe, D. M.; Wilkinson, A. J.; Blow, D. M.; Brick, P.; Carter, P.; Waye, M. M. Y.; Winter, G. *Nature* **1985**, *314*, 235-238.
- (9) Street, I. P.; Armstrong, C. R.; Withers, S. G. *Biochemistry* **1986**, *25*, 6021-6027.
- (10) Cudd, A.; Fridovich, I. *Journal of Biological Chemistry* **1982**, *257*, 1443-1447.
- (11) Tong, L.; Pav, S.; Mui, S.; Lamarre, D.; Yoakim, C.; Beaulieu, P.; Anderson, P. C. *Structure* **1995**, *3*, 33-40.
- (12) Ma, J. C.; Dougherty, D. A. *Chemical Reviews* **1997**, *97*, 1303-1324.
- (13) Kirby, A. J. *Accounts of Chemical Research* **1997**, *30*, 290-296.
- (14) Blow, D. M. *Accounts of Chemical Research* **1976**, *9*, 145-152.
- (15) Perona, J. J.; Craik, C. S. *Protein Science* **1995**, *4*, 337-360.
- (16) Kirby, A. J. *Angewandte Chemie International Edition* **1996**, *35*, 707-724.
- (17) Breslow, R.; Doherty, J. B.; Guillot, G.; Lipsey, C. *Journal of the American Chemical Society* **1978**, *100*, 3227-3229.
- (18) Mattei, P.; Diederich, F. *Helvetica Chimica Acta* **1997**, *80*, 1555-1588.
- (19) Mattei, P.; Diederich, F. *Angewandte Chemie International Edition* **1996**, *35*, 1341-1345.
- (20) Reetz, M. T.; Becker, M. H.; Klein, H. W.; Stockigt, D. *Angewandte Chemie International Edition* **1999**, *38*, 1758-1761.

- (21) Enjalbal, C.; Martinez, J.; Aubagnac, J. L. *Mass Spectrometry Reviews* **2000**, *19*, 139-161.
- (22) Jencks, W. P. *Catalysis in Chemistry and Enzymology*, McGraw Hill, New York **1969**.
- (23) Tramontano, A.; Janda, K. D.; Lerner, R. A. *Science* **1986**, *234*, 1566-1570.
- (24) Pollack, S. J.; Jacobs, J. W.; Schultz, P. G. *Science* **1986**, *234*, 1570-1573.
- (25) Barbas, C. F.; Heine, A.; Zhong, G. F.; Hoffmann, T.; Gramatikova, S.; Bjornestedt, R.; List, B.; Anderson, J.; Stura, E. A.; Wilson, I. A.; Lerner, R. A. *Science* **1997**, *278*, 2085-2092.
- (26) Anslyn, E.; Breslow, R. *Journal of the American Chemical Society* **1989**, *111*, 8931-8932.
- (27) Breslow, R.; Greenspoon, N.; Guo, T.; Zarzycki, R. *Journal of the American Chemical Society* **1989**, *111*, 8296-8297.
- (28) Breslow, R.; Chung, S. *Journal of the American Chemical Society* **1990**, *112*, 9659-9660.
- (29) Tabushi, I.; Kuroda, Y.; Shimokawa, K. *Journal of the American Chemical Society* **1979**, *101*, 1614-1615.
- (30) Yan, J. M.; Breslow, R. *Tetrahedron Letters* **2000**, *41*, 2059-2062.
- (31) Breslow, R.; Yang, J.; Yan, J. M. *Tetrahedron* **2002**, *58*, 653-659.
- (32) Sedewitz, B.; Schleifer, K. H.; Gotz, F. *Journal of Bacteriology* **1984**, *160*, 273-278.
- (33) Muller, Y. A.; Schulz, G. E. *Science* **1993**, *259*, 965-967.
- (34) Breslow, R.; Fang, Z. L. *Tetrahedron Letters* **2002**, *43*, 5197-5200.
- (35) Marty, M.; Clyde-Watson, Z.; Twyman, L. J.; Nakash, M.; Sanders, K. M. *Chemical Communications* **1998**, 2265-2266.
- (36) Clyde-Watson, Z.; Vidal-Ferran, A.; Twyman, L. J.; Walter, C. J.; McCallien, D. W. J.; Fanni, S.; Bampos, N.; Wylie, R. S.; Sanders, J. K. M. *New Journal of Chemistry* **1998**, *22*, 493-502.
- (37) Nakash, M.; Sanders, J. K. M. *Journal of Organic Chemistry* **2000**, *65*, 7266-7271.
- (38) Nakash, M.; Clyde-Watson, Z.; Feeder, N.; Davies, J. E.; Teat, S. J.; Sanders, J. K. M. *Journal of the American Chemical Society* **2000**, *122*, 5286-5293.
- (39) Dewar, M. J. S.; Wade, L. E. *Journal of the American Chemical Society* **1977**, *99*, 4417-4424.

- (40) Ulrich, H. D.; Mundroff, E.; Santarsiero, B. D.; Driggers, E. M.; Stevens, R. C.; Schultz, P. G. *Nature* **1997**, 389, 271-275.
- (41) Hilvert, D.; Hill, K. W.; Nared, K. D.; Auditor, M. T. M. *Journal of the American Chemical Society* **1989**, 111, 9261-9262.
- (42) Li, T. G.; Janda, K. D.; Lerner, R. A. *Nature* **1996**, 379, 326-327.
- (43) Romesberg, F. E.; Flanagan, M. E.; Uno, T.; Schultz, P. G. *Journal of the American Chemical Society* **1998**, 120, 5160-5167.
- (44) Li, T. Y.; Janda, K. D.; Ashley, J. A.; Lerner, R. A. *Science* **1994**, 264, 1289-1293.
- (45) Wentworth, P.; Liu, Y. Q.; Wentworth, A. D.; Fan, P.; Foley, M. J.; Janda, K. D. *Proceedings of the National Academy of Sciences of the United States of America* **1998**, 95, 5971-5975.
- (46) Wirsching, P.; Ashley, J. A.; Lo, C. H. L.; Janda, K. D.; Lerner, R. A. *Science* **1995**, 270, 1775-1782.
- (47) Hoffmann, T.; Zhong, G. F.; List, B.; Shabat, D.; Anderson, J.; Gramatikova, S.; Lerner, R. A.; Barbas, C. F. *Journal of the American Chemical Society* **1998**, 120, 2768-2779.
- (48) Nicholas, K. M.; Wentworth, P.; Harwig, C. W.; Wentworth, A. D.; Shafton, A.; Janda, K. D. *Proceedings of the National Academy of Sciences of the United States of America* **2002**, 99, 2648-2653.
- (49) Smith, G. P.; Petrenko, V. A. *Chemical Reviews* **1997**, 97, 391-410.
- (50) Hanes, J.; Pluckthun, A. *Proceedings of the National Academy of Sciences of the United States of America* **1997**, 94, 4937-4942.
- (51) Taylor, S. J.; Morken, J. P. *Science* **1998**, 280, 267-270.
- (52) Whitcombe, M. J.; Alexander, C.; Vulfson, E. N. *Synlett* **2000**, 911-923.
- (53) Bystrom, S. E.; Borje, A.; Akermark, B. *Journal of the American Chemical Society* **1993**, 115, 2081-2083.
- (54) Liu, J. Q.; Wulff, G. *Angewandte Chemie-International Edition* **2004**, 43, 1287-1290.
- (55) Phillips, M. A.; Fletterick, R.; Rutter, W. J. *Journal of Biological Chemistry* **1990**, 265, 20692-20698.
- (56) Jacobs, J.; Schultz, P. G.; Sugawara, R.; Powell, M. *Journal of the American Chemical Society* **1987**, 109, 2174-2176.
- (57) Visnjeviski, A.; Schomacker, R.; Yilmaz, E.; Bruggemann, O. *Catalysis Communications* **2005**, 6, 601-606.

- (58) Robinson, D. K.; Mosbach, K. *Journal of the Chemical Society-Chemical Communications* **1989**, 969-970.
- (59) Wulff, G.; Gross, T.; Schonfeld, R. *Angewandte Chemie-International Edition in English* **1997**, *36*, 1962-1964.
- (60) Motherwell, W. B.; Bingham, M. J.; Pothier, J.; Six, Y. *Tetrahedron* **2004**, *60*, 3231-3241.
- (61) Alexander, C.; Smith, C. R.; Whitcombe, M. J.; Vulfson, E. N. *Journal of the American Chemical Society* **1999**, *121*, 6640-6651.
- (62) Letsinger, R. L.; Savereid, T. J. *Journal of the American Chemical Society* **1962**, *84*, 3122-&.
- (63) Klotz, I. M.; Sloniews, A. R. *Biochemical and Biophysical Research Communications* **1968**, *31*, 421-&.
- (64) Klotz, I. M.; Royer, G. P.; Scarpa, I. S. *Proceedings of the National Academy of Sciences of the United States of America* **1971**, *68*, 263-&.
- (65) Bruice, T. C.; Schmir, G. L. *Journal of the American Chemical Society* **1957**, *79*, 1663-1667.
- (66) Suh, J.; Oh, S. *Journal of Organic Chemistry* **2000**, *65*, 7534-7540.
- (67) Tahirov, T. H.; Oki, H.; Tsukihara, T.; Ogasahara, K.; Yutani, K.; Ogata, K.; Izu, Y.; Tsunasawa, S.; Kato, I. *Journal of Molecular Biology* **1998**, *284*, 101-124.
- (68) Paul-Soto, R.; Bauer, R.; Frere, J. M.; Galleni, M.; Meyer-Klaucke, W.; Nolting, H.; Rossolini, G. M.; de Seny, D.; Hernandez-Valladares, M.; Zeppezauer, M.; Adolph, H. W. *Journal of Biological Chemistry* **1999**, *274*, 13242-13249.
- (69) Mock, W. L.; Liu, Y. Y. *Journal of Biological Chemistry* **1995**, *270*, 18437-18446.
- (70) Moon, S. J.; Jeon, J. W.; Kim, H.; Suh, M. P.; Suh, J. *Journal of the American Chemical Society* **2000**, *122*, 7742-7749.
- (71) Gao C.; Lavey B.J.; Lo C.H.L.; Datta A.; Wentworth P.; Janda, K. D. *Journal of the American Chemical Society* **1998**, *120*, 2211-2217.
- (72) Williams, N. H.; Takasaki, B.; Wall, M.; Chin, J. *Accounts of Chemical Research* **1999**, *32*, 485-493.
- (73) Hettich, R.; Schneider, H. J. *Journal of the American Chemical Society* **1997**, *119*, 5638-5647.
- (74) Jeung, C. S.; Kim, C. H.; Min, K.; Suh, S. W.; Suh, J. *Bioorganic and Medicinal Chemistry Letters* **2001**, *11*, 2401-2404.

- (75) Menger, F. M.; Eliseev, A. V.; Migulin, V. A. *Journal of Organic Chemistry* **1995**, *60*, 6666-6667.
- (76) Menger, F. M.; Ding, J.; Barragan, V. *Journal of Organic Chemistry* **1998**, *63*, 7578-7579.
- (77) Menger, F. M.; West, C. A.; Ding, J. *Chemical Communications* **1997**, 633-634.
- (78) Dekok, P. M. T.; Bastiaansen, L. A. M.; Vanlier, P. M.; Vekemans, J. A. J. M.; Buck, H. M. *Journal of Organic Chemistry* **1989**, *54*, 1313-1320.
- (79) Reetz, M. T. *Angewandte Chemie-International Edition* **2001**, *40*, 284-310.
- (80) Cadwell, R. C.; Joyce, G. F. *Pcr-Methods and Applications* **1994**, *3*, S136-S140.
- (81) Stemmer, W. P. C. *Nature* **1994**, *370*, 389-391.
- (82) Reetz, M. T.; Becker, M. H.; Kuhling, K. M.; Holzwarth, A. *Angewandte Chemie-International Edition* **1998**, *37*, 2647-2650.
- (83) Reetz, M. T. *Tetrahedron* **2002**, *58*, 6595-6602.
- (84) Fersht, A. R. *Biochemistry* **1987**, *26*, 8031-8037.
- (85) Gerlt, J. A. *Chemical Reviews* **1987**, *87*, 1079-1105.
- (86) Hirose, Y.; Kariya, K.; Nakanishi, Y.; Kurono, Y.; Achiwa, K. *Tetrahedron Letters* **1995**, *36*, 1063-1066.
- (87) Reetz, M. T.; Brunner, B.; Schneider, T.; Schulz, F.; Clouthier, C. M.; Kayser, M. M. *Angewandte Chemie-International Edition* **2004**, *43*, 4075-4078.
- (88) Taschner, M. J.; Black, D. J. *Journal of the American Chemical Society* **1988**, *110*, 6892-6893.
- (89) Stewart, J. D.; Reed, K. W.; Zhu, J.; Chen, G.; Kayser, M. M. *Journal of Organic Chemistry* **1996**, *61*, 7652-7653.
- (90) Atkinson, C. A. *PhD Thesis, University of London* **2001**.
- (91) Motherwell, W. B.; Atkinson, C. E.; Aliev, A. E.; Wong, S. Y. F.; Warrington, B. H. *Angewandte Chemie-International Edition* **2004**, *43*, 1225-1228.
- (92) Clayden, J.; Greeves, N.; Warren, S.; Wothers, P. *'Organic Chemistry', Oxford University Press* **2001**.
- (93) Wolfenden, R. *Annual Review of Biophysics and Bioengineering* **1976**, *5*, 271-306.
- (94) Wu, D.; Chen, A.; Johnson, C. S. *Journal of Magnetic Resonance* **1995**, *115*, 260-264.
- (95) Fielding, L. *Tetrahedron* **2000**, *56*, 6170.

- (96) Atkinson, C. E.; Aliev, A. E.; Motherwell, W. B. *Chemistry-A European Journal* **2003**, *9*, 1714-1723.
- (97) Fersht, A. R. '*Structure and Mechanisms in Protein Science. A Guide to Enzyme Catalysis and Protein Folding*', W.H. Freeman, New York **1999**.
- (98) Chan, W. C.; White, P. D. *Fmoc Solid Phase Peptide Synthesis*, Oxford University Press **2000**.
- (99) Tanaka, N.; Nakagawa, K.; Iwasaki, H.; Hosoya, K.; Kimata, K.; Araki, T.; Patterson, D. G. *Journal of Chromatography A* **1997**, *781*, 139-150.
- (100) Bergeron, R. J.; McManis, J. S. *Journal of Organic Chemistry* **1988**, *53*, 3108-3111.
- (101) Delaney, E. J.; Wood, L. E.; Klotz, I. M. *Journal of the American Chemical Society* **1982**, *104*, 799-807.
- (102) Angell, Y. M.; Garciaecheverria, C.; Rich, D. H. *Tetrahedron Letters* **1994**, *35*, 5981-5984.
- (103) Sarabu, R.; Lovey, K.; Madison, V. S.; Fry, D. C.; Greeley, D. N.; Cook, C. M.; Olson, G. L. *Tetrahedron* **1993**, *49*, 3629-3640.
- (104) Zervas, L.; Theodoropoulos, D. M. *Journal of the American Chemical Society* **1956**, *78*, 1359-1363.
- (105) Boxus, T.; Touillaux, R.; Dive, G.; Marchand-Brynaert, J. *Bioorganic & Medicinal Chemistry* **1998**, *6*, 1577-1595.
- (106) Sheehan, J. C.; Preston, J.; Cruicksh, P. A. *Journal of the American Chemical Society* **1965**, *87*, 2492-&.
- (107) Castro, B.; Dormoy, J. R.; Dourtoglou, B.; Evin, G.; Selve, C.; Ziegler, J. C. *Synthesis-Stuttgart* **1976**, 751-752.
- (108) Bofill, J. M.; Albericio, F. *Tetrahedron Letters* **1999**, *40*, 2641-2644.
- (109) Falorni, M.; Giacomelli, G.; Porcheddu, A.; Dettori, G. *European Journal of Organic Chemistry* **2000**, 3217-3222.
- (110) Felix, A. M.; Heimer, E. P.; Lambros, T. J.; Tzougraki, C.; Meienhofer, J. *Journal of Organic Chemistry* **1978**, *43*, 4194-4196.
- (111) www.rapp-polymere.com **2003**.
- (112) *Third International lectronic Conference on Synthetic Organic Chemistry*, www.mdpi.org **1999**.
- (113) Thoma, G.; Patton, J. T.; Magnani, J. L.; Ernst, B.; Ohrlein, R.; Duthaler, R. O. *Journal of the American Chemical Society* **1999**, *121*, 5919-5929.

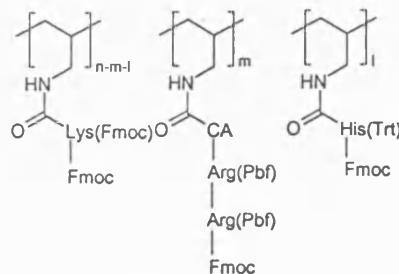
- (114) Hajos, Z. G.; Parrish, D. R. *Journal of Organic Chemistry* **1974**, *39*, 1615-1621.
- (115) List, B.; Lerner, R. A.; Barbas, C. F. *Journal of the American Chemical Society* **2000**, *122*, 2395-2396.
- (116) Zimmerman, H. E.; Traxler, M. D. *Journal of the American Chemical Society* **1957**, *79*, 1920-1923.
- (117) Northrup, A. B.; MacMillan, D. W. C. *Journal of the American Chemical Society* **2002**, *124*, 6798-6799.
- (118) Tang, Z.; Jiang, F.; Yu, L. T.; Cui, X.; Gong, L. Z.; Mi, A. Q.; Jiang, Y. Z.; Wu, Y. D. *Journal of the American Chemical Society* **2003**, *125*, 5262-5263.
- (119) Cobb, A. J. A.; Shaw, D. M.; Longbottom, D. A.; Gold, J. B.; Ley, S. V. *Organic & Biomolecular Chemistry* **2005**, *3*, 84-96.
- (120) List, B. *Journal of the American Chemical Society* **2000**, *122*, 9336-9337.
- (121) Ladlow, M.; Legge, C. H.; Neudeck, T.; Pipe, A. J.; Sheppard, T.; Yang, L. Q. L. *Chemical Communications* **2003**, 2048-2049.
- (122) Shi, L. X.; Sun, Q.; Ge, Z. M.; Zhu, Y. Q.; Cheng, T. M.; Li, R. T. *Synlett* **2004**, 2215-2217.
- (123) Challis, B. C.; Milligan, J. R.; Mitchell, R. C. *Journal of the Chemical Society-Perkin Transactions 1* **1990**, 3103-3108.
- (124) Pfeiffer, F. R.; Chambers, P. A.; Hilbert, E. E.; Woodward, P. W.; Ackerman, D. M. *Journal of Medicinal Chemistry* **1984**, *27*, 325-341.
- (125) Schwarz, H.; Bumpus, F. M.; Page, I. H. *Journal of the American Chemical Society* **1957**, *79*, 5697-5703.
- (126) Clemente, F. R.; Houk, K. N. *Angewandte Chemie-International Edition* **2004**, *43*, 5766-5768.
- (127) Shokat, K.; Uno, T.; Schultz, P. G. *Journal of the American Chemical Society* **1994**, *116*, 2261-2270.
- (128) Lin, C. C.; Shimazaki, M.; Heck, M. P.; Aoki, S.; Wang, R.; Kimura, T.; Ritzen, H.; Takayama, S.; Wu, S. H.; Weitzschmidt, G.; Wong, C. H. *Journal of the American Chemical Society* **1996**, *118*, 6826-6840.
- (129) Rosen, T.; Chu, D. T. W.; Lico, I. M.; Fernandes, P. B.; Marsh, K.; Shen, L.; Cepa, V. G.; Pernet, A. G. *Journal of Medicinal Chemistry* **1988**, *31*, 1598-1611.
- (130) Sato, T.; Kawasaki, S.; Oda, N.; Yagi, S.; El Bialy, S. A. A.; Uenishi, J.; Yamauchi, M.; Ikeda, M. *Journal of the Chemical Society-Perkin Transactions 1* **2001**, 2623-2631.

- (131) Iyer, S.; Liebeskind, L. S. *Journal of the American Chemical Society* **1987**, *109*, 2759-2770.
- (132) Rivero, I. A.; Heredia, S.; Ochoa, A. *Synthetic Communications* **2001**, *31*, 2169-2175.
- (133) Synthesis Notes *Nova Biochem Catalog* **2002**.
- (134) Zhong, G. F.; Lerner, R. A.; Barbas, C. F. *Angewandte Chemie-International Edition* **1999**, *38*, 3738-3741.
- (135) Arno, M.; Domingo, L. R. *Organic & Biomolecular Chemistry* **2003**, *1*, 637-643.
- (136) Solladie, G.; Hutt, J.; Girardin, A. *Synthesis* **1987**, 173.
- (137) Solladie, G. *Synthesis* **1981**, 185-196.
- (138) Solladie, G.; Demailly, G.; Greck, C. *Journal of Organic Chemistry* **1985**, *50*, 1552-1554.
- (139) Dale, S. H.; Elsegood, M. R. J. *Acta Crystallographica Section E-Structure Reports Online* **2003**, *59*, O1205-O1207.
- (140) Pasha, M. K.; Dimmock, J. R.; Hollenberg, M. D.; Sharma, R. K. *Biochemical Pharmacology* **2002**, *64*, 1461-1467.
- (141) Pirkle, W. H.; Hoekstra, M. S. *Journal of the American Chemical Society* **1976**, *98*, 1832-1839.
- (142) Hilton, S. T. *Unpublished results. Thanks to Steve Hilton for synthesising TBDMS protected serine.* **2005**.
- (143) Greene, T. W.; Wuts, P. G. M. *Protective groups in organic synthesis (third edition)*, John Wiley and Sons, Inc. **1999**.
- (144) Li, X. Q.; Feng, D. J.; Jiang, X. K.; Li, Z. T. *Tetrahedron* **2004**, *60*, 8275-8284.
- (145) Kotera, M.; Lehn, J. M.; Vigneron, J. P. *Tetrahedron* **1995**, *51*, 1953-1972.
- (146) Gulikkrzywicki, T.; Fouquey, C.; Lehn, J. M. *Proceedings of the National Academy of Sciences of the United States of America* **1993**, *90*, 163-167.
- (147) Lehn, J. M.; Mascal, M.; Decian, A.; Fischer, J. *Journal of the Chemical Society-Chemical Communications* **1990**, 479-481.
- (148) Brunsveld, L.; Folmer, B. J. B.; Meijer, E. W.; Sijbesma, R. P. *Chemical Reviews* **2001**, *101*, 4071-4097.
- (149) Jacobsen, J. R.; Cochran, A. G.; Stephans, J. C.; King, D. S.; Schultz, P. G. *Journal of the American Chemical Society* **1995**, *117*, 5453-5461.

- (150) Beijer, F. H.; Sijbesma, R. P.; Kooijman, H.; Spek, A. L.; Meijer, E. W. *Journal of the American Chemical Society* **1998**, *120*, 6761-6769.
- (151) Berl, V.; Schmutz, M.; Krische, M. J.; Khoury, R. G.; Lehn, J. M. *Chemistry-A European Journal* **2002**, *8*, 1227-1244.
- (152) Ti, J. S.; Steinfeld, A. S.; Naider, F.; Gulumoglu, A.; Lewis, S. V.; Becker, J. M. *Journal of Medicinal Chemistry* **1980**, *23*, 913-918.
- (153) Janda, K. D.; Ashley, J. A.; Jones, T. M.; McLeod, D. A.; Schloeder, D. M.; Weinhouse, M. I.; Lerner, R. A.; Gibbs, R. A.; Benkovic, P. A.; Hilhorst, R.; Benkovic, S. J. *Journal of the American Chemical Society* **1991**, *113*, 291-297.
- (154) Jacobson, K. A.; Barone, S.; Kammula, U.; Stiles, G. L. *Journal of Medicinal Chemistry* **1989**, *32*, 1043-1051.
- (155) Zhu, Z. L.; Espenson, J. H. *Journal of Organic Chemistry* **1995**, *60*, 7728-7732.
- (156) Cuevas-Yanez, E.; Muchowski, J. M.; Cruz-Almanza, R. *Tetrahedron* **2004**, *60*, 1505-1511.
- (157) Wasner, M.; Suhadolnik, R. J.; Horvath, S. E.; Adelson, M. E.; Kon, N.; Guan, M. X.; Henderson, E. E.; Pfeleiderer, W. *Helvetica Chimica Acta* **1997**, *80*, 1061-1072.
- (158) Zaramella, S.; Heinonen, P.; Yeheskiely, E.; Stromberg, R. *Journal of Organic Chemistry* **2003**, *68*, 7521-7523.
- (159) Adamczyk, M.; Grote, J. *Tetrahedron Letters* **2000**, *41*, 807-809.
- (160) Lindsay, S. *High Performance Liquid Chromatography: Analytical Chemistry by Open Learning*, Wiley, New York **1992**.
- (161) Nakamura, T.; Matsuyama, H.; Kamigata, N.; Iyoda, M. *Journal of Organic Chemistry* **1992**, *57*, 3783-3789.
- (162) Bisang, C.; Jiang, L. Y.; Freund, E.; Emery, F.; Bauch, C.; Matile, H.; Pluschke, G.; Robinson, J. A. *Journal of the American Chemical Society* **1998**, *120*, 7439-7449.
- (163) Greenwood, E. S.; Hitchcock, P. B.; Parsons, P. J. *Tetrahedron* **2003**, *59*, 3307-3314.
- (164) Roberts, S. L.; Furlan, R. L. E.; Otto, S.; Sanders, J. K. M. *Organic & Biomolecular Chemistry* **2003**, *1*, 1625-1633.
- (165) Singh, U.; Ghosh, S. K.; Chadha, M. S.; Mamdapur, V. R. *Tetrahedron Letters* **1991**, *32*, 255-258.
- (166) Scwyzer, R.; Iselin, B.; Kappeler, H.; Riniker, B.; Rittel, W.; Zuber, H. *Helvetica Chimica Acta* **1958**, *41*, 1273-1286.

- (167) Carpino, L. A.; Mansour, E. M. E.; Sadataalae, D. *Journal of Organic Chemistry* **1991**, *56*, 2611-2614.
- (168) Mohapatra, D. K.; Datta, A. *Journal of Organic Chemistry* **1999**, *64*, 6879-6880.
- (169) Rautio, J.; Nevalainen, T.; Taipale, H.; Vepsalainen, J.; Gynther, J.; Laine, K.; Jarvinen, T. *Journal of Medicinal Chemistry* **2000**, *43*, 1489-1494.
- (170) Tang, Z.; Yang, Z. H.; Chen, X. H.; Cun, L. F.; Mi, A. Q.; Jiang, Y. Z.; Gong, L. Z. *Journal of the American Chemical Society* **2005**, *127*, 9285-9289.
- (171) Tsogoeva, S. B.; Wei, S. *Tetrahedron:Asymmetry* **2005**, *16*, 1947-1951.
- (172) Khier, N.; Araujo, C. S.; Alcudia, F.; Fernandez, I. *Journal of Organic Chemistry* **2002**, *67*, 345-356.
- (173) Banfi, L.; Colombo, L.; Gennari, C.; Annunziata, R.; Cozzi, F. *Synthesis* **1982**, 829-831.
- (174) Oppolzer, W.; Froelich, O.; WiauxZamar, C.; Bernardinelli, G. *Tetrahedron Letters* **1997**, *38*, 2825-2828.
- (175) Schwergold, C.; Depecker, G.; Di Giorgio, C.; Patino, N.; Jossinet, F.; Ehresmann, B.; Terreux, R.; Cabrol-Bass, D.; Condom, R. *Tetrahedron* **2002**, *58*, 5675-5687.
- (176) Baker, B. R.; Chheda, G. B. *Journal of Pharmaceutical Sciences* **1965**, *54*, 25-30.
- (177) Zhiqiang, S.; Yuliang, L.; Gong, H.; Liu, M.; Xiao, S.; Liu, H.; Li, H.; Xiao, S.; Zhu, D. *Organic Letters* **2002**, *4*, 1179-1182.

Polymer 157



Current Data Parameters
 NAME Jun18-2003
 EXPNO 80
 PROCNO 1

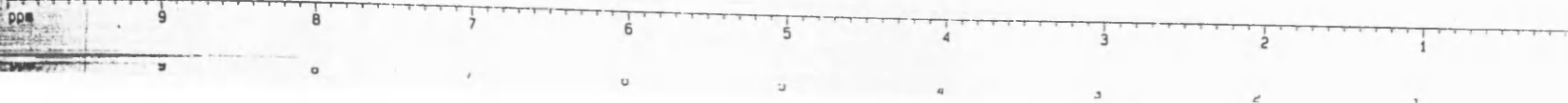
F2 - Acquisition Parameters
 Date_ 20030618
 Time 19.02
 INSTRUM amx300
 PROBHD 5 mm QNP 1H
 PULPROG zg30
 TD 67306
 SOLVENT CDC13
 RO 20
 NS 64
 RO 20
 SNH 8771.930 Hz
 FIDRES 0.130329 Hz
 AQ 3.8364921 sec
 RG 512
 DM 57.000 usec
 DE 81.43 usec
 TE 300.0 K
 HL1 1 dB
 D1 1.0000000 sec
 P1 6.80 usec
 SFO1 299.8758200 MHz
 NUCLEUS 1H

F2 - Processing parameters
 SI 131072
 SF 299.8727940 MHz
 WDW EM
 SSB 0
 LB 0.15 Hz
 GB 0
 PC 1.00
 SR 2794.00 Hz

1D NMR plot parameters
 CX 32.00 cm
 F1P 10.000 ppm
 F1 2998.73 Hz
 F2P 0.000 ppm
 F2 0.00 Hz
 PPMCM 0.31250 ppm/cm
 HZCM 93.71025 Hz/cm

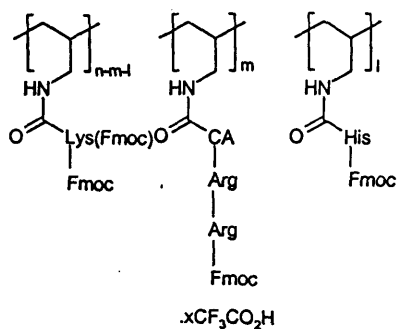
Integral

ppm



ppm

Polymer 162



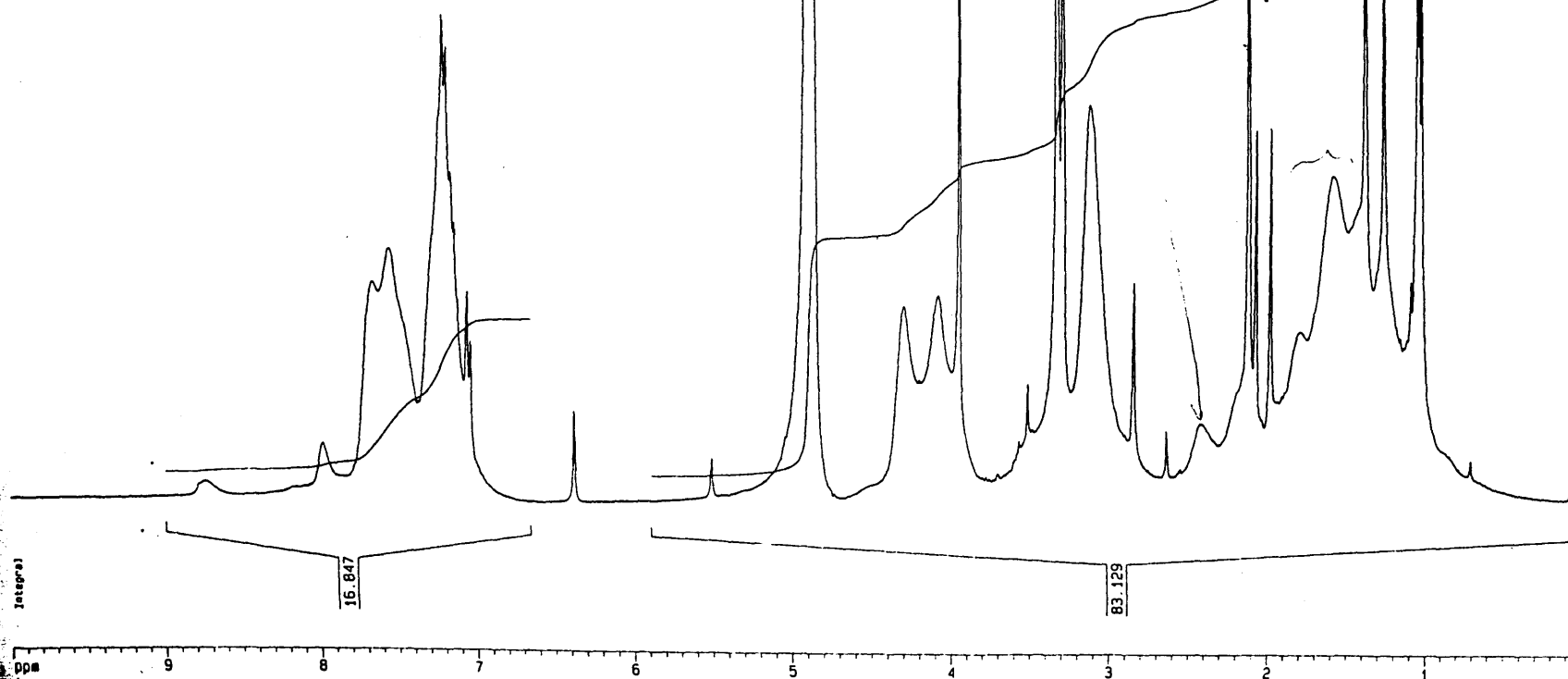
$\times \text{CF}_3\text{CO}_2\text{H}$

Current Data Parameters
NAME Jun20-2003
EXPNO 90
PROCNO 1

F2 - Acquisition Parameters
Date_ 20030620
Time 19.07
INSTRUM amx300
PROBHD 5 mm QNP 1H
PULPROG zg30
TD 67306
SOLVENT MeOH
RO 20
NS 64
R0 20
SWH 8771.965 Hz
FIDRES 0.130330 Hz
AQ 3.8364921 sec
RG 128
DW 57.000 usec
DE 81.43 usec
TE 300.0 K
HL1 1 dB
D1 1.00000000 sec
P1 6.80 usec
SF01 299.8770015 MHz
NUCLEUS 1H

F2 - Processing parameters
SI 131072
SF 299.8739764 MHz
WDW EM
SSB 0
LB 0.15 Hz
GB 0
PC 1.00
SR 3976.36 Hz

1D NMR plot parameters
CX 32.00 cm
F1P 10.000 ppm
F1 2998.74 Hz
F2P 0.000 ppm
F2 0.00 Hz
PPMCM 0.31250 ppm/cm
HZCM 93.71062 Hz/cm



8.77102
8.72076
8.59443

8.09492
7.97932

7.67341
7.56636
7.37138
7.23204
7.20786
7.17668
7.15330
7.06693
7.04300

6.38311

5.80000

5.51458

5.45108

4.90388

4.73750

4.30499

4.20563

4.09141

3.95794

3.79571

3.77512

3.75231

3.70526

3.69682

3.65898

3.56888

3.51263

3.48215

3.33725

3.29861

3.12456

2.84507

2.63735

2.54930

2.40907

2.12480

2.07530

1.98295

1.79199

1.59426

1.39109

1.27533

1.16388

1.13897

1.12190

1.09875

1.06481

1.05234

1.03739

0.74728

0.71609

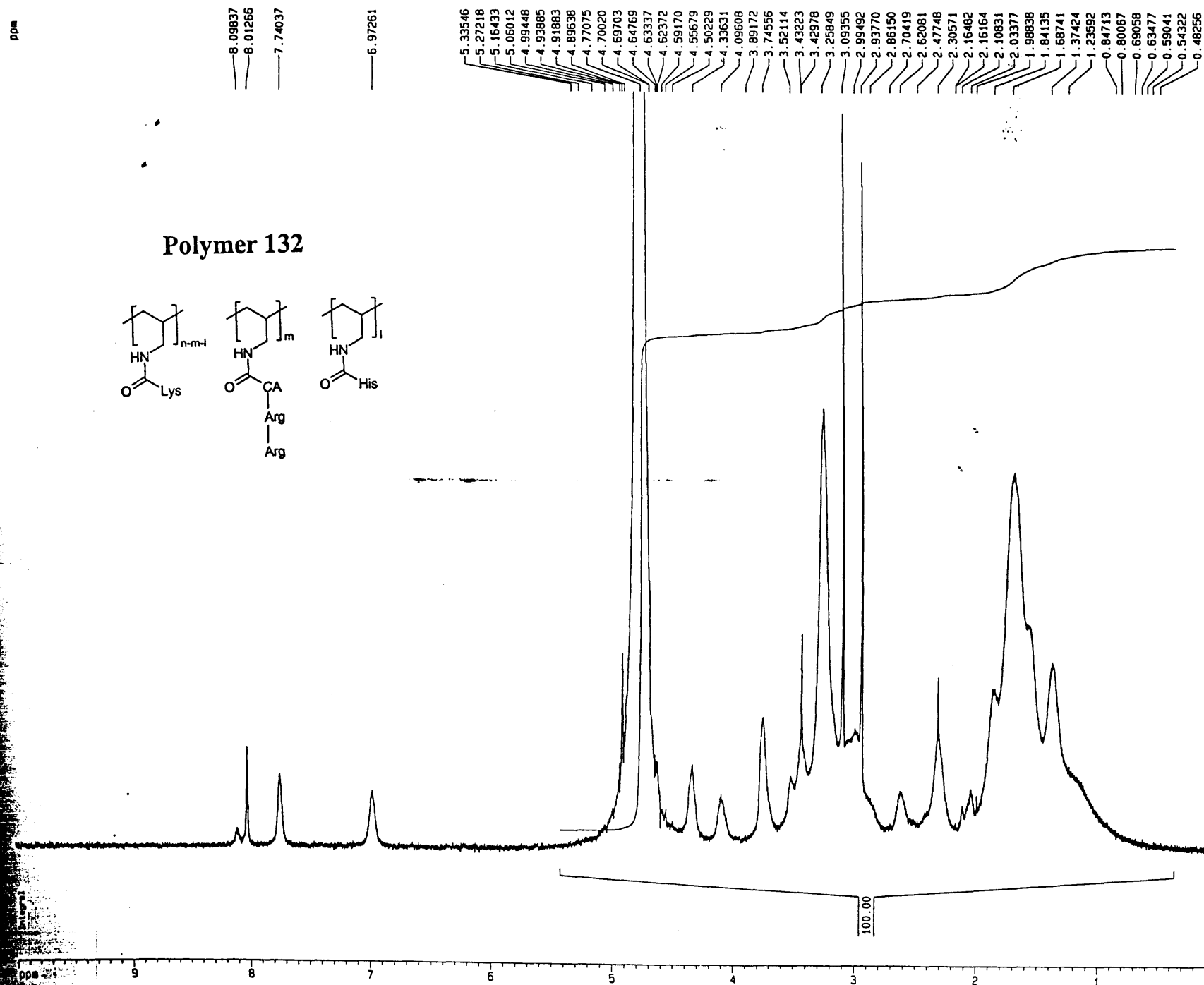
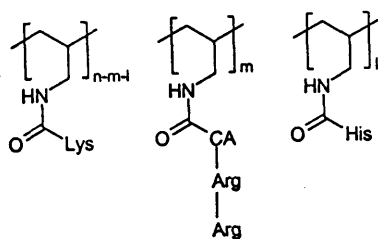
0.46236

0.45200

0.16471

0.09052

Polymer 132



Current Data Parameters
NAME Feb24-2004
EXPNO 140
PROCNO 1

F2 - Acquisition Parameters
Date_ 20040224
Time 20.59
INSTRUM amx300
PROBHD 5 mm QNP 1H
PULPROG zg30
TD 67306
SOLVENT D2O
RO 20
NS 64
R0 20
SWH 8771.952 Hz
FIDRES 0.130329 Hz
AQ 3.8364921 sec
RG 512
OW 57.000 usec
DE 81.43 usec
TE 300.0 K
HL1 1 dB
D1 1.00000000 sec
P1 6.80 usec
SF01 299.8765817 MHz
NUCLEUS 1H

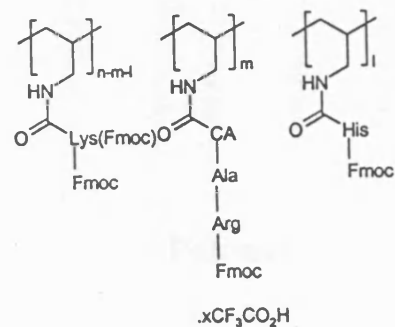
F2 - Processing parameters
SI 131072
SF 299.8735313 MHz
WDW EM
SSB 0
LB 0.15 Hz
GB 0
PC 1.00
SR 3531.32 Hz

1D NMR plot parameters
CX 32.00 cm
F1P 10.000 ppm
F1 2998.74 Hz
F2P 0.000 ppm
F2 0.00 Hz
PPMCH 0.31250 ppm/cm
HZCM 93.71048 Hz/cm

ppm

8.83658
8.78047
8.71945
8.25309
7.96904
7.78559
7.76315
7.64652
7.57939
7.53608
7.25723
7.23426
7.20921
7.17794
7.16264
7.15447
7.13458
7.13076
7.06789
7.04416
6.80395
6.38620
5.58531
5.51745
5.45469
5.25564
5.00680
4.98228
4.83900
4.65227
4.28408
4.08750
3.96038
3.77607
3.59839
3.51516
3.48368
3.38620
3.32455
3.30460
3.29439
3.29439
3.10241
2.90338
2.84799
2.40784
2.16226
2.12175
2.07826
2.04422
2.03409
1.98529
1.90974
1.77332
1.60062
1.39373
1.27831
1.26500
1.18138
1.15595
1.12986
1.09943
1.06739
1.05398
1.03970
1.01925
0.98886
0.97181
0.95606
0.86246

Polymer 164



Current Data Parameters
NAME Jun17-2003
EXPNO 70
PROCNO 1

F2 - Acquisition Parameters

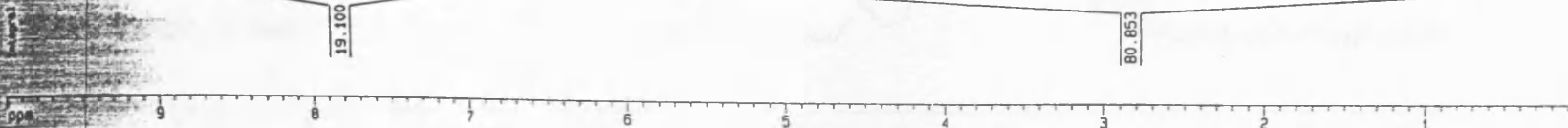
Date_ 20030617
Time 17.04
INSTRUM amx300
PROBHD 5 mm QNP 1H
PULPROG zg30
TD 67306
SOLVENT MeOH
RO 20
NS 64
R0 20
SWH 8771.965 Hz
FIDRES 0.130330 Hz
AQ 3.8364921 sec
RG 256
DW 57.000 usec
DE 81.43 usec
TE 300.0 K
HL1 1 dB
D1 1.00000000 sec
P1 6.80 usec
SFO1 299.8770015 MHz
NUCLEUS 1H

F2 - Processing parameters

SI 131072
SF 299.8739764 MHz
WDW EM
SSB 0
LB 0.15 Hz
GB 0
PC 1.00
SR 3976.36 Hz

1D NMR plot parameters

CX 32.00 cm
F1P 10.000 ppm
F1 2998.74 Hz
F2P 0.000 ppm
F2 0.00 Hz
PPMCH 0.31250 ppm/cm
HZCM 93.71062 Hz/cm

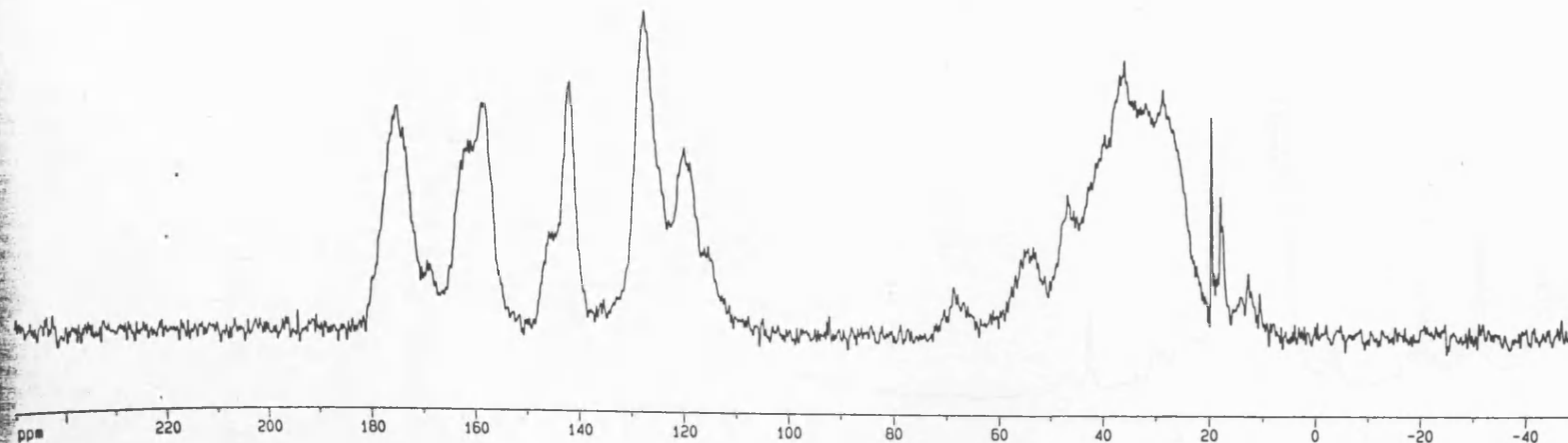
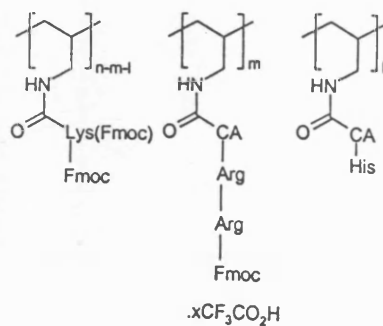


¹³C CPMAS TOSS - SAMPLE ES/D7

ppm

174.514
158.315
141.624
127.566
119.760
68.682
53.396
46.794
36.035
28.729
19.632
17.909
12.768
10.659

Polymer 361



Current Data Parameters

NAME SMILJANC
EXPNO 25
PROCNO 1

F2 - Acquisition Parameters

Date_ 20120703
Time 12.00
INSTRUM msl
PROBHD
PULPROG TOSS5.PC
TD 2048
SOLVENT CDC13
RO 5000
NS 34770
RO 5000
SMH 29411.766 Hz
FIDRES 14.361214 Hz
AQ 0.0348660 sec
RG 1447
DM 17.000 usec
DE 625.00 usec
TE 297.0 K
D11 0.00000530 sec
HL1 0 dB
O5 0.00100000 sec
O25 0.00003653 sec
O2 0.00000810 sec
O26 0.00001648 sec
O27 0.00002674 sec
DO 2.00000000 sec
P1 0.00 usec
L1 1
O1 0.00000400 sec
SFO1 75.4755000 MHz
NUCLEUS

F2 - Processing parameters

SI 16384
SF 75.4674443 MHz
WDW EM
SSB 0
LB 10.00 Hz
GB 0
PC 1.00
SR -555.71 Hz

1D NMR plot parameters

CX 30.00 cm
F1P 250.000 ppm
F1 18866.86 Hz
F2P -50.000 ppm
F2 -3773.37 Hz
PPMCM 10.00000 ppm/cm
HZCM 754.67444 Hz/cm

ES/645

Polymer 238

